

Taxonomic study of the genus *Ischnothyreus* Simon, 1893 from Myanmar (Araneae, Oonopidae)

Yanfeng Tong^{1,2}, Shuqiang Li³, Dongju Bian⁴

1 Life Science College, Shenyang Normal University, Shenyang 110034, China **2** Southeast Asia Biological Diversity Research Institute, Chinese Academy of Sciences, Yezin, Nay Pyi Taw 05282, Myanmar **3** Institute of Zoology, Chinese Academy of Sciences, Beijing 100101, China **4** CAS Key Laboratory of Forest Ecology and Management, Institute of Applied Ecology, Shenyang 110016, China

Corresponding author: Shuqiang Li (lisq@ioz.ac.cn); Dongju Bian (biandongju@163.com)

Academic editor: I. Agnarsson | Received 17 August 2020 | Accepted 19 October 2020 | Published 16 November 2020

<http://zoobank.org/DAFA5BEE-7571-4CA8-99D1-D76DFFCAB875>

Citation: Tong Y, Li S, Bian D (2020) Taxonomic study of the genus *Ischnothyreus* Simon, 1893 from Myanmar (Araneae, Oonopidae). ZooKeys 993: 1–26. <https://doi.org/10.3897/zookeys.993.57676>

Abstract

Seven new species of the genus *Ischnothyreus* Simon, 1893 from the spider family Oonopidae Simon, 1890 are reported from Myanmar: *I. hponkanrazi* **sp. nov.** (♀), *I. jianglangi* **sp. nov.** (♀), *I. meukyawwa* **sp. nov.** (♂♀), *I. putao* **sp. nov.** (♀), *I. qiuxing* **sp. nov.** (♀), *I. taunggyi* **sp. nov.** (♂♀) and *I. zhigangi* **sp. nov.** (♂♀). Morphological descriptions and photographic illustrations of the new species are given. All types are preserved in the Institute of Zoology, Chinese Academy of Sciences in Beijing (IZCAS).

Keywords

Goblin spider, morphology, new species, taxonomy

Introduction

The genus *Ischnothyreus* was established by Simon in 1893, with *Ischnaspis peltifer* Simon, 1892 from Saint Vincent in the Caribbean as the type species (Simon 1893). This genus is an Old World taxon, being represented in the New World by only two species, *I. peltifer* and *I. velox* Jackson, 1908, both of which are assumed to be introduced (Platnick et al. 2012; Brescovit et al. 2019).

The genus *Ischnothyreus* Simon, 1893 can be recognized by the presence of leg spines, the usually small abdominal scutum, the strongly sclerotized male palps, the heavily sclerotized male endites, and the winding genital tube in females (Kranz-Baltensperger 2011). There are currently 107 valid specific names assigned to *Ischnothyreus* (Li 2020; WSC 2020) and even more are waiting to be described (Richard et al. 2016).

In this paper seven new *Ischnothyreus* species collected from Myanmar are described and illustrated. This work presents the first record and description of species *Ischnothyreus* from Myanmar.

Materials and methods

The specimens were examined in 95% ethanol using a Leica M205C stereomicroscope. Details were studied with an Olympus BX51 compound microscope. Photos were taken with a Canon EOS 750D zoom digital camera (18 megapixels) mounted on an Olympus BX51 compound microscope. Vulvae were cleared in lactic acid. Scanning electron microscope images (SEM) were taken under high vacuum with a Hitachi TM3030 after critical point drying and gold-palladium coating. All measurements were taken using an Olympus BX51 compound microscope and are given in millimeters in the text. The specimens are preserved in the Institute of Zoology, Chinese Academy of Sciences (IZCAS) in Beijing, China (curator: Jun Chen).

The following abbreviations are used in the text and figures: **a** = apodemes; **ALE** = anterior lateral eyes; **ass** = anchor-shaped structure; **bsa** = bell-shaped atrium; **csa** = circular atrium; **csp** = crown-shaped sclerotized process; **hsm** = hook-shaped membrane; **llm** = leaf like membrane; **lpp** = leaf-shaped prolateral projection; **nlm** = needle like membrane; **nsa** = nipple-shaped atrium; **oa** = opening of the atrium; **PLE** = posterior lateral eyes; **PME** = posterior median eyes; **rl** = retrolateral lobe; **sem** = serrated exterior margin; **tsa** = triangular shaped atrium; **vpr** = ventral protuberance; **wt** = winding tube.

Taxonomy

Family Oonopidae Simon, 1890

Genus *Ischnothyreus* Simon, 1893

Ischnothyreus hponkanrazi Tong & Li, sp. nov.

<http://zoobank.org/EFA6509C-6C65-46CC-B65D-E54770EAB9E5>

Figures 1, 16A, B

Type material. *Holotype* ♀: MYANMAR, Kachin State, Putao, Hponkanrazi Wildlife Sanctuary, roadside between Camp 2 to Camp 1; 27°36'067"N, 96°59'367"E; elevation ca 1714 m; 17.XII.2016; Wu J. leg. (IZCAS AR-25158).

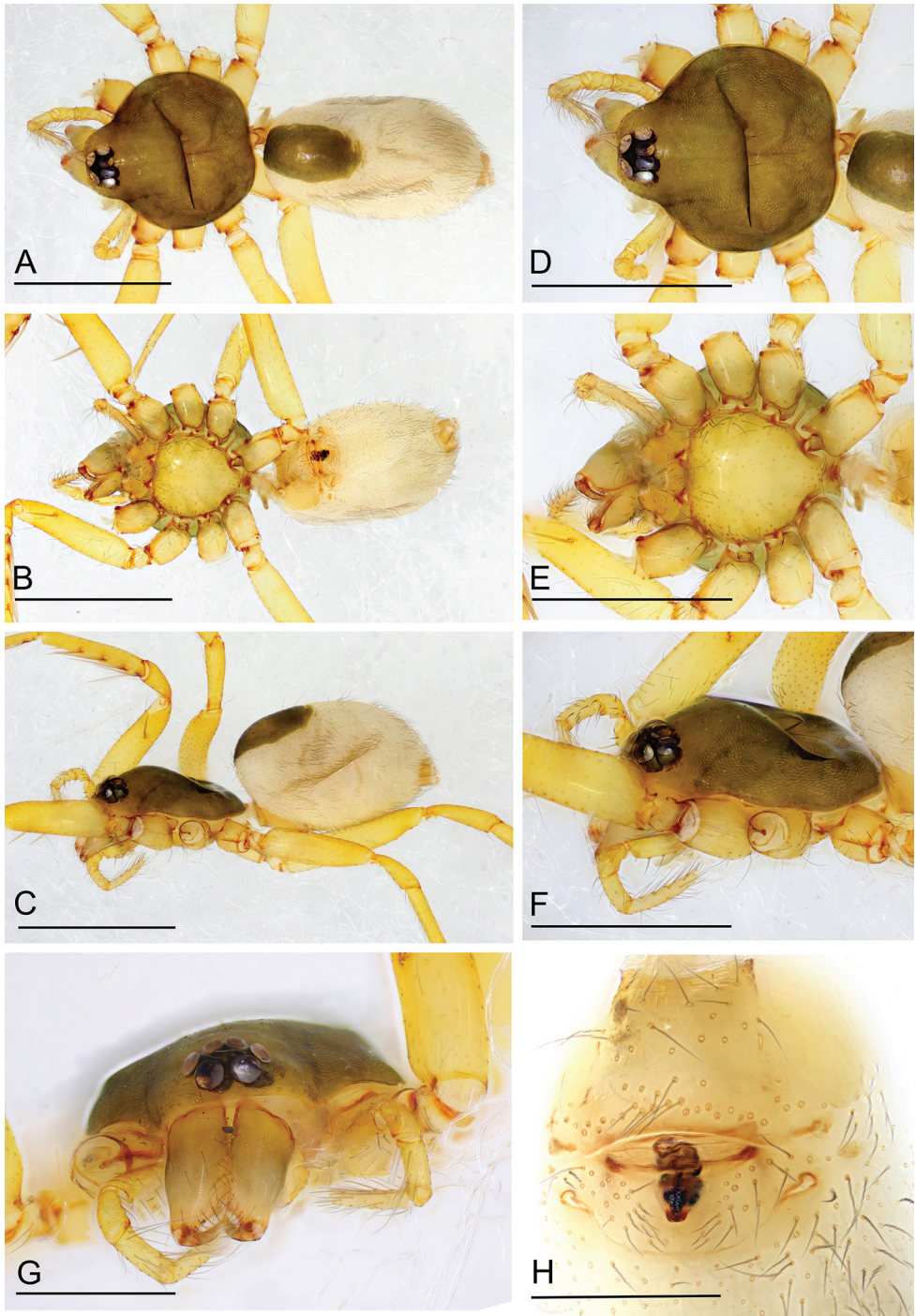


Figure 1. *Ischnothyreus hponkanrazi* sp. nov., female holotype **A–C** habitus, dorsal, ventral and lateral views **D–G** prosoma, dorsal, ventral, lateral and anterior views **H** epigastric region, ventral view. Scale bars: 0.4 mm (**A–F**); 0.2 mm (**G, H**).

Diagnosis. The new species is similar to *I. campanaceus* Tong & Li, 2008 in the bell-shaped atrium, but can be distinguished by the short abdominal dorsal scutum (1/3 of the abdomen length (Fig. 1A) vs 4/5 of the abdomen length (Tong and Li 2008: fig. 1B; Tong 2013: fig. 44B), and the greater sinuosity of the winding tube of endogyne (Fig. 1H) (vs short, simple winding tube; Tong and Li 2008: fig. 1F; Tong 2013: fig. 44F).

Description. Female (holotype). Body: habitus as in Fig. 1A–C; body length 2.40. **Carapace:** 1.08 long, 0.98 wide; pale brown, without any pattern, ovoid in dorsal view, slightly elevated in lateral view, surface finely reticulate, fovea absent, lateral margin straight, smooth (Fig. 1D, F). **Clypeus:** height about equal to ALE radius or more (Fig. 1G). **Eyes:** six, in one group, well developed, subequal, ALE circular, PME and PLE oval, posterior eye row procurved from both above and front (Fig. 1D, G). **Sternum:** as long as wide, pale orange, uniform, not fused to carapace, surface smooth, setae sparse (Fig. 1E). **Mouthparts:** chelicerae, endites and labium orange; chelicerae straight, base of fangs unmodified (Fig. 1G); labium rectangular, not fused to sternum, anterior margin not indented at middle; endites unmodified (Fig. 1E). **Abdomen:** 1.33 long, 0.74 wide; dorsal scutum well sclerotized, pale brown, covering 1/3 of the abdomen width and approximately 1/3 of the abdomen length, not fused to epigastric scutum; epigastric and postgastric scutum well sclerotized, pale orange, unfused (Fig. 1A, B). **Legs:** pale orange, femur I with two prolateral spines, tibia I with four pairs, metatarsus I with two pairs of long ventral spines. Leg II spination is similar to leg I except femur with only one prolateral spine. Legs III and IV spineless. **Epigastric area:** surface without external features (Fig. 1H). **Endogyne:** from the middle of the slightly thickened margin of the postgastric scutum runs a dark winding tube posteriorly, ending in a bell-shaped atrium (Fig. 16A, B).

Male. Unknown.

Etymology. The specific name is a noun in apposition taken from the type locality.

Distribution. Known only from the type locality.

Ischnothyreus jianglangi Tong & Li, sp. nov.

<http://zoobank.org/505F6C65-291C-47C0-8997-23CA63EA5161>

Figures 2, 17A, B

Type material. Holotype ♀: MYANMAR, Kachin State, Putao, Hponkanrazi Wildlife Sanctuary, roadside between Camp 2 to Camp 1; 27°35'806"N, 96°59'532"E; elevation ca 1613 m; 10.V.2017; Wu J. & Chen Z. leg. (IZCAS AR-25159).

Diagnosis. The new species is similar to *I. jojo* Kranz-Baltensperger, 2011 in the triangular shaped atrium, but can be distinguished by shape of the dorsal abdominal scutum (width/length = 1/2 (Fig. 2A) vs approximately 1/3; Kranz-Baltensperger 2011: fig. 25A), and the unmodified exterior surface of postgastric scutum (Fig. 17A) (vs with curved, sclerotized extensions and U-shaped structure; Kranz-Baltensperger 2011: fig. 25E, F).

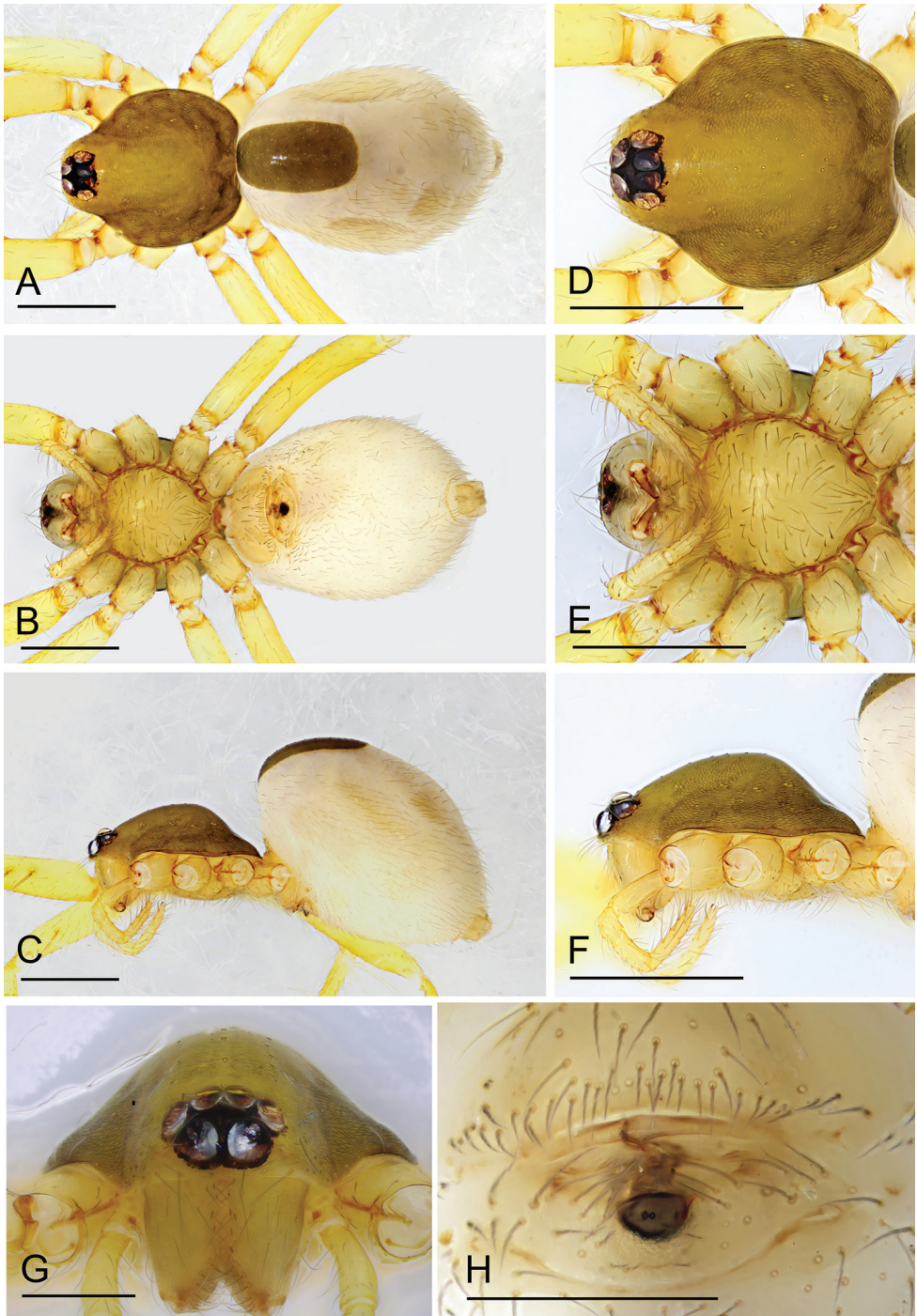


Figure 2. *Ischnothyreus jianglangi* sp. nov., female holotype **A–C** habitus, dorsal, ventral and lateral views **D–G** prosoma, dorsal, ventral, lateral and anterior views **H** epigastric region, ventral view. Scale bars: 0.4 mm (**A–F**); 0.1 mm (**G, H**).

Description. Female (holotype). *Body:* habitus as in Fig. 2A–C; body length 2.35. *Carapace:* 1.02 long, 0.87 wide; brown, without any pattern, ovoid in dorsal view, slightly elevated in lateral view, surface finely reticulate, fovea absent, lateral margin straight, smooth (Fig. 2D, F). *Clypeus:* height about equal to ALE radius or less (Fig. 2G). *Eyes:* six, in one group, well developed, subequal, ALE circular, PME and PLE oval, posterior eye row procurved from both above and front (Fig. 2D, G). *Sternum:* as long as wide, pale brown, uniform, not fused to carapace, surface smooth, setae sparse (Fig. 2E). *Mouthparts:* chelicerae, endites and labium pale brown; chelicerae straight, base of fangs unmodified (Fig. 2G); labium rectangular, not fused to sternum, anterior margin not indented at middle; endites unmodified (Fig. 2E). *Abdomen:* 1.42 long, 1.01 wide; dorsal scutum covering less than 1/2 of the abdomen length and 1/3 of the abdomen width, not fused to epigastric scutum; epigastric and postgastric scutum well sclerotized, pale orange, unfused (Fig. 2A, B). *Legs:* pale orange, femur I with two prolateral spines, tibia I with four pairs, metatarsus I with two pairs of long ventral spines. Leg II spination is similar to leg I except femur with only one prolateral spine. Legs III and IV spineless. *Epigastric area:* surface without external features (Fig. 2H). *Endogyne:* from the middle of the slightly thickened margin of the postgastric scutum runs a dark, simple winding tube posteriorly, ending in a black, triangular shaped atrium (Fig. 17A, B).

Male. Unknown.

Etymology. The species is named after Mr Jianglang Wu, one of the collectors of the holotype; noun in genitive case.

Distribution. Known only from the type locality.

Ischnothyreus meukyawwa Tong & Li, sp. nov.

<http://zoobank.org/08A2A68D-453F-4E7F-8F52-05FB0C49EDAC>

Figures 3–5, 14A–C, 15A, B, 16C, D

Type material. Holotype ♂: MYANMAR, Kachin State, Putao, Meukyawwa Village; 27°20'883"N, 97°22'717"E; elevation ca 464 m; 25.XII.2016; Wu J. leg. (IZCAS AR-25160). **Paratypes:** 5♂ 9♀, same data as for holotype (IZCAS AR-25161–25174).

Diagnosis. The new species is similar to *I. an* Tong & Li, 2016 in the large abdominal dorsal and ventral scutum, but can be distinguished by the unmodified male cheliceral fang (Fig. 3H, I) (vs with thorn-like protrusion; Tong et al. 2016: fig. 1G, H), the acute distal end of male palp (Fig. 14A) (vs blunt distal end of male palp; Tong et al. 2016: fig. 3A, D), and the small bell-shaped atrium (Fig. 16C) (vs a large equilateral triangular shaped atrium; Tong et al. 2016: fig. 2G, I).

Description. Male (holotype). *Body:* habitus as in Fig. 3A–C; body length 1.57. *Carapace:* 0.89 long, 0.74 wide; pale brown, with egg-shaped patches behind eyes, ovoid in dorsal view, strongly elevated in lateral view, surface of elevated portion of pars cephalica smooth, sides finely reticulate, fovea absent, lateral margin straight, smooth

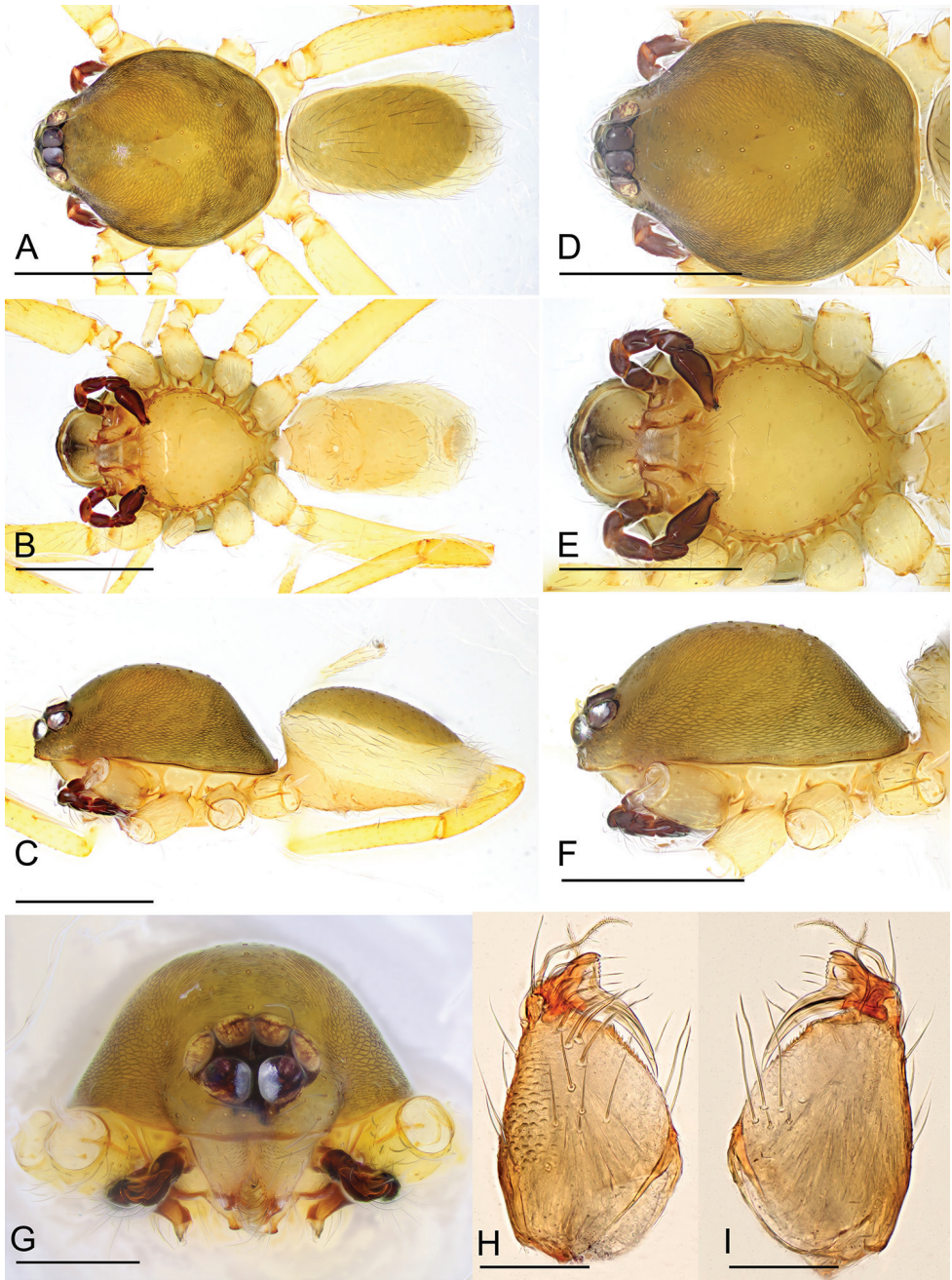


Figure 3. *Ischnothyreus meukyawwa* sp. nov., male holotype **A–C** habitus, dorsal, ventral and lateral views **D–G** prosoma, dorsal, ventral, lateral and anterior views **H, I** left chelicerae, anterior and posterior views. Scale bars: 0.4 mm (**A–F**); 0.2 mm (**G**); 0.1 mm (**H, I**).

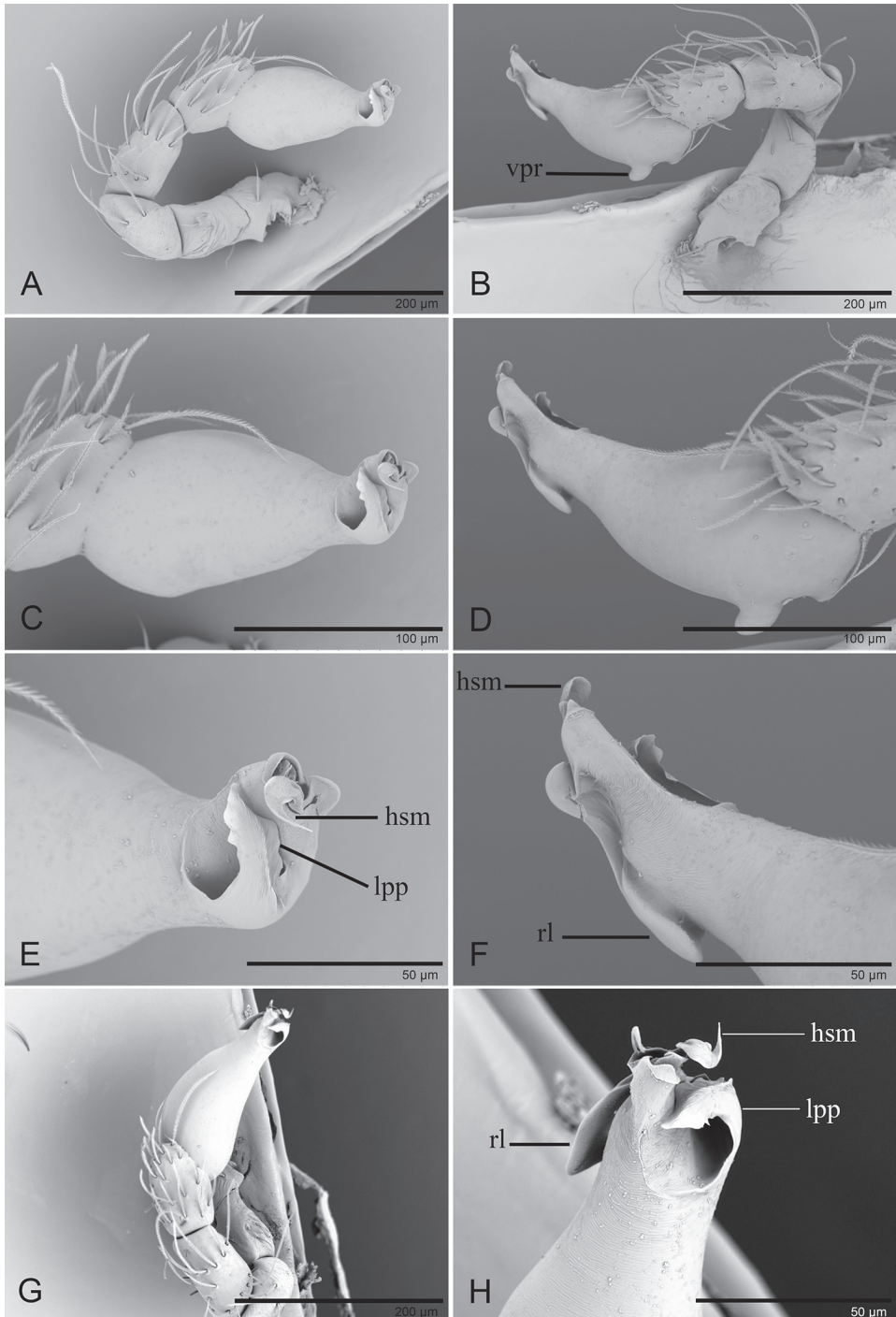


Figure 4. *Ischnothyreus meukyauwa* sp. nov., male holotype, left palp, SEM **A, B, G** prolateral, retrolateral and dorsal views **C, D** palp bulb, prolateral and retrolateral views **E, F, H** distal part of palpal bulb, prolateral, retrolateral and dorsal views. Abbreviations: hsm = hook-shaped membrane; lpp = leaf-shaped prolateral projection; rl = retrolateral lobe; vpr = ventral protuberance.

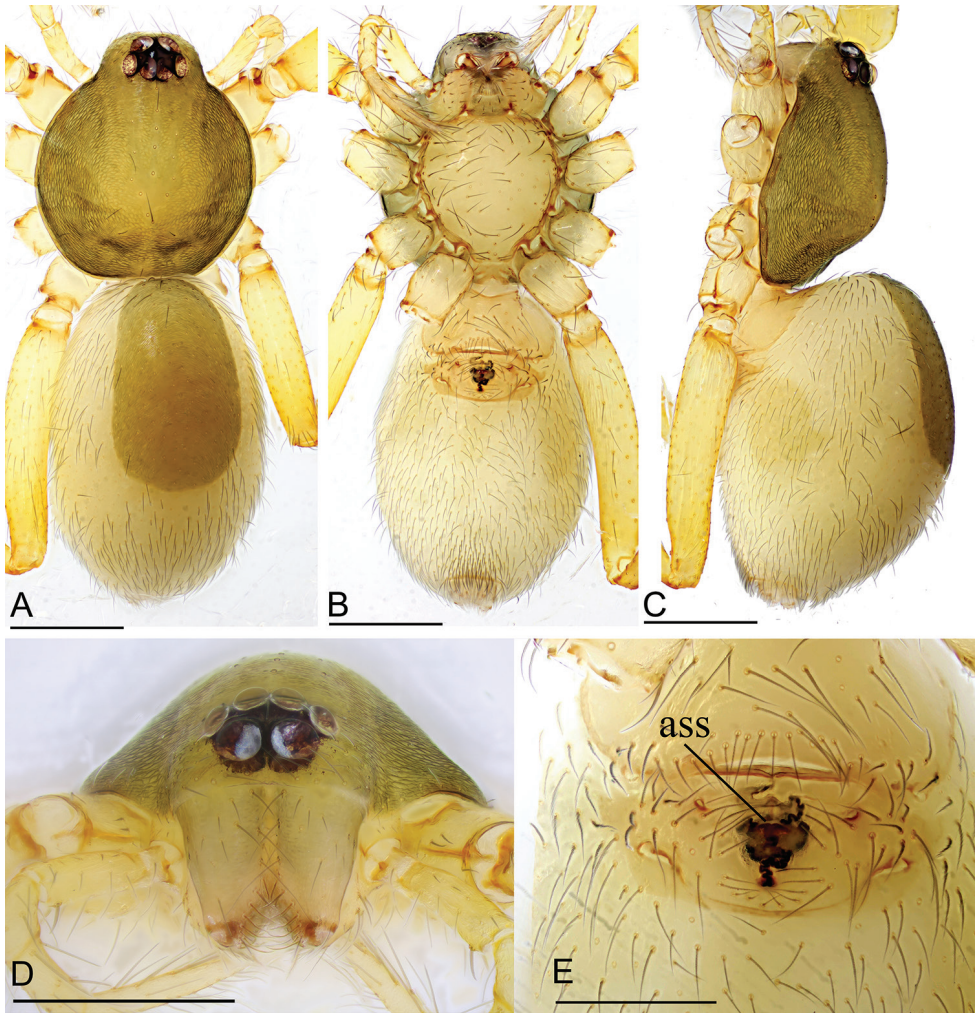


Figure 5. *Ischnothyreus meukyawwa* sp. nov., female paratype **A–C** habitus, dorsal, ventral and lateral views **D** prosoma, anterior view **E** epigastric region, ventral view. Abbreviation: **ass** = anchor-shaped structure. Scale bars: 0.4 mm (**A–C**); 0.2 mm (**D, E**).

(Fig. 3D, F). **Clypeus:** height about 2/3 of ALE diameter (Fig. 3G). **Eyes:** six, in one group, well developed, subequal, ALE circular, PME and PLE oval, posterior eye row recurved from above, procurved from front (Fig. 3D, G). **Sternum:** as long as wide, pale orange, uniform, not fused to carapace, surface smooth, setae sparse (Fig. 3E). **Mouthparts:** chelicerae, endites and labium orange; chelicerae straight, base of fangs with crown-shaped sclerotized process with serrated exterior margin, fang groove with a few small denticles (Figs 3H, I, 15A, B); labium rectangular, not fused to sternum, anterior margin not indented at middle; anteromedian tip of endites with one strong, tooth-like projection (Fig. 3E). **Abdomen:** 0.84 long, 0.43 wide; dorsal scutum well sclerotized, pale orange, covering whole abdomen width and approximately 5/6 of the

abdomen length, not fused to epigastric scutum; epigastric and postgastric scutum well sclerotized, pale orange, fused, postgastric scutum covering about 5/6 of the abdomen length (Fig. 3A–C). **Legs:** pale orange, femur I with three prolateral and two small retrolateral spines, tibia I with four pairs, metatarsus I with two pairs of long ventral spines. Leg II spination is similar to leg I except femur with only two prolateral and one retrolateral spine. Legs III and IV spineless. **Palp:** strongly sclerotized, trochanter with ventral projection, cymbium brown, fused with bulb; bulb brown, with one large and one very small ventral protuberance, distal end of bulb elongated, with one broad leaf-shaped prolateral projection and distal hook-shaped membrane, retrolateral lobe narrow (Figs 4, 14A–C).

Female (paratype, IZCAS AR-25160). Same as male except as noted. **Body:** habitus as in Fig. 5A–C; body length 1.93. **Carapace:** 0.89 long, 0.76 wide; without any pattern. **Mouthparts:** chelicerae and endites unmodified. **Abdomen:** 0.83 long, 0.75 wide; dorsal scutum covering 3/5 of the abdomen length, about 1/2 of the abdomen width. **Epigastric area:** the postgastric scutum with central anchor-shaped structure (Fig. 5E). **Endogyne:** from the middle of the slightly thickened margin of the postgastric scutum runs a dark, simple winding tube posteriorly, ending in a small bell-shaped atrium (Fig. 16C, D).

Etymology. The specific name is a noun in apposition taken from the type locality.

Distribution. Known only from the type locality.

Ischnothyreus putao Tong & Li, sp. nov.

<http://zoobank.org/D96DFBF0-A942-44A3-833A-18EB8FB325B1>

Figures 6, 17C, D

Type material. Holotype ♀: MYANMAR, Kachin State, Putao, Hponkanrazi Wildlife Sanctuary, roadside between Camp 1 to Camp 2; 27°36'567"N, 96°58'850"E; elevation ca 2233 m; 15.XII.2016; Wu J. leg. (IZCAS AR-25175).

Diagnosis. The new species is similar to *I. zhigangi* sp. nov. in the very small abdominal dorsal scutum and the brown carapace, but can be distinguished by the large bell-shaped atrium (Fig. 17C) (vs small, bell-shaped atrium; Fig. 17E), and the smoothly curved posterior margin of postgastric scutum (Fig. 6H) (vs straight posterior margin; Fig. 13H).

Description. Female (holotype). **Body:** habitus as in Fig. 6A–C; body length 1.94. **Carapace:** 0.97 long, 0.88 wide; dark brown, without any pattern, ovoid in dorsal view, strongly elevated in lateral view, surface finely reticulate, fovea absent, lateral margin straight, smooth (Fig. 6D, F). **Clypeus:** height about equal to ALE radius or more (Fig. 6G). **Eyes:** six, in one group, well developed, subequal, ALE circular, PME and PLE oval, posterior eye row procurved from both above and front (Fig. 6D, G). **Sternum:** as long as wide, pale brown, uniform, not fused to carapace, surface smooth, setae sparse (Fig. 6E). **Mouthparts:** chelicerae, endites and labium brown; chelicerae straight, base of fangs unmodified (Fig. 6G); labium rectangular, not fused to sternum, anterior margin not indented at middle; endites unmodified (Fig. 6E). **Abdomen:** 1.30

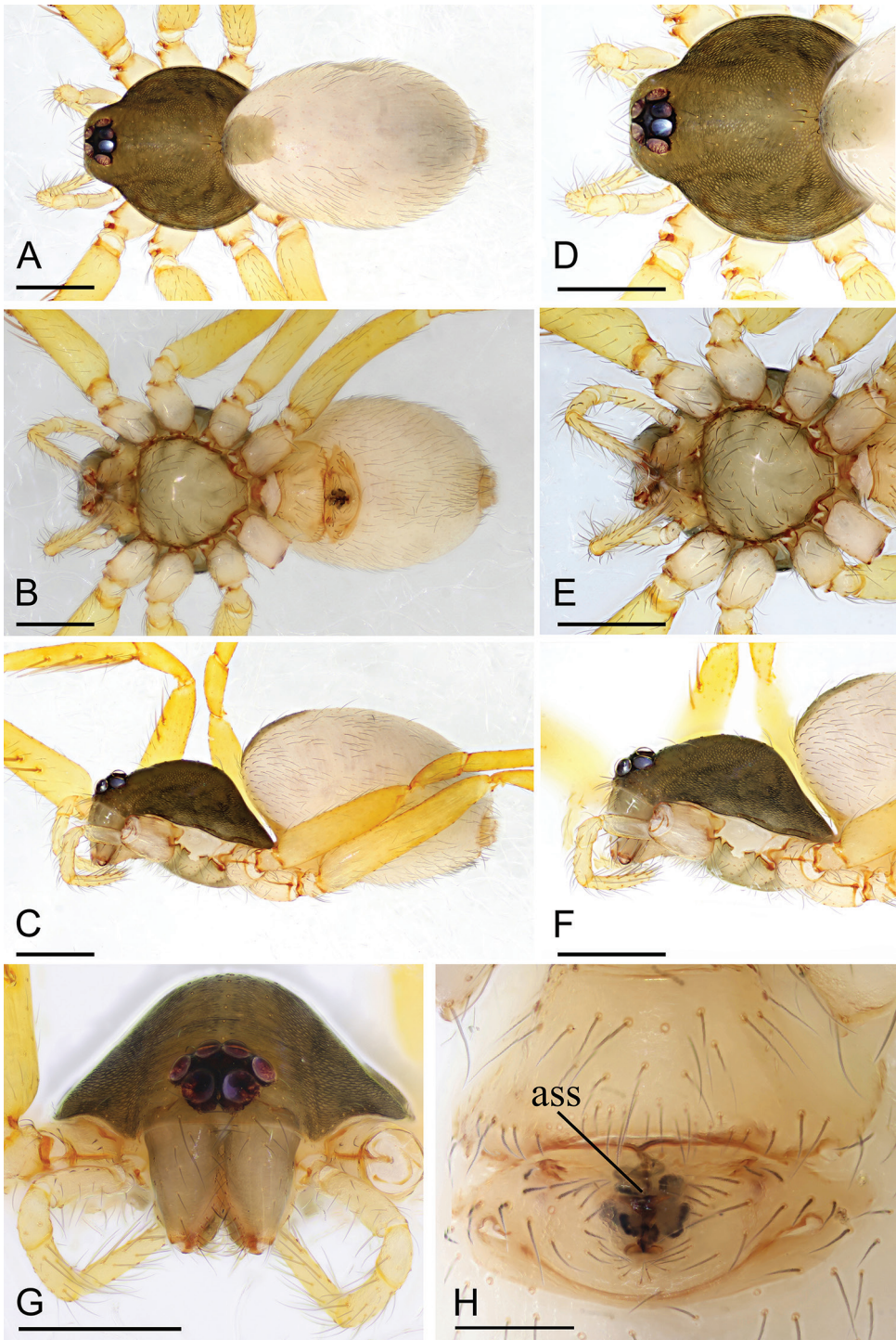


Figure 6. *Ischnothyreus putao* sp. nov., female holotype **A–C** habitus, dorsal, ventral and lateral views **D–G** prosoma, dorsal, ventral, lateral and anterior views **H** epigastric region, ventral view. Abbreviation: ass = anchor-shaped structure. Scale bars: 0.4 mm (**A–F**); 0.2 mm (**G**); 0.1 mm (**H**).

long, 0.89 wide; dorsal scutum weakly sclerotized, very small, not fused to epigastric scutum; epigastric and postgastric scutum well sclerotized, pale orange, unfused (Fig. 6A, B). **Legs:** pale orange, femur I with three prolateral spines, tibia I with four pairs, metatarsus I with two pairs of long ventral spines. Leg II spination is similar to leg I except femur with only two prolateral spine. Legs III and IV spineless. **Epigastric area:** the postgastric scutum with central, anchor-shaped structure, and smoothly curved posterior margin (Fig. 6H). **Endogyne:** from the middle of the slightly thickened margin of the postgastric scutum runs a dark, simple winding tube posteriorly, ending in a large, inverted bell-shaped atrium (Fig. 17C, D).

Male. Unknown.

Etymology. The specific name is a noun in apposition taken from the type locality.

Distribution. Known only from the type locality.

Ischnothyreus qiuxing Tong & Li, sp. nov.

<http://zoobank.org/8B8870A1-6AD1-4C30-B8E3-616837C148B7>

Figures 7, 16E, F

Type material. Holotype ♀: MYANMAR, Kachin State, Putao, Around Ziradum Village; 27°33'465"N, 97°06'580"E; elevation ca 1051 m; 8.V.2017; Wu J. & Chen Z. leg. (IZCAS AR-25176).

Diagnosis. The new species is similar to *I. balu* Kranz-Baltensperger, 2011 in the circular atrium, but can be distinguished by the size of atrium (nearly 1/5 the length of postgastric scutum (Fig. 16E) vs more than 1/3 the length of postgastric scutum; Kranz-Baltensperger 2011: fig. 2F, H) and the greater sinuosity of the winding tube (Fig. 16F) (vs short, simple winding tube; Kranz-Baltensperger 2011: fig. 2G).

Description. Female (holotype). Body: habitus as in Fig. 7A–C; body length 2.01. **Carapace:** 0.87 long, 0.72 wide; yellow, without any pattern, ovoid in dorsal view, strongly elevated in lateral view, surface finely reticulate, fovea absent, lateral margin straight, smooth (Fig. 7D, F). **Clypeus:** height about equal to ALE radius or less (Fig. 7G). **Eyes:** six, in one group, well developed, subequal, ALE circular, PME and PLE oval, posterior eye row recurved from above, procurved from front (Fig. 7D, G). **Sternum:** as long as wide, yellow, uniform, not fused to carapace, surface smooth, setae sparse (Fig. 7E). **Mouthparts:** chelicerae, endites and labium orange; chelicerae straight, base of fangs unmodified (Fig. 7G); labium rectangular, not fused to sternum, anterior margin not indented at middle; endites unmodified (Fig. 7E). **Abdomen:** 1.35 long, 0.92 wide; dorsal scutum weakly sclerotized, very small, not fused to epigastric scutum; epigastric and postgastric scutum well sclerotized, pale orange, unfused (Fig. 7A, B). **Legs:** pale orange, femur I with two prolateral spines, tibia I with four pairs, metatarsus I with two pairs of long ventral spines. Leg II spination is similar to leg I except femur with only one prolateral spine. Legs III and IV spineless. **Epigastric area:** surface without external features (Fig. 7H). **Endogyne:** from the middle of the

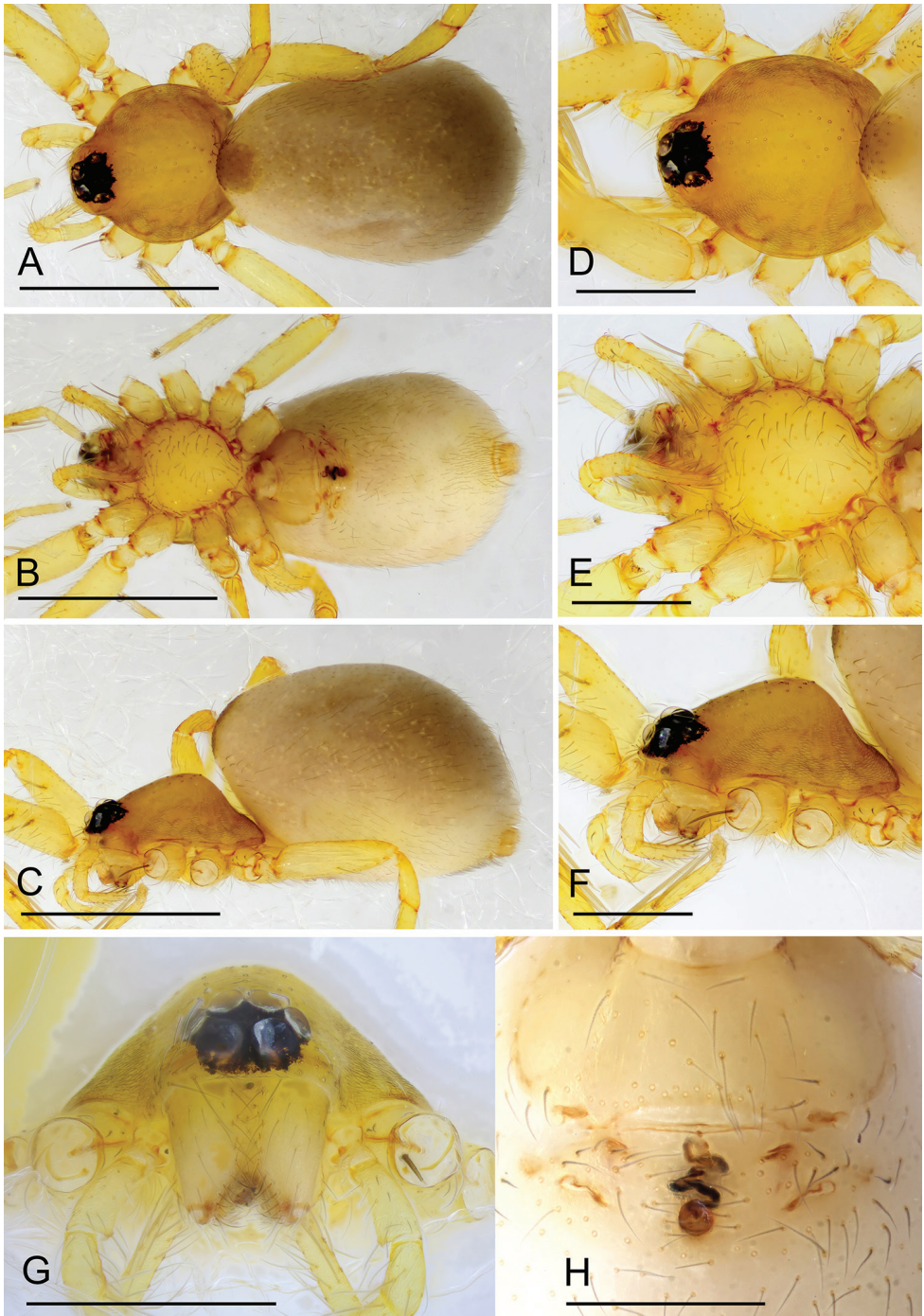


Figure 7. *Ischnothyreus qiuxing* sp. nov., female holotype **A–C** habitus, dorsal, ventral and lateral views **D–G** prosoma, dorsal, ventral, lateral and anterior views **H** epigastric region, ventral view. Scale bars: 0.4 mm (**A–C**); 0.2 mm (**D–H**).

slightly thickened margin of the postgastric scutum runs a dark, very simple winding tube posteriorly, ending in a circular atrium (Fig. 16E, F).

Male. Unknown.

Etymology. The specific name is derived from Chinese pinyin, “qixing”, which means “circular”, referring to the circular atrium; noun in apposition.

Distribution. Known only from the type locality.

***Ischnothyreus taunggyi* Tong & Li, sp. nov.**

<http://zoobank.org/E8228172-15A8-4BCB-8B68-BC87903BCBDE>

Figures 8–10, 14D–F, 15C, D, 16G, H

Type material. *Holotype* ♂: MYANMAR, Shan State, Taunggyi, East of Nyaung Shwe Township; 20°34'700"N, 96°57'450"E; elevation ca 1005 m; 30.XI.2016; Wu J. leg. (IZCAS AR-25177). *Paratypes* 2♀: same data as for holotype (IZCAS AR-25178–25179).

Diagnosis. The new species is similar to *I. zbigangi* sp. nov. in the male palp and the crown-shaped sclerotized process of male cheliceral fang, but can be distinguished by the long abdominal dorsal scutum (3/4 of the abdomen length (Fig. 8A) vs very small; Fig. 11A) and ventral scutum (4/5 of the abdomen length (Fig. 8B) vs very small; Fig. 11B) of male, and the long abdominal dorsal scutum (less than 1/2 of the abdomen length (Fig. 10A) vs very small; Fig. 13A) and the nipple-shaped atrium (Fig. 16G) (vs inverted bell-shaped atrium; Fig. 17E) of female.

Description. Male (holotype). *Body:* habitus as in Fig. 8A–C; body length 1.71. *Carapace:* 0.84 long, 0.63 wide; pale brown, with egg-shaped patches behind eyes, ovoid in dorsal view, strongly elevated in lateral view, surface of elevated portion of pars cephalica smooth, sides finely reticulate, fovea absent, lateral margin straight, smooth (Fig. 8D). *Clypeus:* height about equal to ALE radius or more. *Eyes:* six, in one group, well developed, ALE largest, ALE circular, PME and PLE oval, posterior eye row recurved from above, procurved from front (Fig. 8D). *Sternum:* as long as wide, pale orange, uniform, not fused to carapace, surface smooth, setae sparse (Fig. 8E). *Mouthparts:* chelicerae, endites and labium orange; chelicerae straight, with crown-shaped sclerotized process at base of fangs, fang groove with a few small and one larger denticles (Fig. 15C, D); labium rectangular, not fused to sternum, anterior margin not indented at middle; anteromedian tip of endites with one strong, tooth-like projection (Fig. 8E). *Abdomen:* 0.74 long, 0.49 wide; dorsal scutum well sclerotized, pale orange, covering 2/3 the abdomen width and approximately 3/4 of the abdomen length, unfused to epigastric scutum; epigastric and postgastric scutum well sclerotized, pale orange, fused, postgastric scutum covering about 4/5 of the abdomen length (Fig. 8A, B). *Legs:* pale orange, femur I with three prolateral and one small retrolateral spines, tibia I with four pairs, metatarsus I with two pairs of long ventral spines. Leg II spination is similar to leg I except femur with only two prolateral spines. Legs III and IV spineless. *Palp:* strongly sclerotized, trochanter with ventral projection, cymbium brown, fused with bulb; bulb brown, with two large ventral protuberances, distal end of bulb

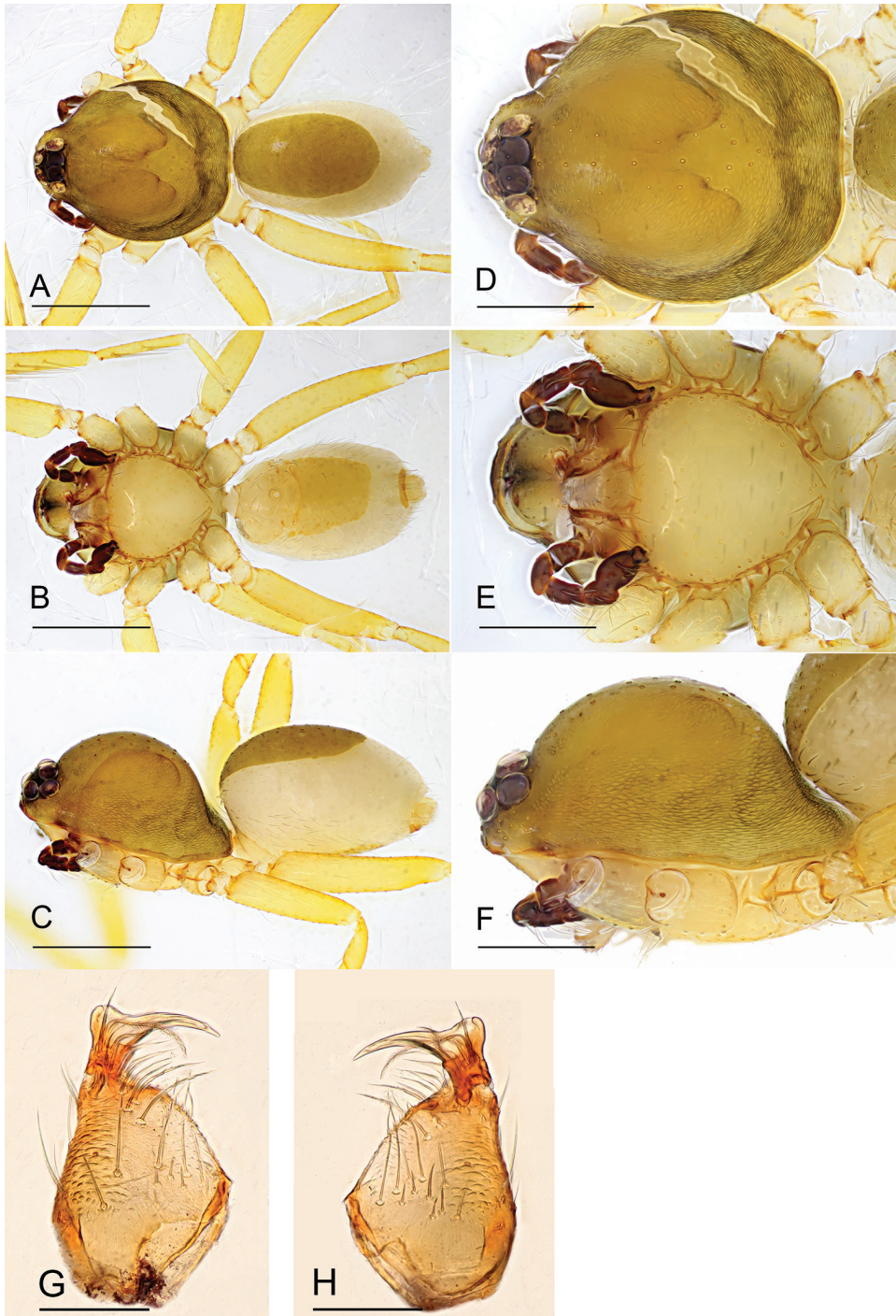


Figure 8. *Ischnothyreus taunggyi* sp. nov., male holotype **A–C** habitus, dorsal, ventral and lateral views **D–F** prosoma, dorsal, ventral and lateral views **G, H** left chelicerae, anterior and posterior views. Scale bars: 0.4 mm (**A–C**); 0.2 mm (**D–F**); 0.1 mm (**G, H**).

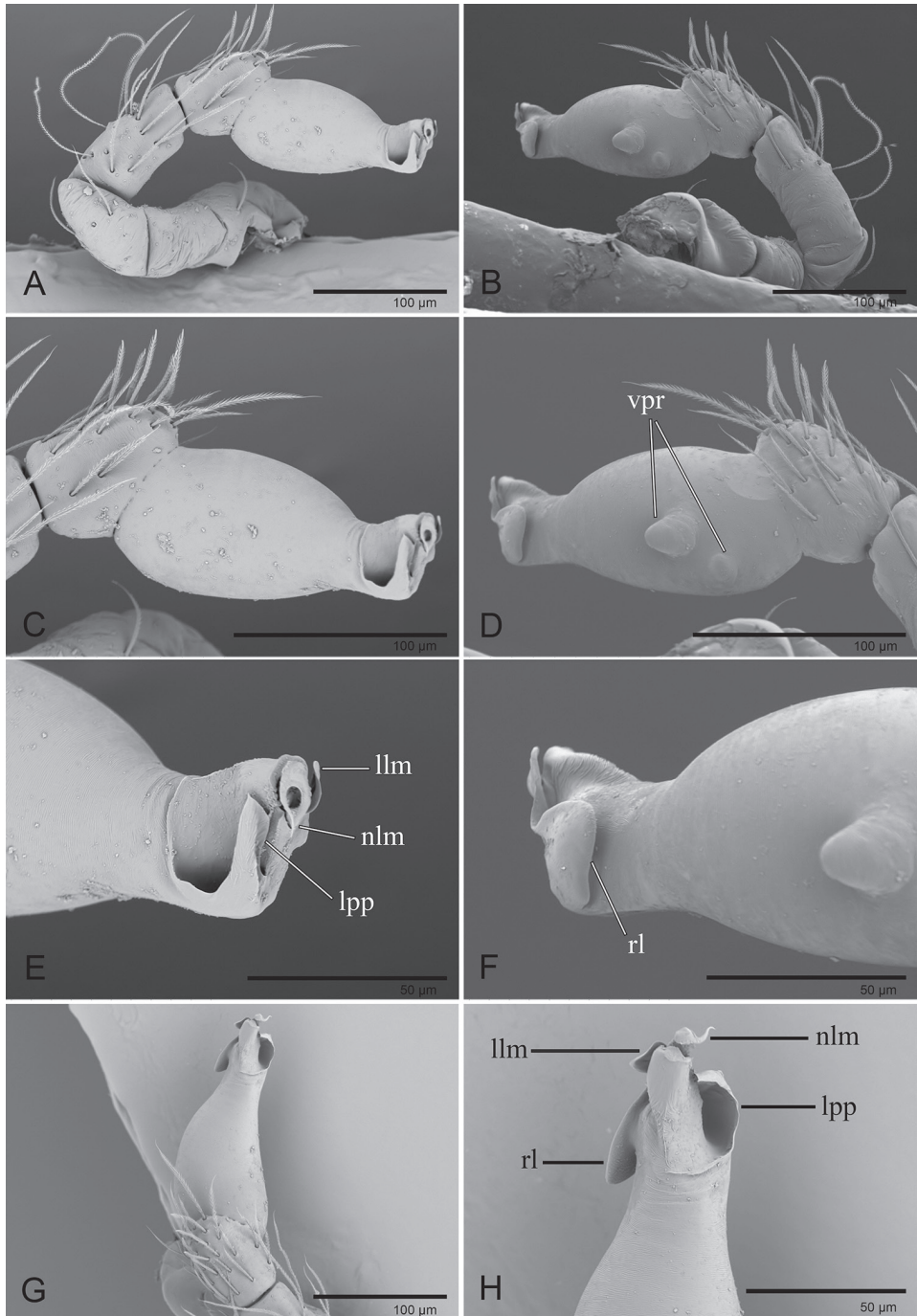


Figure 9. *Ischnothyreus taunggyi* sp. nov., male holotype, left palp, SEM **A, B** prolateral and retrolateral views **C, D, G** palpal bulb, prolateral, retrolateral and dorsal views **E, F, H** distal part of palpal bulb, prolateral, retrolateral and dorsal views. Abbreviations: nlm = needle like membrane; llm = leaf like membrane; lpp = leaf-shaped prolateral projection; rl = retrolateral lobe; vpr = ventral protuberance.

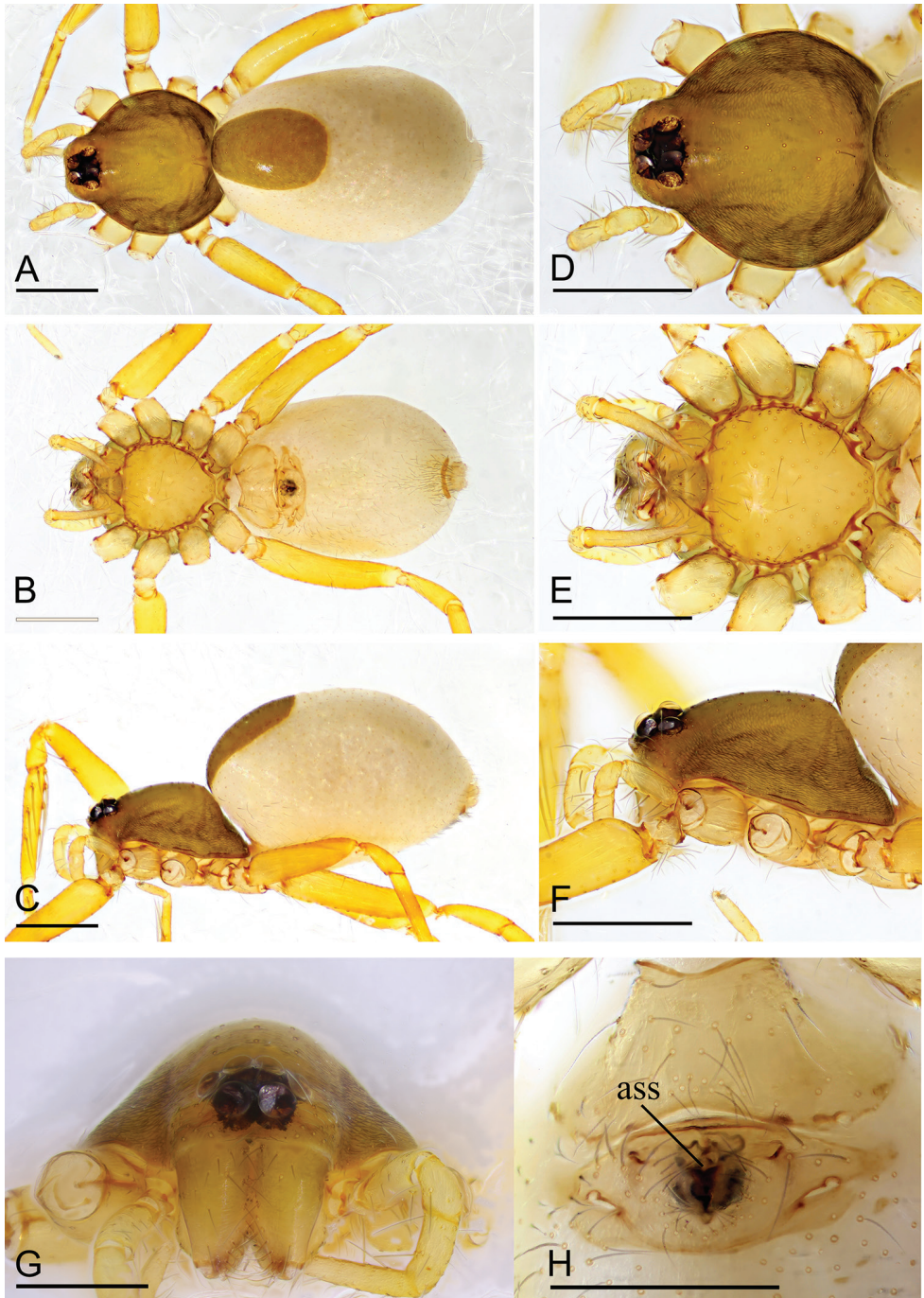


Figure 10. *Ischnothyreus taunggyi* sp. nov., female paratype **A–C** habitus, dorsal, ventral and lateral views **D–F, G** prosoma, dorsal, ventral, lateral and anterior views **H** epigastric region, ventral view. Abbreviation: ass = anchor-shaped structure. Scale bars: 0.4 mm (**A–F**); 0.2 mm (**G, H**).

elongated, with one leaf-shaped prolateral projection and distal needle like membrane, retrolateral lobe broad, ear-shaped (Figs 9, 14D–F).

Female (paratype, IZCAS AR-25178). Same as male except as noted. **Body:** habitus as in Fig. 10A–C; body length 1.98. **Carapace:** 0.83 long, 0.71 wide; without any pattern (Fig. 10D). **Mouthparts:** chelicerae and endites unmodified (Fig. 10E, G). **Abdomen:** 1.27 long, 0.83 wide; dorsal scutum covering less than 1/2 of the abdomen length, about 1/3 of the abdomen width (Fig. 10A). **Epigastric area:** the postgastric scutum with central anchor-shaped structure (Fig. 10H). **Endogyne:** from the middle of the slightly thickened margin of the postgastric scutum runs a dark, very complex winding tube posteriorly, ending in a small, bell-shaped atrium (Fig. 16G, H).

Etymology. The specific name is a noun in apposition taken from the type locality.

Distribution. Known only from the type locality.

Ischnothyreus zhigangi Tong & Li, sp. nov.

<http://zoobank.org/CB6C29F2-AC7C-4511-8F20-7771D82CB329>

Figures 11–13, 14G–I, 15E, F, 17E, F

Type material. **Holotype** ♂: MYANMAR, Putao, Hponkanrazi Wildlife Sanctuary Around Camp 2; 27°36'681"N, 96°58'958"E; elevation ca 2457 m; 11.V.2017; Wu J. & Chen Z. leg. (IZCAS AR-25178). **Paratypes** 4♀: data same as for holotype; 27°31'103"N, 96°57'694"E; elevation ca 2737 m; 16.V.2017; Wu J. & Chen Z. leg. (IZCAS AR-25179–25182).

Diagnosis. The new species is similar to *I. taunggyi* sp. nov. but can be distinguished by the short abdominal dorsal scutum (very small (Fig. 11A) vs 3/4 of the abdomen length; Fig. 8A) and ventral scutum (very small (Fig. 11B) vs 4/5 of the abdomen length; Fig. 8B) of male, and the short abdominal dorsal scutum (very small (Fig. 13A) vs less than 1/2 of the abdomen length; Fig. 10A) and the inverted bell-shaped atrium (Fig. 17E) (vs nipple-shaped atrium (Fig. 16G) of female).

Description. Male (holotype). **Body:** habitus as in Fig. 11A–C; body length 2.08. **Carapace:** 1.03 long, 0.87 wide; pale brown, with egg-shaped patches behind eyes, ovoid in dorsal view, strongly elevated in lateral view, surface of elevated portion of pars cephalica smooth, sides finely reticulate, fovea absent, lateral margin straight, smooth (Fig. 11D). **Clypeus:** height about equal to ALE radius or more. **Eyes:** six, in one group, well developed, subequal, ALE circular, PME and PLE oval, posterior eye row straight from above, procurved from front (Fig. 11D). **Sternum:** as long as wide, pale brown, uniform, not fused to carapace, surface smooth, setae sparse (Fig. 11E). **Mouthparts:** chelicerae, endites and labium orange; chelicerae straight, base of fangs with crown-shaped sclerotized process with serrated exterior margin (Figs 11G, H, 15E, F), fang groove with a few small denticles; labium rectangular, not fused to sternum, anterior margin not indented at middle; anteromedian tip of endites with one strong, tooth-like projection (Fig. 11E). **Abdomen:** 1.07 long, 0.72 wide; dorsal scutum weakly sclerotized, pale orange, very small, not fused to epigastric scutum; epigastric and

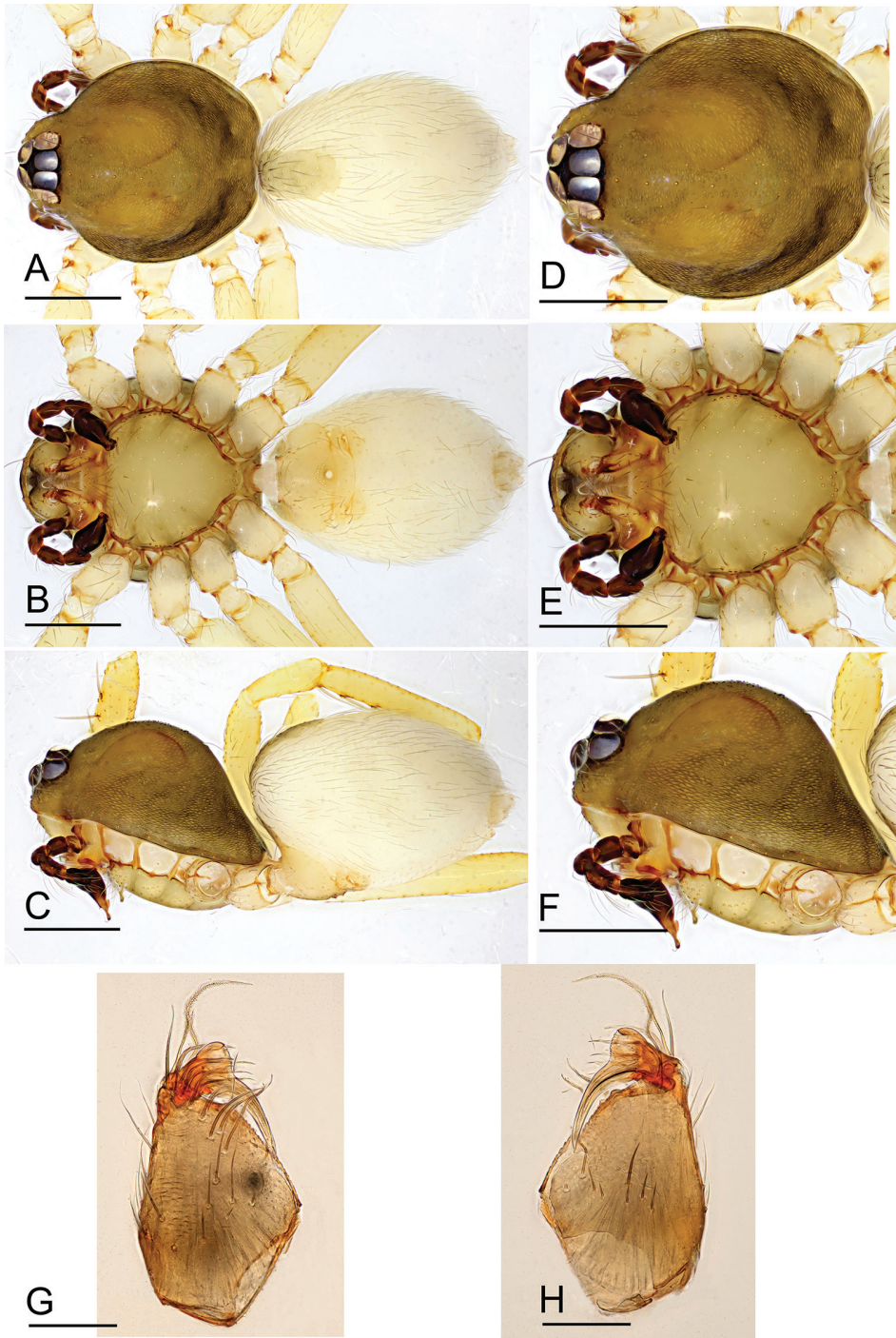


Figure 11. *Ischnothyreus zbigangi* sp. nov., male holotype **A–C** habitus, dorsal, ventral and lateral views **D–F** prosoma, dorsal, ventral and lateral views **G, H** left chelicerae, anterior and posterior views. Scale bars: 0.4 mm (**A–F**); 0.1 mm (**G, H**).

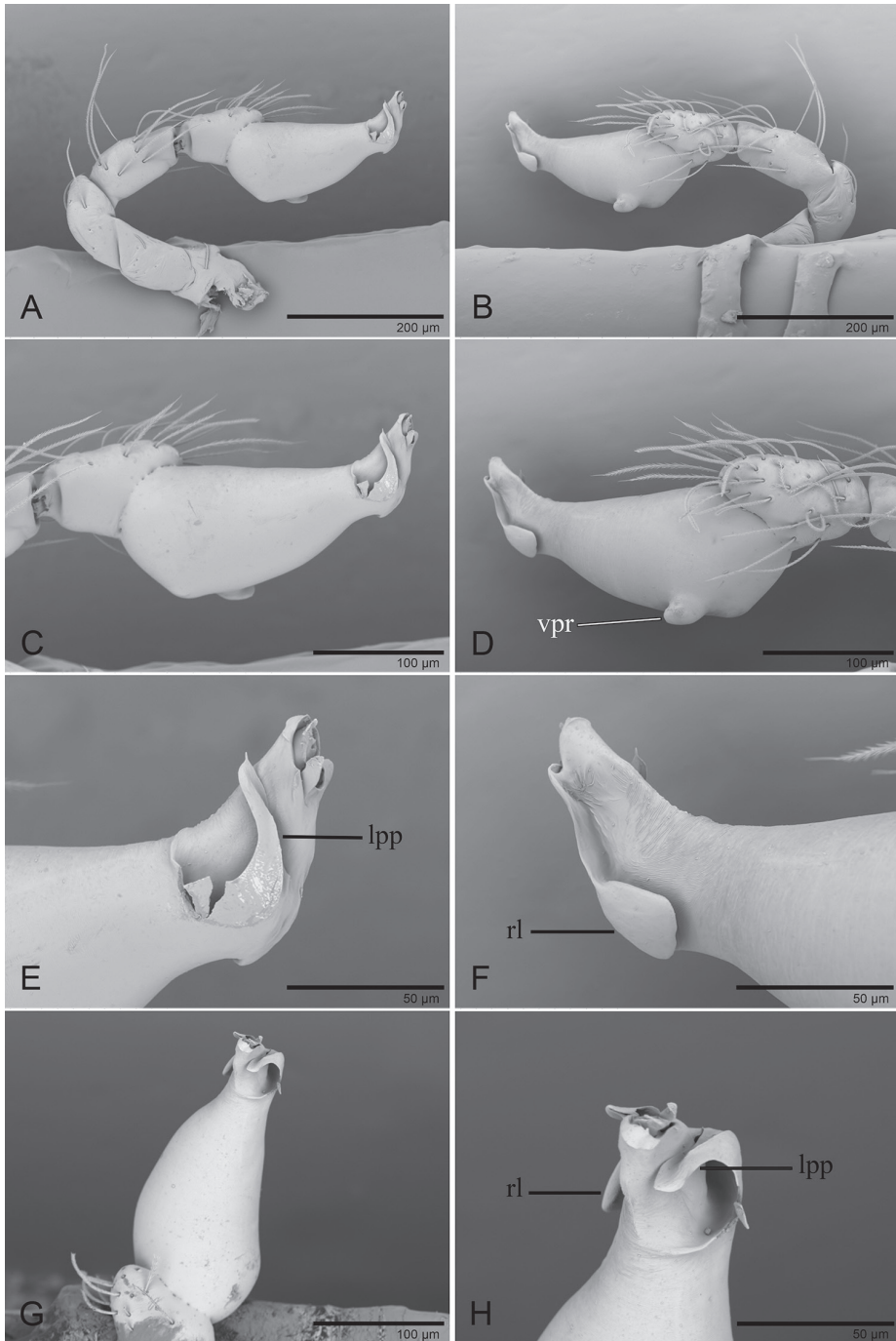


Figure 12. *Ischnothyreus zbigangi* sp. nov., male holotype, left palp, SEM **A, B** prolateral and retrolateral views **C, D, G** palpal bulb, prolateral, retrolateral and dorsal views **E, F, H** distal part of palpal bulb, prolateral, retrolateral and dorsal views. Abbreviations: lpp = leaf-shaped prolateral projection; rl = retrolateral lobe; vpr = ventral protuberance.

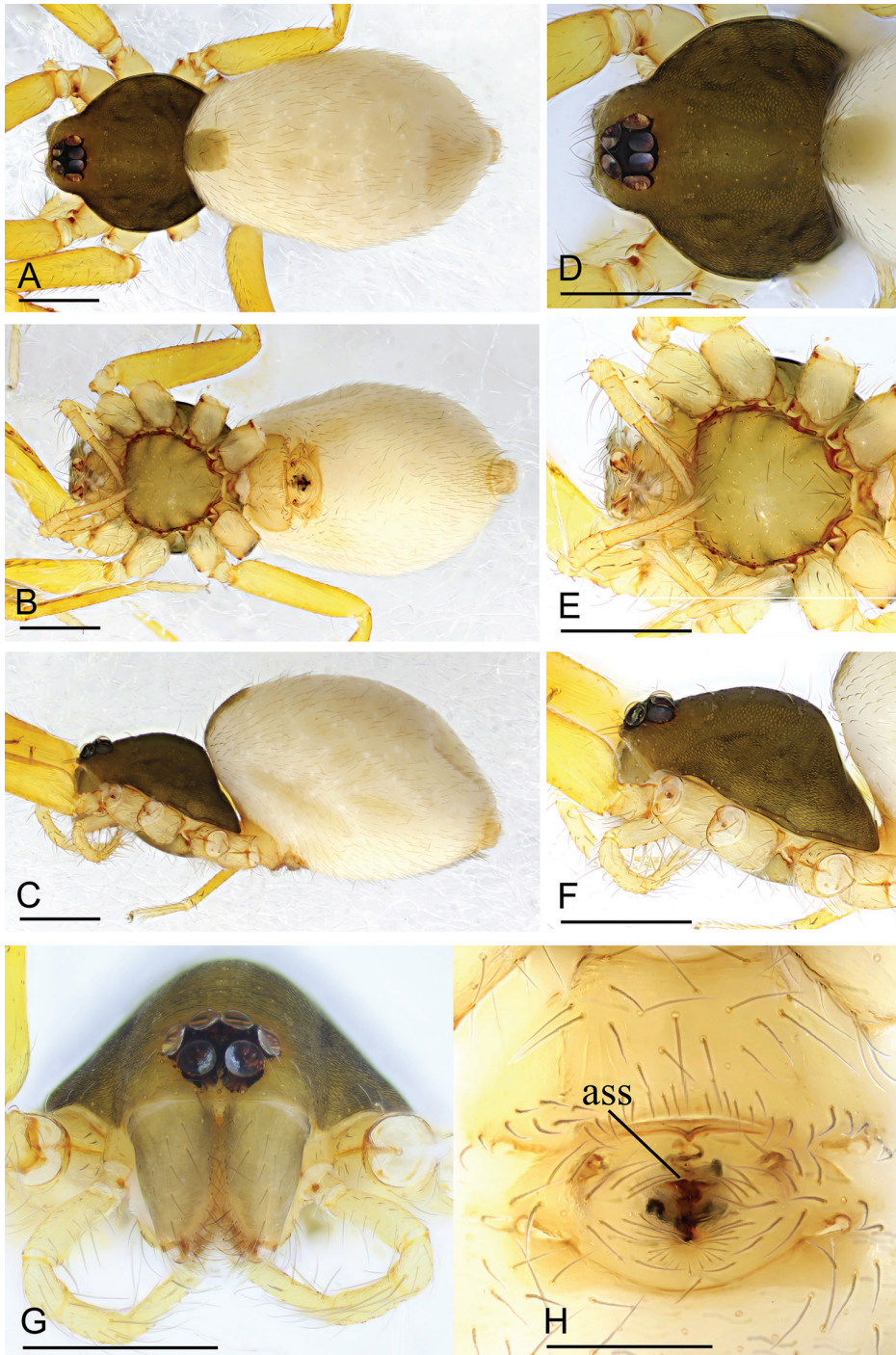


Figure 13. *Ischnothyreus zbigangi* sp. nov., female paratype **A–C** habitus, dorsal, ventral and lateral views **D–G** prosoma, dorsal, ventral, lateral and anterior views **H** epigastric region, ventral view. Abbreviation: ass = anchor-shaped structure. Scale bars: 0.4 mm (**A–G**); 0.1 mm (**H**).

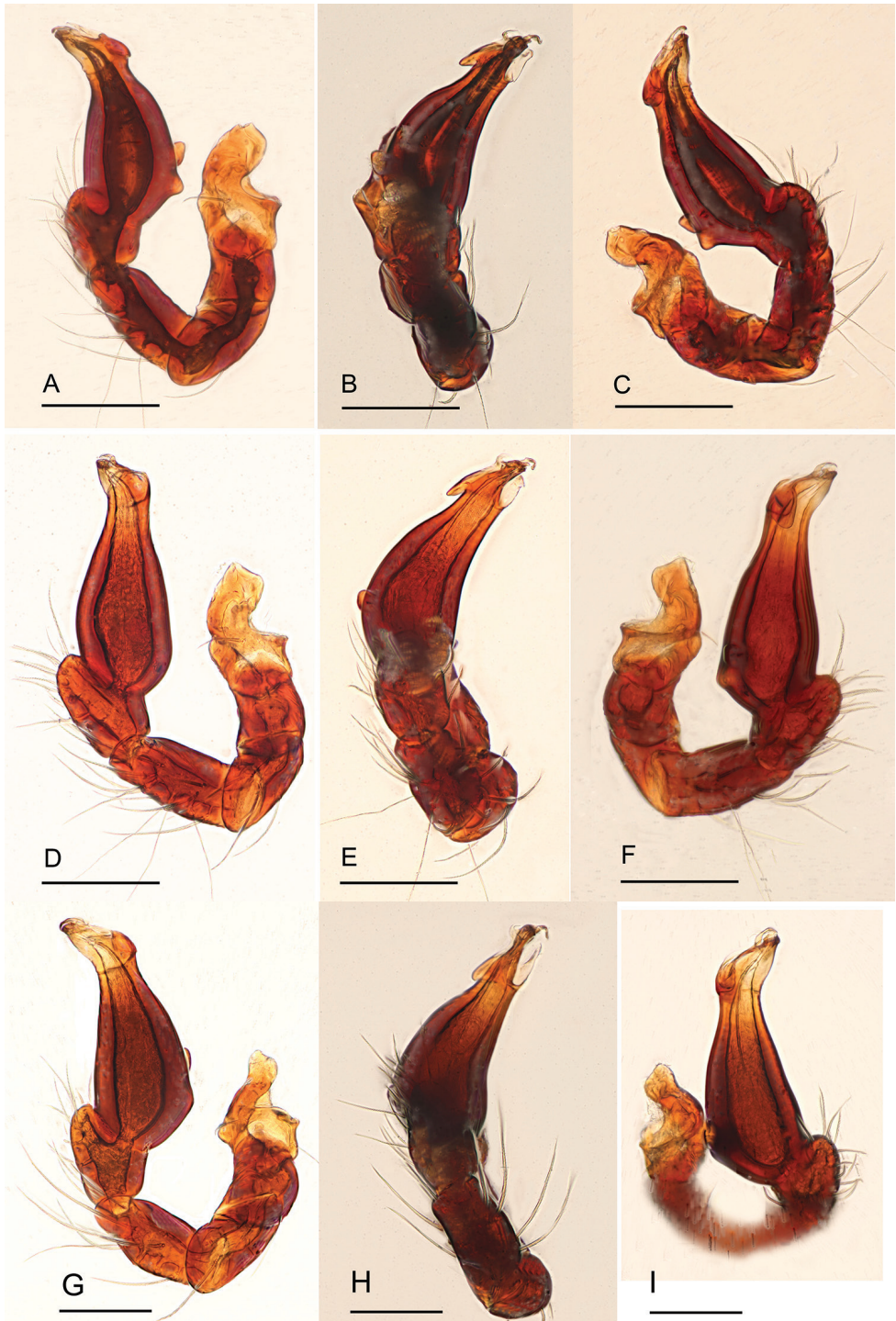


Figure 14. *Ischnothyreus* spp., left male palp **A–C** *I. meukyawwa* sp. nov. **D–F** *I. taunggyi* sp. nov. **G–I** *I. zbigangi* sp. nov. **A, D, G** prolateral view **B, E, H** dorsal view **C, F, I** retrolateral view. Scale bars: 0.1 mm.

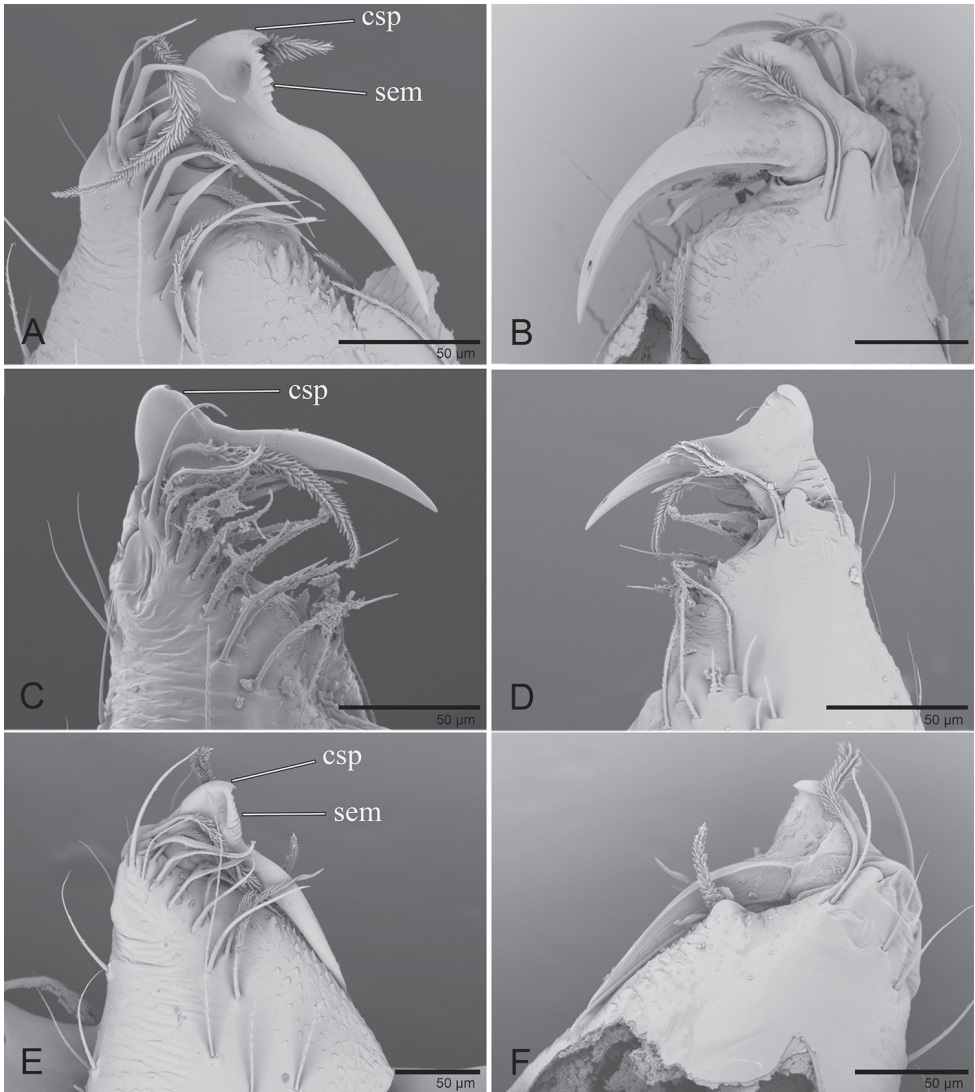


Figure 15. *Ischnothyreus* spp., left male chelicerae. **A, B** *I. meukyauwa* sp. nov. **C, D** *I. taunggyi* sp. nov. **E, F** *I. zbigangi* sp. nov. **A, C, E** anterior view **B, D, F** posterior view. Abbreviations: csp = crown-shaped sclerotized process; sem = serrated exterior margin.

postgastric scutum weakly sclerotized, pale orange, fused, postgastric scutum very small (Fig. 11A, B). **Legs:** pale orange, femur I with three prolateral spines, tibia I with four pairs, metatarsus I with two pairs of long ventral spines. Leg II spination is similar to leg I except femur with only two prolateral spines. Legs III and IV spineless. **Palp:** strongly sclerotized, trochanter with ventral projection, cymbium brown, fused with bulb; bulb brown, with one large ventral protuberance, distal end of bulb elongated, with one narrow leaf-shaped prolateral projection, retrolateral lobe small, simple (Figs 12, 14G–H).

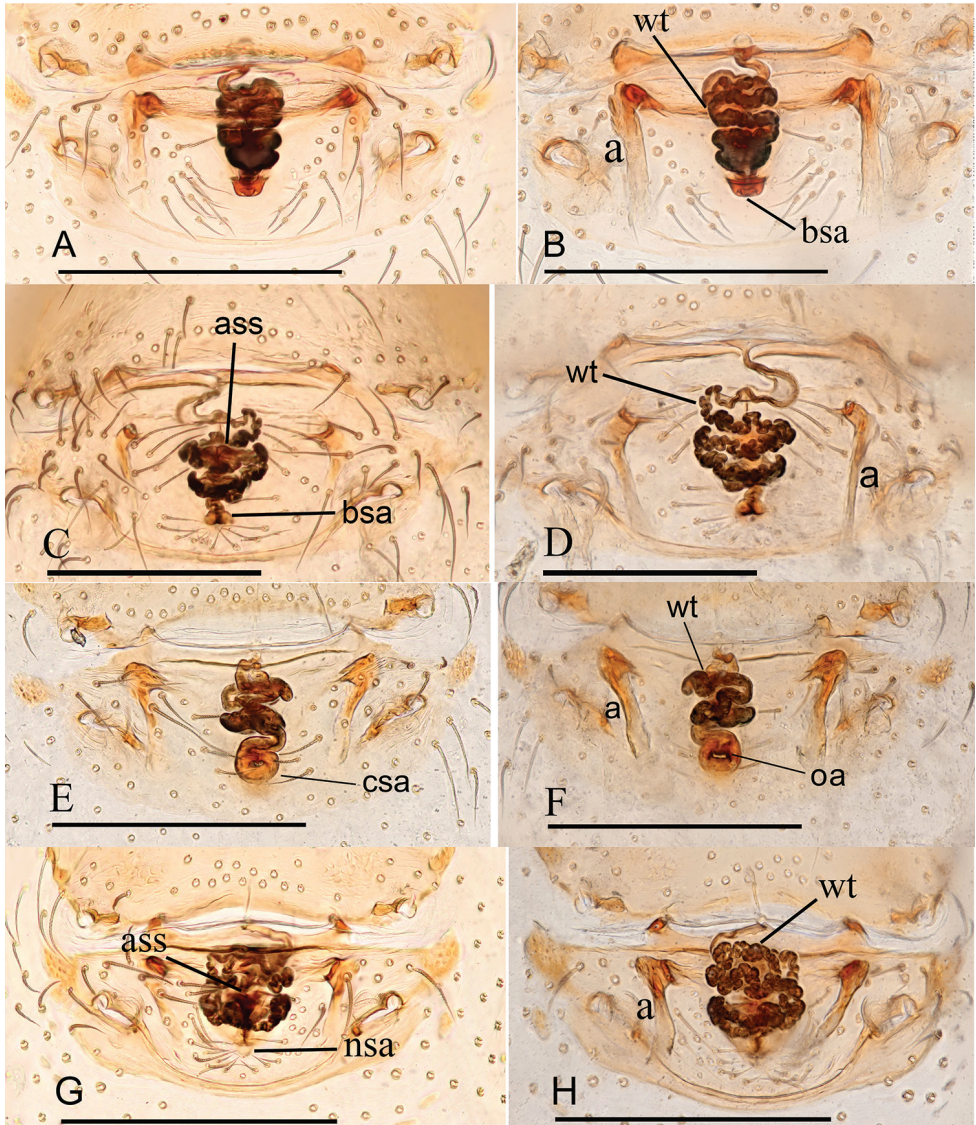


Figure 16. *Ischnothyreus* spp., female copulatory organ **A, B** *I. hponkanrazi* sp. nov. **C, D** *I. meukyawwa* sp. nov. **E, F** *I. qiuxing* sp. nov. **G, H** *I. taunggyi* sp. nov. **A, C, E, G** ventral view **B, D, F, H** dorsal view. Abbreviations: a = apodemes; ass = anchor-shaped structure; bsa = bell-shaped atrium; csa = circular atrium; nsa = nipple-shaped atrium; oa = opening of the atrium; wt = winding tube. Scale bars: 0.2 mm.

Female (paratype, IZCAS AR-25179). Same as male except as noted. **Body:** habitus as in Fig. 13A–C; body length 2.63. **Carapace:** 1.10 long, 0.95 wide; without any pattern, posterior eye row procurved from both above and front (Fig. 13D, G). **Mouthparts:** chelicerae and endites unmodified (Fig. 13E, G). **Abdomen:** 1.82 long, 1.19 wide. **Epigastric area:** the postgastric scutum with central anchor-shaped structure (Fig. 13H). **Endogyne:** from the middle of the slightly thickened margin of the

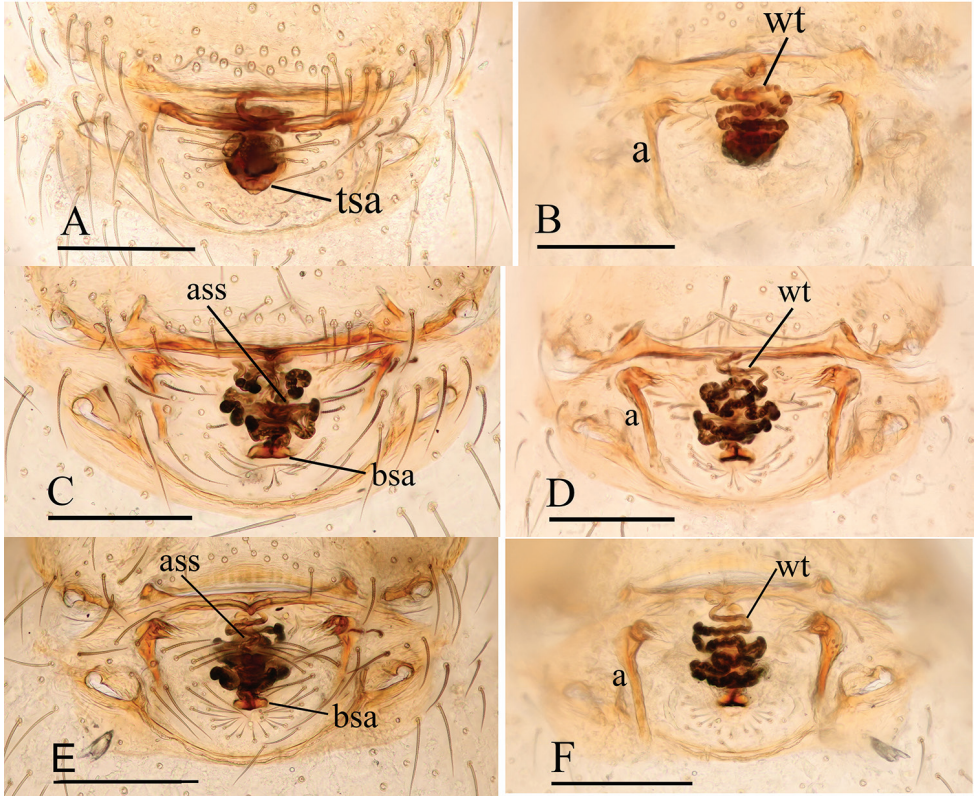


Figure 17. *Ischnothyreus* spp., female copulatory organ **A, B** *I. jianglangi* sp. nov. **C, D** *I. putao* sp. nov. **E, F** *I. zbigangi* sp. nov. **A, C, E** ventral view **B, D, F** dorsal view. Abbreviations: a = apodemes; ass = anchor-shaped structure; bsa = bell-shaped atrium; tsa = triangular shaped atrium; wt = winding tube. Scale bars: 0.1 mm

postgastric scutum runs a dark, simple winding tube posteriorly, ending in a small, inverted bell-shaped atrium (Fig. 17E, F).

Etymology. The species is named after Mr Zhigang Chen, one of the collectors of the holotype; noun in genitive case.

Distribution. Known only from the type locality.

Acknowledgements

The manuscript benefited greatly from constructive comments by Ingi Agnarsson, Antonio Domingos Brescovit, Lily Berniker, and Nadine Dupérré. This study was supported by the National Natural Science Foundation of China (31750002, 31972867) and the Program for Liaoning Innovation Talents in University to Yanfeng Tong, and by the National Natural Science Foundation of China (NSFC-31530067), and the Southeast Asia Biodiversity Research Institute, Chinese Academy of Sciences (2015CASEABRI005, Y4ZK111B01) to Shuqiang Li.

References

- Brescovit AD, Bonaldo AB, Ott R, Chavari JL (2019) To boldly go: on invasive goblin spiders in Brazil (Araneae, Oonopidae). *Iheringia, Série Zoologia* 109: e2019033. <https://doi.org/10.1590/1678-4766e2019033>
- Kranz-Baltensperger Y (2011) The oonopid spider genus *Ischnothyreus* in Borneo (Oonopidae, Araneae). *Zootaxa* 2939: 1–49. <https://doi.org/10.11646/zootaxa.2939.1.1>
- Li S (2020) Spider taxonomy for an advanced China. *Zoological Systematics* 45(2): 73–77.
- Platnick NI, Berniker L, Kranz-Baltensperger Y (2012) The goblin spider genus *Ischnothyreus* (Araneae, Oonopidae) in the New World. *American Museum Novitates* 3759: 1–32. <https://doi.org/10.1206/3759.2>
- Richard M, Graber W, Kropf C (2016) The goblin spider genus *Ischnothyreus* (Araneae, Oonopidae) in Java and Sumatra. *Zootaxa* 4151(1): 1–99. <https://doi.org/10.11646/zootaxa.4151.1.1>
- Simon E (1893) *Histoire naturelle des araignées*. Deuxième édition, tome premier. Roret, Paris, 257–488. <https://doi.org/10.5962/bhl.title.51973>
- Tong Y, Li S (2008) The oonopid spiders (Araneae: Oonopidae) from Hainan Island, China. *Raffles Bulletin of Zoology* 56: 55–66.
- Tong Y (2013) *Haplogynae Spiders from Hainan, China*. Science Press, Beijing, 96 pp. [81 pls]
- Tong Y, Koh JKH, Tong X, Li S (2016) Five new species of the genus *Ischnothyreus* Simon, 1893 from Singapore. *ZooKeys* 618: 39–66. <https://doi.org/10.3897/zookeys.618.9451>
- WSC (2020) *World Spider Catalog, version 21.5*. Natural History Museum Bern. <http://wsc.nmbe.ch> [Accessed on: 2020.08.12]

A new species of *Trachelas* L. Koch, 1872 (Araneae, Trachelidae) from Tajikistan

Yuri M. Marusik^{1,2,3}, Alexander A. Fomichev⁴

1 Institute for Biological Problems of the North RAS, Portovaya Str. 18, Magadan 685000, Russia **2** Department of Zoology and Entomology, University of the Free State, Bloemfontein 9300, South Africa **3** Zoological Museum, Biodiversity Unit, University of Turku, FI-20014, Finland **4** Altai State University, Lenina Prospect, 61, Barnaul, RF-656049, Russia

Corresponding author: Yuri M. Marusik (yurmar@mail.ru)

Academic editor: S. Li | Received 22 October 2020 | Accepted 31 October 2020 | Published 16 November 2020

<http://zoobank.org/72AB7A43-5D29-44A4-BAFB-58ACB1207D55>

Citation: Marusik YM, Fomichev AA (2020) A new species of *Trachelas* L. Koch, 1872 (Araneae, Trachelidae) from Tajikistan. ZooKeys 993: 27–34. <https://doi.org/10.3897/zookeys.993.59932>

Abstract

A new species of trachelid spiders, *Trachelas crewsae* **sp. nov.** is described from south-western Tajikistan based on both sexes. The new species is closely related to *T. vulcani* Simon, 1896 from South-East Asia but differs in the conformation of the copulatory organs and color pattern.

Keywords

Aranei, Central Asia, taxonomy, trachelids

Introduction

Trachelidae Simon, 1897 is a small spider group recently elevated to the family-level, consisting of 246 species in 19 genera (Ramírez 2014; WSC 2020). *Trachelas* L. Koch, 1872 is the most speciose genus of the family, accounting for 89 valid species distributed worldwide except for polar regions, Australia and New Zealand, with most of the species being known from the Americas (Platnick and Shadab 1974a, b; WSC 2020). The genus is well studied in the Palearctic and Indomalayan regions thanks to several revisions dealing with the Mediterranean, Russian and south Chinese species (Bos-selaers et al. 2009; Zhang et al. 2009; Marusik and Kovblyuk 2010; Jin et al. 2017).

To date, only a single *Trachelas* species – *T. minor* O. Pickard-Cambridge, 1872, one of the most widespread species of the family – is known from Central Asia: viz., from Turkmenistan and Uzbekistan (Mikhailov 2013). While examining spiders recently collected by the senior author from Tajikistan, we found *Trachelas* specimens that belong to an undescribed species similar to the Indomalayan *T. vulcani* Simon, 1896. The goal of this paper is to provide a detailed description and diagnosis of this new species.

Material and methods

Specimens were photographed using a Canon EOS 7D camera attached to an Olympus SZX16 stereomicroscope and a SEM JEOL JSM-5200 scanning electron microscope at the Zoological Museum, University of Turku, Finland. Photographs were taken in a dish filled with alcohol, with cotton at the bottom. The epigyne was macerated in a KOH/water solution until the soft tissues were dissolved. Digital images were prepared using Helicon Focus software (<https://www.photo-soft.ru/helicon-focus/>). All measurements are in millimeters. Length of leg segments were measured on their dorsal sides. Leg measurements are shown as: femur, patella, tibia, metatarsus, tarsus (total length). The terminology follows Jin et al. (2017), with some modifications. The types will be deposited in the Zoological Museum of the Moscow State University, Russia (ZMMU; curator: K.G. Mikhailov).

Taxonomy

Family Trachelidae Simon, 1897

Genus *Trachelas* L. Koch, 1872

***Trachelas crewsae* sp. nov.**

<http://zoobank.org/9FBFFDD9-4C50-420B-ADA2-D85CB1E5CF97>

Figs 1, 2, 3A–F, 4B, 5

Type material. Holotype: ♂ (ZMMU), TAJIKISTAN: Khatlon Region; Tigrovaya Balka Reserve; 37°21'20.6"N, 68°28'12.4"E; tugai (gallery) forest with thick litter; 06.05.2015 (Y.M. Marusik). **Paratype:** 1 ♀ (ZMMU) together with the holotype.

Diagnosis. The male of the new species resembles those of *T. vulcani* in having a similar long, coiled embolus and long, apically oriented patellar apophysis (*Pa*) but can be distinguished from it by having a distinct abdominal scutum occupying 2/3 of the abdomen length (vs. absent) (cf. Figs 1A, B and 4A), the patellar apophysis (*Pa*) with almost parallel edges (vs. triangular), the ♂-shaped sperm duct (*Sd*) (vs. J-shaped) and the haematodocha (*Hd*) being almost as wide as the tegulum in ventral view (vs. significantly narrower) (cf. Figs 2B–D, F, 3B and 4D). Males of both species are also distinguishable in the relative length/width ratio of the palpal femur (as

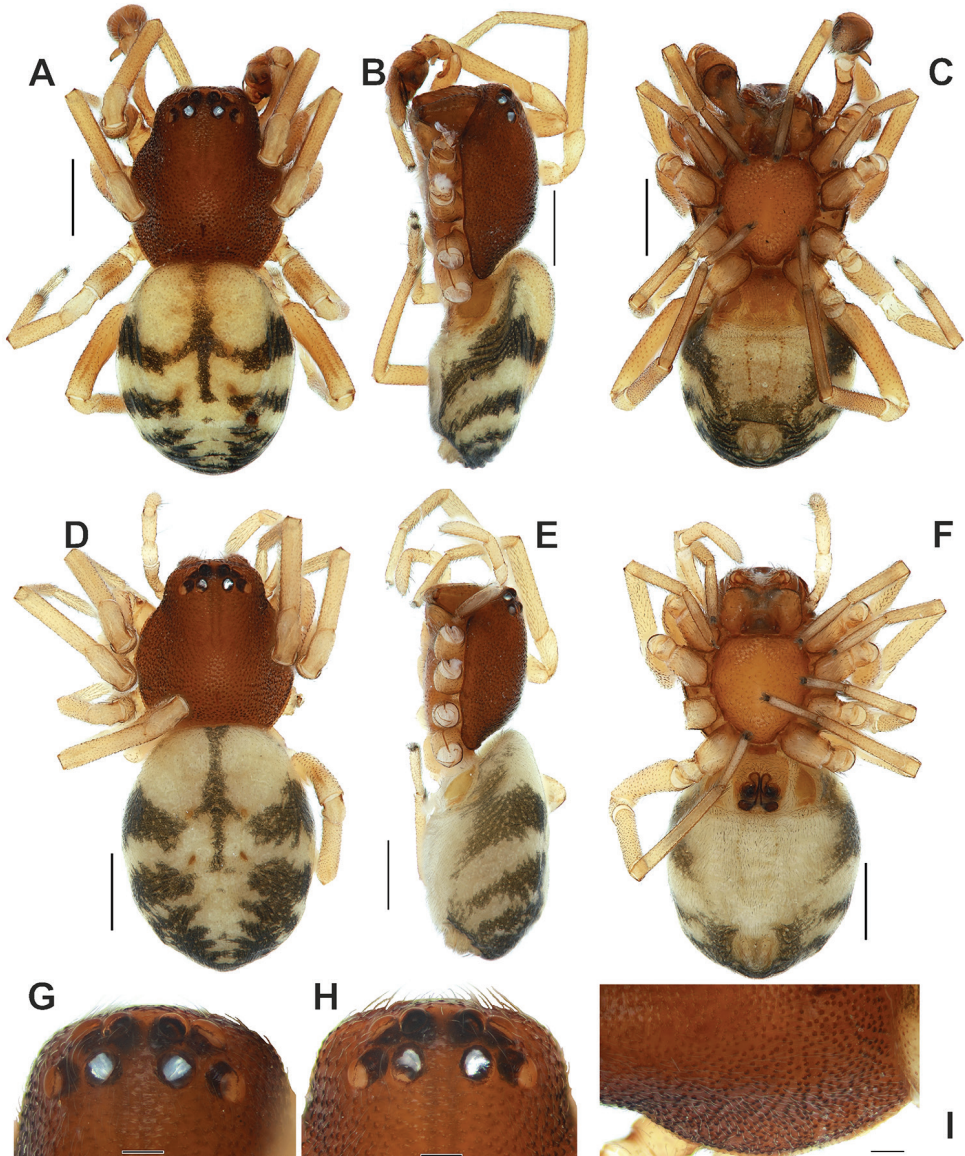


Figure 1. *Trachelas crewsae* sp. nov.: **A–C, G, I** male **D–F, H** female **A–F** habitus, dorsal, lateral and ventral **G–H** cephalic part, dorsal **I** carapace left side. Scale bars: 0.5 mm (**A–F**), 0.1 mm (**G–I**).

long as cymbium in the new species vs. shorter than cymbium) (cf. Fig. 4B, C), and the much longer embolus with its base situated postero-retrolaterally vs. antero-prolaterally. The female of *T. crewsae* sp. nov. also resembles that of *T. vulcani* in having copulatory ducts packed in several coils and primary receptacles (*Pr*), consisting of two subunits, but can be separated from the latter by the copulatory openings (*Co*) situated laterally (vs. anteriorly) (cf. Fig. 3D, G), the copulatory ducts (*Cd*) packed

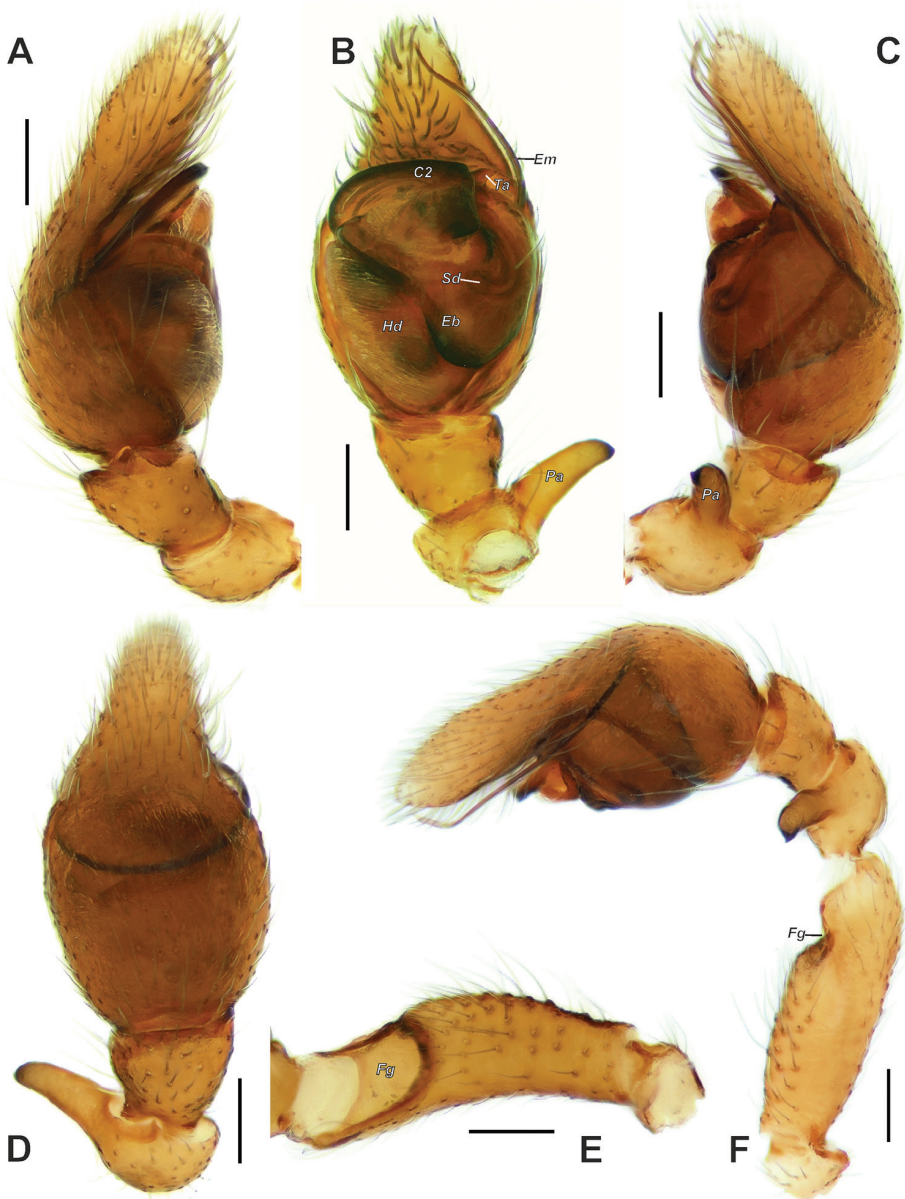


Figure 2. Male palp of *Trachelas crewsae* sp. nov.: **A–D** terminal part, prolateral, ventral, retrolateral, dorsal **F** whole palp, retrolateral **E** femur, ventral. Abbreviations: *C2* coil 2, *Hd* haematodocha, *Eb* embolic base, *Em* embolus, *Fg* femoral groove, *Pa* patellar apophysis, *Sd* sperm duct, *Ta* tegular apophysis. Scale bars: 0.1 mm.

in four tight coils (vs. three loose coils) and the secondary receptacles (*Sr*) directed posteriad (vs. anteriolaterad) (cf. Fig. 3E, F, H). Both sexes of *T. crewsae* sp. nov. differ reliably from those of *T. vulcani* in having an abdominal colour pattern formed by transverse dark grey stripes (cf. Figs 1A–F, 4A).

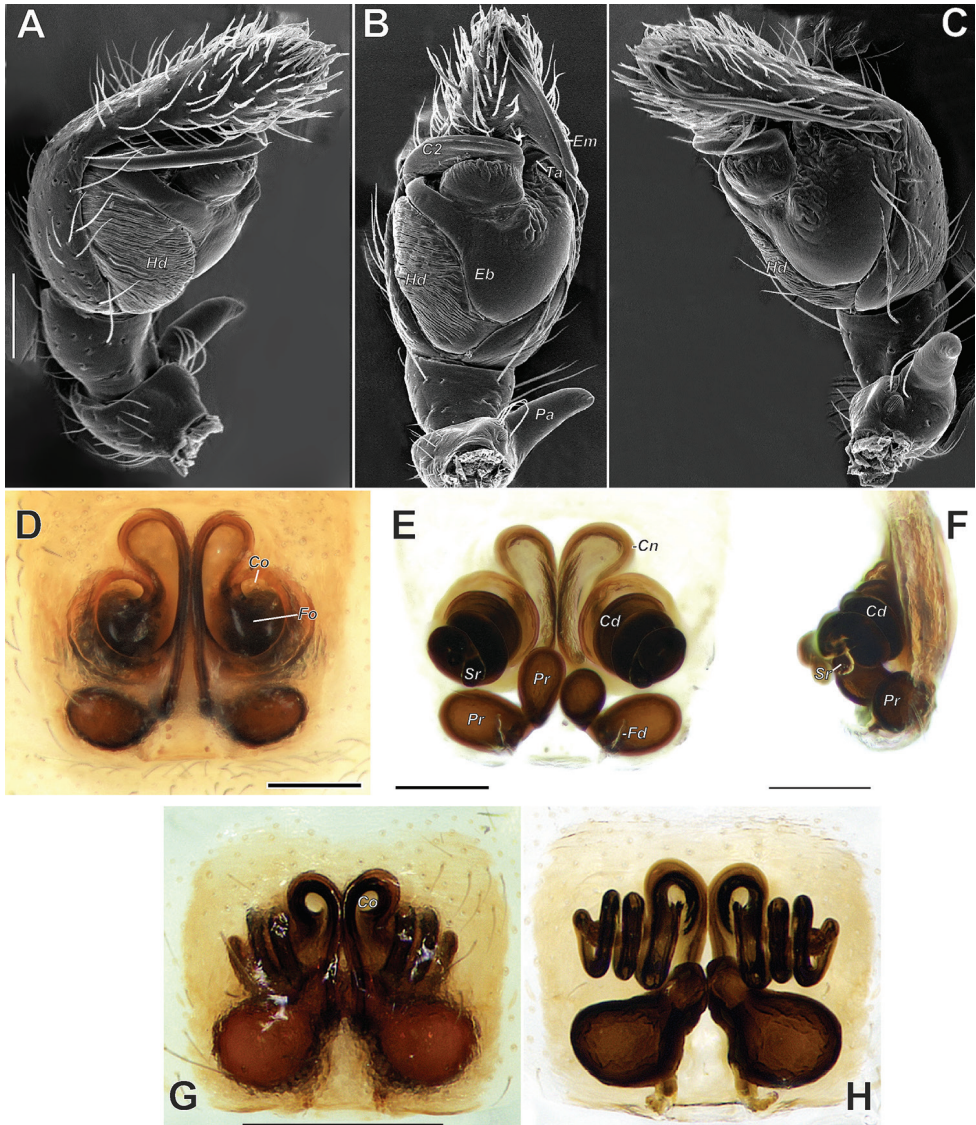


Figure 3. Male palp (**A–C**) and epigyne (**D–H**) of *Trachelas crewsae* sp. nov. (**A–F**) and *T. vulcani* (**G–H**) **A** prolateral **B, D, G** ventral **C** retrolateral **E, H** dorsal **F** lateral. Abbreviations: C2 coil 2, Cd copulatory duct, Cn connecting duct, Co copulatory opening, Hd haematodocha, Eb embolic base, Em embolus, Fd fertilization duct, Fo fovea, Pa patellar apophysis, Pr primary receptacle, Sr secondary receptacle, Ta tegular apophysis. Scale bars: 0.1 mm.

Description. Male (holotype). Total length 2.55. Carapace: 1.27 long, 1.07 wide. Carapace dark brown, granulated. Chelicerae and labium brown. Sternum yellow-orange. Maxillae light brown. Palps and legs yellow. Abdomen yellow-beige, with elongate scutum occupying 2/3 of abdomen; with dark grey dorsal pattern formed by transverse stripes; venter with epigastral scutum occupying whole ventral surface;

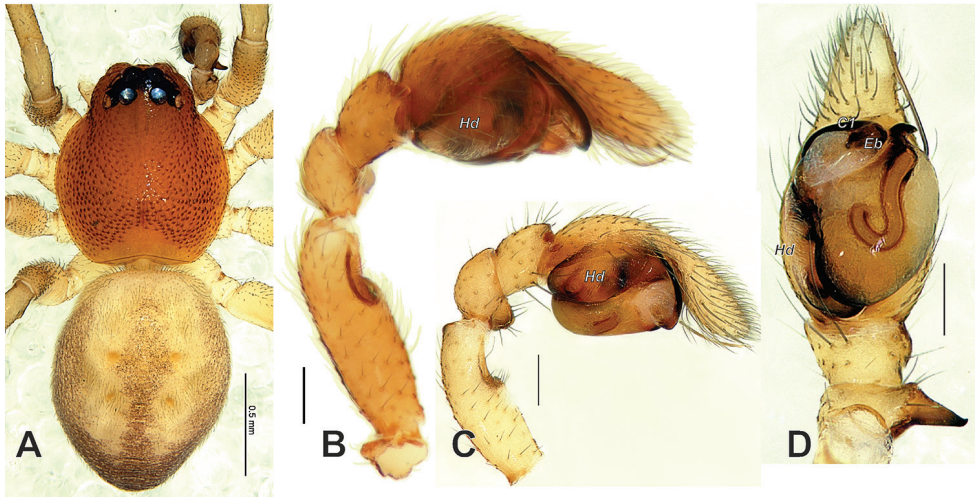


Figure 4. *Trachelas vulcani* (A, C–D from Guangxi, China) and *T. crewsae* sp. nov. (B) A male habitus, dorsal B–C male palp, proteral D male palp, ventral. A, C–D courtesy of Feng Zhang. Abbreviations: C1 coil 1 of embolus, Eb embolic base, Hd haematodocha. Scale bars: 0.5 mm (A), 0.1 mm (B–D).

book lung opercula large; postgaster with broad light band bordered with black lateral stripes. Spinnerets light yellow (Fig. 1A–C). Measurements of legs. I: 0.89, 0.37, 0.73, 0.56, 0.43 (2.98). II: 0.83, 0.36, 0.69, 0.53, 0.41 (2.82). III: 0.64, 0.3, 0.47, 0.5, 0.29 (2.2). IV: 0.93, 0.31, 0.79, 0.8, 0.34 (3.17).

Palp as in Figs 2A–F, 3A–C, 4B; femur as long as cymbium, three times longer than wide, with wide ventral groove (*Fg*) occupying an anterior third of segment; patellar apophysis finger-like as long as patella's width, with a pointed tip; tegulum expanded anteriorly; ♂-shaped sperm duct poorly visible; embolus (*Em*) long, whip-like, coiled almost across entire tegulum; tegular apophysis (*Ta*) small, claw-shaped.

Female. Total length 2.7. Carapace: 1.2 long, 1.06 wide. Coloration as in the male, with lighter dorsal abdominal pattern (Fig. 1D–F). Measurements of legs: I: 0.86, 0.37, 0.67, 0.53, 0.41 (2.84). II: 0.79, 0.36, 0.64, 0.51, 0.39 (2.69). III: 0.64, 0.31, 0.47, 0.49, 0.27 (2.18). IV: 0.93, 0.33, 0.81, 0.8, 0.34 (3.21).

Epigyne as in Fig. 3D–F; epigynal plate semitransparent, through which the copulatory ducts and primary receptacles are clearly visible; fovea divided by septum 'db' shaped; copulatory openings small, located at anteriorly on fovea; copulatory ducts, forming four coils, packed in helix directed posteriolaterad; connecting ducts (*Cn*) looped; secondary receptacles small; primary receptacles consisting of two subunits, connected by a narrow constriction; fertilization ducts (*Fd*) weakly sclerotized.

Etymology. The new species is named after our colleague Sarah C. Crews (San Francisco, USA), who continuously helps us with editing the English and providing fruitful comments on our manuscripts.

Distribution. Known only from the type locality (Fig. 5A–C).

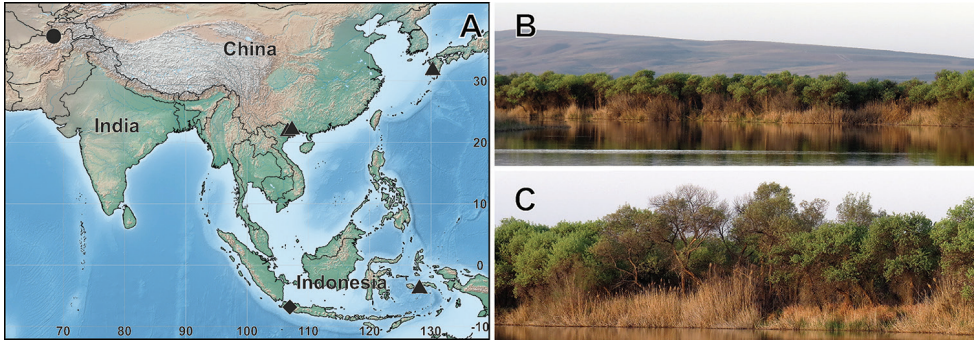


Figure 5. Distributional records of *Trachelas crewsae* sp. nov. and *T. vulcani* (**A**) and habitat of *T. crewsae* sp. nov. (**B–C**). Circle – *T. crewsae* sp. nov., diamond – type locality of *T. vulcani*, triangle – recent findings of *T. vulcani* outside of the type locality **B** Tigrovaya Balka Reserve **C** tugai (gallery) forest **B–C** courtesy of R.V. Yakovlev.

Discussion

Trachelas vulcani, the sibling species of *T. crewsae* sp. nov., was described from Java, Indonesia (Simon 1896). Thereafter, the species has been recorded from Maluku Islands (Indonesia), southern China and southern Japan (Deeleman-Reinhold 2001; Jin et al. 2017; Ono and Ogata 2018) (Fig. 5A). Based on the figures from the aforementioned papers, specimens of *T. vulcani* from different localities differ in details of the male palp and epigyne. Ono and Ogata (2018) argued that these differences lie within the range of species variation, considering the wide species range. However, it is also possible that all separated populations of *T. vulcani* could belong to different, closely related species. It is necessary to re-examine the holotype of *T. vulcani* in order to resolve the matter. The present diagnosis of *T. crewsae* sp. nov. from *T. vulcani* is based on the Chinese specimens considered by Jin et al. (2017: figs 5, 6, 7, 8, 9A, B).

Acknowledgements

We thank Murod Saidov and Rustam Muratov (both from Dushanbe, Tajikistan) for organizing the expedition to Tajikistan in 2015, in which the material presented here was collected. We also wish to cordially thank S. Koponen and I. Sääksjärvi (Zoological Museum, University of Turku, Finland) for allowing us to use their museum facilities, Roman V. Yakovlev (Barnaul, Russia) for providing photographs of the type locality of *T. crewsae* sp. nov., and Feng Zhang (Baoding, China) for the photographs of *T. vulcani*. We thank Alireza Zamani (Turku, Finland) and Hao Yu (Guiyang, China) who reviewed our manuscript and provided valuable comments. The English of the final draft was kindly checked by Dmitri V. Logunov (Manchester, UK).

References

- Bosselaers J, Urones C, Barrientos JA, Alberdi JM (2009) On the Mediterranean species of Trachelinae (Araneae, Corinnidae) with a revision of *Trachelas* L. Koch 1872 on the Iberian Peninsula. *Journal of Arachnology* 37: 15–38. <https://doi.org/10.1636/A08-33.1>
- Deeleman-Reinhold CL (2001) Forest spiders of South East Asia: with a revision of the sac and ground spiders (Araneae: Clubionidae, Corinnidae, Liocranidae, Gnaphosidae, Prodidomidae and Trochanterriidae [sic]). Brill, Leiden, 591 pp.
- Jin C, Yin XC, Zhang F (2017) Four new species of the genus *Trachelas* L. Koch, 1872 and the first record of *T. vulcani* Simon, 1896 from south-west China (Araneae: Trachelidae). *Zootaxa* 4324(1): 23–49. <https://doi.org/10.11646/zootaxa.4324.1.2>
- Marusik YM, Kovblyuk MM (2010) The spider genus *Trachelas* L. Koch, 1872 (Aranei: Corinnidae) in Russia. *Arthropoda Selecta* 19(1): 21–27. <https://doi.org/10.15298/arth-sel.19.1.04>
- Mikhailov KG (2013) The spiders (Arachnida: Aranei) of Russia and adjacent countries: a non-annotated checklist. *Arthropoda Selecta* 3 (Supplement): 1–262.
- Ono H, Ogata K (2018) Spiders of Japan: their natural history and diversity. Tokai University Press, Kanagawa, 713 pp.
- Platnick NI, Shadab MU (1974a) A revision of the *tranquillus* and *speciosus* groups of the spider genus *Trachelas* (Araneae, Clubionidae) in North and Central America. *American Museum Novitates* 2553: 1–34.
- Platnick NI, Shadab MU (1974b) A revision of the *bispinosus* and *bicolor* groups of the spider genus *Trachelas* (Araneae, Clubionidae) in North and Central America and the West Indies. *American Museum Novitates* 2560: 1–34.
- Ramírez MJ (2014) The morphology and phylogeny of dionychan spiders (Araneae: Araneomorphae). *Bulletin of the American Museum of Natural History* 390: 1–374. <https://doi.org/10.1206/821.1>
- Simon E (1896) Descriptions d'arachnides nouveaux de la famille des Clubionidae. *Annales de la Société Entomologique de Belgique* 40: 400–422. <https://doi.org/10.5962/bhl.part.2026>
- World Spider Catalog (2020). World Spider Catalog. Version 21.5. Natural History Museum Bern. <https://doi.org/10.24436/2> [accessed on October 2020]
- Zhang F, Fu JY, Zhu MS (2009) A review of the genus *Trachelas* (Araneae: Corinnidae) from China. *Zootaxa* 2235: 40–58. <https://doi.org/10.11646/zootaxa.2235.1.2>

Three new species of *Diplotaxis* Kirby from Guatemala and Mexico (Coleoptera, Scarabaeidae, Melolonthinae), with a key to the species of the *trapezifera* group

Leonardo Delgado^{1,2}, Víctor Hugo Toledo-Hernández¹

1 Centro de Investigación en Biodiversidad y Conservación, Universidad Autónoma del Estado de Morelos, Avenida Universidad No. 1001, Col. Chamilpa, 62209 Cuernavaca, Morelos, México **2** Instituto de Ecología, A. C. Carretera Antigua a Coatepec 351, 91070 Xalapa, Veracruz, México

Corresponding author: Leonardo Delgado (leonardo.delgado@inecol.mx)

Academic editor: A. Frolov | Received 16 December 2019 | Accepted 7 October 2020 | Published 16 November 2020

<http://zoobank.org/F50BE60A-8CFA-4A65-9A99-0C9E908F526F>

Citation: Delgado L, Toledo-Hernández VH (2020) Three new species of *Diplotaxis* Kirby from Guatemala and Mexico (Coleoptera, Scarabaeidae, Melolonthinae), with a key to the species of the *trapezifera* group. ZooKeys 993: 35–46. <https://doi.org/10.3897/zookeys.993.49434>

Abstract

Three new species of *Diplotaxis* Kirby are described and illustrated, *D. balam* **sp. nov.** from Guatemala, and *D. chiapasensis* **sp. nov.** and *D. complanatis* **sp. nov.** from Mexico. The new species have a flattened body and are included in the *trapezifera* species group. An updated key to the *trapezifera* species group is given.

Keywords

Cloud forests, Description, Diplotaxini, Insecta, Mesoamerica, taxonomy

Introduction

The American genus *Diplotaxis* Kirby is the third most diverse genus among the New World Melolonthinae and the second largest Diplotaxini genus worldwide (Bezdek 2004; Evans and Smith 2009). This genus contains 237 described species distributed from Canada through the West Indies to Brazil. Mexico has the highest diversity with 181 species, followed by the United States with 105 species (Vaurie 1958, 1960; McCleve 1993; Delgado and Mora-Aguilar 2012; Cherman et al. 2016). The species of this genus are

arranged in 37 species-groups, with nine species unassigned to any group (Vaurie 1958, 1960; Delgado and Capistrán 1992; Davidson and Davidson 2006).

In this work we describe three new species of *Diplotaxis*, which share with *D. xalapensis* Delgado & Capistrán, 1992 the following characters: body dorsoventrally flattened, clypeus setose, pronotum and elytra glabrous or nearly so. These species are diagnosed and included in the key to the species of the *trapezifera* group below.

Materials and methods

Morphological structures were studied using a Zeiss Stemi SV-6 stereomicroscope. Photographs were taken with a Nikon SMZ25 stereomicroscope and a DS-Fi2 camera and images were processed with the NIS-Elements software. Measurements were taken with an ocular micrometer. The length of the beetles was measured from the apex of the clypeus to the apex of the pygidium, whereas the width was measured across the maximum width of the elytra. Morphological terminology follows that of Vaurie (1958, 1960).

Abbreviations for collections cited in this work are as follows: **UVGC** – Colección Entomológica de la Universidad del Valle de Guatemala (Guatemala, Guatemala), **CNIN** – Colección Nacional de Insectos de la Universidad Nacional Autónoma de México, (Mexico City), **ECO-SC** – Colección Entomológica de El Colegio de la Frontera Sur (Chiapas, Mexico), **IEXA** – Colección Entomológica del Instituto de Ecología, A. C. (Veracruz, Mexico), **SMC** – Scott McCleve private collection (Arizona, USA), and **LLDC** – Leonardo Delgado private collection (Veracruz, Mexico).

Results

Diplotaxis balam sp. nov.

<http://zoobank.org/75CDF203-6811-4A1E-8D85-40547CEC4FBD>

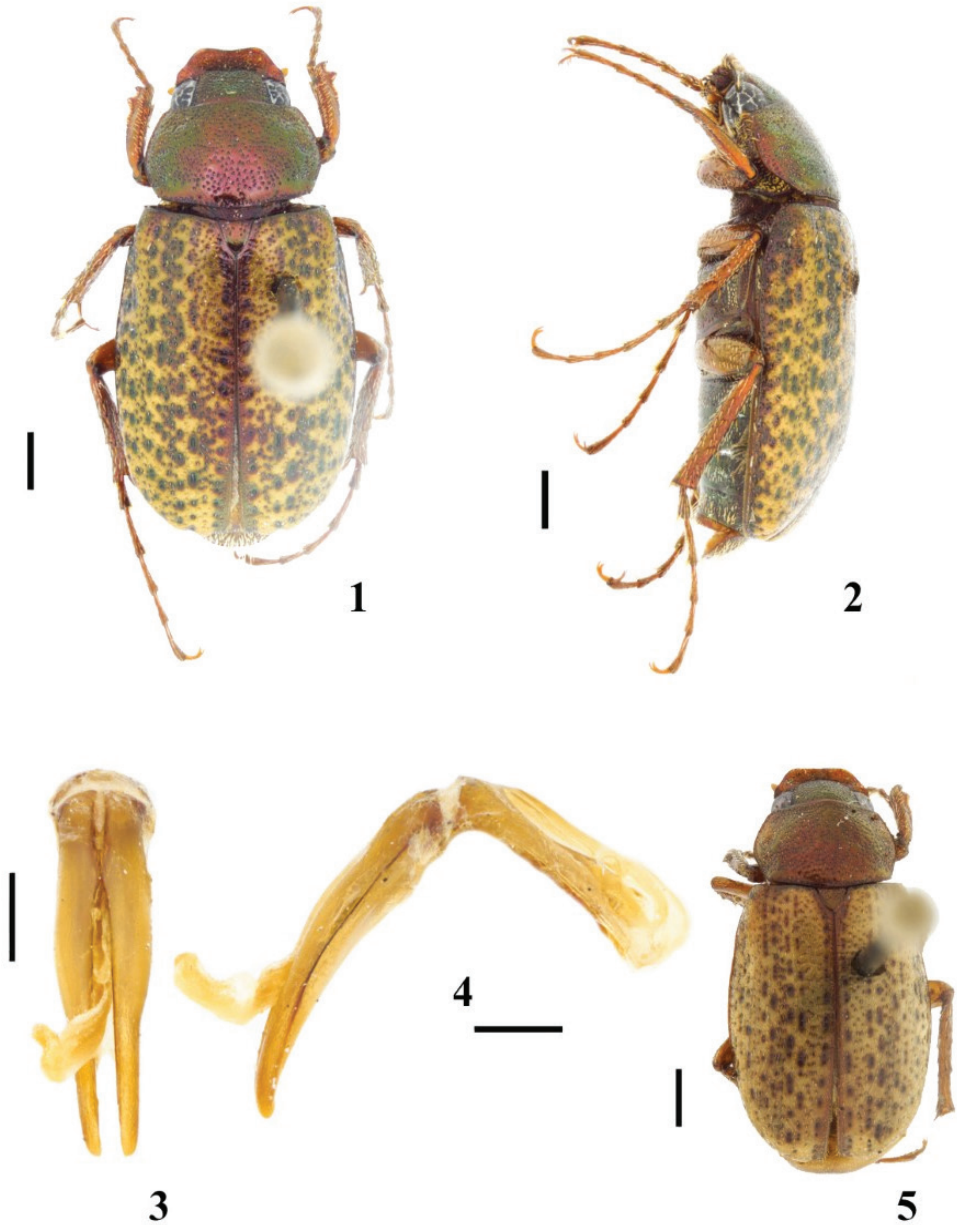
Figs 1–5

Material examined. *Holotype* male, “GUATEMALA: Zacapa, arriba de La Unión, 16-III-1996, Alt. 1,550 m, bosque nuboso, J. C. Schuster col.” (UVGC). *Paratype* female, same data as holotype (LLDC).

Diagnosis. This species is easily recognized by the color of the elytra (Figs 1–2, 5): ground color yellow with black, irregular foveae distributed throughout entire surface. No other described species of this genus shows this color pattern.

Description. *Holotype. Male* (Figs 1–4). Length 8.55 mm; width 4.21 mm. Body elongate and dorsoventrally flattened. Clypeus red with a metallic green tinge, frons and pronotum metallic green, elytra yellow and black with irregular foveae throughout entire surface, venter metallic green, legs tan with a weak metallic green tinge.

Head. Clypeus trapezoidal in shape, 0.4 length of frons, apex broadly sinuated with anterior angles rounded, sides indented in front of eyes; clypeal surface concave,



Figures 1–5. *Diplotaxis balam* sp. nov. **1** male habitus, dorsal view **2** male habitus, lateral view **3** aedeagus, dorsal view **4** aedeagus, lateral view **5** female habitus. Scale bars: 1 mm (**1, 2, 5**); 0.5 mm (**3, 4**).

rugose, with distinct setae; frontoclypeal suture absent; frons flat, gradually declivous to clypeus, with coarse, dense punctures; transverse eye diameter 0.33 interocular width; antennae 10-segmented; labrum flat, flush with, and 0.20 times longer than reflexed underside face of clypeus, surface with dense punctures; mandibles slender in

frontal view; mentum slightly convex, with weak anterior declivity marked by a suture; last article of maxillary palps not impressed dorsally.

Pronotum. Hexagonal in shape; with anterior angles acute, lateral margins angled and situated behind middle, posterior angles obtuse; pronotal surface almost evenly convex, with three lateral foveae on each side; pronotal punctuation regular with dense, medium-sized punctures on disc, confluent near sides; basal margin with bead not cariniform, with a continuous row of punctures; most punctures bearing a minute seta slightly longer than one puncture diameter.

Scutellum. With medium-sized punctures at sides. **Elytra.** 1.7 times longer than width, elytral surface with irregular, shallow, black foveae, most of them on the intervals; elytral striae with separated, ocellate punctures, intervals with small, moderately dense punctures; elytral punctures with setae minute but slightly longer than those of pronotum.

Abdomen. Without lateral carina; propygidium without groove above of pygidium; ventrites 2–5 subequal in length, surface with setae medially and with whitish scales laterally; pygidium 1.7 times wider than long, surface with coarse, deep, setigerous punctures; setae dense, longer on apical half.

Legs. Protibiae tridentate, basal tooth weak and situated in distal half; claws long, slightly curved, cleft subapically, inner rami of claws shorter than apex; tarsi longer than respective tibiae; mesotarsomere 1 slightly shorter than 2; metacoxal plate rounded and margined laterally; metafemora straight and slender; metatibial spurs slender, long, acute; metatarsomere 1 shorter than the 2 and slightly longer than longest spur.

Genitalia. Basal piece shorter than parameres, which are joined on inner margin at basal fifth, moderately widened at middle, apices blunt (Figs 3–4).

Female. One female paratype (Fig. 5). Length 6.97 mm; width 3.53 mm. The female differs from the male in the following respects: clypeus slightly shorter; frons and vertex more convex; transverse eye diameter 0.31 interocular width; pronotum with anterior angles obtuse and lateral angles rounded; elytra 1.3 times longer than width; abdomen nearly flat; pygidium 1.6 times wider than long; tibiae broader and robust; metafemora slightly broader; inner metatibial spur wider and longer than metatarsomere 1.

Etymology. The specific epithet *balam*, meaning jaguar in the Mayan language, refers to the color pattern of the elytra, similar to the skin of this feline.

Distribution. This species is only known from the type locality, situated in the Sierra de Las Minas, Guatemala, near the border with Honduras (14°56'45.6"N, 89°16'40.1"W) (Fig. 17). The locality is at 1550 m altitude, covered by a cloud forest.

Taxonomic remarks. The features of *D. balam* sp. nov. agree in part with those of the *trapezifera* species group [see key to species groups by Vaurie (1960)]. The group is mainly characterized by the presence of setae on the clypeal surface, the rest of the dorsum being glabrous or with minute setae only. However, *D. balam* sp. nov. (as well as *D. xalapensis* and the two new species described below) has a dorsoventrally flattened body, unlike species of the *trapezifera* group which have a convex body. *Diplotaxis balam* sp. nov. is distinguished from all other *Diplotaxis* by the unique color pattern of the elytra (Figs 1–2, 5).

***Diptotaxis chiapasensis* sp. nov.**

<http://zoobank.org/DE89ABE0-49DA-4BEF-A743-B0A08FAEEA7F>

Figs 6–10

Material examined. *Holotype* male, “MÉXICO: Chiapas, Unión Juárez, Talquián, 7-X-2002, B. Gómez y Gómez col.” (ECO-SC). *Paratype* female, same data as holotype (LLDC).

Diagnosis. This new species is recognized by the following combination of characters: body dorsoventrally flattened; clypeus setose, rest of dorsum glabrous; dorsum with a metallic green cast; pronotum and elytra shiny, without microreticulation.

Description. *Holotype. Male* (Figs 6–9). Length 8.14 mm; width 3.63 mm. Body elongate and dorsoventrally flattened. Clypeus, sides of pronotum and scutellum reddish-brown, frons and vertex black, most of pronotum and elytra dark brown, legs and venter reddish-brown; head, pronotum and elytra with metallic green cast.

Head. Clypeus subrectangular in shape, short, length equals 0.80 of that of frons and vertex combined, apex broadly sinuated, anterior angles rounded, clypeal surface with short, sparse setae; frons with anterior half gradually declivous to clypeus and slightly concave; punctuation of clypeus rugose, frons with punctures of medium size, moderately dense; transverse eye diameter 0.32 interocular width; antennae 10-segmented; labrum concave, flush with, and slightly longer than, reflexed underside of clypeus, surface with moderately dense punctures; mandibles slender in frontal view; mentum with anterior declivity marked by transverse, curved, setiferous ridge; last article of maxillary palps not impressed dorsally.

Pronotum. Hexagonal in shape, anterior angles acute, lateral margins obtusely angled, posterior angles obtuse; pronotal surface almost evenly flat, reticulated, with large, ocellate punctures; lateral and basal borders narrowly beaded.

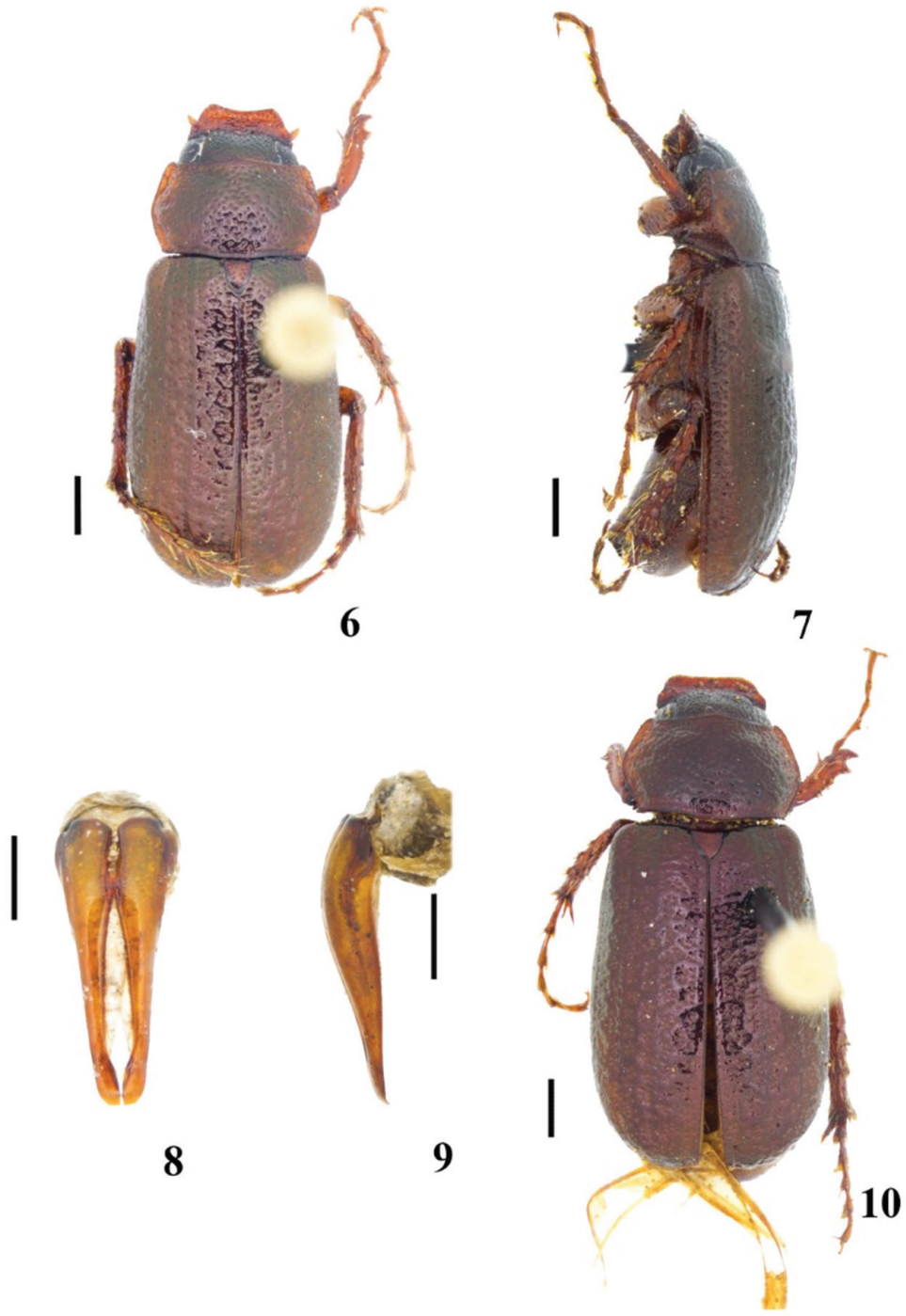
Scutellum. Moderately punctate. **Elytra.** 1.6 times longer than width, surface moderately rugose and densely punctate, punctures larger than those on pronotum; striae indistinct; marginal lateral setae scarce and minute, only present on basal fourth.

Abdomen. Without lateral carina, propygidium without groove anterior to pygidium, ventrites 2–5 subequal in length, with sparse setae; pygidium 1.6 times wider than long, with confluent punctures and moderately dense setae.

Legs. Protibiae tridentate, basal tooth small and situated on apical 2/5 of protibia; protarsal claws slightly curved, subapically cleft, both rami equal in length; all tarsi longer than respective tibiae, mesotarsomere 1 as long as 2; metacoxal plates truncate and margined laterally; metafemora straight and slender; metatibial spurs slender and shorter than metatarsomere 1; metatarsomere 1 shorter than 2; meso- and metatarsal claws abruptly curved, with subapical ramus large.

Genitalia. Basal piece damaged, parameres joined on inner margin at basal fourth, narrowing distally to moderately widened apices (Figs 8–9).

Female. One female paratype (Fig. 10). Length 8.59 mm; width 3.90 mm. The female differs from the male in the following respects: clypeus slightly shorter; frons and vertex more convex; pronotum with anterior angles obtuse and lateral angles rounded; elytra 1.7 times longer than wide; abdomen almost flat; pygidium 1.7 times wider than



Figures 6–10. *Diplotaxis chiapasensis* sp. nov. **6** male habitus, dorsal view **7** male habitus, lateral view **8** male genitalia, frontal view **9** male genitalia, lateral view **10** female habitus. Scale bars: 1 mm (**6, 7, 10**); 0.5 mm (**8, 9**).

long; tibiae broader and robust; metafemora slightly broader; and inner metatibial spur wider and longer than metatarsomere 1.

Etymology. The specific epithet is derived from Chiapas, the state of Mexico where this species was collected, combined with the Latin suffix *-ensis*, meaning belonging to.

Distribution. *Diplotaxis chiapasensis* sp. nov. is only known from the type locality, situated on the Pacific side of the state of Chiapas, Mexico, near the border with Guatemala (15°05'6.9"N, 92°05'02.24"W) (Fig. 17). This locality is at 1660 m altitude, with cloud forests with different degrees of disturbance.

Taxonomic remarks. *Diplotaxis chiapasensis* sp. nov. is similar to *D. xalapensis*. Both species belong to the *trapezifera* group because of the setose clypeus and the rest of the dorsum glabrous, but both species can be distinguished from the remaining species of this group by the dorsoventrally flattened body and the elytra dark brown. *Diplotaxis chiapasensis* sp. nov. is clearly separated from *D. xalapensis* by the shiny elytra (not matt or with sericeous surface).

***Diplotaxis complanatis* sp. nov.**

<http://zoobank.org/8908C72D-8A47-4A2E-B8B9-3249B5B62155>

Figs 11–16

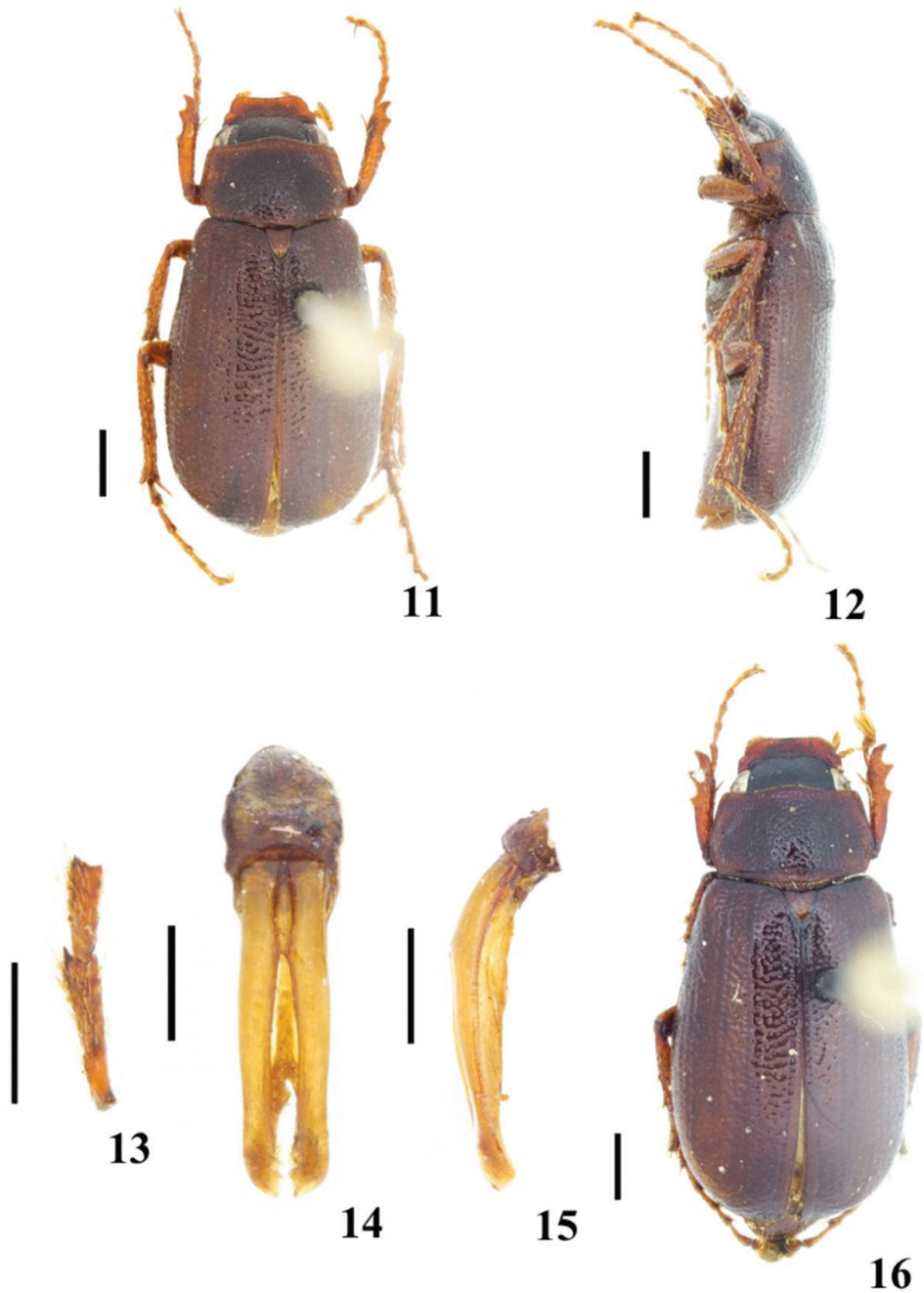
Material examined. *Holotype* male, “MÉXICO: Oaxaca, km 21 Carr. Yolotepec-Juquila, VIII-1993, Alt. 1,900 m, bosque mesófilo, luz, L. Delgado col.” (IEXA). *Paratype* female, same data as holotype (IEXA). Three male and one female *paratypes*, same data except: “31-VII–1-VIII-1991, luz u.v., J. L. Navarrete, G. Quiroz y L. Delgado cols.” (CNIN, SMC, LLDC).

Diagnosis. This tiny species is recognized by the following combination of characters: body dorsoventrally flattened, clypeal surface with a few and minute setae, pronotum and elytra glabrous or with scarcely visible setae (shorter than diameter of one puncture), and dorsum shiny but without a metallic cast.

Description. *Holotype. Male* (Figs 11–15). Length 6.58 mm; width 3.26 mm. Body elongate and dorsoventrally flattened. Clypeus reddish, frons and vertex black, pronotum reddish, elytra reddish-brown; dorsum shiny, without metallic cast.

Head. Clypeus trapezoidal in shape, length equals 0.66 that of frons, apex broadly emarginated with anterior angles rounded, and sides indented in front of eyes; surface concave, coarsely rugose, with scarce, minute setae near external margins; frontoclypeal suture barely marked; frons slightly concave, gradually declivous to clypeus, with large and dense punctures; transverse eye diameter 0.34 interocular width; antennae 10-segmented; labrum with anterior half slightly convex and posterior half concave, length equals 0.50 of that of reflexed underside of clypeus, surface with small, sparse punctures; mandibles moderately robust in frontal view; mentum convex, with anterior declivity marked by an arcuate, setiferous ridge; last article of maxillary palps not impressed dorsally.

Pronotum. Hexagonal in shape, anterior angles right, lateral margins obtusely angled near middle, posterior angles obtuse; surface slightly convex, with a shallow fovea



Figures 11–16. *Diplotaxis complanatis* sp. nov. **11** male habitus, dorsal view **12** male habitus, lateral view **13** male protarsomeres **14** male genitalia, frontal view **15** male genitalia, lateral view **16** female habitus. Scale bars: 1 mm (**11**, **12**, **16**); 0.5 mm (**13–15**).

on each side; punctuation coarse on disc, confluent along sides; basal margin beaded, with a row of small punctures.

Scutellum. With sparse, medium-sized punctures. **Elytra.** 1.7 times longer than width, broad intervals with coarse punctures, many of which confluent, narrow intervals slightly raised; elytral punctures with setae minute, barely visible.

Abdomen. Without lateral carina; propygidium without groove anterior to pygidium; ventrites 2–5 subequal in length, surface with small setae; pygidium 1.8 times wider than long, slightly convex in basal 3/4, apical fourth flat; surface with coarse, deep punctures, with sparse setae on apical third.

Legs. Protibiae tridentate, basal tooth situated nearly at middle and removed from apical teeth; claws bent and subapically cleft; tarsi longer than respective tibiae; apex of protarsomere 2 with a small denticle (Fig. 13), mesotarsomere 1 longer than 2; metacoxal plates margined and rounded laterally; metafemora straight and slender; metatibial spurs long and acute; metatarsomere 1 shorter than 2, and almost as long as longest spur.

Genitalia. Basal piece almost as long as parameres, parameres joined along inner margin in basal third, almost parallel, and with apices rounded and slightly widened (Figs 14–15).

Variation. Three male and two female paratypes. Males: length 6.5–7.2 mm, width 3.1–3.3 mm. Females: length 7.2–7.6 mm, width 3.6–3.9. In both sexes, the color and punctuation varies slightly. Females differ from males in having frons more convex; abdomen slightly more convex; tibiae and femora broader and robust, protarsomere 2 without a denticle; inner metatibial spur longer than metatarsomere 1.

Etymology. The name of this species is derived from the Latin *complanatae*, meaning flat, in relation to the dorsoventrally flattened body.

Distribution. This species is known only from the type locality, which is situated in the Sierra Madre del Sur, in the state of Oaxaca, Mexico (16°14'33.4"N, 97°15'01"W) (Fig. 17). The locality is on the slope facing southward to the coast, at 1900 m altitude, in a transition between pine-oak and cloud forests. The specimens were attracted to ultraviolet light traps.

Taxonomic remarks. This small species has a dimorphic character which is so far unique for this genus: the presence in the males of a minute denticle on the apex of protarsomere 2 (Fig. 13). The clypeus with minute setae and the rest of the dorsum glabrous (or nearly so) relate this species with the *trapezifera* group, however, *D. complanatis* sp. nov. exhibits a dorsoventrally flattened body. This species can be distinguished from *D. chiapasensis* sp. nov. and *D. xalapensis* by its shiny body, but without a metallic green cast (Figs 11, 16).

Discussion

The three species herein described, in addition to *D. xalapensis*, are distinguished from the other species of the genus *Diplotaxis* by the following combination of

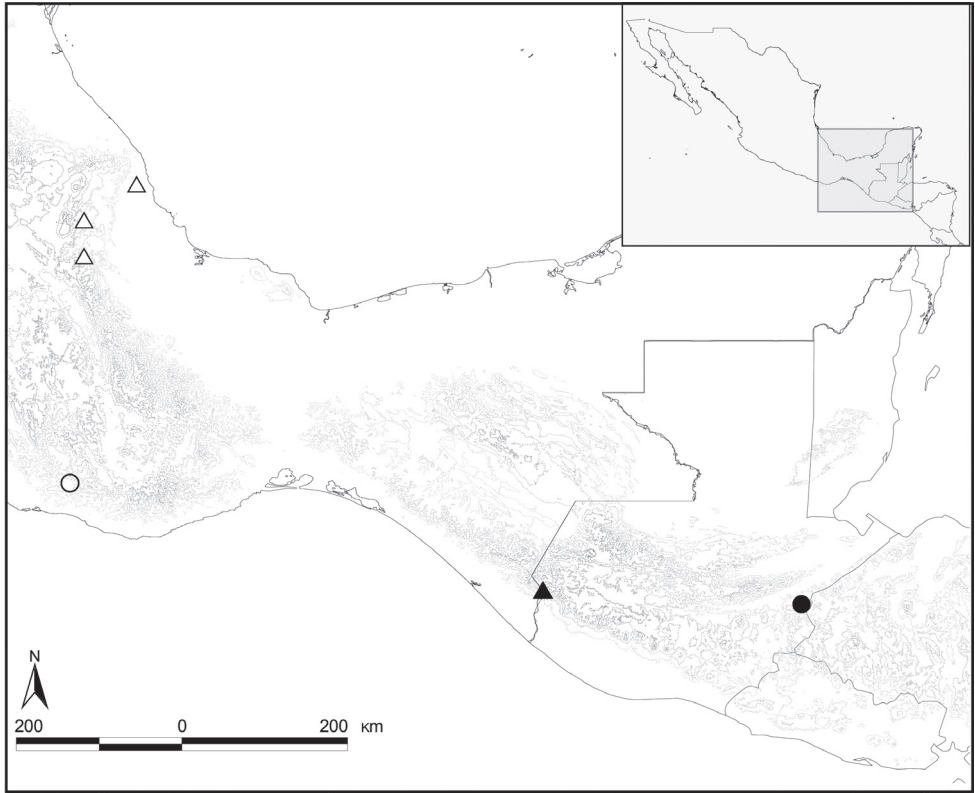


Figure 17. Distribution of *Diplotaxis* species. *Diplotaxis balam* sp. nov. (black circle), *D. chiapasensis* sp. nov. (black triangle), *D. complanatis* sp. nov. (white circle), *D. xalapensis* Delgado and Capistrán (white triangle).

characters: body dorsoventrally flattened, clypeal surface with at least a few and distinct setae, and pronotum and elytra glabrous or with scarcely visible setae (most setae shorter than one puncture diameter). The presence of setae on the clypeal surface, together with the pronotum and elytra glabrous or nearly, could include these species in the *trapezifera* species group. The species of this group, however, exhibit a convex body, a character widespread in this genus. Without an analysis of the phylogenetic relationships of the species of this genus (which is currently being carried out by the senior author), the flattened body character state should not, at this time, be considered as a synapomorphy, but only as an uncommon character state.

Besides these species, there are two species showing a flattened body, *D. hallei* Vaurie and *D. pilifera* Burmeister, but these species are included in the *pilifera* group by their distinctive scales on the dorsum and venter (Vaurie 1958). Because the new species here described, along with *D. xalapensis*, share the characters mentioned above with the *trapezifera* group, we included them in this group, and modified Vaurie's key accordingly (modifications are indicated by a lowercase letter).

Key to the *trapezifera* group [partly modified from Vaurie (1960)]

- 26 Front margin of pronotum at sides drawn forward to acute angle27
- 26' Front margin of pronotum at sides truncate or virtually so, forming obtuse or right angle..... 27a
- 27 Pronotum with sides strongly arcuate behind middle, and hind angles rounded; lateral margins of clypeus almost parallel with indentation in front of eyes..... *D. incisa* Vaurie
- 27' Pronotum with sides scarcely arcuate and hind angles distinctly angulate; lateral margins of clypeus without indentation in front of eyes
.....*D. saltensis* Vaurie (in part)
- 27a Dorsum red or reddish-brown27b
- 27a' Dorsum of different color, sometimes with metallic cast27d
- 27b Head and pronotum shiny; elytra yellowish, with scattered black foveae
..... *D. balam* sp. nov.
- 27b' Head and pronotum with metallic green cast; elytra of different color, without black foveae 27c
- 27c Elytra dull green, sericeous..... *D. xalapensis* Delgado & Capistrán
- 27c' Elytra shiny green*D. chiapasensis* sp. nov.
- 27d Body dorsoventrally flattened; clypeus rectangular, with front angles rounded*D. complanatis* sp. nov.
- 27d' Body dorsoventrally convex; clypeus trapezoidal, with front angles right or acute28
- 28 Eyes very large, each eye about 1/3 or nearly of width of head; size small (6 to 7 mm)29
- 28' Eyes not quite so large, each 1/5 or 1/4 of width of head; size usually larger than 7 mm.....30

Acknowledgments

We thank Enio Cano for the loan and donation of specimens from the Collection of the Universidad del Valle de Guatemala. We thank Benigno Gómez y Gómez for the loan and donation of specimens from Chiapas. We thank Eder F. Mora-Aguilar for taking the photographs, preparation of figure plates, and comments on the manuscript. We also thank José Luis Navarrete-Heredia and Georgina Quiroz for their help with collecting in the state of Oaxaca. We also thank Daniel Curoe for his linguistic review of the manuscript.

References

- Bezdek A (2004) Catalogue of Diplotaxini (Coleoptera: Scarabaeidae: Melolonthidae) of the Old World. *Zootaxa* 463: 1–90. <https://doi.org/10.11646/zootaxa.463.1.1>

- Cherman MA, Morón MA, Almeida LM (2016) Phylogenetic relationships within *Diplotaxini* Kirby (Coleoptera: Melolonthidae: Melolonthinae) with emphasis on *Liogenys* Guérin-Méneville. *Systematic Entomology* 41(4): 744–770. <https://doi.org/10.1111/syen.12188>
- Davidson JP, Davidson JM (2006) Two new species of *Diplotaxis* Kirby, 1837, from Arizona with a key and notes on the *D. misella* group (Coleoptera: Scarabaeidae). *The Pan-Pacific Entomologist* 82(1): 74–81.
- Delgado L, Capistrán F (1992) Two new species of *Diplotaxis* from Biosphere Reserve of El Cielo. *Revista Brasileira de Entomologia* 37(2): 267–272.
- Delgado L, Mora-Aguilar EF (2012) *Diplotaxis multicarinata* (Coleoptera: Scarabaeidae), a new species from a relict forest in Oaxaca, Mexico. *Florida Entomologist* 95(2): 285–289. <https://doi.org/10.1653/024.095.0207>
- Evans AV, Smith ABT (2009) An Electronic Checklist of the New World Chafers (Coleoptera: Scarabaeidae: Melolonthinae), Version 3. <http://www.museum.unl.edu> [Accessed on 15 May 2019]
- McCleve S (1993) Three new species of flightless *Diplotaxis* from Oaxaca, Mexico (Coleoptera: Scarabaeidae: Melolonthinae). *The Coleopterists Bulletin* 47(1): 43–50.
- Vaurie P (1958) A revision of the genus *Diplotaxis* (Coleoptera, Scarabaeidae, Melolonthinae), Part I. *Bulletin of the American Museum of Natural History* 115(5): 267–396.
- Vaurie P (1960) A revision of the genus *Diplotaxis* (Coleoptera, Scarabaeidae, Melolonthinae), Part II. *Bulletin of the American Museum of Natural History* 120(2): 161–434.

Revision of Chinese *Phorocardius* species (Coleoptera, Elateridae, Cardiophorinae)

Yongying Ruan¹, Hume B. Douglas², Lu Qiu³, Xiaoqin Chen¹, Shihong Jiang¹

1 School of Applied Chemistry and Biological Technology, Shenzhen Polytechnic, Shenzhen, Guangdong 518055, China **2** Canadian National Collection of Insects, Arachnids and Nematodes, Agriculture and Agri-Food Canada, 960 Carling Ave., Ottawa, Ontario, K1A 0C6, Canada **3** Institute of Entomology, College of Plant Protection, Southwest University, Beibei, Chongqing 400716, China

Corresponding author: Yongying Ruan (yongyingruan@szpt.edu.cn); Shihong Jiang (sjiang@szpt.edu.cn)

Academic editor: Aaron Smith | Received 1 May 2020 | Accepted 13 October 2020 | Published 16 November 2020

<http://zoobank.org/C40989DB-8063-4C9F-A481-E7AA82CA924B>

Citation: Ruan Y, Douglas HB, Qiu L, Chen X, Jiang S (2020) Revision of Chinese *Phorocardius* species (Coleoptera, Elateridae, Cardiophorinae). ZooKeys 993: 47–120. <https://doi.org/10.3897/zookeys.993.53805>

Abstract

The Chinese species of *Phorocardius* Fleutiaux, 1931 have been studied and six species are described as new: *P. alterlineatus* Ruan & Douglas, **sp. nov.**; *P. flavistriolatus* Ruan & Douglas, **sp. nov.**; *P. minutus* Ruan & Douglas, **sp. nov.**; *P. rufiposterus* Ruan & Douglas, **sp. nov.**; *P. yunnanensis* Ruan & Douglas, **sp. nov.**; and *P. zhiweii* Ruan, Douglas & Qiu, **sp. nov.** Lectotypes are designated for *Cardiophorus comptus* Candèze, 1860, *Cardiophorus contemptus* Candèze, 1860, *Phorocardius magnus* Fleutiaux, 1931, and *Cardiophorus manuleatus* Candèze, 1888. The holotype is identified for *Cardiophorus yanagiharae* Miwa, 1927. *Phorocardius florentini* (Fleutiaux, 1895) and *P. manuleatus* (Candèze, 1888) are newly reported from China; *P. comptus* (Candèze, 1860) is excluded from the Chinese fauna. A key to the 11 *Phorocardius* species known from China is given. *Phorocardius* is newly recorded from deep within the Palearctic Region. The procoxal cavities of *P. rufiposterus* Ruan & Douglas, **sp. nov.** are closed, which is different from all other species of *Phorocardius*. An annotated checklist of the 21 *Phorocardius* species of the world is provided. Additionally, *Phorocardius contemptus* (Candèze, 1860), **comb. nov.** is transferred from *Cardiophorus* to *Phorocardius*; four species are transferred from *Phorocardius* to *Displatynychus*: *Displatynychus bombycinus* (Candèze, 1895), **comb. nov.**, *Displatynychus pakistanicus* (Platia & Ahmed, 2016), **comb. nov.**, *Displatynychus sobrinus* (Laporte, 1840), **comb. nov.**, and *Displatynychus tibialis* (Platia & Ahmed, 2016), **comb. nov.**

Keywords

Cardiophorus, checklist, click beetles, *Displatynychus*, diversity, elaterid, new species, review

Introduction

Phorocardius Fleutiaux, 1931 is a small Asian genus of elaterids with 15 species known previously (Douglas et al. 2018), placed in the subfamily Cardiophorinae Candèze, 1859 (Fleutiaux 1931; Douglas 2017; Douglas et al. 2018). Fleutiaux (1931) established *Phorocardius* and its two subgenera for Cardiophorinae with tarsal claws bidentate near their apices. Subsequently, Fleutiaux (1947) revised eight species from French Indo-China (Vietnam, Laos, and Cambodia). Since 1947, only a few new studies have been published: Platia (2015) and Platia and Ahmed (2016) described new species from Pakistan and Maldives respectively; and Douglas (2017) redefined the genus based on a phylogeny using adult morphological characters.

Previously, *Phorocardius* included a second subgenus: *Diocarphus* Fleutiaux, 1947. *Diocarphus* was recognized by the reduced ventral apex of the tarsal claw and more pronounced pronotal lateral carina “sutures inferieures” in comparison to subgenus *Phorocardius*. However, Douglas (2017) found *Phorocardius* polyphyletic and elevated *Diocarphus* to genus status with diagnoses including procoxal cavity closure and female internal genitalic structures.

With only three species previously known (Cate et al. 2007), the *Phorocardius* fauna of China remained little known. In this paper, we study the taxonomy of Chinese *Phorocardius* and describe six new species. Additionally, we designate lectotypes for *Cardiophorus comptus* Candèze, 1860, *Cardiophorus contemptus* Candèze, 1860, *Phorocardius magnus* Fleutiaux, 1931, and *Cardiophorus manuleatus* Candèze, 1888; and the holotype of *Cardiophorus yanagiharae* Miwa, 1927 is identified. These were designated (or identified) to fix species concepts and to ensure their universal and consistent interpretation.

Materials and methods

Observations of the habitus and diagnostic characters were made using a NIKON SMZ645 stereo microscope and a NIKON E100 optical microscope. Digital images were taken using a CANNON D800 camera attached to a CANNON MP-E 65 mm Lens or NIKON E100 microscope. Before dissection, dry specimens were submerged in hot water for 10 minutes. Male genitalia were subsequently dissected and glued to card papers pinned under the specimens. Female genitalia were submerged in hot 10% NaOH solution for approximately 1 minute, surrounding tissues were cleared, mounted in glycerin on slides for photography, and then glued to card papers pinned under the specimens. Specimen measurements were made as shown in Fig. 1.

Specimens were identified using species identification keys (e.g., Candèze 1860; Fleutiaux 1947), and additional species descriptions. We were able to examine type material for most species only occurring outside the study area. The remainder were excluded from the Chinese fauna based on literature alone. Details are presented in Results: Checklist and synonymy of world *Phorocardius* species.

Morphological terminology and the generic concept of *Phorocardius* follow Douglas (2017).

Definition of Oriental and Palearctic Regions mainly follows Wallace (1876) and Morrone (2015), south Tibet and the Yangtze River valley in central China is treated as the boundary (or transition zone) between the two regions. In the ‘Type Material’ and ‘Material’ sections of each species, specimen data are recorded verbatim from labels. Specimens were examined from the following insect collections:

- IZCAS** Institute of Zoology, Chinese Academy of Sciences, Beijing, China.
LQCC Lu Qiu Personal Collection, Chongqing, China.
MNHN Museum national d’Histoire naturelle, Paris, France.
NHMUK The Natural History Museum (formerly British Museum), London, United Kingdom.
NHMW Naturhistorisches Museum Wien, Wien (Vienna), Austria.
RBINS Royal Belgian Institute of Natural Sciences (Institut Royal des Sciences Naturelles de Belgique), Brussels, Belgium.
SZPT School of Applied Chemistry and Biological Technology, Shenzhen Polytechnic, Shenzhen, Guangdong, China.
TARI Taiwan Agricultural Research Institute, Taichung, Taiwan, China.

Results

Phorocardius Fleutiaux, 1931

Phorocardius Fleutiaux, 1931: 308. Type species: *Cardiophorus florentini* Fleutiaux, 1895.

Distribution of known species. Oriental and southeast Palearctic Regions: China (Inner Mongolia, Shaanxi, Henan, Sichuan, Hubei, Guizhou, Yunnan, Guangxi, Taiwan, Hainan), Myanmar, India, Laos, Nepal, Thailand, Vietnam, Sri Lanka, Cambodia, Maldives (doubtful).

Description of *Phorocardius* based on species from China. Body length 5–13.9 mm. Width 1.6–4.5 mm. Integument black, brown, yellow and/or red, some with spots or stripes on pronotum or elytra. Body with yellow to yellow-grey pubescence (brown setae present on disc of pronotum in *P. florentini* and *P. zhiweii* Ruan Douglas & Qiu, sp. nov.).

Head. Hypognathous. Frons and vertex convex, flat or weakly concave; frontal carina (joined supraantennal carinae, raised above labrum) convex or straight in dorsal view; carina smooth and glabrous; supraantennal carinae forked near junctures with compound eyes (Fig. 23, indicated by arrows), weakly separated in rare cases (e.g., in *P. manuleatus*, see Fig. 23E); frons with supraorbital and orbital grooves present and shallow (Fig. 1F). Antennae not reaching or slightly exceeding posterior angles of pronotum; antennal sensory elements beginning on antennomere 3. Mandible with apex

bidentate to tridentate; apical palpomere of maxillary hatchet-shaped or polygonal, longer than wide. Labrum evenly convex. Area between each antennal fossa and adjacent compound eye unsculptured, or with groove or pit(s).

Prothorax. Pronotum in dorsal view with sides straight, convex, or sinuate near posterior fourth. Pronotum with punctures circular or oval on dorsal surface, punctures larger and deeper on disc and anterad, sparser and smaller posterad; sublateral incisions and carinae present (with carinae obsolete, see Fig. 1B); posterior edge of pronotum sinuate, with three apices mesally (tridentate antescutellar lobe, i.e., the median basal lobe in Douglas 2003); lateral carina on hypomeron not present (or not distinguishable from hind angle carina); posterior angles not truncate dorsally; hind angle carina not extending anterad beyond posterior third; anterior angles obtuse and not projecting anterad, posterior angles straight-sided, slightly convex or strongly bulged laterally (e.g., Fig. 17C, D), parallel to weakly divergent; hypomeral hind edges rectangularly emarginate (Fig. 12B, indicated by arrow) immediately meso-ventrad of posterior angles. Procoxal cavities open or closed. Prosternum with sides concave in ventral view; anterior prosternal lobe long, covering labium when head is retracted; prosternal process curved dorsad or not, ventral surface convex to flat, carinate laterally or not; prosternal process approximately twice as long as procoxal cavity length.

Pterothorax. Scutellar shield heart-symbol shaped, with anterior edge emarginate (Fig. 13D), anterolateral edges sinuate to evenly convex, posterior apex narrowly rounded (Fig. 13D) to pointed (Figs 11A, 15A), strongly elongate and produced posteriorly in some (e.g., in *P. florentini*). In lateral view, mesosternum with anterior edges concave (Fig. 24); anterior facing projections on posterior edge of mesosternum (i.e., on antero-ventral angle of mesosternal fossa according to Douglas (2003)) strongly developed, sharp and produced anteriorly to absent (Fig. 25, indicated by solid line and lower red arrow). In ventral view, mesosternal fossa approximately diamond-symbol shaped (Fig. 25), with lateral edges sinuate anterad of mesocoxae (Fig. 25); antero-mesal angle of mesepisternum broadly rounded to acute, facing antero-mesally (Fig. 25, indicated by dashed line and green arrow). Elytra with humeral angle angulate or tuberculate in dorsal view; interstriae prominently convex near base in most, gradually becoming less convex on apical half; upper edge of epipleura with minute serrations. Hind wings large, and apparently capable of flight; notched in anal area or not (Douglas 2017).

Legs. Tarsi simple; tarsomere V longest; tarsal claws each with two apices, apices separated in apical half of claw, with ventral surface of claw sinuate basad of ventral apex, ventral apex much smaller than to almost as large as dorsal apex. Metacoxal plate large, covering 1/2–2/3 of metatrochanter with legs withdrawn.

Abdomen. Lateral edges of visible abdominal ventrites I–V (i.e., urosternites III–VII) with or without minute serrations.

Male genitalia. Urosternite VIII straight to anteriorly pointed, with two lateral posterior lobes, without median posterior lobe; abdominal segment IX with tergite and sternites articulated at sides. Aedeagus: paramere, with or without preapical lateral expansion (Fig. 1G), with preapical ventral (or apical mesal) expansion in some

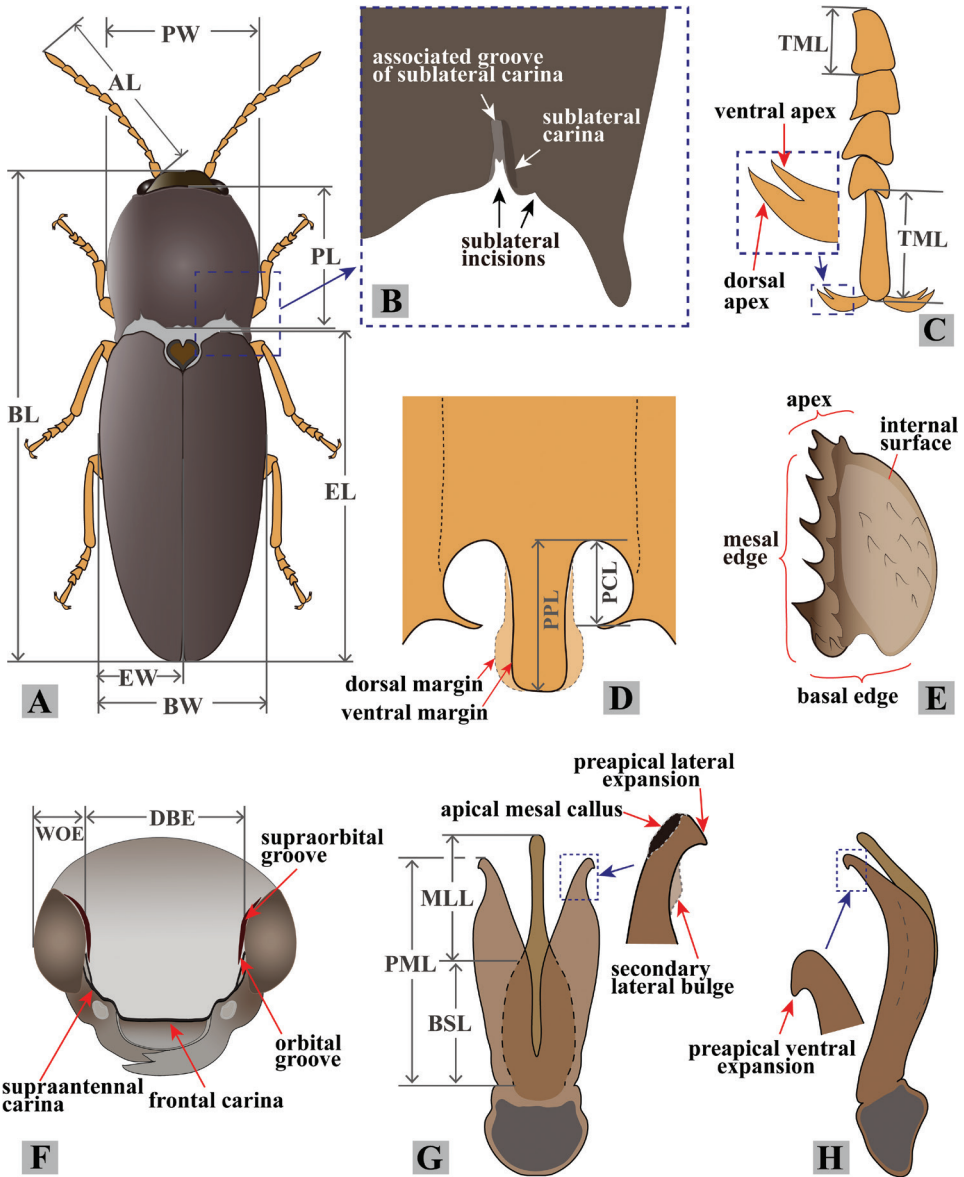


Figure 1. Explanation of measurement and terminology. **A** male habitus (AL: antenna length; BL: body length; BW: body width; EL: elytron length; EW: elytron width; PL: pronotum length; PW: pronotum width) **B** postero-lateral part of pronotum **C** tarsomeres I to V (TML: tarsomere length), with inset showing bifid claw **D** posterior part of prosternum, showing prosternal process, arrows showing its dorsal and ventral margins (PCL: procoxal cavity length; PPL: prosternal process length) **E** proximal sclerite of bursa copulatrix, showing internal surface: with a concavity on basal edge, large spines on mesal edge and minute ones on disc **F** head, frontal view (DBE: distance between eyes; WOE: width of eye) **G** aedeagus, ventral view (BSL: basal strut length; MLL: median lobe length; PML: paramere length), inset showing apical part of paramere **H** aedeagus, lateral view, inset showing apical part of paramere.

(Fig. 1H), apical mesal callus (in most oval, disc-like, with sclerotized sharp edge; see Figs 1G, 4G) present or absent, lateral side with two setae near apex; aedeagus with basal strut ca. 0.8–1.0 × median lobe length; in ventral or dorsal view, median lobe tapered, parallel-sided or apically expanded, apex pointed to rounded to blunt; in lateral view, apex of median lobe bent abruptly dorsad in some (e.g., in *P. magnus*); in lateral view, paramere and median lobe bent 30–45° ventrad near mid-length or apical third.

Female. Body of same or different color as male, some slightly longer and wider than male. Antennae of some shorter than in male. Apex of abdominal ventrite V arcuate to truncate, with deep to shallow incision on each side (Figs 9D, E, 20D), or with elongate deep invagination containing slender blade-like projection (Fig. 15C) (in male: apex of abdominal ventrite V simple, arcuate to slightly sinuate, without incision or invagination). Ovipositor with baculae present; coxites heavily sclerotized. Bursa copulatrix without sclerotized spermathecae; with paired distal and spine-bearing proximal sclerites, proximal sclerites ovoid with emarginate base to elongate and parallel-sided; distal sclerites claw-like and not fused, gradually narrowed to pointed apex; spermathecal gland duct with row of diverticulae in some, base not sclerotized inside bursa (Douglas 2017); anterior end of bursa with a single pedunculate sac.

Checklist and synonymy of world *Phorocardius* species

1. *Phorocardius alterlineatus* Ruan & Douglas, sp. nov. (details under species treatment)

2. *Phorocardius astutus* (Candèze, 1888)

Cardiophorus astutus Candèze, 1888: 681. Type locality: “Teinzò”, Myanmar.

Phorocardius astutus: Fleutiaux 1931: 311 (key to species).

Distribution. Cambodia (Fleutiaux 1931), Laos (Fleutiaux 1931), Vietnam (Fleutiaux 1931), Myanmar (Candèze 1888).

Remarks. Cotype specimens examined (NHMUK). Recognizable by brown-black body with dark appendages; legs with red-brown joints; parameres wedge-like with pre-apical lateral expansions.

3. *Phorocardius bifidus* (Fleutiaux, 1918)

Cardiophorus bifidus Fleutiaux, 1918: 222. Type locality: Bangkok, Thailand.

Phorocardius bifidus: Fleutiaux 1931: 311 (key to species).

Distribution. Thailand (Fleutiaux 1918), Laos (Fleutiaux 1931).

Remarks. Type specimen examined (MNHN). Body brown-black with red-brown appendages; and yellow pubescence. Aedeagus with median lobe parallel-sided, with rounded apex, parameres narrowed to a point without preapical expansions.

4. *Phorocardius comptus* (Candèze, 1860) (details under species treatment)

5. *Phorocardius contemptus* (Candèze, 1860), **comb. nov.**

Fig. 29

Cardiophorus contemptus Candèze, 1860: 202. Type locality: “Hindustan meridional; Pondichery et Mysore” (India: Pudicherry; Karnataka, Mysore). Lectotype designated here.

Distribution. India (Candèze 1860), Myanmar (‘Thagatà’; Candèze 1888), Bangladesh (‘Bengale’; Candèze 1891), Vietnam? (‘Cochinchine’; Fleutiaux 1918; doubtful record).

Remarks. Only a single female syntype was discovered in NHMUK: integument entirely black with dark legs, pubescence yellow. Bursa copulatrix with proximal sclerites (from internal view) ovoid with slight basal concavity; spines present on convex mesal edge, both sides of apex and flattened internal surface. The male syntype described in the original paper was not seen in NHMUK. Since Candèze’s collection before 1869 had been transferred to the NHMUK (Bousquet 2016), this female specimen is studied and designated as the lectotype to fix species concepts.

The examination of the lectotype shows that it resembles *P. comptus* Candèze (1860) in the female genitalia and external characters except for the all-black elytral color. Candèze (1860) also commented that “This may be an entirely black variety of *comptus*”. It is possible that *C. contemptus* is conspecific with *P. comptus*. Because we have not studied any male specimen, *C. contemptus* is treated here as valid.

Type material. (NHMUK) (Photographs of syntype provided by Ms Karine Savard, Agriculture and Agri-food Canada). **Lectotype.** ♀, labels: 1) Syntype [blue ringed disk]; 2) [female symbol]; 3) [red square]; 4) [red square]; 5) 215; 6) C75; 7) Ind. Or Moussour ca; 8) *Cardioph. Contemptus* Cdzé sec. Cdze; 9) Janson Coll. Ex. Deyrolle. 1903.130; 10) NHMUK04016800; 11) Lectotype, *Cardiophorus contemptus* Candèze, 1860, Des. Ruan & Douglas, 2020.

6. *Phorocardius erythronotus* (Candèze, 1860)

Cardiophorus erythronotus Candèze, 1860: 212. Type locality: India: Patna, Dinapur. *Phorocardius erythronotus*: Ôhira 1978: 96 (distribution, photograph of habitus and diagnostic characters).

Distribution. India (Candèze 1860), Nepal (Ôhira 1978).

Remarks. Type material examined (NHMUK). Body brown-black; prothorax, head and antennae red-yellow to red-brown; pronotum in lateral view with lateral carina diverging from hind angle carina. This species is probably not *Phorocardius* because of the presence of pronotal lateral carina. It was not transferred outside *Phorocardius* because we were unable to make a well-supported generic placement without data from female morphology.

7. *Phorocardius flavistriolatus* Ruan & Douglas, sp. nov. (details under species treatment)

8. *Phorocardius florentini* (Fleutiaux, 1895) (details under species treatment)

9. *Phorocardius magnus* Fleutiaux, 1931 (details under species treatment)

10. *Phorocardius maldivianus* Platia, 2015

Phorocardius maldivianus Platia, 2015: 184. Type locality: “Maldives, Meemu Atoll, Kureli Island”.

Distribution. Maldives (Platia 2015).

Remarks. This species is unlikely to truly belong to *Phorocardius* because the pronotal lateral carina diverges from the hind angle carina. The distinctive arcuate parameres with bulbous apices distinguish this species from those of any *Phorocardius* examined by the authors. However, *P. maldivianus* was not transferred outside *Phorocardius* because we were unable to make a well-supported generic placement without data from female morphology or DNA.

11. *Phorocardius manuleatus* (Candèze, 1888) (details under species treatment)

12. *Phorocardius melanopterus* (Candèze, 1878)

Cardiophorus melanopterus Candèze, 1878: 38. Type locality: Cambodia.
Phorocardius melanopterus: Fleutiaux 1931: 311 (key to species).

Distribution. Cambodia (Candèze 1878).

Remarks. Type material examined (RBINS, photograph examined): the head is brown-black, the remainder of the body is brown throughout including the legs and basal four antennomeres (remaining antennomeres are lost), and pronotum with lateral carina diverging from hind angle carina. This species is probably not *Phorocardius* because of having a pronotal lateral carina. It was not transferred outside *Phorocardius* because we were unable to make a well-supported generic placement without data from female morphology.

13. *Phorocardius minutus* Ruan & Douglas, sp. nov. (details under species treatment)

14. *Phorocardius moorii* (Candèze, 1860)

Cardiophorus moorii Candèze, 1860: 206. Type locality: “Madras” (India).

Phorocardius moorii: Ôhira 1978: 96 (distribution, photograph of habitus and diagnostic characters)

Phorocardius moorii: Cate et al. 2007: 206 (distribution).

Distribution. India (Candèze 1860). Nepal (Ôhira 1978).

Remarks. Body black, with four round yellow spots on its elytra. This species is probably a junior synonym of *Elater tetraspilotus* Hope (syntypes of *E. tetraspilotus* and *C. moorii* housed in NHMUK examined). However, dissection of type specimens is required to confirm possible synonymy.

15. *Phorocardius rufiposterus* Ruan & Douglas, sp. nov. (details under species treatment)

16. *Phorocardius systemus* (Candèze, 1860)

Cardiophorus systemus Candèze, 1860: 210. Type locality: “Hindoustan” (India).

Platynychus systemus: Miwa 1934: 212 (distribution).

Phorocardius systemus: Ôhira, 1978: 96 (distribution, photograph of habitus, and diagnostic characters).

Distribution. India (Candèze 1860), Nepal (Ôhira 1978).

Remarks. Type examined (NHMUK). *Cardiophorus systemus* Candèze, 1860 was transferred to *Phorocardius* by Ôhira (1978). However, Miwa (1934) had already treated the same species as a member of the genus *Platynychus*. This species was treated separately as both *Platynychus* and *Phorocardius* by Cate et al. (2007). This species is closer to *Platynychus* rather than *Phorocardius* because, in lateral view, the pronotum has the lateral carina diverging from hind angle carina. However, here we treat this species as a member of *Phorocardius* until more evidence is gathered for transferring it to another genus. Furthermore, the examination of the type specimens of *Cardiophorus bucculatus* Candèze, 1860 and *Cardiophorus systemus* Candèze, 1860 indicates they are probably conspecific.

17. *Phorocardius unguicularis* Fleutiaux, 1918 (details under species treatment)

18. *Phorocardius vicinus* (Kollar, 1848)

Cardiophorus vicinus Kollar, 1848: 507. Type locality: Kashmir.

Phorocardius vicinus: Cate et al. 2007: 206 (distribution).

Distribution. India: Kashmir (Cate 2007).

Remarks. Type specimen examined by photographs (NHMW): 9 mm long, black with dark legs, pubescence yellow. Bursa copulatrix with proximal sclerites ovoid without basal concavity; spines present on convex mesal edge, both sides of apex and flattened internal surface.

19. *Phorocardius yanagiharae* (Miwa, 1927) (details under species treatment)

20. *Phorocardius yunnanensis* Ruan & Douglas, sp. nov. (details under species treatment)

21. *Phorocardius zhiweii* Ruan, Douglas & Qiu, sp. nov. (details under species treatment)

Species transferred from *Phorocardius* to *Displatynychus*

The following *Phorocardius* species are shown, in their original publications (or in the examined type specimens) to have the diagnostic characters of *Displatynychus* and not *Phorocardius*. While these species have *Phorocardius*-like claws, they are shown to have the following diagnostic characters of *Displatynychus*: pronotal lateral carina distinct from hind-angle carina and hidden in dorsal view by overhanging edge of upper part of pronotum; and female bursa copulatrix with base of spermathecal gland duct sclerotized into complex tube-like structure.

Recently described *Phorocardius* species from south Asia (*P. maldivianus* Platia, 2015; *P. pakistanicus* Platia & Ahmed, 2016; *P. tibialis* Platia & Ahmed, 2016) could be distinguished from all Chinese *Phorocardius* species using the species descriptions. We recommend the transfer of *P. pakistanicus* and *P. tibialis* to *Displatynychus* Ôhira, 1987. However, we do not recommend the transfer of *P. maldivianus* outside *Phorocardius* because we were unable to make a well-supported generic placement without data from female morphology or DNA.

1. *Displatynychus bombycinus* (Candèze, 1895), **comb. nov.**

Cardiophorus bombycinus Candèze, 1895: 46. Type locality: “Darjeeling” (India).
Phorocardius bombycinus: Cate et al. 2007: 206 (distribution).

Distribution. India: west Bengal (Candèze 1895).

Remarks. This species matches *Displatynychus* and not *Phorocardius* in two key diagnostic characters listed above. Type specimen examined (RBINS): “Coll. R.I.Sc.N.B./ Inde Kurseong”; “Collection/ E. Candèze”; “n.sp. 11. 1982/ Bombycinus/ Cand./ Kurseong”; type has pronotum with lateral carina diverging from hind angle carina and nearly reaching the anterior edge of the pronotum. Female specimen from India (NHMUK): Darjeeling (NHMUK014016975), with base of spermathecal gland duct sclerotized into complex tube-like structure and distal sclerites absent.

2. *Displatynychus pakistanicus* (Platia & Ahmed, 2016), **comb. nov.**

Phorocardius pakistanicus Platia & Ahmed, 2016: 16. Type locality: “Pakistan, Thar”.

Distribution. Pakistan (Platia and Ahmed 2016).

3. *Displatynychus sobrinus* (Laporte, 1840), **comb. nov.**

Caloderus sobrinus Laporte, 1840: 250. Type locality: “Hindoustan” (south Asia).
Cardiophorus sobrinus: Candèze 1860: 210. (key to species, redescription).

Dicronychus sobrinus: Ôhira 1973: 38 (distribution).

Phorocardius sobrinus: Ôhira 1978: 95 (distribution, photograph of habitus, and diagnostic characters).

Phorocardius sobrinus: Cate et al. 2007: 206 (distribution).

Distribution. India (Ôhira 1973), Sri Lanka (Laporte 1840; Candèze 1860; Ôhira 1973), Cambodia (Fleutiaux 1918), Nepal (Ôhira 1978).

Remarks. This species matches *Displatynychus* and not *Phorocardius* in two key diagnostic characters mentioned above. Type material was not examined (probably in MNHN), but non-type specimens at NHMUK (Janson Coll.) had pronotum with lateral carina diverging from hind angle carina and nearly reaching the anterior edge of the pronotum. Female specimen at NHMUK (NHMUK014017117) with base of spermathecal gland duct sclerotized into complex tube-like structure and distal sclerites absent.

4. *Displatynychus tibialis* (Platia & Ahmed, 2016), comb. nov.

Phorocardius tibialis Platia & Ahmed, 2016: 17. Type locality: “Pakistan, Chakri, Islamabad”.

Distribution. Pakistan (Platia and Ahmed 2016).

Taxonomy of Chinese *Phorocardius* species

Key to Chinese *Phorocardius* species

- 1 Procoxal cavities closed (Fig. 15E, narrowly open in rare cases); color of dorsum and venter anteriorly black, fading to red-brown or yellow-brown posterad; apex of last abdominal ventrite (ventrite V) of female deeply emarginate, with slender blade-like projection at middle (Fig. 15C); from dorsal and ventral views, paramere of aedeagus with preapical lateral expansion triangular, not acute (Fig. 14G) *P. rufiposterus* sp. nov.
- Procoxal cavities open (e.g., Fig. 25A); body color not fading from black to paler posterad; apex of last abdominal ventrite (ventrite V) of female without longitudinal slender blade-like structure; from dorsal and ventral views, paramere of aedeagus with preapical lateral expansion absent, rounded or acute, not triangular **2**
- 2 Body length less than 7.0 mm; scutellar shield with antero-lateral edge evenly convex and posterior apex narrowly rounded; tarsal claw with ventral apex much smaller than dorsal one (Fig. 12A, indicated by arrow); apex of paramere pointed and turned laterad in ventral view (Fig. 12E, I, indicated by arrows) *P. minutus* sp. nov.
- Body length greater than 7.0 mm; scutellar shield with antero-lateral edge sinuate and posterior apex pointed; tarsal claw with ventral apex as large as dorsal one

- (Figs 4A, 10B, indicated by blue arrow); paramere apex not pointed and bent laterad..... **3**
- 3 Elytra with metallic luster; pronotum and hypomeron entirely red except posterior edge red-brown or black..... **4**
- Elytra without metallic luster; pronotum and hypomeron black, brown or with longitudinal midline black and remainder red..... **5**
- 4 Elytra black, with metallic blue to purple luster; paramere with preapical lateral expansion in ventral view, (Fig. 7E), with sides rounded, facing laterally, without apical mesal callus; prosternal process with outline of ventral apex rounded-rectangular in ventral view (Fig. 25C)..... ***P. florentini* (Fleutiaux, 1895)**
- Elytra metallic green; paramere of aedeagus without preapical lateral expansion, with apical mesal callus (Fig. 21D); prosternal process with outline of ventral apex evenly rounded in ventral view (Fig. 25I) ***P. zhiweii* sp. nov.**
- 5 Dorsum bicolored, with yellow to red maculation; if dorsum unicolor, apex of median lobe of aedeagus dilated in ventral view (Figs 10D, E, 11F)..... **6**
- Dorsum unicolored, without maculation; in ventral view, apex of median lobe of aedeagus not dilated..... **8**
- 6 Body dark brown, elytra with longitudinal yellow stripes; ventral surface of prosternal process not strongly narrowed posterad in ventral view, with apex truncate to slightly convex (Fig. 25A, B); paramere without preapical lateral expansion in ventral view..... **7**
- Body entirely black, yellow or mixed with both yellow and black (Fig. 11A); ventral surface of prosternal process strongly narrowed posterad in ventral view, with apex acute (Fig. 25E); paramere with small and round preapical lateral expansion in ventral view (Fig. 11F) ***P. manuleatus* (Candèze, 1888)**
- 7 Each elytron with three separate slender longitudinal yellow stripes on interstriae III, V and VII (Fig. 2A); aedeagus gradually narrowed from base to apex in lateral view (Fig. 2H); apex of median lobe narrowly rounded to angulate in ventral view (as in Fig. 2G, I) ***P. alterlineatus* sp. nov.**
- Each elytron with a single longitudinal yellow stripe covering basal half of interstria IV and interstriae V to VII. (Fig. 4A, C); in lateral view, aedeagus of equal thickness from base to apical fifth, only slightly narrowed at apical fifth (as in Fig. 4N); apex of median lobe truncate to broadly rounded in ventral view ***P. flavistriolatus* sp. nov.**
- 8 Head with frontal carina convex in frontal view (Fig. 16C). Pronotum with interspaces between punctures 0.3–1 × average puncture diameter (Fig. 16D). Elytral length to pronotal length ratio 2.7–3.1. Paramere of aedeagus with apex needle-like and simple, without preapical lateral expansion (Fig. 16F)..... ***P. unguicularis* (Fleutiaux, 1918)**
- Head with frontal carina straight in frontal view. Pronotum with interspaces between punctures 1–3 × average puncture diameter. Elytral length to pronotal length ratio 2.5–2.7. Paramere of aedeagus not needle-like at apex, with preapical lateral expansion **9**

- 9 Posterior angle of pronotum with lateral edge convex, strongly bulged laterally in dorsal view (Fig. 17C, D). Median lobe of aedeagus with apex not dilated or bent dorsad in lateral view (Fig. 17G)..... *P. yanagiharae* (Miwa, 1927)
- Posterior angle of pronotum with lateral edge straight to slightly convex, not strongly bulged in dorsal view. Median lobe of aedeagus with apex dilated (Fig. 19F) or bent dorsad (Fig. 8G) in lateral view **10**
- 10 Dorsum matt, brown to red-brown. Aedeagus with apex of median lobe bent abruptly dorsad in lateral view (Fig. 8G); in ventral and dorsal views, paramere with a secondary lateral bulge present before preapical lateral expansion (Fig. 8D, E, F, indicated by arrows)..... *P. magnus* Fleutiaux, 1931
- Dorsum entirely black and shiny. Aedeagus with apex of median lobe not bent dorsad in lateral view (Fig. 19F); in ventral and dorsal views, paramere without a secondary lateral bulge (Fig. 19D, E) *P. yunnanensis* sp. nov.

1. *Phorocardius alterlineatus* Ruan & Douglas, sp. nov.

<http://zoobank.org/E5EEBBF2-D73F-498B-88C4-99452A547603>

Figs 2, 3, 23A, 24A, 25A, 26A

Type locality. Shaanxi Prov., Yan-an (36.622°N, 109.457°E, alt. 993 m).

Etymology. The name of this species refers to the alternating longitudinal maculation on elytra.

Distribution. China (Shaanxi, Hubei, Sichuan, Guangxi).

Differential diagnosis. Body length greater than 7.0 mm; integument dark brown (non-metallic), each elytron with three separate yellow stripes along interstriae III, V, and VII. Prothorax: procoxal cavities open. Prosternal process not strongly narrowed posterad to ventral apex in ventral view, with apex truncate to slightly rounded. Pterothorax: scutellar shield with posterior apex pointed. Tarsal claw with ventral apex not smaller than dorsal apex. Male genitalia: paramere without preapical lateral expansion or apical mesal callus. Female: apex of last abdominal ventrite (ventrite V) simple, not emarginate at apex.

This species is unique in *Phorocardius* in its alternating dark and yellow stripes on the elytra, the aedeagus is also unique due to its simple shape: without any preapical lateral expansion (but with ventral hook-like expansion).

Phorocardius alterlineatus Ruan & Douglas, sp. nov. resembles *P. flavistriolatus* Ruan & Douglas, sp. nov. and *P. comptus* (Candèze, 1860) in having longitudinal yellow maculation on the elytron, but it could be distinguished from the latter two species by the following characters. In *P. alterlineatus* Ruan & Douglas, sp. nov., aedeagus gradually narrowed from base to apex in lateral view; apex of median lobe narrowly rounded in ventral view; and each elytron with three slender longitudinal stripes present separately on interstriae III, V, and VII, which partly merged near base and apex; while in *P. flavistriolatus* Ruan & Douglas, sp. nov., in lateral view, aedeagus with equal breadth from base to apical fifth, only slightly narrowed at apical fifth; apex of median

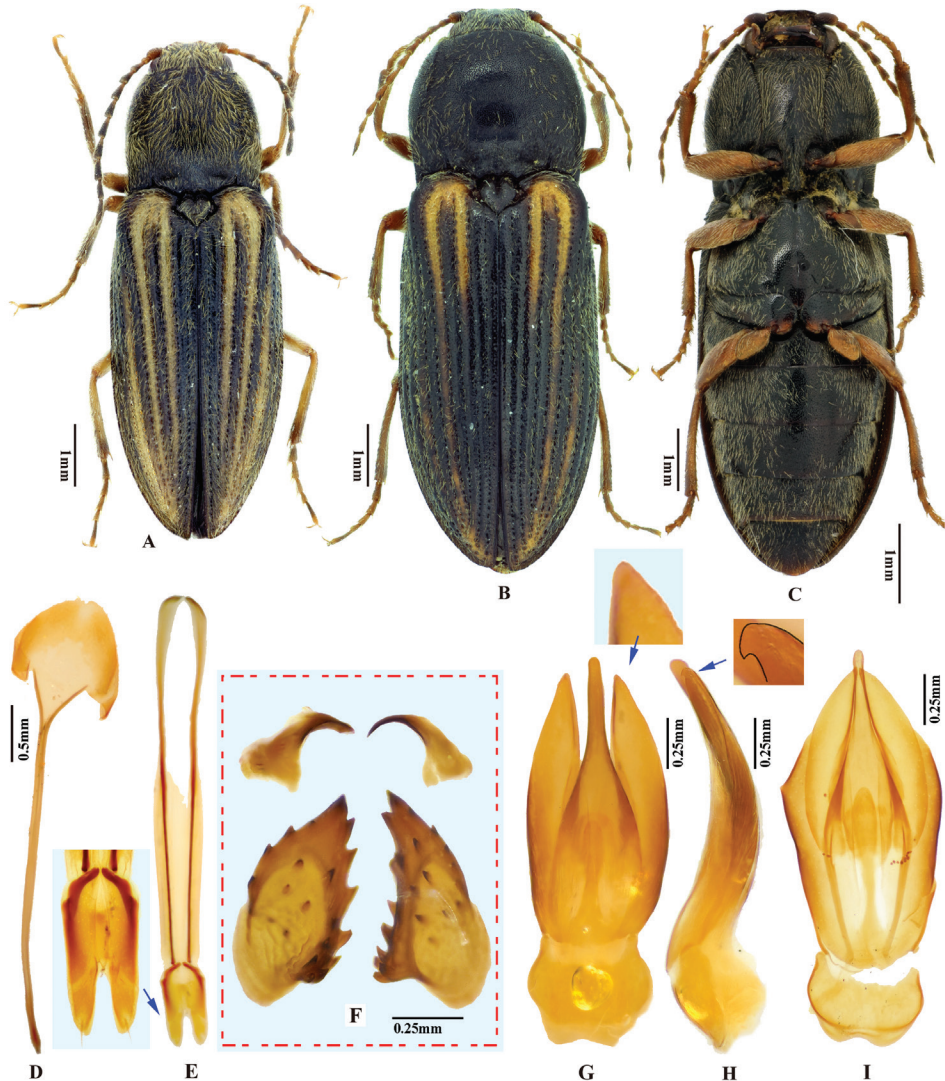


Figure 2. *Phorocardius alterlineatus* Ruan & Douglas, sp. nov. **A** male habitus, paratype (Shaanxi, Zha-shui County, Niu-bei-liang), dorsal view **B** female habitus, paratype (Shaanxi, Shan-luo, Zha-shui County, Ying-pan township), dorsal view **C** female habitus, paratype (same individual as in inset B), ventral view **D** female abdominal sternite VIII **E** ovipositor, dorsal view (paratype), arrow indicating coxites **F** distal (upper side) and proximal sclerites of bursa copulatrix (the two proximal sclerites are viewed from different angles, resulting in different shapes shown above) **G** aedeagus, dorsal view (paratype, dry), arrow indicating apex of paramere **H** aedeagus, lateral view (paratype, dry), arrow indicating apex of paramere. **I** aedeagus (mounted in glycerin), dorsal view (paratype).

lobe truncate to broadly rounded in ventral view; and each elytron with a single broad stripe covering basal half of interstria IV and interstriae V–VII.

In *Phorocardius alterlineatus* Ruan & Douglas, sp. nov., the parameres of the aedeagus have apical lateral expansions in dorsal view and lack preapical ventral expansions in

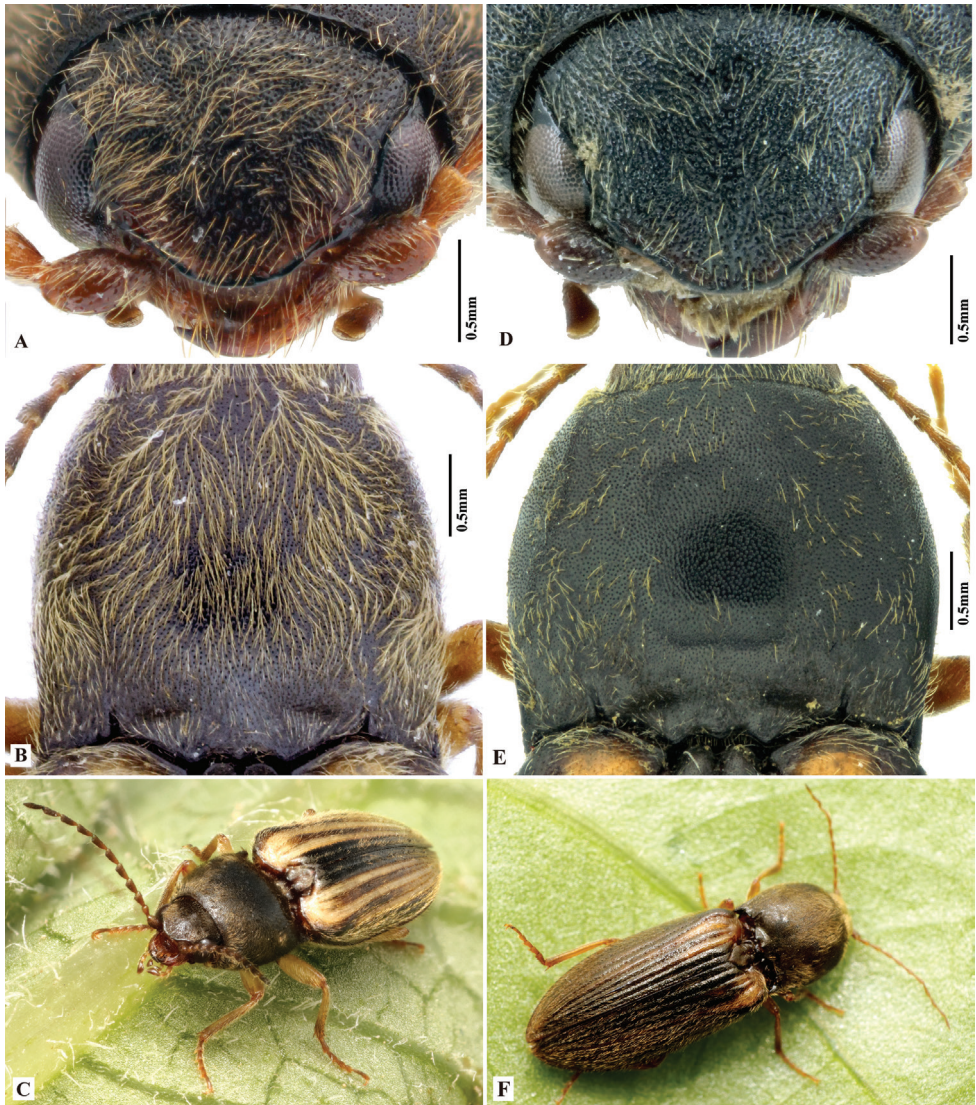


Figure 3. *Phorocardius alterlineatus* Ruan & Douglas, sp. nov. **A** male head, frontal view (paratype) **B** male pronotum, dorsal view (paratype) **C** male on foliage (indoors; holotype) **D** female head, frontal view (paratype) **E** female pronotum, dorsal view (paratype) **F** female on foliage (indoors; paratype; collected from Shaanxi, Yan-an).

lateral view; body brown-black; and each elytron with three slender longitudinal stripes present separately on interstriae III, V, and VII, with pale stripes partly joined near base and apex; while in *P. comptus* (Candèze, 1860), the parameres lack apical lateral expansions in dorsal view and have preapical ventral expansions in lateral view; body black; and a single broad longitudinal stripe covering four interstriae (interstriae V–VIII).

Description. (Based on all type specimens) Body brown-black. Each elytron with three separate longitudinal yellow stripes along interstriae III, V, and VII, partly joined

near base and apex; stripes on mid-length of elytron absent or reduced in some females. Elytral stripes pale yellow in most males, orange in females. Antenna brown to dark brown, with first two antennomeres paler. Legs yellow-brown to brown, darker on tarsomere V and tibial apex. Body with yellow pubescence.

Measurements. (based on all type specimens) Male body length 7.3–9.2 mm, width 2.3–3.0 mm. Female body length 8.2–10.6 mm, width 2.7–3.7 mm. Body length to width ratio 2.7–3.0. Pronotal width to length ratio 1.1–1.2. Pronotal width to body width ratio 0.83–0.90. Elytral length to pronotal length ratio 2.6–2.8; elytron length to width ratio 4.0–4.2.

Head. Frons and vertex with interspaces between punctures $0.5\text{--}1.0 \times$ average puncture diameter; punctures slightly sparser at centre of vertex. Frontal carina convex in frontal view. Distance between eyes to width of eye ratio 4.2–4.5. Antenna with last antennomere entirely reaching beyond posterior angle of pronotum in male, only reaching to posterior angle in female. Antenna length to body length ratio, in male 0.39–0.41; in female 0.35–0.37. Proportions of antennomere lengths (male): 100 (scape); 53–58; 75–81; 82–83; 81–85; 83–88; 84–86; 85–90; 85–90; 85–90; 100–130.

Prothorax. Pronotum in dorsal view: sides evenly convex from anterior edge to constriction near posterior fourth, widest near mid-length; posterior angles with lateral sides almost straight, not bulged; surface with deep punctures, interspaces between punctures $0.5\text{--}1.0 \times$ average puncture diameter. In ventral view, ventral surface of prosternal process with sides carinate and slightly and gradually narrow from anterior to posterior end, with apex almost truncate (Fig. 25A). In lateral view, prosternal process with ventral surface curved slightly dorsad; with posterior end (i.e., area between ventral and dorsal apices (sensu Douglas 2011, 2017)) slightly concave to almost straight (Fig. 24A, upper arrow). Procoxal cavities open.

Pterothorax (Figs 24A, 25A). Mesepisternum in ventral view with antero-mesal corner broadly rounded, facing antero-mesally (Fig. 25A, upper (green) arrow). Projections on posterior edge of mesosternum: in ventral view present (Fig. 25A, lower (red) arrow); in lateral view present, acute, produced anteriorly (Fig. 24A, red arrow). Scutellar shield: width to length ratio 0.97–1.00; anterolateral edges slightly sinuate; posterior apex pointed. Elytra: upper edge of epipleura with minute serrations.

Legs. Length ratio of metatarsomeres I–V (excluding claws): 100; 68–74; 66–70; 51–53; 125–128. Claw with ventral apex almost as large as dorsal apex.

Abdomen. Lateral edges of visible abdominal ventrites I–V with minute serrations.

Male genitalia. Robust in dorsal view (Fig. 2G); in lateral view slender, gradually narrowing from base to apex. Median lobe in ventral view narrowed from base to mid-length; parallel-sided and slender on apical half, apex narrowly rounded. Median lobe in lateral view gently and evenly curved ventrad from base to apex, apex rounded. Paramere in dorsal view: wide from base to mid-length, gradually narrowed beyond mid-length, angulate at apex; preapical lateral expansion and apical mesal callus absent; width $2.5\text{--}3.5 \times$ median lobe width (measured at mid-length of paramere and median lobe respectively). Paramere in lateral view: slender, gradually narrowed and evenly curved ventrad from base to apex; apex with sharp hook-shaped preapical ventral expansion (Fig. 2H, indicated by blue arrow).

Female. Body color slightly blacker than male (Fig. 2B), elytral longitudinal yellow stripes partly absent on mid-length of elytron. Apex of abdominal ventrite V convex (Fig. 26A). Bursa copulatrix with proximal sclerites ovoid, apex acute, base slightly concave; with numerous spines on concave internal surface: each with 9–12 large spines on mesal edge, 6–8 smaller ones on disc.

Type material. Holotype. ♂ (SZPT), labels: 1) **Shaanxi**, Yan-an (延安), Yan-an University, Yao-yuan Holiday Hotel, leg. Yongying Ruan et al. 2018-VI-22–23 [in Chinese]; 2) 36.622°N, 109.457°E, 993 m; 3) Holotype *Phorocardius alterlineatus* sp. nov. Des. Ruan & Douglas, 2019.

Paratypes (100♂, 136♀). 3♀ (SZPT), labels: 1) **Shaanxi**, Yan-an (延安), Yan-an University, Yao-yuan Holiday Hotel, leg. Yongying Ruan et al. 2018-VI-22–23, light trap [in Chinese]; 2) 36.622°N, 109.457°E, 993 m; 3) Paratype *Phorocardius alterlineatus* sp. nov. Des. Ruan & Douglas, 2019. • 2♀ (IZCAS), labels: 1) **Shaanxi**, Liu-ba County (留坝县), Huo-shao-dian, Hong-ya-gou, 2012.VI.23, 33.51°N 106.93°E, 986 m, leg. Yi Hua [in Chinese]; 2) Paratype *Phorocardius alterlineatus* sp. nov. Des. Ruan & Douglas, 2019. • 1♀ (IZCAS), labels: 1) **Shaanxi**, Tai-bai County (太白县), Huang-bai-yuan, He-tao-ping, 2012.VI.19, 33.822°N 107.556°E, leg. Li Sha, light trap [in Chinese]; 2) Paratype *Phorocardius alterlineatus* sp. nov. Des. Ruan & Douglas, 2019. • 1♂ (IZCAS), labels: 1) **Shaanxi**, Liu-ba County (留坝县), 2012.VI.21, 33.616°N 106.907°E, 980 m, leg. Li Sha; 2) Paratype *Phorocardius alterlineatus* sp. nov. Des. Ruan & Douglas, 2019. • 1♂7♀ (in IZCAS, 1♀ to be transferred to LQCC), labels: 1) **Shaanxi**, Qin-ling Botanical Garden (秦岭植物园), grand canyon, 2012.VII.5, 33.9282°N 108.3525°E, leg. Hua Yi, 925 m [in Chinese]; 2) Paratype *Phorocardius alterlineatus* sp. nov. Des. Ruan & Douglas, 2019. • 1♀ (IZCAS), labels: 1) **Shaanxi**, Qin-ling Botanical Garden (秦岭植物园), Bai-yang-ji-li-gou, 2012.VII.6, 33.9827°N 108.3282°E, leg. Hua Yi, 698–738 m [in Chinese]; 2) Paratype *Phorocardius alterlineatus* sp. nov. Des. Ruan & Douglas, 2019. • 1♂ (IZCAS), labels: 1) **Shaanxi**, Zha-shui County, Niu-bei-liang (牛背梁), 2013.VII.1–2, leg. Junzhi Cui & Yuanyuan Lu, 33.85742°N, 108.99886°E [in Chinese]; 2) Paratype *Phorocardius alterlineatus* sp. nov. Des. Ruan & Douglas, 2019. • 1♀ (IZCAS), labels: 1) **Shaanxi**, Shan-luo, Zha-shui County, Ying-pan township (营盘镇), Light trap 2014.VII.29, leg. Yuanyuan Lu, Chinese Academy of Sciences [in Chinese]; 2) 955 m, pure ethanol, 33.776572°N 109.043397°E, Chinese Academy of Sciences [in Chinese]; 3) Paratype *Phorocardius alterlineatus* sp. nov. Des. Ruan & Douglas, 2019. • 53♂67♀ (SZPT), labels: 1) **Shaanxi**, Zi-wu-ling reserve (子午岭保护区), Hua-shu-gou, collecting method FIT, 2019.VI–VII [in Chinese]; 2) Paratype *Phorocardius alterlineatus* sp. nov. Des. Ruan & Douglas, 2020. • 28♂38♀ (SZPT), labels: 1) **Shaanxi**, Zi-wu-ling reserve (子午岭保护区), Shi-hui-gou, collecting method FIT, 2019.VI–VII [in Chinese]; 2) Paratype *Phorocardius alterlineatus* sp. nov. Des. Ruan & Douglas, 2020. • 9♂3♀ (SZPT), labels: 1) **Shaanxi**, Zi-wu-ling reserve (子午岭保护区), Chen-jia-he, sweeping, leg. Lei Dang, 2019.VI.26 [in Chinese]; 2) Paratype *Phorocardius alterlineatus* sp. nov. Des. Ruan & Douglas, 2020. • 5♂9♀ (SZPT), labels: 1) **Shaanxi**, Zi-wu-ling reserve (子午岭保护区), Chen-jia-he, collecting method MT-5, 2019.VII.5–19 [in Chinese]; 2) Paratype *Phorocardius alterlineatus* sp. nov. Des. Ruan & Douglas, 2020. • 1♀ (SZPT),

ex. LQCC), labels: 1) **Sichuan**, Jiu-zai-gou (九寨沟), 2015.6.11, leg. Hao Huang [in Chinese]; 2) Paratype *Phorocardius alterlineatus* sp. nov. Des. Ruan & Douglas, 2019. • 1♂ (SZPT), labels: 1) **Hubei**, Wu-dang Mts., Chao-tian-gong (朝天宫), 1982.VII.5; 2) *Phorocardius comptus* (Candèze), det. Shihong Jiang 19; 3) 7.30*2.60 cm; 4) Paratype *Phorocardius alterlineatus* sp. nov. Des. Ruan & Douglas, 2019. • 1♂ (SZPT), labels: 1) **Hubei**, Wu-dang Mts., Zi-xiao (紫霄), 1982.VII.10; 2) *Phorocardius comptus* (Candèze), det. Shihong Jiang 1993; 3) Paratype *Phorocardius alterlineatus* sp. nov. Des. Ruan & Douglas, 2019. • 1♀ (SZPT), labels: 1) **Hubei**, Wu-dang Mts., Jin-ding (金顶), 1982.VII.9; 2) *Phorocardius comptus* (Candèze), det. Shihong Jiang 1993; 3) Paratype *Phorocardius alterlineatus* sp. nov. Des. Ruan & Douglas, 2019. • 1♀ (SZPT), labels: 1) **Hubei**, Wu-dang Mts., Lao-yan (老燕), 1983.VII.2; 2) *Phorocardius comptus* (Candèze), det. Shihong Jiang 1993; 3) Paratype *Phorocardius alterlineatus* sp. nov. Des. Ruan & Douglas, 2019. • 1♀ (SZPT), labels: 1) **Hubei**, Wu-dang Mts., Nan-yan (南岩), 1983.VII.2; 2) *Phorocardius comptus* (Candèze), det. Shihong Jiang 1991; 3) Paratype *Phorocardius alterlineatus* sp. nov. Des. Ruan & Douglas, 2019. • 1♂ (TARI, ex. SZPT), labels: 1) **Guangxi**, Jin-xiu, Tong-shui township (桐水镇), VI-25.2006, Shenzhen Polytechnic [in Chinese]; 2) Paratype *Phorocardius alterlineatus* sp. nov. Des. Ruan & Douglas, 2019.

Remarks. Specimens examined were from low to middle elevations (0–2500 m), temperate to subtropical mountain evergreen forests in central and south China. Specimens of this species were collected at different environments using variable collecting methods, including flight interception trap (in forests), malaise trap (in forests), sweeping (on shrubs), and light trap (near a hill in suburbs of a city). Specimens came to light traps, or were caught by sweep-netting vegetation in daylight. This suggests that this species is nocturnal and diurnal. This species is known from central China (i.e., the boundary between the Palearctic and Oriental Regions), only one specimen examined is from south China (Oriental Region).

In the field, this beetle was spotted running on multiple plants. We have observed one live adult in the field with an aphid in its mouthparts. However, individuals taken back to containers in the laboratory were not observed to feed on live aphids presented there. Further evidence is required to learn the adult and larval feeding habits of this species.

Some of the paratype specimens of *P. alterlineatus* sp. nov. Ruan & Douglas were previously misidentified and used for distributional records as *P. comptus* in Jiang (1993) and Jiang and Wang (1999). The label information for these specimens is listed as follows. 1♂ (SZPT), labels: 1) Hubei, Wu-dang Mts., Chao-tian-gong (朝天宫), 1982.VII.5; 2) *Phorocardius comptus* (Candèze), det. Shihong Jiang 19; 3) 7.30*2.60 cm. • 1♂ (SZPT), labels: 1) Hubei, Wu-dang Mts., Zi-xiao (紫霄), 1982.VII.10; 2) *Phorocardius comptus* (Candèze), det. Shihong Jiang 1993. • 1♀ (SZPT), labels: 1) Hubei, Wu-dang Mts., Jin-ding (金顶), 1982.VII.9; 2) *Phorocardius comptus* (Candèze), det. Shihong Jiang 1993. • 1♀ (SZPT), labels: 1) Hubei, Wu-dang Mts., Lao-yan (老燕), 1983.VII.2; 2) *Phorocardius comptus* (Candèze), det. Shihong Jiang 1993. • 1♀ (SZPT), labels: 1) Hubei, Wu-dang Mts., Nan-yan (南岩), 1983.VII.2; 2) *Phorocardius comptus* (Candèze), det. Shihong Jiang 1991.

2. *Phorocardius flavistriolatus* Ruan & Douglas, sp. nov.

<http://zoobank.org/64BB27C0-B42E-40C7-A0AD-5CE7217C549B>

Figs 4–6, 23B, 24B, 25B, 26B

Type locality. China: Henan Prov., Nan-Yang City, Bao-tian-man National Nature Reserve.

Etymology. The name of this species is derived from the yellow stripes on its elytra.

Distribution. Central China (Henan, Shaanxi, Sichuan).

Differential diagnosis. Body length 7.0–12 mm; integument dark brown (non-metallic), each elytron with a longitudinal yellow stripe covering basal half of interstria IV and interstriae V to VII. Prothorax: procoxal cavities open; prosternal process not strongly narrowed from anterior base posterad to ventral apex in ventral view, ventral apex straight to slightly concave. Pterothorax: scutellar shield with posterior apex pointed. Tarsal claw with ventral apex not smaller than dorsal apex. Male genitalia: paramere without preapical lateral expansion, with apical mesal callus present. Female: apex of last abdominal ventrite (ventrite V) simple, not emarginate at apex.

This species is unique in its longitudinal yellow elytral maculation, aedeagus with apical fourth of paramere compressed and gradually narrowing towards apex, and with apical mesal part of paramere turned ventrad (Fig. 6).

Phorocardius flavistriolatus Ruan & Douglas, sp. nov. resembles *P. comptus* in having a longitudinal yellow stripe on each elytron. They can be separated by the following combination of characters: in *P. flavistriolatus* Ruan & Douglas, sp. nov., each elytron with a longitudinal yellow stripe covering basal half of interstria IV and interstriae V–VII, interstria VIII is entirely brown-black; female with pronotum not strongly enlarged, sides of pronotum only gently convex, width of pronotum to elytra ratio ca. 0.83–0.85, and proximal sclerites of bursa copulatrix with deep basal emargination; while in *P. comptus*, each elytron with a longitudinal yellow stripe covering interstriae V–VIII, interstria IV is entirely black; female with pronotum strongly enlarged, sides of pronotum strongly convex, width of pronotum to elytra ratio ca. 0.90–0.92 (measured in two specimens), and proximal sclerites of bursa copulatrix without basal emargination or with emargination narrower than 1/3 width of sclerite. The aedeagus of *P. flavistriolatus* Ruan & Douglas, sp. nov. has parameres with no apical or preapical expansion, with apical mesal callus present; while *P. comptus* has acute apical lateral expansions, without apical mesal callus.

Phorocardius flavistriolatus Ruan & Douglas, sp. nov. is similar to *P. alterlineatus* Ruan & Douglas, sp. nov. in having yellow stripes on the elytra. However, they can be separated by the following characters: in *P. flavistriolatus* Ruan & Douglas, sp. nov., in lateral view, aedeagus with equal breadth from base to apical fifth, only slightly narrowed at apical fifth; apex of median lobe truncate to broadly rounded in ventral view; and each elytron with a single broad stripe covering basal half of interstria IV and interstriae V–VII; while in *P. alterlineatus* Ruan & Douglas, sp. nov., aedeagus gradually narrowed from base to apex in lateral view; apex of median lobe narrowly rounded in ventral view; and each elytron with three slender longitudinal stripes present separately on interstriae III, V, and VII, which partly merged near base and apex.

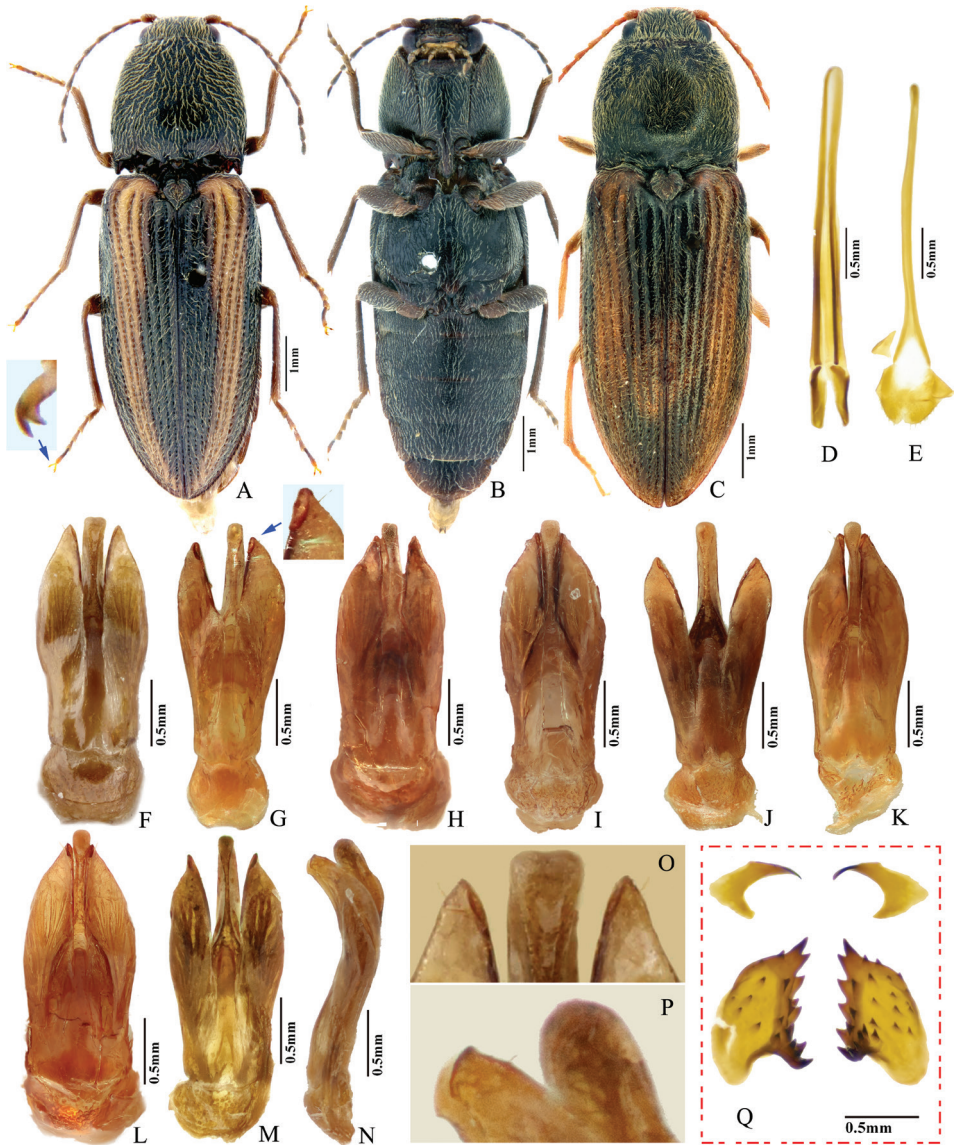


Figure 4. *Phorcardius flavistriolatus* Ruan & Douglas, sp. nov. **A** habitus of holotype, male, dorsal view, arrow indicating claw **B** habitus of holotype, male, ventral view **C** female habitus, dorsal view (paratype; Sichuan, Bao-xing County, Feng-tong-zai National Nature Reserve) **D** ovipositor, dorsal view (paratype) **E** female abdominal sternite VIII, dorsal view (paratype) **F–N** aedeagus of holotype, ventral view **G–N** ventral or lateral view of aedeagi of paratype specimens from different localities, indicating variations in shape [collecting information as follows **G, H** Sichuan Prov., Shi-mian, Li-zi-ping National Nature Reserve, Zi-ma reserve station, VII-27-2016 **I** Sichuan, Lu-ding County, Xin-xing township, 2000 m, 2009.VII.2–7 **J, K** Sichuan Prov., Lu-ding County, Mo-xi township, 1500 m–1600 m, 1983.VI.17–19 **L** Shaanxi Prov., Fo-ping County, alt. 843 m, 2007.VIII.16 **M, N** Shaanxi Prov., Ning-shan County, Shi-ba-zhang-pu-bu Scenic Spot, 15.VIII.2013], arrow indicating apex of paramere **O** apical part of aedeagus of holotype, ventral view **P** apex of aedeagus of paratype, lateral view **Q** distal (upper side) and proximal sclerites of bursa copulatrix (paratype).

Description. (based on all type specimens) Body brown-black, matt; antennae and legs paler, brown to yellow-brown. Head brown-black. Pronotum brown-black, with posterior edge brown. Scutellar shield brown-black. Elytra brown-black, each elytron with a longitudinal yellow stripe covering basal half of interstria IV and interstriae V to VII, epipleura orange at base, dark orange on remainder. Ventral surface entirely brown-black. Body with yellow-grey pubescence.

Measurements. (based on all type specimens) Male body length 7.1–9.6 mm, width 2.2–2.9 mm. Female body length 8.0–11.0 mm, width 2.7–3.7 mm. Body length to width ratio 2.9–3.0. Pronotal width to length ratio 1.1–1.2. Pronotal width to body width ratio 0.82–0.85. Elytral length to pronotal length ratio 2.6–2.7; elytron length to width ratio 3.9–4.2.

Head. Frons and vertex punctures with interspaces $0.5\text{--}1.0 \times$ average puncture diameter; punctures sparser at centre of vertex. Frontal carina in frontal view convex, not straight. Distance between eyes to width of eye ratio 3.6–3.9. Antenna barely extending beyond posterior angle of pronotum. Antenna length to body length ratio, in male 0.39–0.41, in female 0.36–0.38. Proportions of antennomere lengths: 100 (scape); 52–60; 71–73; 71–73; 72–76; 72–76; 72–76; 73–78; 73–78; 73–78; 90–100.

Prothorax. Pronotum in dorsal view: sides evenly convex from anterior edge to constriction near posterior fourth, nearly straight at posterior fourth, widest near posterior third; posterior angles with lateral sides almost straight, not bulged; surface with interspaces between punctures $1\text{--}2 \times$ average puncture diameter. In ventral view, ventral surface of prosternal process with sides carinate and slightly and gradually narrow from anterior to mid-length, parallel from mid-length to apex, with apex slightly convex to almost straight. In lateral view, prosternal process with ventral surface curved slightly dorsad; posterior end weakly concave or not (Fig. 24B, upper arrow). Procoxal cavities open.

Pterothorax (Figs 24B, 25B). Mesepisternum in ventral view with antero-mesal corner angulate (Fig. 25B, upper (green) arrow). Projections on posterior edge of mesosternum: in ventral view present (Fig. 25B, lower (red) arrow); in lateral view present, acute, strongly produced anteriorly (Fig. 24B, lower (red) arrow). Scutellar shield: width to length ratio 0.84–0.9; anterolateral edges slightly sinuate; posterior apex pointed. Elytra: upper edge of epipleura with minute serrations.

Legs. Length ratio of metatarsomeres I–V (excluding claws): 100; 77–81; 65–69; 48–60; 121–123. Claw with ventral apex almost as large as dorsal apex.

Abdomen. Lateral edges of visible abdominal ventrites I–V with minute serrations.

Male genitalia (Fig. 4F–P). Robust from ventral and lateral views. Median lobe in ventral view with ridge along midline; narrowed from base to basal third, parallel-sided from basal third to apex, apex broadly rounded to truncate. Median lobe in lateral view curved ventrad from base to apex, apex rounded with angulate dorsal and ventral corners (Fig. 4P). Paramere in ventral view: robust, widest near mid-length, gradually narrowing towards apex, apical part with mesal side turned ventrad in varying degree (Fig. 6), result in different shapes in ventral view; apex with apical mesal callus present (Figs 4O, 6), without preapical lateral expansion; width $1.5\text{--}2.5 \times$ median lobe width (measured at mid-length of paramere and median lobe respectively). Paramere

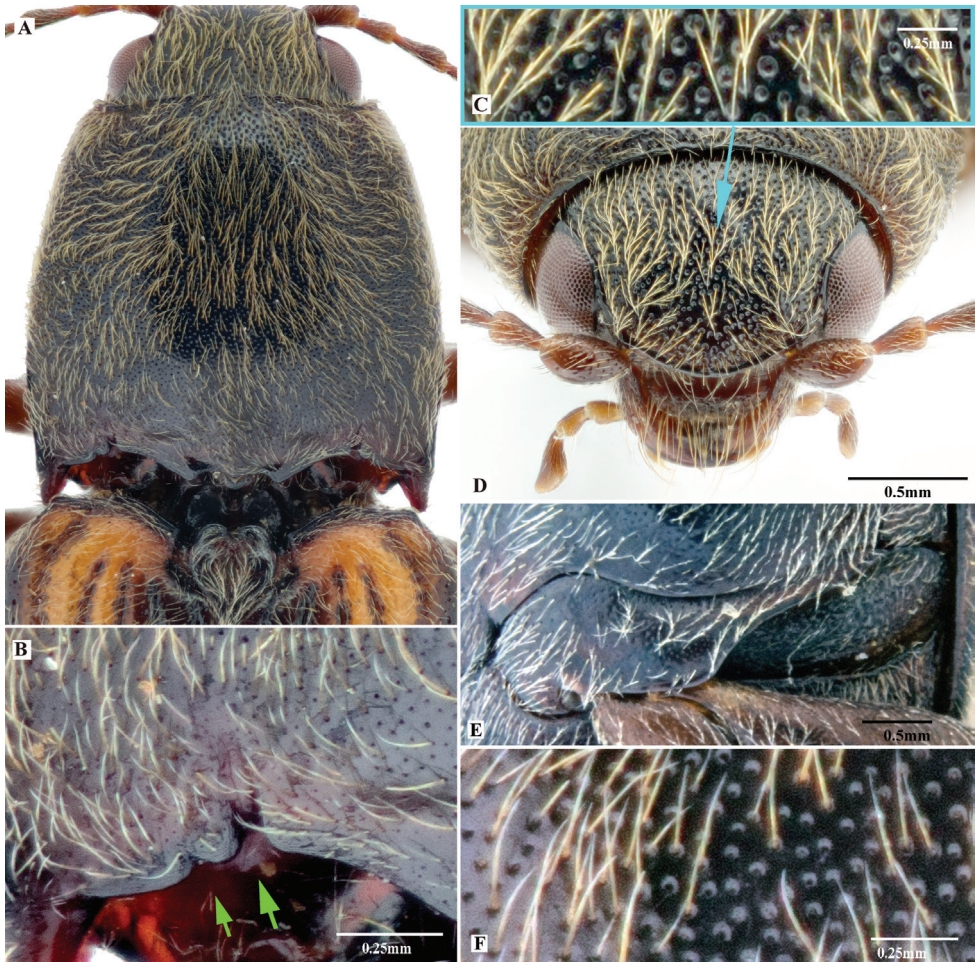


Figure 5. *Phorocardius flavistriolatus* Ruan & Douglas, sp. nov. **A** pronotum, dorsal view (holotype) **B** posterior edge of pronotum, left side, arrow indicating sublateral incisions **C** punctation on centre of vertex of head **D** head, frontal view **E** left metacoxal plate, ventral view **F** punctation on disc of pronotum.

in lateral view (Fig. 4N): robust; apical fourth compressed and turned ventrad; preapical ventral expansion obtuse, not sharp hook-shaped (Fig. 4P).

Female. Color pattern like male. Apex of abdominal ventrite V convex (Fig. 26B). Proximal sclerites of bursa copulatrix wide and somewhat diamond-shaped (Fig. 4Q), with concave basal edge, flat mesal edge and acute apex; each sclerite with seven or eight large spines arranged along mesal edge, and with 10–15 smaller scattered spines on disc.

Type material. Holotype. male (SZPT), labels: 1) **Henan** Province, Nan-Yang City, Bao-tian-man National Nature Reserve (宝天曼自然保护区), Outward Bound Center, VIII-26-2015, leg. Mei-rong Liang, light trap, Shenzhen Polytechnic [in Chinese]; 2) Holotype, *Phorocardius flavistriolatus* sp. nov., Des. Ruan et al., 2019.

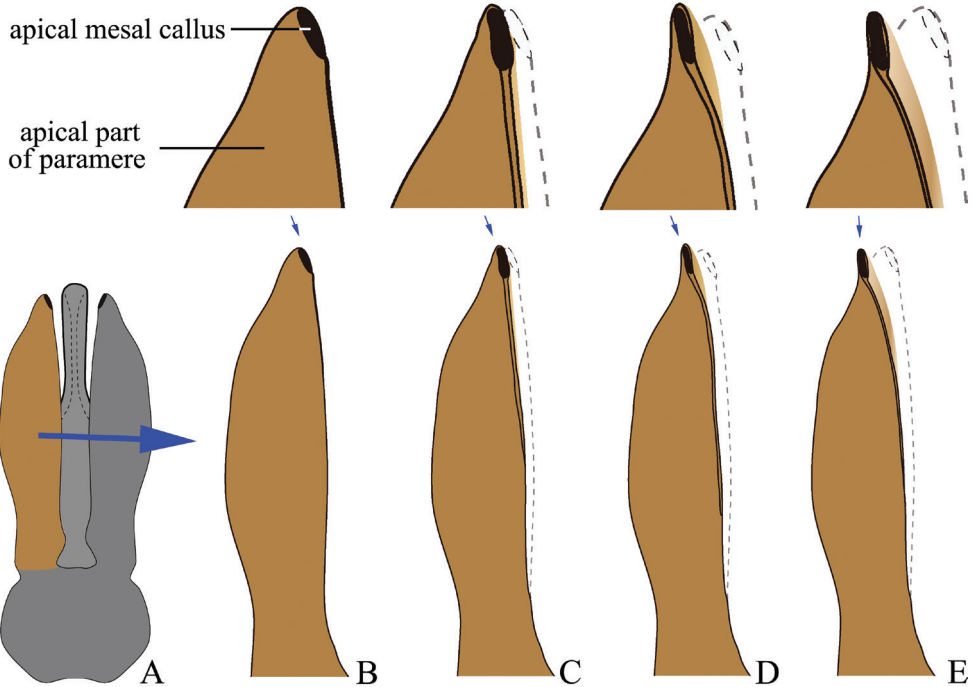


Figure 6. Shape variation due to rotation of paramere in *Phorcardius flavistriolatus* Ruan & Douglas, sp. nov. **A** aedeagus, ventral view **B–E** ventral view of paramere, showing variation; the mesal side of apical part of paramere rotated ventrad to increasing degrees, resulting in different observed shapes in ventral view, apex of paramere are shown in upper insets.

Paratypes (16♂, 11♀). 2♂ (IZCAS), labels: 1) **Sichuan**, Lu-ding County, Xin-xing township (新兴乡), 2000 m, 2009.VII.2–7, leg. Hua-kang Zhang, Chinese Academy of Sciences [in Chinese]; 2) Paratype, *Phorcardius flavistriolatus* sp. nov., Des. Ruan et al., 2019. • 1♂ (LQCC), labels: 1) Lu-ding (泸定) (**Sichuan**), De-tuo township (得妥乡), 2015.8.6, QL, leg. Lu Qiu, Shenzhen Polytechnic [in Chinese]; 2) Paratype, *Phorcardius flavistriolatus* sp. nov., Des. Ruan et al., 2019. • 2♂ (SZPT, ex. LQCC), labels: 1) Lu-ding (泸定) (**Sichuan**), Xin-xing township (新兴乡), 2016. VI.23, Q.X, leg. Jianyue Qiu & Hao Xu, Shenzhen Polytechnic [in Chinese]; 2) Paratype, *Phorcardius flavistriolatus* sp. nov., Des. Ruan et al., 2019. • 4♂1♀ (SZPT), labels: 1) **Sichuan**, Shi-mian (石棉), Li-zi-ping National Nature Reserve, Zi-ma reserve station, VII-27-2016, leg. Li-ting Yu et al., Shenzhen Polytechnic [in Chinese]; 2) Paratype, *Phorcardius flavistriolatus* sp. nov., Des. Ruan et al., 2019. • 1♂2♀ (SZPT), labels: 1) **Sichuan**, Shi-mian County (石棉), Li-zi-ping National Nature Reserve, Gong-yi-hai reserve station, Ma-ma-di, VII-24-2016, leg. Huang-qiang Liu, Shenzhen Polytechnic [in Chinese]; 2) Paratype, *Phorcardius flavistriolatus* sp. nov., Des. Ruan et al., 2019. • 1♀ (SZPT), labels: 1) **Sichuan**, Bao-xing County (宝兴), Feng-tong-zai National Nature Reserve, Deng-chi-gou village, VIII-1-2016, leg. Huang-qiang Liu, Shenzhen Polytechnic [in Chinese]; 2) Paratype, *Phorcardius flavistriolatus* sp. nov.,

Des. Ruan et al., 2019. • 2♂1♀ (IZCAS), labels: 1) **Sichuan**, Lu-ding County (泸定), Mo-xi township, 1500 m–1600 m, Chinese Academy of Sciences [in Chinese]; 2) 1983.VI.17–19 leg. Shuyong Wang & Xue-zhong Zhang [in Chinese]; 3) *Phorocardius comptus* Cand. Det. Ge; 4) Paratype, *Phorocardius flavistriolatus* sp. nov., Des. Ruan et al., 2019. • 1♂ (SZPT), labels: 1) Gong-ga Mts. (**Sichuan**), Mo-xi (墨西), 2016. VI.26, leg. Chenglong Ren, SZPT [in Chinese]; 2) Paratype, *Phorocardius flavistriolatus* sp. nov., Des. Ruan et al., 2019. • 1♂ (SZPT), labels: 1) **Shaanxi**, Ning-shan County (宁陕), Shi-ba-zhang-pu-bu Scenic Spot, 15.VIII.2013, leg. Jun Xu [in Chinese]; 2) Paratype, *Phorocardius flavistriolatus* sp. nov., Des. Ruan et al., 2019. • 1♂ (IZCAS), labels: 1) **Shaanxi**, Fo-ping County (佛坪), alt.843 m, 2007.VIII.16, Chinese Academy of Sciences [in Chinese]; 2) 33.52°N, 107.98°E, leg. Yu-xia Yang, Chinese Academy of Sciences [in Chinese]; 3) IOZ(E)1882863; 4) Paratype, *Phorocardius flavistriolatus* sp. nov., Des. Ruan et al., 2019. • 1♂1♀ (SZPT, ex. LQCC), labels: 1) **Henan**, Bai-yun-shan (白云山), Yu-huang-ding (玉皇顶), 1800–2200 m, 2016.8.12, leg. Weipeng Qiao, Shenzhen Polytechnic [in Chinese]; 2) Paratype, *Phorocardius flavistriolatus* sp. nov., Des. Ruan et al., 2019. • 5♀ (SZPT, ex. LQCC), labels: 1) Nei-xiang (内乡县) (**Henan** prov.), Bao-tian-man (宝天曼), 1200–1400 m, 2016.8.15–20, leg. Qiaozhi Yang & Weipeng Qiao, Shenzhen Polytechnic [in Chinese]; 2) Paratype, *Phorocardius flavistriolatus* sp. nov., Des. Ruan et al., 2019.

Remarks. Although there are variations in the shape of aedeagi, all the male specimens are identical in color patterns and other external structures. Females are stable in both external characters and the shape of sclerites of bursa copulatrix. Variations are found even in the specimens collected at the same place and time. For instance, Fig. 4G, H shows aedeagi of two externally identical males collected on the same day and same locality in Shi-mian, Sichuan; the two aedeagi are different from each other in the basal width and the shape of the apex of paramere. In Fig. 4J, K, these are aedeagi of two males collected on the same date and same locality in Lu-ding County, Sichuan; the two aedeagi are different from each other in the basal width, median lobe shape, and the shape of the apex of paramere. Additional mitochondrial DNA sequence comparisons would be useful to further test species limits.

Variation of the shape of aedeagus: in some cases, the base of the aedeagus is much narrower (e.g., Fig. 4G, J). Variations in the paramere: apical half of paramere of aedeagus compressed; additionally, apical part with mesal side turned ventrad to a varying degree (Fig. 6), resulting in different shapes in ventral view. In ventral view, when the turning is minimal, the apical part of paramere is nearly horizontal to the observers, therefore the paramere apex is broad and gradually narrowed in appearance (e.g., Fig. 4F, G); but, when the turning is stronger, the paramere apex would be nearly vertical to the observers, in which circumstance the paramere apex we see is acute and abruptly narrowed (e.g., Fig. 4K, M). Variations in the median lobe: in ventral view, apex usually truncate, in rare cases broadly rounded (Fig. 4K, L), lateral sides very slightly concave in rare cases (Fig. 4K).

Most specimens of this species were collected from low to middle elevations (ca. 500–2500 m) in central China on the boundary of the Oriental Palearctic Regions.

Based on collecting information, it inhabits mountainous areas with evergreen forest and temperate to subtropical climate. Specimens were collected at light traps, indicating nocturnal activity. Specimens collected by sweep-netting indicate their presence on vegetation during daylight.

3. *Phorocardius florentini* (Fleutiaux, 1895)

Figs 7, 23C, 24C, 25C, 26C

Cardiophorus florentini Fleutiaux, 1895: 687. Type locality: “Tonkin: Lang-son”, interpreted as Vietnam: Lạng Sơn Province.

Phorocardius florentini: Fleutiaux 1931: 311.

Distribution. China (Guizhou, new record); Vietnam (Fleutiaux 1895).

Differential diagnosis. Body length greater than 7.0 mm; pronotum and hypomeron red, elytra black with metallic blue to purple luster. Prothorax: procoxal cavities open; prosternal process not strongly narrowed from anterior base posterad to ventral apex in ventral view, with apex convex. Pterothorax: scutellar shield elongate, with posterior apex pointed. Tarsal claw with ventral apex not smaller than dorsal apex. Male genitalia: paramere with preapical lateral expansion present, apical mesal callus absent. Female: apex of last abdominal ventrite (ventrite V) simple, not emarginate at apex.

This species is distinctive for its elytral color: black with metallic blue to purple luster.

Phorocardius florentini (Fleutiaux, 1895) resembles *P. zhiweii* Ruan, Douglas & Qiu, sp. nov. in its entirely red pronotum and metallic elytra. *P. florentini* (Fleutiaux, 1895) can be easily separated from *P. zhiweii* Ruan, Douglas & Qiu, sp. nov. by the following characters. In *P. florentini* (Fleutiaux, 1895): aedeagus strongly narrowed from mid-length to apex in lateral view; in dorsal view, paramere with preapical lateral expansion minute, acute to rounded, facing laterally, with apical mesal callus absent; scutellar shield elongate (width to length ratio: 0.81–0.86); and elytra black, with metallic blue to purple luster; while in *P. zhiweii* Ruan, Douglas & Qiu, sp. nov., the aedeagus is only slightly narrowed from mid-length to apex in lateral view; in dorsal view, paramere with preapical lateral expansion absent, apical mesal callus present, apex narrow and slightly bent laterad; scutellar shield not elongate (width to length ratio: 1.0); and elytra metallic green with slight purple luster.

Description. (Based on holotype and three non-type specimens examined) Body black, red and metallic blue-purple (Fig. 7A–D). Pronotum and hypomera red. Elytra black, with metallic blue to purple luster. Head brown-black to black; antennae brown-black. Prosternum red, black or mixed with red and black; meso- and meta- sternum black; abdominal ventrites black; legs brown-black to black. Body with short, yellow pubescence; brown setae also present on disc of pronotum.

Measurements. (based on type and non-type specimens) Male body length 9.0–11.5 mm, width 3.3–3.8 mm. Female body length 10.0–13.0 mm, width 3.7–4.0 mm. Body length to width ratio 2.6–2.8. Pronotal width to length ratio 1.1–1.2,

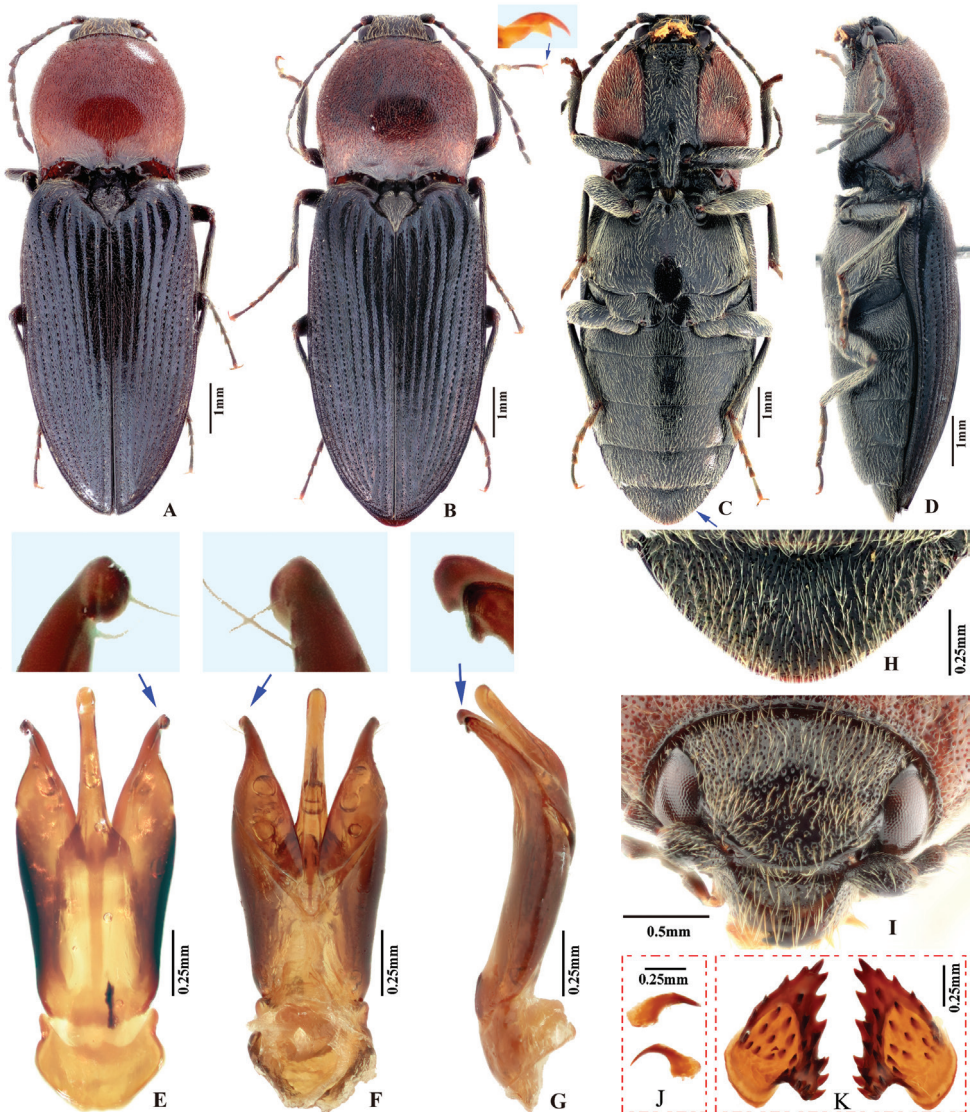


Figure 7. *Phorocardius florentini* (Fleutiaux, 1895). **A** male habitus, dorsal view **B** female habitus, dorsal view, arrow indicating claw **C** female habitus, ventral view, arrow indicating last visible ventrite **D** female habitus, lateral view **E** aedeagus, ventral view, arrow indicating preapical lateral expansion **F** aedeagus, dorsal view, arrow indicating preapical lateral expansion **G** aedeagus, lateral view, arrow indicating preapical ventral expansion **H** last visible ventrite of female, ventral view **I** head, frontal view **J** distal sclerites of bursa copulatrix **K** proximal sclerites of bursa copulatrix.

Pronotal width to body width ratio 0.86–0.91. Elytral length to pronotal length ratio 2.3–2.5; elytron length to width ratio 3.7–3.9.

Head. Frons and vertex punctures with interspaces $0.5\text{--}1 \times$ average puncture diameter; punctures sparser at centre of vertex, with interspaces $1.5\text{--}2 \times$ average

puncture diameter. Frontal carina in frontal view convex, not straight (Fig. 7I). Antenna with last antennomere not reaching beyond posterior angle of pronotum. Distance between eyes to width of eye ratio 3.8–3.9. Antenna length to body length ratio, in male 0.36–0.38; in female 0.37–0.39. Proportions of antennomere lengths (male): 100 (scape); 60–65; 75–83; 75–83; 75–83; 78–85; 81–86; 85–90; 85–90; 81–85; 90–100.

Prothorax. Pronotum in dorsal view: sides evenly convex from anterior edge to constriction near posterior end, widest near mid-length; posterior angles with lateral sides almost straight, not bulged; surface with interspaces between punctures $1-2 \times$ average puncture diameter. In ventral view, ventral surface of prosternal process with sides carinate and slightly and gradually narrow from anterior to mid-length, parallel from mid-length to posterior end, with apex convex. In lateral view, prosternal process with ventral surface curved slightly dorsad, posterior end somewhat concave or not (Fig. 24C, upper arrow). Procoxal cavities open.

Pterothorax (Figs 24C, 25C). Mesepisternum in ventral view with antero-mesal corner angulate (Fig. 25C, upper (green) arrow). Projections on posterior edge of mesosternum: in ventral view present (Fig. 25C, red arrow); in lateral view present, acute, strongly produced anteriorly (Fig. 24C). Scutellar shield: elongate, width to length ratio 0.81–0.86; anterolateral edges slightly sinuate; posterior edge gradually narrowed and elongate, strongly protruding posterad, pointed at apex. Elytra: upper edge of epipleura with minute serrations.

Legs. Length ratio of metatarsomeres I–V (excluding claws): 100; 80–85; 70–75; 50–55; 135–140. Claw with ventral apex almost as large as dorsal apex.

Abdomen. Lateral edges of visible abdominal ventrites I–V with minute serrations.

Male genitalia (Fig. 7E–G). Robust from ventral and lateral views. Median lobe in ventral view slightly narrowed from base to basal third, parallel-sided from basal third to near apex, apex rounded and very slightly dilated. Median lobe in lateral view wide from base to mid-length, narrow from mid-length to apex; gently and evenly curved ventrad from base to mid-length, straight from mid-length to apex; apex rounded. Paramere in ventral view: wide and equal wide from base to apical third; abruptly narrowed from apical third to apex; preapical lateral expansion present, minute and rounded, facing laterally; apical mesal callus absent; paramere width $3-4 \times$ median lobe width (measured at mid-length of paramere and median lobe respectively). Paramere in lateral view: robust, almost straight from base to mid-length, curved ventrad and narrowed from mid-length to apex; apex with hook-like preapical expansion with barb facing base.

Female. Body color like male (Fig. 7B). Apex of abdominal ventrite V convex (Fig. 7H). Proximal sclerites of bursa copulatrix wide with apex acute, base concave, and mesal edge flat (Fig. 7K); each with 8–10 large spines on mesal edge, 14–18 smaller spines on disc.

Type material. Lectotype. ♀ (MNHN), labels: 1) Tonkin Florentin; 2) Type [red label]; 3) Museum Paris Coll. E. Fleutiaux; 4) *Cardiophorus florentini* Fleut. Type; 5) Fleut Ann. Soc. Ent. Fr., 1894. P. 687, Collection Fleutiaux; 6) *C. florentini* Fleut., type, Collection Fleutiaux; 7) LECTOTYPE *Cardiophorus florentini* Fleutiaux desig. Douglas 2015.

Additional material. 2♂1♀ (SZPT, ex. LQCC), labels: 1) **Guizhou**, Li-bo, Mao-lan, Dong-duo, 2000 m, 2018.VI.11–17, leg. Jianyue Qiu & Hao Xu [in Chinese]; 2) *Phorocardius florentini* (Fleutiaux, 1894) Det. Ruan, 2019.

Remarks. Based on examined material, this species inhabits low to middle elevations (0–2000 m) in south China and north Vietnam. Recent Chinese specimens were collected in daylight in a mountainous area with evergreen forest and subtropical climate. Known from the Oriental Region only.

4. *Phorocardius magnus* Fleutiaux, 1931

Figs 8, 9, 23D, 24D, 25D, 26D

Phorocardius magnus Fleutiaux, 1931: 310. Type locality: Vietnam (Hanoi). Lectotype designated here.

Distribution. China (Yunnan, Hainan), Vietnam (Fleutiaux 1931).

Differential diagnosis. Body length greater than 7.0 mm; integument entirely red-brown to brown throughout. Prothorax: procoxal cavities open; prosternal process gradually narrowed posterad to ventral apex in ventral view, with apex narrowly rounded. Pterothorax: scutellar shield with posterior apex pointed. Tarsal claw with ventral apex not smaller than dorsal apex. Male genitalia: paramere with preapical lateral expansion and secondary lateral bulge present, apical mesal callus absent. Female: apex of last abdominal ventrite (ventrite V) tri-lobed, emarginate between middle and lateral lobes.

Phorocardius magnus Fleutiaux, 1931 resembles *P. unguicularis* (Fleutiaux, 1918) in body color and size. They can be separated by the following combination of characters: in *P. magnus* Fleutiaux, 1931, aedeagus robust in lateral view (more than 4 × thicker at mid-length than at apical 1/5 of parameres); in ventral view, paramere slightly narrowed from base to apical fourth, apical fourth abruptly narrowed to 1/4 width at mid-length, with hook-like preapical lateral expansion; pronotum with shallow punctures, interspaces between punctures 1–2.5 × average puncture diameter; and head with frontal carina straight in frontal view; while *P. unguicularis* (Fleutiaux, 1918) has aedeagus slender in lateral view, in ventral view paramere slightly widened from base to mid-length, gradually narrowed from mid-length to apex, apex pointed and without preapical lateral expansion; pronotum with deep punctures, interspaces between punctures 0.3–1 × average puncture diameter; and head with frontal carina convex in frontal view.

Description. (based on photographs of eight type specimens and four non-type specimens) Body robust. Color entirely red-brown to brown throughout, including legs and antennae; pronotum slightly darker than remainder. Integument matt, with yellow pubescence.

Measurements. (based on lectotype and examined specimens) Male body length 9.5–12.0 mm, width 3.0–4.1 mm. Female body length 11.0–13.9 mm, width 3.9–4.5 mm. Body length to width ratio 2.9–3.2. Pronotal width to length ratio 1.0–1.2.

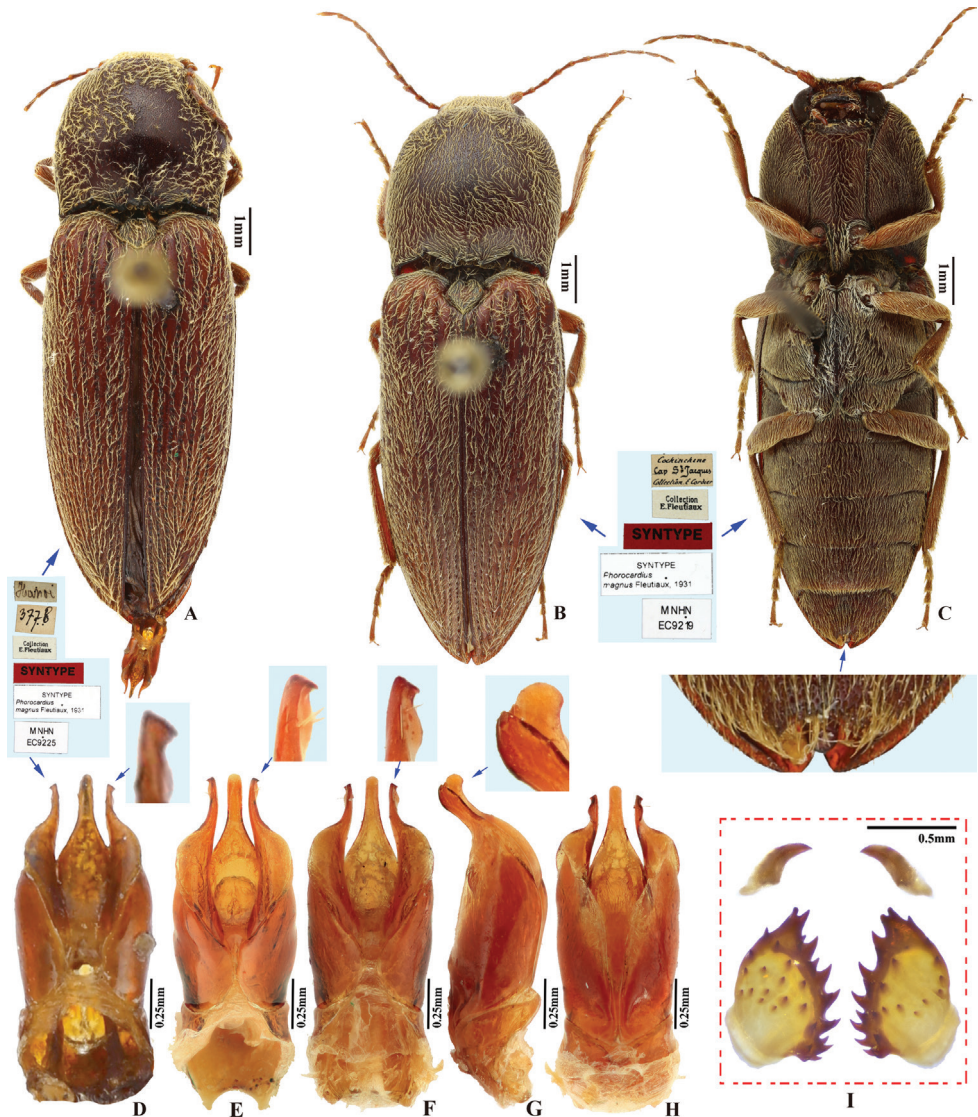


Figure 8. *Phorocardius magnus* Fleutiaux, 1931. **A** lectotype, male, from Hanoi, Vietnam, dorsal view (photograph: Dr Antoine Mantilleri, MNHN), arrow indicating specimen labels **B** paralectotype, female, from Vung Tau, Vietnam, dorsal view (photograph: Dr Antoine Mantilleri, MNHN), arrow indicating specimen labels **C** the same female as **B**, ventral view (photograph: Dr Antoine Mantilleri, MNHN), arrows indicating specimen labels and last visible ventrite **D** aedeagus of lectotype, dorsal view (photograph: Dr Antoine Mantilleri, MNHN), arrows indicating specimen labels and apex of paramere **E** aedeagus of non-type specimen, individual-1 (Yunnan, Xi-shuang-ban-na, Meng-zhe), dorsal view, arrow indicating apex of paramere **F** aedeagus of non-type specimen (Yunnan, Jing-dong, Dong-jia-feng), individual-2, dorsal view, arrow indicating apex of paramere **G** aedeagus, individual-2, lateral view, arrow indicating apex of paramere **H** aedeagus, individual-2, ventral view **I** distal (upper side) and proximal sclerites of bursa copulatrix, non-type specimen.

Pronotal width to body width ratio 0.90–0.97. Elytral length to pronotal length ratio 2.5–2.7; elytron length to width ratio 3.9–4.1.

Head. Frons and vertex with interspaces between punctures $0.3\text{--}1 \times$ average puncture diameter (Fig. 9B). Frontal carina in frontal view transversely straight (Fig. 9C). Antenna with apex extending to posterior angle of pronotum. Distance between eyes to width of eye ratio 2.9–3.1. Antenna length to body length ratio, in male 0.35–0.36, in female 0.32–0.33. Proportions of antennomere lengths (male): 100 (scape); 46–53; 57–63; 55–58; 50–55; 59–60; 59–65; 57–63; 60–63; 60–67; 80–87.

Prothorax. Pronotum in dorsal view: robust, comparatively larger than other Chinese *Phorocardius* species, with sides evenly convex, widest near mid-length, straighter posterad; posterior angles with lateral sides straight to slightly convex, not bulged; surface with shallow punctures, interspaces between punctures $1\text{--}2.5 \times$ average puncture diameter. In ventral view, ventral surface of prosternal process with sides carinate and gradually narrow from anterior to posterior end, with apex narrowly rounded. In lateral view, prosternal process with ventral surface curved slightly dorsad, posterior end somewhat concave (Fig. 24D, upper arrow). Procoxal cavities narrowly open.

Pterothorax (Figs 24D, 25D). Mesepisternum in ventral view with antero-mesal corner narrowly rounded (Fig. 25D, upper (green) arrow). Projections on posterior edge of mesosternum: in ventral view present (Fig. 25D, lower (red) arrow); in lateral view present, acute, strongly produced anteriorly (Fig. 24D, lower (red) arrow). Scutellar shield: width to length ratio 0.92–1.10; anterolateral edges slightly sinuate; posterior apex pointed. Elytra: upper edge of epipleura with very weak minute serrations (barely visible).

Legs. Length ratio of metatarsomeres I–V (excluding claws): 100; 90–98; 70–79; 61–75; 145–152. Claw with ventral apex almost as large as dorsal apex.

Abdomen. Lateral edges of visible abdominal ventrites I–V with minute serrations. Male genitalia. Robust from ventral and lateral views (Fig. 8). Median lobe in ventral view gradually narrowing from base to apical third, parallel-sided near rounded apex. Median lobe in lateral view robust at base, curved ventrad and gradually narrowed from base to apical third, apical third slender, apex globose and recurved dorsad (Fig. 8G, indicated by arrow). Paramere in ventral view: robust, widest near mid-length ($4\text{--}5 \times$ wider than at apical fifth); width $1.5\text{--}2.5 \times$ median lobe width (measured at mid-length part of paramere and median lobe respectively); apical fourth gradually narrowing towards apex, with a secondary lateral bulge present before apex (Fig. 8D–F, indicated by arrow); secondary lateral bulge turned and bent ventrad; preapical lateral expansion small, sharp, hook like; apical mesal callus absent. Paramere in lateral view: robust; parallel from base to mid-length, abruptly narrowed from mid-length to apical fourth, nearly parallel from apical fourth to apex; preapical ventral expansion absent, without hook-shaped structure.

Female. Color like male. Apex of abdominal ventrite V tri-lobed; with shape of middle lobe semicircular to longitudinal with apex rounded; deeply to gently incised between middle and lateral lobes (Fig. 9D–G). [In non-type specimens: proximal sclerites of bursa copulatrix ovoid (Fig. 8I), with shallow basal concavity; apex acute, each with 8–11 large spines on convex mesal edge, 15–17 smaller spines on disc.]

Type material. (all in MNHN) (photographs provided by Dr Antoine Mantilleri). **Lectotype.** ♂, labels: 1) Hanoi; 2) 3778; 3) Collection E. Fleutiaux; 4) Syntype

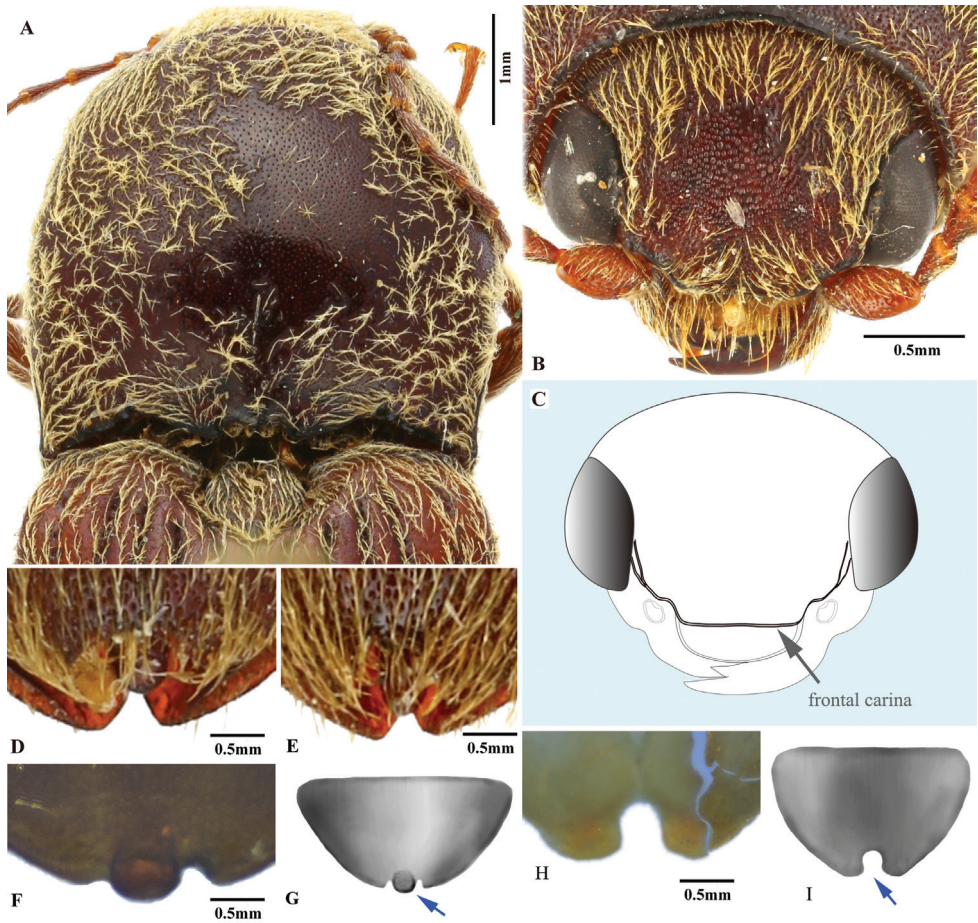


Figure 9. *Phorcardius magnus* Fleutiaux, 1931. **A** pronotum of lectotype, dorsal view (photograph: Dr Antoine Mantilleri, MNHN) **B** head of paralectotype, frontal view (photograph: Dr Antoine Mantilleri, MNHN) **C** head, frontal view, hand drawing, arrow indicating straight frontal carina **D, E** apex of last visible abdominal ventrite (ventrite V) of female, ventral view, paralectotype (photograph: Dr Antoine Mantilleri, MNHN) **F** apex of last visible abdominal ventrite (ventrite V) of female, dorsal view, non-type specimen **G** a model of last visible abdominal ventrite (ventrite V) of female, ventral view, hand drawing, arrow indicating tri-lobed apex **H** apex of last visible abdominal tergite (tergite VII) of female, dorsal view, non-type specimen **I** a model of last visible abdominal tergite (tergite VII) of female, dorsal view, hand drawing, arrow indicating concave apex.

[red label]; 5) Syntype *Phorcardius magnus* Fleutiaux, 1931; 6) MNHN EC9225; 7) Lectotype, *Phorcardius magnus* Fleutiaux, 1931, Des. Ruan & Douglas, 2019.

Paralectotypes. 1 ♀, labels: 1) Cochinchine, Cap St. Jacques, Collection E Cordier; 2) *Phorcardius magnus* Fleut., type, Collection Fleutiaux; 3) Collection E. Fleutiaux; 4) Syntype [red label]; 5) Syntype *Phorcardius magnus* Fleutiaux, 1931; 6) MNHN EC9218; 7) Paralectotype, *Phorcardius magnus* Fleutiaux, 1931, Des. Ruan & Douglas, 2020. • 1 ♀, labels: 1) Cochinchine, Cap St. Jacques, Collection E Cordier; 2) Collection E. Fleutiaux; 3) Syntype [red label]; 4) Syntype *Phorcardius magnus*

Fleutiaux, 1931; 5) MNHN EC9219; 6) Paralectotype, *Phorocardius magnus* Fleutiaux, 1931, Des. Ruan & Douglas, 2020. • 1 (sex unknown), labels: 1) Cochinchine, Cap St. Jacques, Collection E Cordier; 2) Collection E. Fleutiaux; 3) Syntype [red label]; 4) Syntype *Phorocardius magnus* Fleutiaux, 1931; 5) MNHN EC9220; 6) Paralectotype, *Phorocardius magnus* Fleutiaux, 1931, Des. Ruan & Douglas, 2020. • 1 (sex unknown), labels: 1) Cochinchine, Cap St. Jacques, Collection E Cordier; 2) Collection E. Fleutiaux; 3) Syntype [red label]; 4) Syntype *Phorocardius magnus* Fleutiaux, 1931; 5) MNHN EC9221; 6) Paralectotype, *Phorocardius magnus* Fleutiaux, 1931, Des. Ruan & Douglas, 2020. • 1♀, labels: 1) Cochinchine, Cap St. Jacques, Collection E Cordier; 2) type,[characters illegible] Collection Fleutiaux; 3) Collection E. Fleutiaux; 4) ex Coll Fleut., *Phorocardius magnus*. 5) Syntype [red label]; 6) Syntype *Phorocardius magnus* Fleutiaux, 1931; 6) MNHN EC9222; 7) ♀ genitalia See slide Coll No. 105; 8) Paralectotype, *Phorocardius magnus* Fleutiaux, 1931, Des. Ruan & Douglas, 2020. • 1 (sex unknown), labels: 1) Dap Cau, 1 au 9. 7. 06 [= 1 to 9 July, 1906]; 2) Collection E. Fleutiaux; 3) *Phorocardius magnus* Fleut., Collection E. Fleutiaux; 4) Syntype [red label]; 5) Syntype *Phorocardius magnus* Fleutiaux, 1931; 6) MNHN EC9223; 7) Paralectotype, *Phorocardius magnus* Fleutiaux, 1931, Des. Ruan & Douglas, 2020. • 1 (sex unknown), label: 1) Dap Cau, 1 au 9. 7. 06' [= 1 to 9 July, 1906]; 2) Collection E. Fleutiaux; 3) Syntype [red label]; 4) Syntype *Phorocardius magnus* Fleutiaux, 1931; 5) MNHN EC9224; 6) Paralectotype, *Phorocardius magnus* Fleutiaux, 1931, Des. Ruan & Douglas, 2020.

Additional material. One female and two males. 1♀ (IZCAS), labels: 1) **Hainan** Prov., Na-da (那大), Beijing Natural History Museum, leg. Sikong Liu, 1964.V.14 [in Chinese]; 2) *Phorocardius magnus* Fleut. Det. Siqin Ge; 3) *Phorocardius magnus* Fleutiaux, 1931 Det. Ruan, 2018. • 1♂ (IZCAS), labels: 1) **Yunnan**, Xi-shuang-ban-na, Meng-zhe (勐遮), 1700 m, Chinese Academy of Sciences [in Chinese]; 2) 1958.IV.22, leg. Shuyong Wang [in Chinese]; 3) *Phorocardius magnus* Fleutiaux, 1931 Det. Ruan, 2018. • 1♂ (IZCAS), labels: 1) **Yunnan**, Jing-dong, Dong-jia-feng (董家坟), 1250 m, 1956.VI.2; 2) *Phorocardius magnus* Fleutiaux, 1931 Det. Ruan, 2018.

Remarks. This species has the largest body size in Chinese *Phorocardius* species, with females up to 13.9 mm long and 4.5 mm wide.

Based on specimen information, this species inhabits low to middle elevations (0–1700 m) in south China and throughout Vietnam. It inhabits mountainous areas with subtropical to tropical climates and much rainfall. One specimen was collected in or near to tropical rain forest (“Xi-shuang-ban-na tropical rain forest”). Known from the Oriental Region only.

5. *Phorocardius manuleatus* (Candèze, 1888)

Figs 10, 11, 23E, 24E, 25E, 26E

Cardiophorus manuleatus Candèze, 1888: 681. Type locality: “Thagatà, Tenasserim”, interpreted as Myanmar, Kayin State, mountains east of Kyaikdon using Hallermann et al. (2002). Lectotype designated here.

Phorocardius melanopterus manuleatus: Fleutiaux 1931: 311.

Phorocardius manuleatus: Fleutiaux 1947: 366.

Differential diagnosis. Body length greater than 7.0 mm; integument shiny, black with yellow in most, entirely black to black-brown in some. Prothorax: procoxal cavities open; prosternal process strongly narrowed posterad to ventral apex in ventral view, with apex acute. Pterothorax: scutellar shield with posterior apex pointed. Tarsal claw with ventral apex not smaller than dorsal apex. Male genitalia: paramere with preapical lateral expansion present, without apical mesal callus. Female: apex of last abdominal ventrite (ventrite V) simple, not emarginate at apex.

Phorocardius manuleatus (Candèze, 1888) is unique among Chinese *Phorocardius* species for its variable color pattern. Some individuals are entirely black to black-brown throughout body, resembling *P. yanagiharae* (Miwa, 1927) and *P. yunnanensis* sp. nov.

This species can be differentiated from *P. yanagiharae* by the following combination of characters. In *P. manuleatus*: in ventral view, parameres of aedeagus with sides gently narrowed from mid-length to apex (not abruptly narrowed from apical third to near apex), with width $1.5\text{--}2 \times$ that of median lobe (measured at apical fourth); and in dorsal view, pronotum with lateral sides of posterior angles almost straight, slightly convex (bulged) at posterior half in a few cases (e.g., in Fig. 11A); while in *P. yanagiharae*, in ventral view, paramere of aedeagus with sides abruptly narrowed from apical third to near apex, with width $2\text{--}3 \times$ that of median lobe (measured at apical fourth); and in dorsal view, pronotum with lateral sides of posterior angles strongly bulged and convex (Fig. 18C, D).

This species can be differentiated from *P. yunnanensis* Ruan & Douglas, sp. nov. by the following combination of characters. In *P. manuleatus*, in ventral view, paramere of aedeagus narrow and slender near apex, with width to that of median lobe ratio $0.5\text{--}0.7$ (measured at the area posterior of preapical lateral expansion); legs darker in apical half, not unicolor yellow-brown to brown; while in *P. yunnanensis* Ruan & Douglas, sp. nov., in ventral view, paramere of aedeagus wide and strong near apex, with width to that of median lobe ratio $1.0\text{--}1.2$ (measured at the area posterior of preapical lateral expansion); and legs unicolor, entirely yellow-brown.

Distribution. China (Yunnan, new record), Myanmar (Candèze 1888), Laos (Fleutiaux 1931, 1947), Vietnam (Fleutiaux 1918, 1947).

Description. (based on lectotype and 24 non-type specimens) Integument shiny, black with yellow in most, or entirely black to black-brown. Pronotum entirely black or orange with variable median black stripe (Fig. 11E). Ventral side of prothorax yellow, orange, black or orange with black prosternum. Elytra black, yellow, or black with orange spot at elytral bases. Mesosternum brown to black. Metasternum yellow to black. Abdominal ventrites yellow, black, or bicolored (I–IV orange, V yellow). Head red-brown to black. Antennae brown. Legs variably orange to yellow-brown from coxa to mid tibia, yellow-brown to brown from mid tibia to last tarsomere. Body with yellow pubescence.

Measurements. (based on lectotype and examined specimens) Male body length 7.2–9.6 mm, width 2.2–2.6 mm. Female body length 8.5–9.7 mm, width 2.5–2.9 mm.

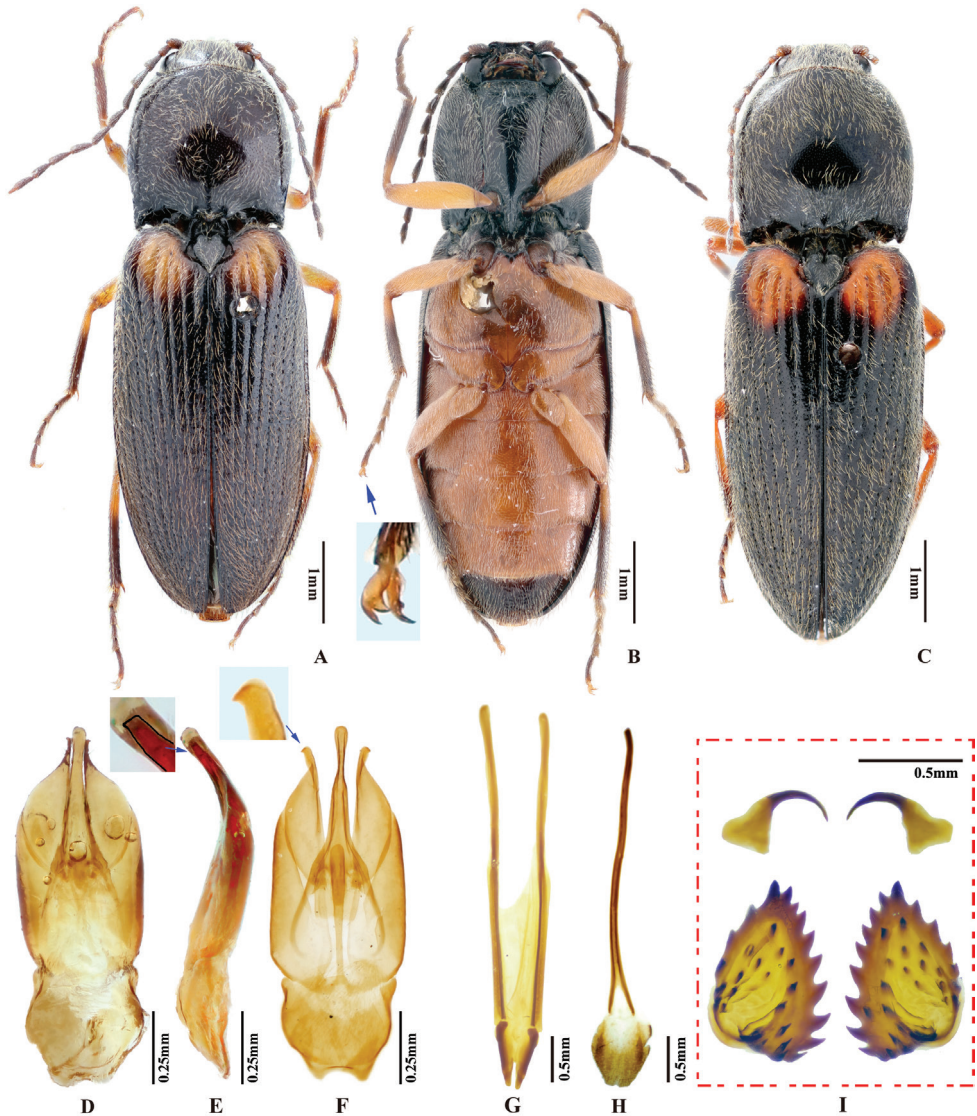


Figure 10. *Phorocardius manuleatus* Candèze, 1888. **A** male habitus, dorsal view **B** male habitus, ventral view, arrow indicating claws **C** female habitus, dorsal view **D** aedeagus, ventral view (immersed in glycerin) **E** aedeagus, lateral view, arrow indicating apex of paramere **F** aedeagus, dorsal view (immersed in glycerin), arrow indicating apex of paramere **G** ovipositor, dorsal view **H** female abdominal sternite VIII, dorsal view (near type locality) **I** distal (top) and proximal sclerites of bursa copulatrix.

Body length to width ratio 3.0–3.1. Pronotal width to length ratio 1.1–1.2. Pronotum narrower than elytra, pronotal width to body width ratio 0.87–0.90. Elytral length to pronotal length ratio 2.4–2.6; elytron length to width ratio 4.1–4.2.

Head. Frons and vertex with interspaces between punctures 2.5–6 × average diameter of puncture (Fig. 11D). Frontal carina in frontal view convex, not straight.

Antenna with apex extending to posterior angle of pronotum. Distance between eyes to width of eye ratio 2.7–3.1. Antenna length to body length ratio, in male 0.41–0.42, in female 0.39–0.40. Proportions of antennomere lengths (male): 100 (scape); 51–55; 72–80; 75–82; 82–88; 82–84; 72–78; 72–78; 80–88; 80–89; 114–120.

Prothorax. Pronotum in dorsal view: sides convex near mid-length, nearly straight at ends, widest near mid-length; posterior angles with lateral sides almost straight, slightly convex (bulged) at basal half in a few cases (e.g., Fig. 11A); surface with interspaces between punctures $4-8 \times$ average puncture diameter (Fig. 11C). In ventral view, ventral surface of prosternal process with sides carinate and strongly narrowed from anterior to posterior end, with apex acute. In lateral view, prosternal process with ventral surface curved slightly dorsad, posterior end strongly concave (Fig. 24E, upper arrow). Procoxal cavities open.

Pterothorax (Figs 24E, 25E). Mesepisternum in ventral view with antero-mesal corner angulate mesad of a notch (Fig. 25E, upper (green) arrow). Projections on posterior edge of mesosternum: in ventral view present (Fig. 25E, lower (red) arrow); in lateral view present, acute, strongly produced anteriorly (Fig. 24E, lower (red) arrow). Scutellar shield: width to length ratio 1.0, anterolateral edges slightly sinuate, posterior apex pointed. Elytra: upper edge of epipleura with minute serrations.

Legs. Length ratio of metatarsomeres I–V: 100; 82–92; 67–75; 60–70; 155–180. Claw with ventral apex almost as large as dorsal apex.

Abdomen. Serrations on lateral edges of visible abdominal ventrites I–V absent.

Male genitalia. Robust in ventral view, slender in lateral view. Median lobe in ventral view gradually narrowing from base to near apex, then dilated to rounded apex. Median lobe in lateral view curved ventrad at base, straight from basal third to apex; apex broadly rounded. Paramere in ventral view: robust, width $3-4 \times$ median lobe width (measured at mid-length of paramere and median lobe respectively), widest near mid-length; apical fourth gradually narrowing towards apex, with mesal side bent and turned ventrad in varying degree, result in slightly different shapes in ventral view; apex of paramere slender and sharp, with preapical lateral expansion acute, hook-like to rounded, facing laterally (Figs 10F, 11F, indicated by blue arrow), without apical mesal callus. Paramere in lateral view: slender, almost straight from base to mid-length, curved ventrad and gradually narrowed from mid-length to apex; apex obliquely truncate; preapical ventral expansion acute but not hook-like (Figs 10E, 11F, indicated by blue arrows).

Female. Body color like male. Apex of abdominal ventrite V convex, somewhat angulate (Fig. 26E). Proximal sclerites of bursa copulatrix ovoid-triangular shaped (Fig. 10I), basal edge almost without concavity: each with 9–11 large spines mainly on the convex mesal edge, 15–20 smaller spines on disc.

Type material. Lectotype. ♂ (RBINS): 1) Coll. R. I. SC. N. B., Inde; 2) Tenasserim, Thagatà, Fea. Apr. 1887; 3) Collection E. Candèze; 4) *Manuleatus* cdz., Tenasserim; 5) *Cardiophorus manuleatus*, Cd., dét. E. Candèze; 6) Probably syntype var. a., Det. W. Suzuki, 1986; 7) Lectotype, *Cardiophorus manuleatus* Candèze, 1888, Des. Ruan & Douglas, 2020.

Additional material. 1♂ (NHMUK), labels: 1) Cotype; 2) Carin Chebà, 900–1100 m, L. Fea, V XII-88; 3) Andrewes Bequest. B. M. 1922-221. 4) *Cardiophorus manuleatus* Cand. Co.type.; 5) Not paratype of *manuleatus* Cand., wrong loc., C.M.F. von Hayek. det., 1957. [Notes: locality of this specimen (“Chebà”) differs from what Candèze (1888) provided (“Thagatà, Tenasserim”). Although “Thagatà” and “Chebà” are both in “Carin State” (Now Kayin State), Myanmar and there is a ‘Cotype’ label under the specimen, it is still unknown if this specimen belongs to the syntypes described by the author.]

3♂1♀ (IZCAS), labels: 1) **Yunnan**, Xi-shuang-ban-na, Meng-a (勐阿), 1050–1080 m, Chinese Academy of Sciences [in Chinese]; 2) 1958.VI.2–10, leg. Shuyong Wang [in Chinese]; 3) *Phorocardius flavus* Det. Shihong Jiang, 1999; 4) *Phorocardius manuleatus* (Candèze, 1888) Det. Ruan, 2018. • 1♂ (IZCAS), labels: 1) **Yunnan**, Xi-shuang-ban-na, Meng-zhe (勐遮), 1200 m, Chinese Academy of Sciences [in Chinese]; 2) 1958.IV.14, leg. Shuyong Wang [in Chinese]; 3) *Phorocardius manuleatus* (Candèze, 1888) Det. Ruan, 2018. • 1♂ (IZCAS), labels: 1) Da-nuo-you IV B 26.04.2009 leg. L.Z.Meng, gift from Na-ban-he Nature reserve [in Chinese]; 2) **Yunnan**, Jing-hong, Na-ban-he Nature reserve, Meng-song county, Da-nuo-you (大糯有), 2009.IV.26, 770 m, Chinese Academy of Sciences [in Chinese]; 3) 22.20699°N, 100.63761°E, Malaise trap, leg. Linzeng Meng, Chinese Academy of Sciences [in Chinese]; 4) *Phorocardius manuleatus* (Candèze, 1888) Det. Ruan, 2018. • 1♀ (SZPT), labels: 1) **Yunnan**, Xi-shuang-ban-na, Meng-hun (勐混), Chinese Academy of Sciences [in Chinese]; 2) 1958.V.31, leg. Chun-pei Hong [in Chinese]; 3) *Phorocardius flavus* Det. Shihong Jiang, 1999; 4) *Phorocardius manuleatus* (Candèze, 1888) Det. Ruan, 2018. • 1♀ (IZCAS), labels: 1) **Yunnan**, Xi-shuang-ban-na, Meng-hun (勐混), Chinese Academy of Sciences [in Chinese]; 2) 1958.VI.12, leg. Yirang Zhang [in Chinese]; 3) *Phorocardius manuleatus* (Candèze, 1888) Det. Ruan, 2018. • 1♂ (IZCAS), labels: 1) **Yunnan**, Xi-shuang-ban-na, Da-meng-long (大勐龙), 650 m, Chinese Academy of Sciences [in Chinese]; 2) 1958.IV.18, leg. Fu-ji Pu [in Chinese]; 3) *Phorocardius manuleatus* (Candèze, 1888) Det. Ruan, 2018. • 1♂ (IZCAS), labels: 1) **Yunnan**, Xi-shuang-ban-na, Meng-la (勐腊), 620–650 m, Chinese Academy of Sciences [in Chinese]; 2) 1958.V.17, leg. Fa-cai Zhang [in Chinese]; 3) *Phorocardius manuleatus* (Candèze, 1888) Det. Ruan, 2018. • 4♂2♀ (IZCAS), labels: 1) **Yunnan**, Meng-la (勐腊), 670 m, Chinese Academy of Sciences [in Chinese]; 2) 1982.IV.20, leg. Subai Liao [in Chinese]; 3) *Phorocardius manuleatus* (Candèze, 1888) Det. Ruan, 2018. • 3♂1♀ (IZCAS), labels: 1) **Yunnan**, Gan-lang-ba (橄欖坝), 560 m, Chinese Academy of Sciences [in Chinese]; 2) 1957.IV.19, leg. Guangji Hong [in Chinese]; 3) *Phorocardius flavus* Det. Shihong Jiang, 1999; 4) *Phorocardius manuleatus* (Candèze, 1888) Det. Ruan, 2018. • 1♂1♀ (IZCAS), labels: 1) **Yunnan**, Si-mao (思茅), 1200 m, 1957.V.11, leg. Shuyong Wang [in Chinese]; 2) leg. Guangji Hong [in Chinese]; 3) *Phorocardius flavus* Det. Shihong Jiang, 1999; 4) *Phorocardius manuleatus* (Candèze, 1888) Det. Ruan, 2018. • 1♂ (IZCAS), labels: 1) **Yunnan**, close to Si-mao (思茅), 750 m, 1957.V.11, leg. Д. панфилов [Russian name, written in Chinese]; 2) *Phorocardius manuleatus* (Candèze, 1888) Det. Ruan, 2018.

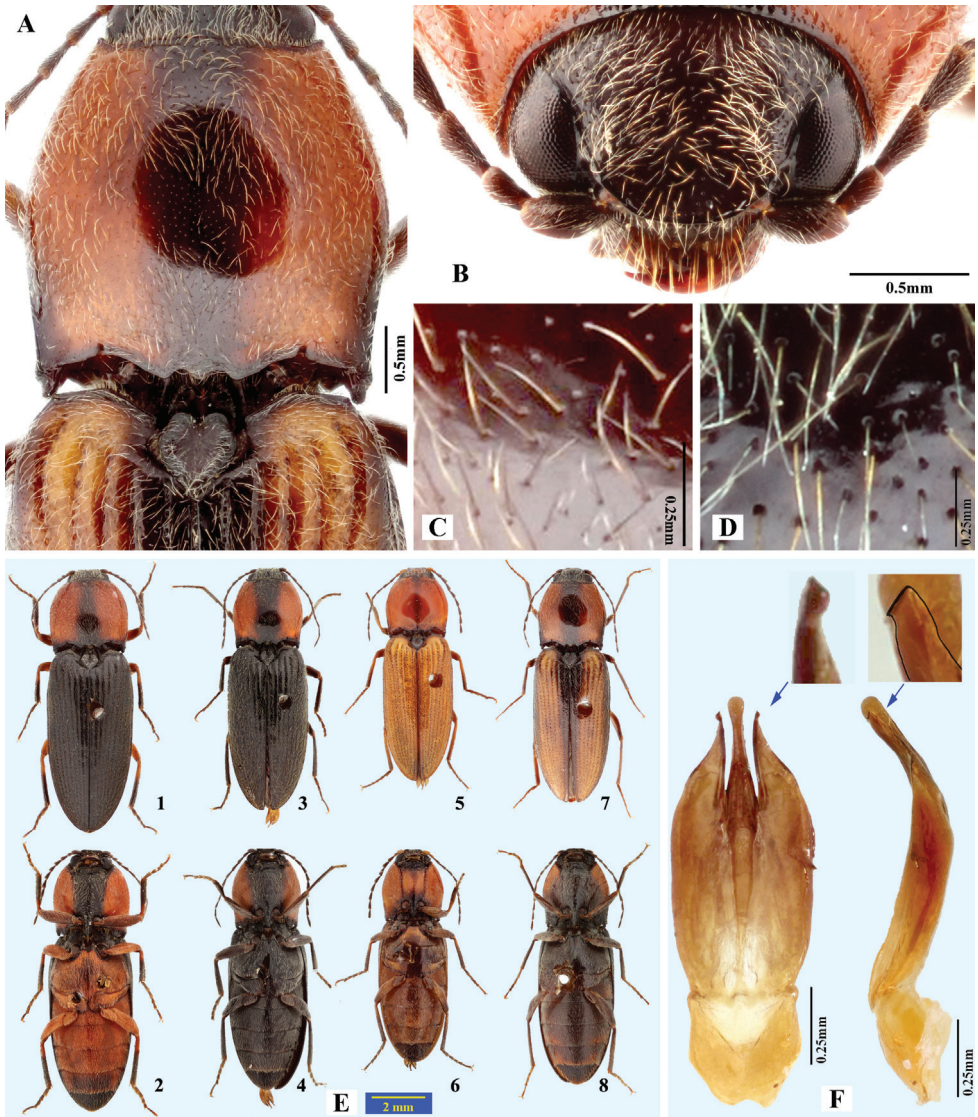


Figure 11. *Phorocardius manuleatus* Candèze (1888). **A** pronotum and scutellar shield, dorsal view **B** head, frontal view **C** punctation on disc of pronotum **D** punctation on vertex of head **E** color variation between four individuals; insets 2, 4, 6, 8 are the ventral views of 1, 3, 5, 7 **F** aedeagus, in dorsal view and lateral view, arrows indicating apices of parameres.

Remarks. This species is unusual for its extensively varied body color. The following three main patterns were found in examined specimens. Color pattern 1 (Fig. 10A, C): black on dorsum, with orange or yellow spot on base of each elytron; venter black before mesocoxae, orange from mesocoxae to abdominal ventrite IV, brown-black on abdominal ventrite V; antenna brown; and leg orange, yellow from coxa to mid-length of tibia in some, brown from mid-length of tibia to apex. Color pattern 2 (Fig. 11E):

head black; pronotum with different combinations and proportions of colors, orange at sides in most, black near midline and posterior; elytron black, yellow or mixed with brown and yellow; venter mixed with orange and black; and leg orange or yellow from coxa to mid-length of tibia, brown from mid-length of tibia to apex. Color pattern 3: dorsum and venter entirely black to black-brown, antennae brown, and legs yellow-brown on basal half, brown on apical half.

The aedeagus slightly varied in the apex shapes of the median lobe and parameres. In rare cases, the sides of the pronotum are dramatically wider and more robust (e.g., Fig. 11E₁). A comparison of specimens using mitochondrial DNA would be useful to test species boundaries.

Based on specimens from Yunnan, this species inhabits low to middle elevations (ca. 500–1200 m). Yunnan is mountainous, rainy, subtropical to tropical, with subtropical evergreen broad-leaf forest or tropical rain forest. Some of our specimens are collected from Xi-shuang-ban-na tropical rain forest. Known from Oriental Region only.

This species was treated as a subspecies of *Phorocardius melanopterus* (Candèze, 1878) by Fleutiaux (1931: 311). We have studied the photograph of the single type specimen of *P. melanopterus* [RBINS, label information: Coll. R. I. SC. N. B., CAMBODGE // Collection E. Candèze // n. sp. *Melanopterus* cdz., Cambodia // *Cardiophorus melanopterus*, Cd., dét. E. Candèze // Type]. In that specimen, the head is brown-black, the rest of the body is entirely brown throughout including legs and basal four antennomeres (all other antennomeres are missing on the type specimen), and the pronotum with lateral carina diverging from hind angle carina. Its color is different from all known color patterns of *P. manuleatus*. Additionally, *P. melanopterus* probably does not belong to *Phorocardius* because of the presence of pronotal lateral carina (see checklist above).

6. *Phorocardius minutus* Ruan & Douglas, sp. nov.

<http://zoobank.org/00316F6E-6213-4A86-A88D-8430EBC4165B>

Figs 12, 13, 23F, 24F, 25F

Type locality. Inner Mongolia: Da-yin-zi, Linxi County (“Ta-Yngtse, Linsisien”).

Etymology. This species is named for its small body size.

Distribution. China (Inner Mongolia).

Differential diagnosis. Body length 5–7 mm. Prothorax: procoxal cavities open; prosternal process gradually narrowed posterad to ventral apex in ventral view, with apex narrowly rounded. Pterothorax: scutellar shield with posterior apex narrowly rounded. Tarsal claw with ventral apex smaller than dorsal apex. Male genitalia: paramere with apex pointed and bent laterad and ventrad, without preapical lateral expansion or apical mesal callus. Female unknown.

Phorocardius minutus Ruan & Douglas, sp. nov. is distinct for its small body size, color, and more robust appendages compared to other Chinese species. Its partly yellow elytra resemble *P. flavistriolatus* Ruan & Douglas, sp. nov., and *P. comptus* (Candèze, 1860).

This species can be differentiated from *P. flavistriolatus* Ruan & Douglas, sp. nov. by the following characters: in *P. minutus* Ruan & Douglas, sp. nov., aedeagus with paramere apex claw-like, produced laterally; males are less than 6.3 mm in body length; and body brown, elytra yellow, with suture and lateral-basal edges near epipleura brown; while in *P. flavistriolatus* Ruan & Douglas, sp. nov., aedeagus with apex of paramere not claw like or produced laterally; males are longer than 7 mm; body black-brown; and elytra black-brown with two longitudinal yellow stripes.

P. minutus Ruan & Douglas, sp. nov. can be differentiated from *P. comptus* by the following characters: in *P. minutus* Ruan & Douglas, sp. nov., males are less than 6.3 mm in body length; and body brown, elytra yellow, with suture and lateral-basal edges near epipleura brown; while in *P. comptus*, males are longer than 7 mm; and body black, elytra black with two longitudinal yellow stripes.

Description. (Based on all type specimens) Dorsum matt. Head brown, with mouthparts red-brown to pale brown. Antennae pale brown. Pronotum brown, with posterior edge dark brown. Scutellar shield brown. Elytra yellow, with suture and lateral-basal edges near epipleura brown. Ventral surfaces brown, including hypomera. Epipleura brown. Legs pale brown to brown. Body with yellow pubescence.

Measurements. (based on all type specimens) Male body length 5.2–6.3 mm, width 1.6–2.2 mm. Body length to width ratio 2.9–3.2. Pronotal width to length ratio 1.1–1.2. Pronotum slightly narrower than elytra, Pronotal width to body width ratio 0.86–0.87. Elytral length to pronotal length ratio 2.7–2.9; elytron length to width ratio 3.9–4.3.

Head. Frons and vertex with interspaces between punctures 1–3 × average puncture diameter. In frontal view, edge of frontal carina convex. Antenna with apex extending slightly over posterior angle of pronotum. Distance between eyes to width of eye ratio 4.1–4.5. Antenna length to body length ratio 0.40–0.45; proportions of antennomere length as follows: 100 (scape); 66–70; 98–100; 88–95; 97–107; 97–110; 108–112; 110–115; 109–120; 104–110; 139–142.

Prothorax. Pronotum in dorsal view (Fig. 13A): sides convex from anterior to near posterior fourth, concave on posterior fourth, widest near mid-length; posterior angles with lateral sides slightly and evenly convex; surface with interspaces between punctures 1–2 × average puncture diameter. In ventral view, ventral surface of prosternal process with sides carinate at basal half (not carinate at apical half), gradually narrow from anterior to posterior end, with apex narrowly rounded. In lateral view, prosternal process with ventral surface curved strongly dorsad, posterior end weakly concave (Fig. 24F, upper arrow). Procoxal cavities open.

Pterothorax (Figs 24F, 25F). Mesepisternum in ventral view with antero-mesal angle broadly rounded (Fig. 25F, upper (green) arrow). Projections on posterior edge of mesosternum absent in ventral view (Fig. 25F, lower (red) arrow) and lateral view (Fig. 24F, lower (red) arrow). Scutellar shield: short, width to length ratio 0.85–0.94; anterolateral edges evenly convex; posterior apex narrowly rounded. Elytra: upper edge of epipleura with minute serrations.

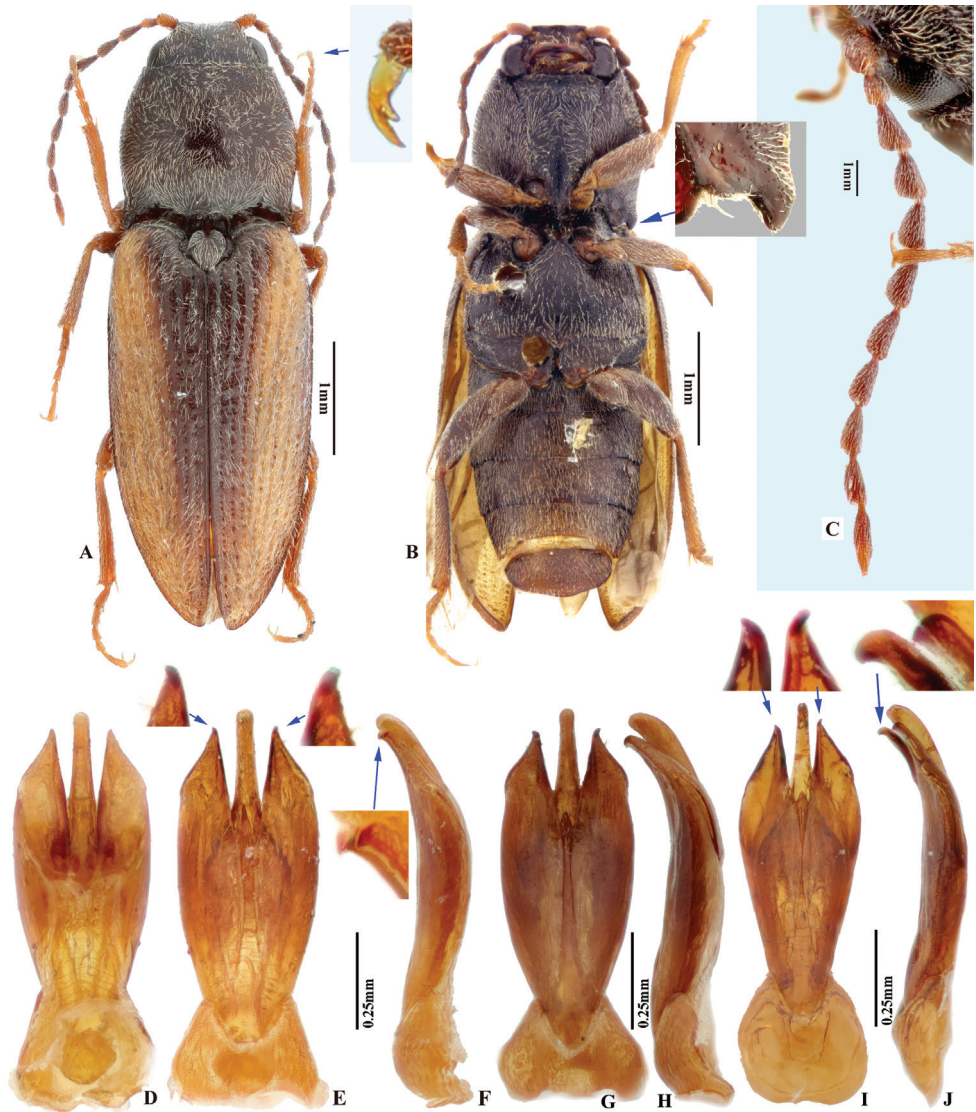


Figure 12. *Phorocardius minutus* Ruan & Douglas, sp. nov. **A** holotype, habitus, dorsal view, arrow indicating claw **B** paratype, habitus, ventral view, arrow indicating hypomeral hind edges **C** antennae of holotype, showing triangular antennomeres III–IV **D–F** aedeagus of holotype **D** dorsal view **E** ventral view, arrows indicating apices of parameres **F** lateral view, arrow indicating apices of parameres **G, H** aedeagus of paratype collected from Da-qing-gou, Inner Mongolia, ventral and lateral views **I, J** aedeagus of paratype collected from Ke-you-zhong-qi, Inner Mongolia, ventral and lateral views, arrows indicating apices of parameres.

Legs. Femora and tibiae thick. Length ratio of metatarsomeres I–V (excluding claws): 100; 66–76; 60–63; 45–48; 110–120. Claw with ventral apex much smaller than dorsal apex.

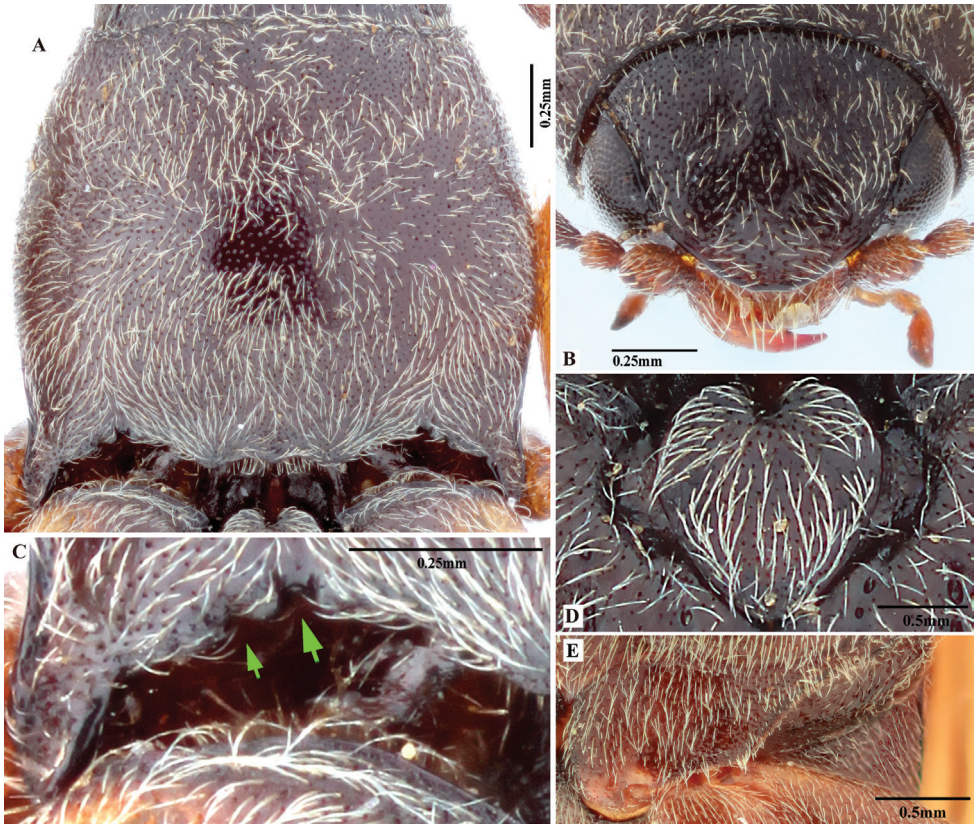


Figure 13. *Phorocardius minutus* Ruan & Douglas, sp. nov. **A** pronotum of holotype, dorsal view **B** head of holotype, dorsal-frontal view **C** posterior edge of pronotum of holotype, left side, dorsal view, arrows indicating sublateral incisions **D** scutellar shield of holotype, dorsal view **E** metacoxal plate of paratype, ventral view.

Abdomen. Lateral edges of visible abdominal ventrites I–V with minute serrations.

Male genitalia. Slender in ventral and lateral views. Median lobe in ventral view gradually narrowed from base to rounded apex. Median lobe in lateral view gently curved ventrad, apex rounded. Paramere in ventral view: wide, width 2–2.5 × median lobe width (measured across the mid-length of paramere and median lobe respectively), widest near apical third, abruptly narrowed near apex; apex pointed, bent laterally; preapical lateral expansion and apical mesal callus absent. Paramere in lateral view: robust, almost straight from base to mid-length; bent ventrad from mid-length to apex; apex pointed and facing ventrad, claw-like, but not hooked.

Female. Unknown.

Type material. Holotype. ♂ (IZCAS), labels: 1) Manchoukuo, Ta-Yngtse (大营子), Linsisien (林西县), leg. E. Bourgault, VII.1940; 2) *Phorocardius comptus* Cand. Det. Siqin Ge; 3) Holotype *Phorocardius minutus* sp. nov. Des. Ruan et al., 2019.

Paratypes (3♂). 1♂ (IZCAS), labels: 1) Inner Mongolia, Ke-you-zhong-qi (科右中旗), stock farm, 1995.VII.15 [in Chinese]; 2) leg. Mingzhi Yang [in Chinese]; 3) Cardiopnorine; 4) Elateridae; 5) Paratype *Phorocardius minutus* sp. nov. Des. Ruan et al., 2019. • 1♂ (SZPT), labels: 1) Inner Mongolia, Da-qing-gou (大青沟), Xiao-qing-hu, 19.VII.2013, leg. Kai Shi [in Chinese]; 2) Paratype *Phorocardius minutus* sp. nov. Des. Ruan et al., 2019. • 1♂ (SZPT), labels: 1) Inner Mongolia, Da-qing-gou (大青沟), Xiao-qing-hu, sweeping, 20.VII.2013, leg. Kai Shi [in Chinese]; 2) Paratype *Phorocardius minutus* sp. nov. Des. Ruan et al., 2019.

Remarks. The aedeagus of one paratype collected from ‘Ke-you-zhong-qi, Inner Mongolia’ is slightly different from that of the holotype by being slender in ventral and lateral views (Fig. 11I, J). However, all external characters of this individual (e.g., body color, shape and length, punctures on head and pronotum) are identical with the Holotype. The slight differences in the shape of aedeagus are treated as intraspecific variation here.

Previously, the genus *Phorocardius* was only known from the Oriental Region. The discovery of *P. minutus* Ruan & Douglas, sp. nov. from the Palearctic Region indicates that the members of this genus can survive in areas with freezing winter temperatures (in Ke-you-zhong-qi, Inner Mongolia, the minimum temperature is approximately -20°C in January). Examination of female genitalia or phylogenetic studies would be useful to see how closely this species is related to other *Phorocardius*. The thick tibiae and ascendant prosternal process of this species are similar to many fossorial elaterids (Douglas 2011), including many species with flightless females. Females of this species are currently unknown.

Phorocardius minutus Ruan & Douglas, sp. nov. is like *Diocarpus solitarius* (Fleutiaux, 1931) in the ventral apex of the tarsal claw is much smaller than the dorsal apex. However, *P. minutus* can be easily separated from *Diocarpus* by its open procoxal cavities and the pronotum without pronotal lateral carina.

Based on specimen information, this species inhabits low elevation areas (ca. 0–500 m) in Inner Mongolia, north China. This area is arid with temperate grassland and shrubland and cold winters. Known only from the Palearctic Region.

7. *Phorocardius rufiposterus* Ruan & Douglas, sp. nov.

<http://zoobank.org/60CF4626-B266-496A-8B46-344DB7BCF2E6>

Figs 14, 15, 23G, 24G, 25G, 26F

Type locality. Yunnan, Xi-shuang-ban-na, Xiao-meng-yang.

Etymology. This species is named after the red-brown color of the posterior half of the body.

Distribution. China (Yunnan).

Differential diagnosis. Body length greater than 7.0 mm; integument black (non-metallic) anteriorly, fading to red-brown or yellow-brown on posterior half. Prothorax: procoxal cavities closed (narrowly open in a few); prosternal process not strongly

narrowed posterad from base to ventral apex in ventral view, ventral apex almost truncate. Male genitalia: paramere acute beyond preapical lateral expansion; with preapical lateral expansion present, without apical mesal callus. Female: apex of last abdominal ventrite (ventrite V) with longitudinal slender blade-shaped projection at middle, deeply emarginate at sides.

This species is unique for its closed procoxal cavities.

It resembles *Phorocardius magnus* Fleutiaux, 1931 in the general body shape and the lighter color on the posterior half of body. They can be distinguished by the following characters: in *P. rufiposterus* Ruan & Douglas, sp. nov., aedeagus with apex of paramere robust (sides convex in dorsal view before large preapical expansion), apex spear-shaped in ventral view with acute tip and triangular preapical lateral expansion; head with frontal carina convex in frontal view; and female with ventrite V deeply emarginate, a slender blade-shaped projection present at middle (Fig. 15C), while in *P. magnus*, body entirely red-brown to brown throughout, with pronotum slightly darker; aedeagus with paramere narrow and concave before small preapical expansion in ventral view; head with frontal carina straight in frontal view; and female with the apex of abdominal ventrite V tri-lobed, middle lobe semicircular to longitudinal with apex rounded, not slender blade-shaped.

Description. (based on all type specimens) Body black anteriorly, fading to red-brown or yellow-brown on posterior half. Dorsum glabrous and shiny. Head black, with mouthparts red-brown to dark brown. Antennae brown. Pronotum black, with anterior and posterior edge brown. Elytra black to dark red-brown anteriorly, fading to red-brown or yellow-brown posteriorly. Venter black to dark red-brown on anterior half, fading to red-brown or yellow-brown on posterior half. Epipleura red-brown. Legs red-brown to dark red-brown. Body surface covered with yellow-grey pubescence.

Measurements. (based on all type specimens) Male body length 8.2–10.2 mm, width 2.6–3.2 mm. Female body length 8.5–10.6 mm, width 3.0–3.5 mm. Body length to width ratio 3.0–3.2. Pronotal width to length ratio 1.0–1.1. Pronotal width to body width ratio 0.87–0.90. Elytral length to pronotal length ratio 2.3–2.4; elytron length to width ratio 4.1–4.2.

Head. Frons and vertex with interspaces between punctures $1.5\text{--}4 \times$ average puncture diameter, sparsest at centre of frons. Frontal carina in frontal view convex, not straight. Antenna with apex not reaching beyond posterior angle of pronotum. Distance between eyes to width of eye ratio in frontal view 3.0–3.2. Antenna length to body length ratio, in male 0.36–0.37, in female 0.33–0.34; proportions of antennomere length (male) as follows: 100 (scape); 51–59; 75–80; 71–76; 75–80; 73–80; 68–78; 67–75; 73–80; 78–80; 92–99.

Prothorax. Pronotum in dorsal view (Fig. 14A): sides evenly convex from apex to slight concavity near posterior third, widest near mid-length; posterior angles with lateral sides almost straight, not bulged; surface with interspaces between punctures $1.5\text{--}2.5 \times$ average puncture diameter. Punctures much smaller or nearly absent posterad than at centre of disc. In ventral view, ventral surface of prosternal process with sides

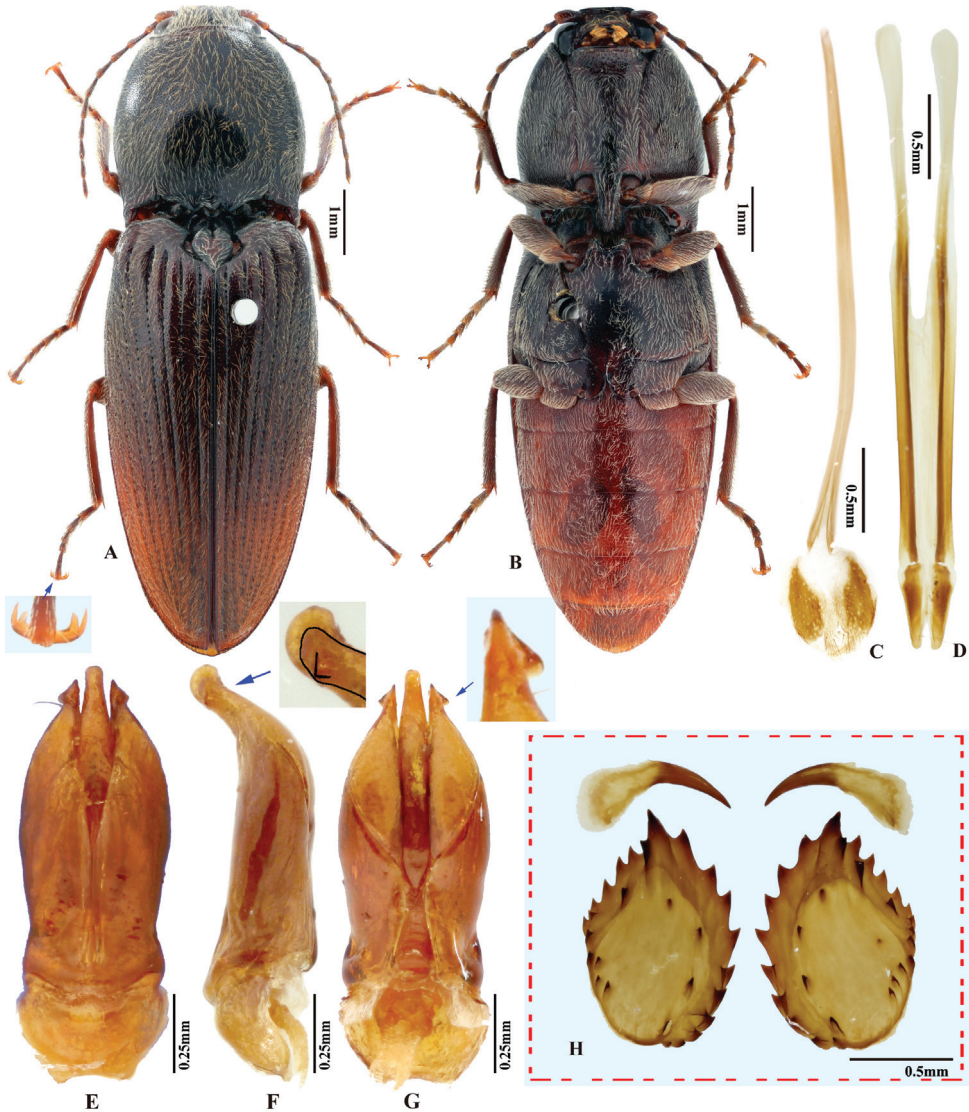


Figure 14. *Phorocardius rufiposterus* Ruan & Douglas, sp. nov. **A** holotype, habitus, dorsal view, arrow indicating claws **B** holotype, habitus, ventral view **C** female abdominal sternite VIII, dorsal view (paratype) **D** ovipositor, dorsal view (paratype) **E** aedeagus, ventral view (paratype) **F** aedeagus, lateral view (paratype), arrow indicating apex of paramere and median lobe **G** aedeagus, dorsal view (paratype), arrow indicating apex of paramere **H** distal (upper side) and proximal sclerites of bursa copulatrix.

carinate and slightly and gradually narrow from anterior to mid-length, parallel-sided from mid-length to posterior end, apex almost truncate. In lateral view, prosternal process with ventral surface curved slightly dorsad, posterior end with ventral 2/3 almost straight, dorsal 1/3 produced posteriorly (Fig. 24G, upper arrow). Procoxal cavity closed (Fig. 15E), narrowly open in a few.

Pterothorax (Figs 24G, 25G). Mesepisternum in ventral view with antero-mesal angle acute, long (Fig. 25G, upper (green) arrow). Projections on posterior edge of mesosternum: in ventral view weakly developed (Fig. 25G, lower (red) arrow); in lateral view almost absent (Fig. 24G, lower (red) arrow). Scutellar shield: width to length ratio 0.88–0.90; anterolateral edges slightly sinuate; posterior apex pointed. Elytra: upper edge of epipleura with minute serrations.

Legs. Length ratio of metatarsomeres I–V (excluding claws): 100; 80–90; 65–75; 57–62; 137–155. Claw with ventral apex almost as large as dorsal apex.

Abdomen. Lateral edges of visible abdominal ventrites I–V with minute serrations.

Male genitalia. Robust in ventral and lateral views. Median lobe in ventral view gradually narrowed from base to near apex, apex rounded to apically flattened. Median lobe in lateral view curved ventrad, with apex dilated and recurved dorsad. Paramere in ventral view: wide, width 2.5–3.5 × median lobe width (measured at mid-length of paramere and median lobe respectively); widest near mid-length, gradually narrowed and with outer sides evenly convex towards apex; apex spear-shaped, with acute tip and triangular preapical lateral expansion, apical mesal callus absent. Paramere in lateral view: robust, almost straight from base to apical third, gradually narrowed and bent ventrad from apical third to apex; apex slightly recurved dorsad, preapical ventral expansion absent, with an angulate structure near apex (see Fig. 14F), without hook-shaped structure.

Female. Body color like male. Ventrite V deeply emarginate at apex, with longitudinal slender blade-shaped projection at midline (Fig. 15C) (male with ventrite V entirely convex and rounded). Proximal sclerites of bursa copulatrix oval, apex acute (Fig. 14H): base with without concavity, each with 14–16 large spines occupying two-thirds of edges, 9–10 smaller spines on disc.

Type material. Holotype. ♂ (IZCAS), labels: 1) **Yunnan**, Xi-shuang-ban-na, Xiao-meng-yang (小勐养), 850 m, Chinese Academy of Sciences [in Chinese]; 2) 1957.VI.18, leg. Linchao Zang [in Chinese]; 3) Holotype *Phorocardius rufiposterus* sp. nov. Des. Ruan et al., 2019.

Paratypes (23♂, 11♀). 1♂ (SZPT), labels: 1) **Yunnan**, Xi-shuang-ban-na, Xiao-meng-yang (小勐养), 850 m, Chinese Academy of Sciences [in Chinese]; 2) 1957.IX.13, leg. Shuyong Wang [in Chinese]; 3) *Phorocardius* sp. det. Shihong Jiang, 1999; 4) Paratype *Phorocardius rufiposterus* sp. nov. Des. Ruan et al., 2019. • 2♀ (SZPT), labels: 1) **Yunnan**, Lin-cang, Yun-xian County, Man-wang township (漫湾镇), light trap, VI–VII, leg. Zichun Xiong, Shenzhen Polytechnic [in Chinese]; 2) Paratype *Phorocardius rufiposterus* sp. nov. Des. Ruan et al., 2019. • 2♂ (SZPT), labels: 1) CN: **Yunnan**, Xiping County (新平), 2013.VI.7, Collector unknown, Shenzhen Polytechnic [partly in Chinese]; 2) Paratype *Phorocardius rufiposterus* sp. nov. Des. Ruan et al., 2019. • 1♂ (SZPT), labels: 1) **Yunnan**, Xi-shuang-ban-na, Meng-a (勐阿), 1000 m, Chinese Academy of Sciences [in Chinese]; 2) 1958.VI.21, leg. Shuyong Wang [in Chinese]; 3) *Phorocardius* sp. det. Shihong Jiang, 1999; 4) Paratype *Phorocardius rufiposterus* sp. nov. Des. Ruan et al., 2019. • 2♂2♀ (IZCAS), labels: 1) **Yunnan**, Xi-shuang-ban-na, Xiao-meng-yang (小勐养), 850 m, Chinese Academy of Sciences [in Chinese]; 2) 1957.VI.14–20, leg. Shuyong Wang & Linchao Zang [in Chinese];

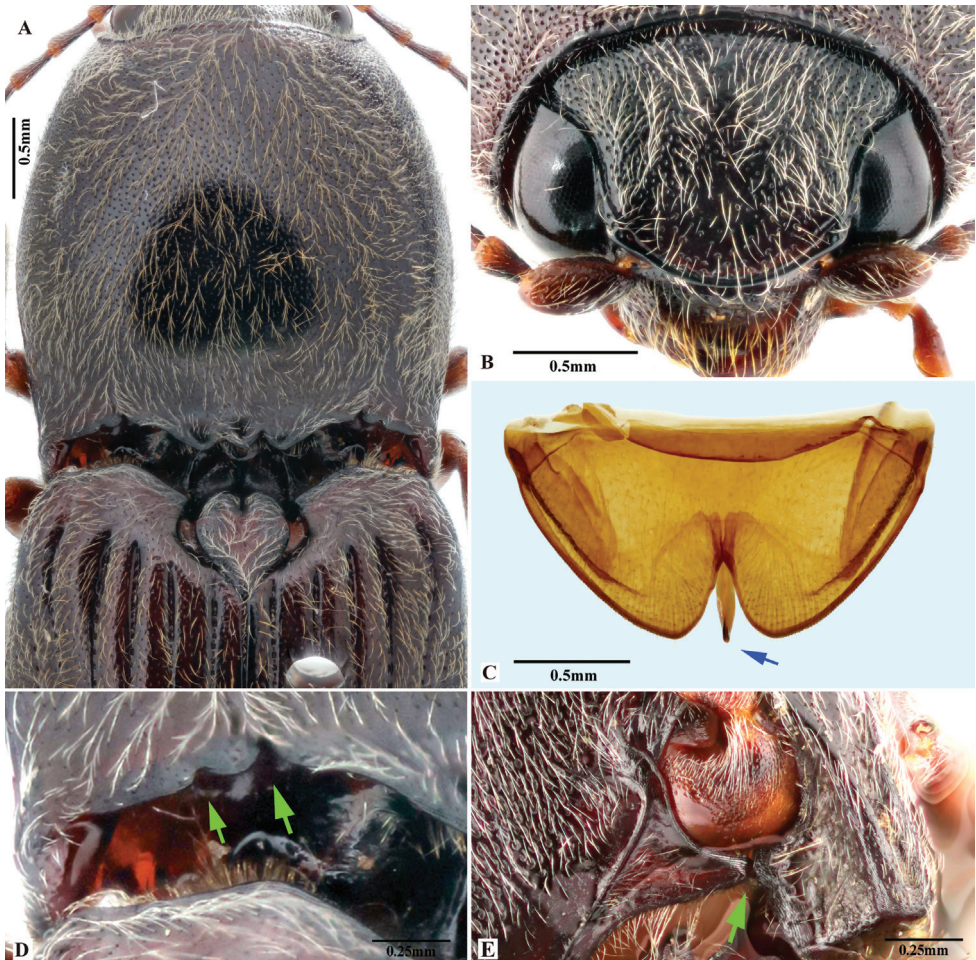


Figure 15. *Phorocardius rufiposterus* Ruan & Douglas, sp. nov. **A** pronotum and scutellar shield of holotype, dorsal view **B** head, frontal view **C** last abdominal ventrite (ventrite V) of female, dorsal view, arrow indicating blade-like projection **D** posterior edge of pronotum, left side, dorsal view, arrows indicating sublateral incisions **E** procoxa, lateral-ventral view, arrow indicating closed procoxal cavity.

3) Paratype *Phorocardius rufiposterus* sp. nov. Des. Ruan et al., 2019. • 2♂ (IZCAS), labels: 1) Shuan Jiang (双江县), 55-VI; 2) Paratype *Phorocardius rufiposterus* sp. nov. Des. Ruan et al., 2019. • 1♂ (IZCAS), labels: 1) **Yunnan**, Xi-shuang-ban-na, Meng-la (勐腊), 620–650 m, Chinese Academy of Sciences [in Chinese]; 2) 1958.VI.10, leg. Yirang Zhang [in Chinese]; 3) Paratype *Phorocardius rufiposterus* sp. nov. Des. Ruan et al., 2019. • 3♂4♀ (IZCAS), labels: 1) **Yunnan**, Xi-shuang-ban-na, Meng-a (勐阿), 800–1080 m, Chinese Academy of Sciences [in Chinese]; 2) 1958.V–VIII, leg. Shuyong Wang & Fuji Pu [in Chinese]; 4) Paratype *Phorocardius rufiposterus* sp. nov. Des. Ruan et al., 2019. • 4♂2♀ (IZCAS), labels: 1) **Yunnan**, Xi-shuang-ban-na, Meng-hun (勐混), 650–950 m, Chinese Academy of Sciences [in Chinese]; 2) 1958.

VI.3–15, leg. Xuwu Meng, Shuyong Wang & Chunpei Hong [in Chinese]; 3) Paratype *Phorocardius rufiposterus* sp. nov. Des. Ruan et al., 2019. • 4♂ (IZCAS), labels: 1) **Yunnan**, Xi-shuang-ban-na, Meng-hun (勐混), 650–1200 m, Chinese Academy of Sciences [in Chinese]; 2) 1958.V–VII, leg. Xuwu Meng & Zhixing Chen [in Chinese]; 3) Paratype *Phorocardius rufiposterus* sp. nov. Des. Ruan et al., 2019. • 1♂ (TARI, ex. SZPT), labels: 1) **Yunnan**, Xi-shuang-ban-na, Meng-hun (勐混), 750 m, Chinese Academy of Sciences [in Chinese]; 2) 1958.V-31, leg. Xuwu Meng [in Chinese]; 3) Paratype *Phorocardius rufiposterus* sp. nov. Des. Ruan, 2018. • 1♀ (IZCAS), labels: 1) **Yunnan**, Jing-dong (景东), 1170 m, 1958.VII.3 [in Chinese]; 2) Paratype *Phorocardius rufiposterus* sp. nov. Des. Ruan et al., 2019. • 1♂ (IZCAS), labels: 1) southwest **Yunnan**, close to Jing-ping (金平), 1170 m, 1956.VII.27, leg. панфилов [written in Russian]; 2) Paratype *Phorocardius rufiposterus* sp. nov. Des. Ruan et al., 2019. • 1♂ (IZCAS), labels: 1) **Yunnan**, Lan-cang (澜沧), 1000 m, 1957.VII.29, leg. Lingchao Zang [in Chinese]; 2) Paratype *Phorocardius rufiposterus* sp. nov. Des. Ruan et al., 2019.

Remarks. This species is unique for its closed procoxal cavities, which has not been reported in other *Phorocardius* species. However, other aspects of this species are consistent with generic traits of *Phorocardius*. These are: characteristic claws and female and male genitalia.

Integument color varies slightly between individuals. However, the gradual change of color from anterior to posterior end of the body can be observed in all specimens.

Based on specimen information, this species inhabits low to middle elevations (ca. 500–1500 m) in Yunnan Prov., south China. Yunnan is rainy, subtropical to tropical, with evergreen broad-leaf forest or tropical rain forest. This species is distributed only in the Oriental Region.

8. *Phorocardius unguicularis* (Fleutiaux, 1918)

Figs 16, 23H, 24H, 25H, 26G

Cardiophorus unguicularis Fleutiaux, 1918: 222. Type locality: “Tonkin: Région de Lao-Kay et de Ho-Khéou, frontière de Chine”, interpreted as Vietnam: the area near frontier of Lao-Cai city (Vietnam) and He-Kou city (China).

Phorocardius unguicularis: Fleutiaux 1913: 311.

Distribution. China: Yunnan (Fleutiaux 1931, 1947), Hainan (new record), Sichuan (“Se-Tchouen, Aubert” – Fleutiaux (1931)); Vietnam (Fleutiaux 1918).

Differential diagnosis. Body length greater than 7.0 mm; integument brown to dark brown. Prothorax: procoxal cavities open; prosternal process gradually and only slightly narrowed posterad to ventral apex in ventral view, with apex almost truncate. Pterothorax: scutellar shield with posterior apex pointed. Tarsal claw with ventral apex not smaller than dorsal apex. Male genitalia: paramere without preapical lateral expansion or apical mesal callus in any view. Female: apex of last abdominal ventrite (ventrite V) simple, not emarginate at apex.

This species is unique among Chinese *Phorocardius* species by having extremely dense pronotal punctation (interspaces between pronotal punctures $0.3\text{--}1 \times$ average puncture diameter).

Phorocardius unguicularis (Fleutiaux, 1918) resembles *P. magnus* Fleutiaux, 1931 in body color and size. They can be separated by the following combination of characters: in *P. unguicularis* (Fleutiaux, 1918), aedeagus slender in lateral view (paramere maximum thickness $1/5$ paramere length), in ventral view paramere widened from base to mid-length, narrowed from mid-length to apex, apex pointed and without preapical lateral expansion; pronotum with deep punctures, interspaces between punctures $0.3\text{--}1 \times$ average puncture diameter; and head with frontal carina convex at middle in frontal view; while in *P. magnus* Fleutiaux, 1931, aedeagus robust in lateral view (paramere maximum thickness $1/3$ paramere length); in ventral view, paramere slightly widened from base to apical fourth, apical fourth abruptly narrowed, with hook-like preapical lateral expansion; pronotum with interspaces between punctures $1\text{--}2.5 \times$ average puncture diameter; and head with frontal carina straight in frontal view.

Phorocardius unguicularis (Fleutiaux, 1918) resembles *P. yanagiharae* (Miwa, 1927) in body color. They can be separated by the following combination of characters. In *P. unguicularis* (Fleutiaux, 1918), in ventral view, aedeagus with paramere gradually narrowed from mid-length to apex, apex pointed and without preapical lateral expansion; pronotum with deep punctures, interspaces between punctures $0.3\text{--}1 \times$ average puncture diameter; and head with frontal carina convex in frontal view; while in *P. yanagiharae* (Miwa, 1927), in ventral view, aedeagus with paramere, abruptly narrowed from apical third to apex, apex with hook-like preapical lateral expansion; pronotum with shallow punctures, interspaces between punctures $1\text{--}2 \times$ average puncture diameter; and head with frontal carina straight in frontal view.

Phorocardius unguicularis is also similar to *P. astutus* (Candèze, 1888), it differs from the latter based on the following characters: body brown to dark-brown with yellow-brown appendages; legs yellow-brown throughout; proximal sclerites of copulatrix kidney-shaped with slight basal concavity; and parameres of aedeagus without pre-apical lateral expansions. In *P. astutus*: body brown-black with dark appendages; legs with red-brown joints; proximal sclerites of copulatrix oval, not kidney-shaped, without basal concavity; and parameres wedge-like with pre-apical lateral expansions. Additionally, *P. unguicularis* has narrower pronotum and body, and larger body length. Further study of these two species would be important to verify their status.

Description. (Based on photographs of the holotype and all examined specimens) Body brown to dark brown (brown-black in a few); legs and antennae brown; pronotum slightly darker than rest (Fig. 16A, B). Integument matt, with yellow pubescence.

Measurements. (based on the type and non-type specimens) Male body length 8.6–11.2 mm, width 2.2–3.2 mm. Female body length 9.6–12.8 mm, width 3.0–4.0 mm. Body length to width ratio 2.9–3.1. Pronotal width to length ratio 1.1–1.2. Pronotal width to body width ratio 0.76–0.81. Elytral length to pronotal length ratio 2.7–3.1; elytron length to width ratio 4.4–4.7.

Head. Frons and vertex with interspaces between punctures $0.5\text{--}1.5 \times$ average puncture diameter. Frontal carina in frontal view convex, not straight. Antenna with

apex slightly extending over base of elytron, slightly varied long in different individuals. Distance between eyes to width of eye ratio 3.6–3.8. Antenna length to body length ratio, in male 0.39–0.42, in female 0.37–0.39. Proportions of antennomere lengths (male): 100 (scape); 60–65; 80–85; 95–99; 95–99; 91–95; 94–104; 92–95; 86–90; 73–83; 100–105.

Prothorax. Pronotum in dorsal view: sides evenly convex, widest near mid-length (Fig. 16C); posterior angles with lateral sides almost straight, slightly convex and bulged at basal half in some cases; surface with interspaces between punctures $0.3\text{--}1 \times$ average puncture diameter. In ventral view, ventral surface of prosternal process with sides not carinate and gradually narrowed from anterior to near posterior end, apex almost truncate. In lateral view, prosternal process with ventral surface curved slightly dorsad, posterior end with ventral $2/3$ almost straight, dorsal $1/3$ produced posteriorly (Fig. 24H, upper arrow). Procoxal cavities open.

Pterothorax (Figs 24H, 25H). Mesepisternum in ventral view with antero-mesal angle right-angled (Fig. 25H, upper (green) arrow). Projections on posterior edge of mesosternum: almost absent in ventral view (Fig. 25H, lower (red) arrow), and lateral view (Fig. 24H, lower (red) arrow). Scutellar shield: width to length ratio 0.94–0.95; anterolateral edges slightly sinuate; posterior apex pointed. Elytra: upper edge of epipleura with minute serrations.

Legs. Length ratio of metatarsomeres I–V (excluding claws): 100; 78–85; 70–78; 50–57; 125–134. Claw with ventral apex almost as large as dorsal apex.

Abdomen. Lateral edges of visible abdominal ventrites I–V with minute serrations.

Male genitalia. Robust from ventral and dorsal views, slender in lateral view. Median lobe in ventral view gradually narrowing from base to near mid-length, apical half elongate with sides parallel-sided to slightly convex, apex narrowly rounded. Median lobe in lateral view almost straight, apex narrowly rounded. Paramere in ventral view: robust, width $3\text{--}4 \times$ median lobe width (measured at mid-length of paramere and median lobe respectively), widest near mid-length; gradually narrowing from mid-length to apex, apex elongate and needle-like, without preapical lateral expansion or apical mesal callus (Fig. 16E). Paramere in lateral view: slender, gradually narrowing and curved ventrad from base to near apex; preapical ventral expansion absent, without hook-shaped structure.

Female. Body color like male. Apex of abdominal ventrite V slightly sinuate (Fig. 26G). Proximal sclerites of bursa copulatrix elongate-kidney shaped, apex acute (Fig. 16H), base with slight concavity: each with 13–15 large spines mainly on the convex mesal edge, 10–12 smaller spines on disc.

Type material. *Holotype* (sex unknown, in MNHN, photographs of holotype provided by Dr Antoine Mantilleri), labels: 1) Museum Paris, Frontière Chine-Tonkin, Region De Lao-Kay, Et Ho-Kheou, Ch. Dupont; 2) *Cardiophorus unguicularis* Fleut., type, Fleutiaux det.; 3) Collection E. Fleutiaux; 4) Holotype [red label]; 5) Holotype, *Phorocardius unguicularis* (Fleutiaux, 1918); 6) MNHN EC9217.

Additional material. 1♀ (TARI), without information of locality, with only one label: *Phorocardius unguicularis* Fleut., Coll. E. Fleutiaux. 1♂16♀ (IZCAS), labels: 1) **Yunnan**, Li-jiang, Yu-long-shan (玉龙山), 2700 m, Chinese Academy of Sciences

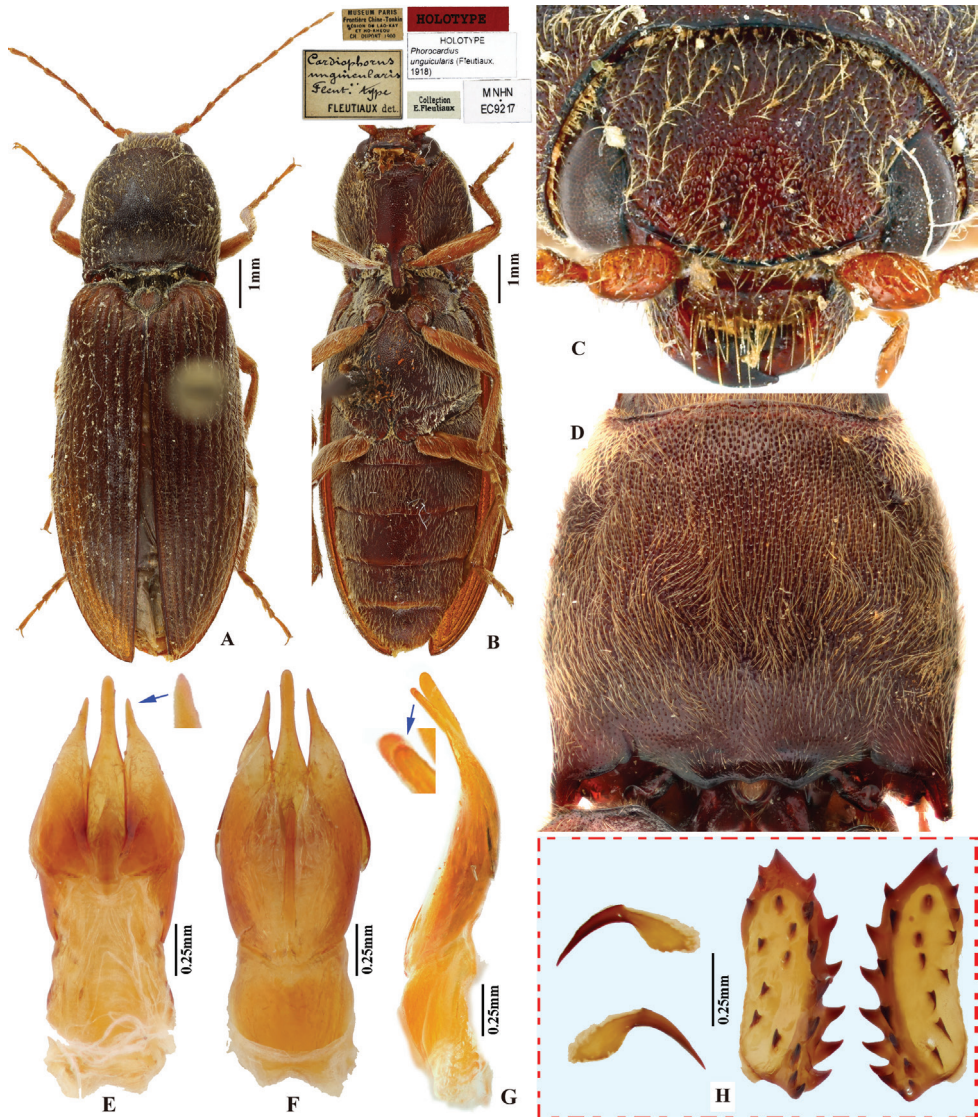


Figure 16. *Phorocardius unguicularis* (Fleutiaux, 1918). **A** holotype habitus, dorsal view (photograph: Dr Antoine Mantilleri, MNHN) **B** holotype habitus, ventral view with specimen labels (photograph: Dr Antoine Mantilleri, MNHN) **C** head of holotype, frontal view **D** pronotum (non-type specimen) **E** aedeagus, dorsal view (non-type specimen), arrow indicating apex of paramere **F** aedeagus, ventral view (non-type specimen) **G** aedeagus, lateral view (non-type specimen), arrow indicating apices of parameres **H** distal (left side) and proximal sclerites of bursa copulatrix (inner view, non-type specimen).

[in Chinese]; 2) 1984.VII.27, leg. Shuyong Wang [in Chinese]; 3) *Phorocardius unguicularis* (Fleutiaux, 1918) Det. Ruan, 2018. • 4♂4♀ (IZCAS), labels: 1) **Yunnan**, Li-jiang, Yu-hu (玉湖), 2750 m, Chinese Academy of Sciences [in Chinese]; 2) 1984.VII.21–23, leg. Jianguo Fang / Changfang Li [in Chinese]; 3) *Phorocardius unguicularis* (Fleutiaux, 1918) Det. Ruan, 2018. • 1♀ (IZCAS), labels: 1) *Cardiophorus*, **Yunnan**,

Collection Fleutiaux, Li-jiang, Yu-long-shan (玉龙山), 2700 m, Chinese Academy of Sciences [in Chinese]; 2) 1984.VII.27, leg. Shuyong Wang [in Chinese]; 3) *Phorocardius unguicularis* (Fleutiaux, 1918) Det. Ruan, 2018. • 2♂7♀ (IZCAS), labels: 1) **Yunnan**, Yong-sheng, Liu-de (六德), 2250–2750 m, Chinese Academy of Sciences [in Chinese]; 2) 1984.VII, leg. Shuyong Wang et al. [in Chinese]; 3) *Phorocardius unguicularis* (Fleutiaux, 1918) Det. Ruan, 2018. • 1♂ (IZCAS), labels: 1) **Hainan** Prov., Chang-jiang County, Ba-wang-ling, 145 m, 2007.V.7N, Chinese Academy of Sciences [in Chinese]; 2) 19.1104N 109.08168E, leg. Hongbin Liang, Chinese Academy of Sciences [in Chinese]; 3) *Phorocardius unguicularis* (Fleutiaux, 1918) Det. Ruan, 2018.

Remarks. Based on specimen information, this species inhabits low to high elevations in south China and north Vietnam. The highest elevation record for this species is around 2750 m. Some specimens were collected at the foot of Yu-long-shan Mountain (also known as Yu-long Snow Mountain), whose main peak is 5596 m, and with snowfall all the year-round above 3500 m. South China and north Vietnam are rainy, with subtropical to tropical climates, with subtropical evergreen broad-leaf forest or tropical rain forest. This species is known only from the Oriental Region.

9. *Phorocardius yanagiharae* (Miwa, 1927)

Figs 17, 18

Cardiophorus yanagiharae Miwa, 1927: 109. Type locality: Taiwan, Tainan (China).
Phorocardius yanagiharae: Miwa 1934: 209.

Distribution. China: Taiwan (Miwa 1927, 1931).

Differential diagnosis. Body length greater than 7.0 mm; integument red-brown to brown throughout. Prothorax: procoxal cavities open. Pterothorax: scutellar shield with posterior edge pointed. Tarsal claw with ventral apex not smaller than dorsal apex. Male genitalia: paramere with preapical lateral expansion present, without apical mesal callus. Female unknown.

Phorocardius yanagiharae (Miwa, 1927) resembles *P. magnus* Fleutiaux, 1931 in general body color and shape. They can be separated by the following combination of characters. In *P. yanagiharae* (Miwa, 1927), in lateral view, aedeagus with median lobe straight at apex, with paramere slender and ca. 1/2 as wide as median lobe (measured near middle part); pronotum narrower than in *P. magnus*, pronotal width to body width ratio 0.86; and in dorsal view, pronotum with sides of posterior angles strongly bulged and convex (Fig. 18C, D); while in *P. magnus* Fleutiaux, 1931: in lateral view, aedeagus with median lobe recurved dorsally at apex, with paramere robust and as wide as median lobe (measured near middle part); pronotum wider than in *P. yanagiharae*, pronotal width to body width ratio 0.90–0.97; and in dorsal view, pronotum with sides of posterior angles not bulged, straight to slightly convex (Fig. 9A).

Phorocardius yanagiharae (Miwa, 1927) also resembles *P. unguicularis* (Fleutiaux, 1918) in body color. They can be separated by the following combination of characters. In *P. yanagiharae* (Miwa, 1927), in ventral view, aedeagus with paramere, abruptly

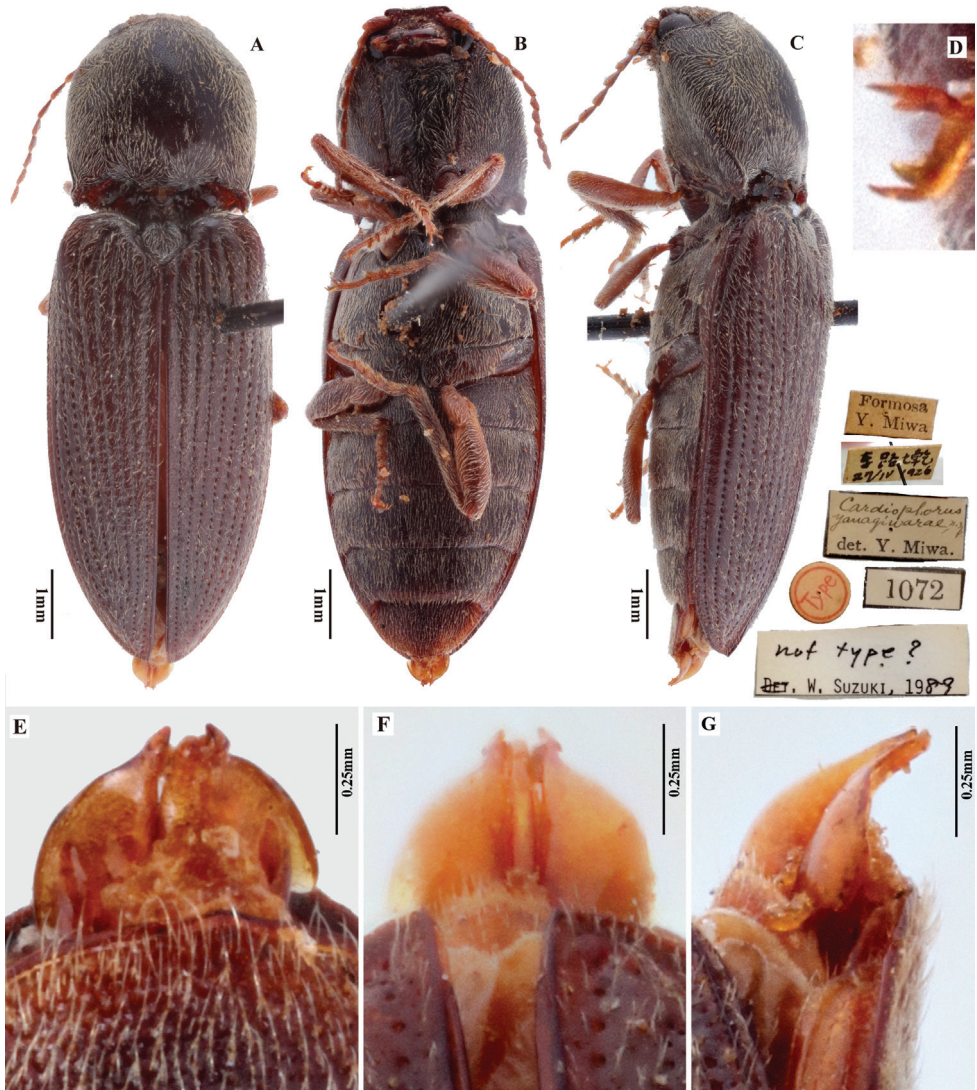


Figure 17. *Phorocardius yanagiharae* (Miwa, 1927). **A** holotype, habitus, dorsal view **B** holotype, habitus, ventral view **C** holotype, habitus, lateral view with specimen labels **D** claw of holotype **E** apical part of aedeagus of holotype, ventral view **F** apical part of aedeagus of holotype, dorsal view **G** apical part of aedeagus of holotype, lateral view.

narrowed from apical third to apex, apex with hook-like preapical lateral expansion; pronotum with shallow punctures, interspaces between punctures 1–2 × average puncture diameter; and head with frontal carina straight in frontal view; while in *P. unguicularis* (Fleutiaux, 1918), in ventral view, aedeagus with paramere gradually narrowed from mid-length to apex, apex pointed and without preapical lateral expansion;

pronotum with deep punctures, interspaces between punctures $0.3\text{--}1 \times$ average puncture diameter; and head with frontal carina convex in frontal view.

Description. (based on holotype) Color entirely red-brown to brown throughout, with legs and antennae yellow-brown to brown; pronotum and venter slightly darker than elytra. Integument matt, with light yellow pubescence.

Measurements. (based on holotype) Body length 9.4 mm. Body width 3.3 mm. Body length to width ratio 2.9. Pronotal width to length ratio 1.1. Pronotal width to body width ratio 0.86. Elytral length to pronotal length ratio 2.6; elytron length to width ratio 4.3.

Head. Frons and vertex with interspaces between punctures $1\text{--}3 \times$ average puncture diameter. Frontal carina in frontal view transversely straight. Antenna with apex extending to posterior angle of pronotum. Distance between eyes to width of eye ratio 3.0. Antenna length to body length ratio 0.36.

Prothorax. Pronotum in dorsal view (Fig. 18A): sides strongly convex from anterior edge to posterior fourth, slightly convex from posterior fourth to base of posterior angle, concave at base of posterior angle; widest near posterior third; posterior angles with lateral margin convex, strongly bulged laterally (Fig. 18C, D); surface with interspaces between punctures $1\text{--}2 \times$ average puncture diameter.

Pterothorax. Projections on posterior edge of mesosternum: in lateral view present, acute, (Fig. 17C). Scutellar shield: width to length ratio 1.0; anterolateral edges slightly sinuate; posterior apex pointed. Elytra: upper edge of epipleura with minute serrations.

Legs. Length ratio of metatarsomeres I–V (excluding claws): 100; 66; 61; 47; 122. Claw with ventral apex almost as large as dorsal apex.

Abdomen. Lateral edges of visible abdominal ventrites I–V with minute serrations.

Male genitalia (only apical third observed in current study, see Fig. 17E–G). Apical third robust in ventral and lateral views. Apical third of median lobe in ventral view (Fig. 17E) narrowing from base to apex, apex rounded. Apical third of median lobe in lateral view bent ventrad (Fig. 17G). Apical third of paramere in ventral view: extremely wide, $2\text{--}3 \times$ wider than median lobe (measured at base of apical third), sides convex and narrowed to near apex, preapical lateral expansion triangular, facing laterally (Fig. 17F); apex acute beyond preapical lateral expansion, apical mesal callus absent. Apical third of paramere in lateral view: bent ventrad and gradually narrowed towards apex, preapical ventral expansion absent, without hook-shaped structure near apex.

Female. Unknown.

Type material. Holotype. male (TARI), labels: 1) Formosa, Y. Miwa; 車路壩, 27/IV, 1926; 2) *Cardiophorus yanagiharae* n. sp., det. Y. Miwa; 3) Type; 4) 1072; 5) Not type?, det. W. Suzuki, 1989; 6) Holotype of *Cardiophorus yanagiharae* Miwa, 1927, Identified by Ruan & Douglas, 2020.

Remarks. Miwa (1927) stated that only one specimen was used for description of *Cardiophorus yanagiharae* Miwa, 1927 in the original publication. Therefore, according to ICZN (Art. 73.1.2.), the single specimen he described was fixed as holotype.

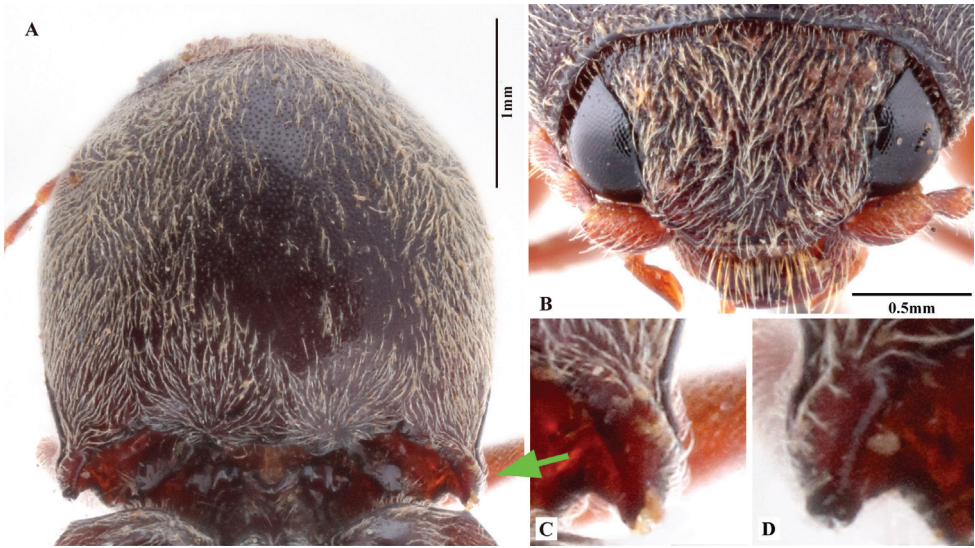


Figure 18. *Phorocardius yanagiharae* (Miwa, 1927). **A** holotype, pronotum, dorsal view **B** holotype, head, frontal view **C** right posterior angle of pronotum, dorsal view **D** left posterior angle of pronotum, dorsal view.

We have investigated the TARI Elateridae collection. Only one single specimen labeled as “*Cardiophorus yanagiharae* sp. nov.” was discovered, which we have identified as the holotype for the following reasons: 1) it is preserved in the type collection with a circular type label and a rectangular TARI type number label; 2) it has a label indicating “*Phorocardius yanagiharae* n. sp.” in Miwa’s handwriting; and 3) it has a label that indicates the specimen locality “車路墘”, which is a location in the city “Tainan”, which matches the type locality Miwa (1927) provided.

We believe Miwa had incorrectly reported the sex of the type as female. Moreover, Miwa implied the collecting date is “21/IV, 1926”. However, according to our examination, the date on the label is “27/IV, 1926”.

The previous record of *Phorocardius yanagiharae* from Sichuan province (Jiang 1993; Jiang and Wang 1999) are erroneous. We investigated those specimens the authors used, and they turned out to be a new species (i.e., *Phorocardius yunnanensis* Ruan & Douglas, sp. nov., see following text).

Based on specimen information, this species inhabits low elevations (below 100 m) in south Taiwan island. The area is rainy, with subtropical to tropical climate. This species is currently considered endemic to Taiwan.

10. *Phorocardius yunnanensis* Ruan & Douglas, sp. nov.

<http://zoobank.org/66DD489B-D095-4CCE-86A0-40676B3F1DA3>

Figs 19, 20, 23I, 24I, 26H

Type locality. Yunnan Prov., Xi-shuang-ban-na, Meng-a (alt. 1050–1080 m).

Etymology. The name of this species refers to the type locality.

Distribution. China (currently endemic to Yunnan).

Differential diagnosis. Body length greater than 7.0 mm; integument black and shiny (non-metallic), elytron without yellow stripes, appendages yellow-brown. Prothorax: procoxal cavities narrowly open; prosternal process not strongly narrowed posterad to ventral apex in ventral view, with apex truncate to slightly rounded. Pterothorax: scutellar shield with posterior apex pointed. Tarsal claw with ventral apex not smaller than dorsal apex. Male genitalia: paramere acute in ventral view with small, acute preapical lateral expansion, without apical mesal callus. Female: apex of last abdominal ventrite (ventrite V) truncate to slightly convex, bent dorsad, each side with an incision.

This species is distinctive for having the dorsum entirely black and shiny and legs entirely yellow-brown (except for brown-black coxae).

Phorocardius yunnanensis Ruan & Douglas, sp. nov. is close to *P. vicinus* in brown-black body color, but distinguishable by the following. In *P. yunnanensis* Ruan & Douglas, sp. nov., pronotum longer with length of pronotum to elytra ratio 0.37–0.40 (excluding posterior angle) or ca. 0.43 (including posterior angle); antennae, palpi of mouthparts and legs yellow-brown to brown; and proximal sclerites of bursa copulatrix with basal edge concave. According to Kollar (1848) and type material (NHMW), *P. vicinus* has length of pronotum to elytra ratio only 0.33; appendages brown-black to black; and proximal sclerites of bursa copulatrix not concave at basal edge.

Description. (based on all type specimens (25♂, 24♀)) Dorsum black and shiny, venter brown-black with last 2–3 ventrites yellow-brown. Antennae brown to yellow-brown, with first two antennomeres slightly lighter in color. Legs entirely yellow-brown (except coxae brown-black). Surface of body with yellow pubescence.

Measurements. (based on all type specimens) Male body length 7.3–8.6 mm, width 2.6–3.3 mm. Female body length 7.3–10.4 mm, width 2.8–3.8 mm. Body length to width ratio 2.6–2.9. Pronotal width to length ratio 1.1–1.2. Pronotal width to body width ratio 0.84–0.91. Elytral length to pronotal length ratio 2.5–2.7; elytron length to width ratio 3.6–3.9.

Head. Frons and vertex with interspaces between punctures 1–2 × average puncture diameter; punctures slightly sparser at centre of vertex. Frontal carina in frontal view straight at middle, curved dorsally at sides. Distance between eyes to width of eye ratio 3.4–4.1. Antenna with apex reaching to or slightly reaching beyond posterior angle of pronotum in male, not reaching to posterior angle in female. Antenna length to body length ratio, in male 0.34–0.39; in female 0.32–0.36. Proportions of antennomere lengths (male): 100 (scape); 57–65; 73–79; 78–80; 77–84; 78–89; 74–89; 77–89; 75–79; 73–83; 105–116.

Prothorax. Pronotum in dorsal view: sides evenly convex from anterior edge to constriction near posterior fifth, widest near mid-length; posterior angles with lateral sides almost straight, not bulged; surface with small punctures, interspaces between punctures 1.5–3 × average puncture diameter. In ventral view, ventral surface of prosternal process with sides carinate and gradually narrow from anterior to posterior end, with apex rounded. In lateral view, prosternal process with ventral surface curved slightly dorsad, posterior end concave (Fig. 24I, upper arrow). Procoxal cavities narrowly open.

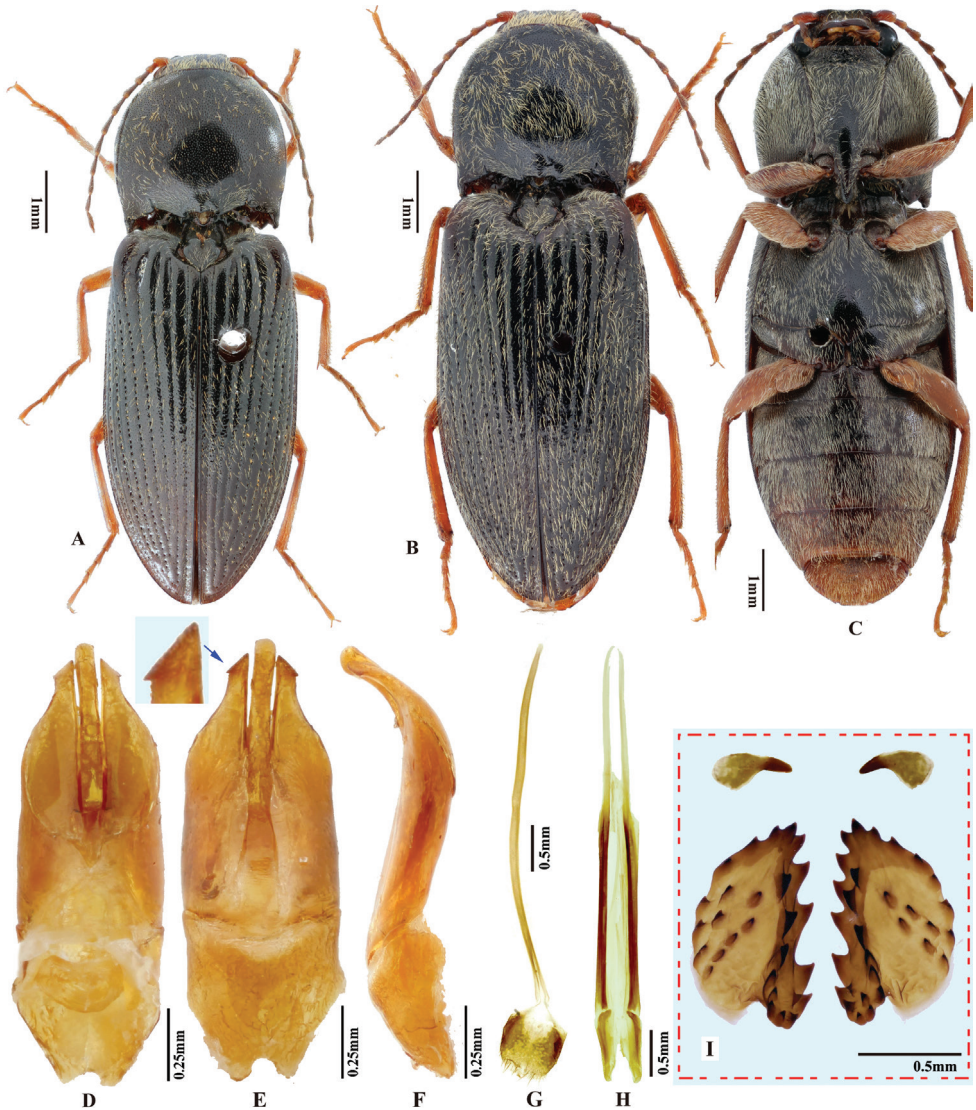


Figure 19. *Phorocardius yunnanensis* Ruan & Douglas, sp. nov. **A** holotype, male, dorsal view **B** paratype, female, dorsal view **C** paratype, female (Yunnan, Xi-shuan-ban-na, Meng-zhe), ventral view **D** aedeagus of holotype, dorsal view **E** aedeagus of holotype, ventral view, arrow indicating apex of paramere **F** aedeagus of holotype, lateral view **G** female abdominal sternite VIII, dorsal view (paratype) **H** ovipositor of paratype, dorsal view **I** distal (upper side) and proximal sclerites of bursa copulatrix (paratype).

Pterothorax (Figs 20E, 24I). Mesepisternum in ventral view with antero-mesal angle broadly rounded mesad of a notch, facing antero-mesally (Fig. 20E, upper (green) arrow); Projections on posterior edge of mesosternum: in ventral view weak (Fig. 20E, lower (red) arrow); in lateral view weak to absent, not produced anteriorly (Fig. 24I, lower

(red) arrow). Scutellar shield: width to length ratio 0.7–0.93; anterolateral edges slightly sinuate; posterior edge pointed. Elytra: upper edge of epipleura with minute serrations.

Legs. Length ratio of metatarsomeres I–V (excluding claws): 100; 73–79; 65–79; 45–54; 138–154. Claw with ventral apex almost as large as dorsal apex.

Abdomen. Lateral edges of visible abdominal ventrites I–V with minute serrations.

Male genitalia (Fig. 19D–F). Robust in dorsal view, slender in lateral view. Median lobe in ventral view narrowing from base to basal third, parallel-sided and slender from basal third to apex, apex broadly rounded to truncate. Median lobe in lateral view evenly curved ventrad from base to apex, apex rounded and dilated. Paramere in dorsal view: wide from base to mid-length, gradually narrowed beyond mid-length, apex slanted; preapical lateral expansion small and sharp, facing laterally; apical mesal callus absent; width 2–2.5 × median lobe width (measured at mid-length of paramere and median lobe respectively). Paramere in lateral view straight from base to mid-length, curved ventrad from mid-length to apex; apex without sharp hook-shaped preapical ventral expansion.

Female. Body length slightly larger than male (Fig. 19B, C), apex of abdominal ventrite V in ventral view truncate to slightly convex, bent dorsad, each side with an incision (Figs 20D, 26H, indicated by blue arrow) (in male, apex of abdominal ventrite V not bent dorsad, each side weakly concave, see Fig. 20D). Bursa copulatrix with proximal sclerites large, semi-spherical, base with deep concavity, apex narrowed and angulate; with many spines on internal surface: each with 9–11 large ones on mesal edge, 10–12 smaller ones on disc.

Type material. Holotype. ♂ (IZCAS), labels: 1) **Yunnan**, Xi-shuang-ban-na, Meng-a (勐阿), 1050–1080 m, Chinese Academy of Sciences [in Chinese]; 2) 1958.VI.6, leg. Fuji Pu [in Chinese]; 3) Holotype *Phorocardius yunnanensis* sp. nov. Des. Ruan & Douglas, 2019.

Paratypes (34♂42♀). 1♂1♀ (IZCAS), labels: 1) **Yunnan**, Xi-shuang-ban-na, Meng-a (勐阿), 1050–1080 m, Chinese Academy of Sciences [in Chinese]; 2) 1958.VI.9–10, leg. Shuyong Wang [in Chinese]; 3) Paratype *Phorocardius yunnanensis* sp. nov. Des. Ruan & Douglas, 2019. • 1♀ (IZCAS), labels: 1) **Yunnan**, Xi-shuang-ban-na, Meng-a (勐阿), 1000 m, Chinese Academy of Sciences [in Chinese]; 2) 1958.V.19, leg. Fuji Pu [in Chinese]; 3) Paratype *Phorocardius yunnanensis* sp. nov. Des. Ruan & Douglas, 2019. • 2♂3♀ (IZCAS), labels: 1) **Yunnan**, Xi-shuang-ban-na, Meng-zhe (勐遮), 1200 m, Chinese Academy of Sciences [in Chinese]; 2) 1958.VI.15, leg. Fuji Pu [in Chinese]; 3) *Phorocardius yanagiharae*, det. Siqin Ge; 4) Paratype *Phorocardius yunnanensis* sp. nov. Des. Ruan & Douglas, 2019. • 5♂6♀ (IZCAS), labels: 1) **Yunnan**, Xi-shuang-ban-na, Meng-zhe (勐遮), 1200 m, Chinese Academy of Sciences [in Chinese]; 2) 1958.VI.15, leg. Shuyong Wang [in Chinese]; 3) *Phorocardius yanagiharae* (Miwa), det. Shihong Jiang, 1998; 4) Paratype *Phorocardius yunnanensis* sp. nov. Des. Ruan & Douglas, 2019. • 1♀ (IZCAS), labels: 1) **Yunnan**, Xi-shuang-ban-na, Meng-zhe (勐遮), 1200 m, Chinese Academy of Sciences [in Chinese]; 2) 1958.IV.14, leg. Shuyong Wang [in Chinese]; 3) Paratype *Phorocardius yunnanensis* sp. nov. Des. Ruan & Douglas, 2019. • 1♂ (IZCAS), labels: 1) **Yunnan**, Xi-shuang-ban-na, Meng-zhe

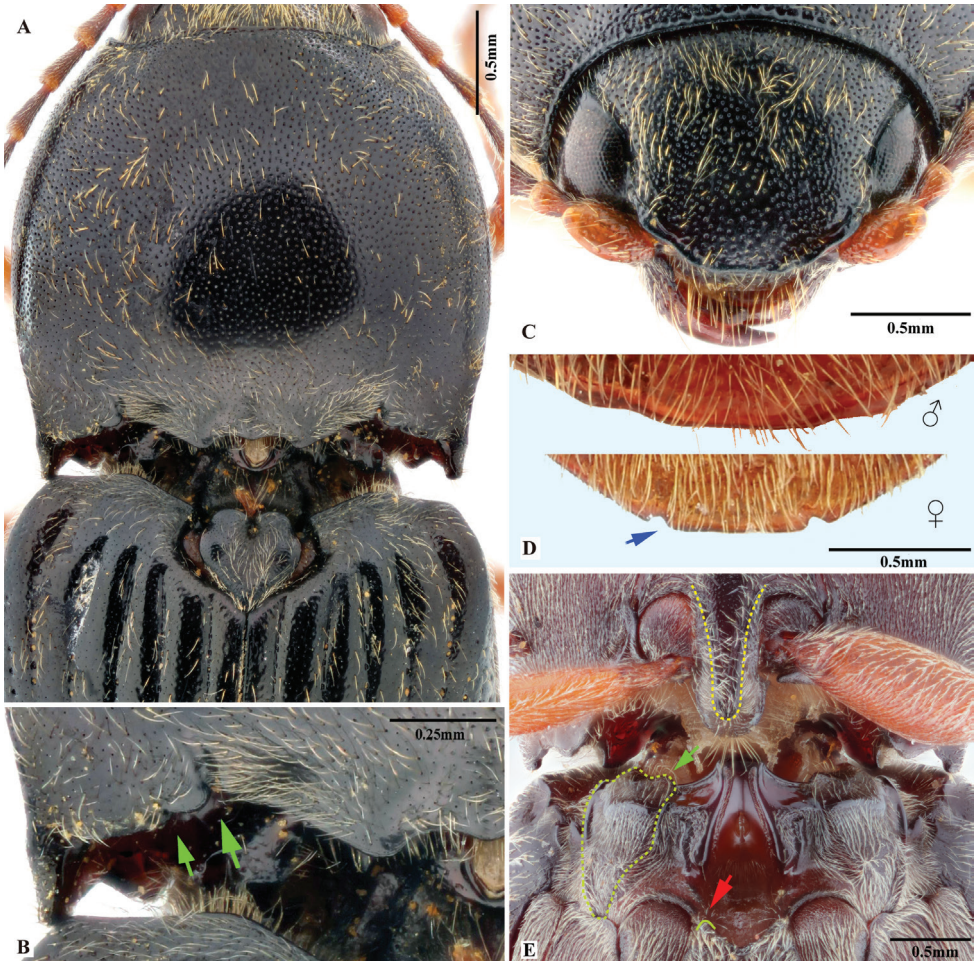


Figure 20. *Phorocardius yunnanensis* Ruan & Douglas, sp. nov. **A** pronotum and scutellum of holotype, dorsal view **B** posterior edge of pronotum, left side, dorsal view, arrows showing sublateral incisions **C** head of holotype, frontal view **D** apex of last abdominal ventrite (ventrite V) of male and female, ventral view (paratypes), arrow showing apical lateral incisions **E** paratype, ventral view of pro- and mesothorax; indicating shapes of prosternal process, mesepisternum (upper, green arrow on antero-mesal angle) and projections on posterior edge of mesosternum (lower, red arrow).

(勐遮), 1200 m, Chinese Academy of Sciences [in Chinese]; 2) 1958.VI.17, leg. Zhi-zi Chen [in Chinese]; 3) Paratype *Phorocardius yunnanensis* sp. nov. Des. Ruan & Douglas, 2019. • 1♂ (IZCAS), labels: 1) **Yunnan**, Xi-shuang-ban-na, Meng-zhe (勐遮), 870 m, Chinese Academy of Sciences [in Chinese]; 2) 1958.VII.7, leg. Fuji-Pu [in Chinese]; 3) Paratype *Phorocardius yunnanensis* sp. nov. Des. Ruan & Douglas, 2019. • 1♂ (IZCAS), labels: 1) **Yunnan**, Meng-zhe (勐遮), Nan-nuo-shan, 1100 m, 1957.IV.28, leg. Fuji Pu, light trap [in Chinese]; 2) [same information as label 1, in Russian]; 3) Paratype *Phorocardius yunnanensis* sp. nov. Des. Ruan & Douglas, 2019. • 1♂ (IZCAS), labels: 1)

Yunnan, Xi-shuang-ban-na, Meng-hun (勐混), 1200 m, Chinese Academy of Sciences [in Chinese]; 2) 1958.V.28, leg. Shuyong Wang [in Chinese]; 3) Paratype *Phorocardius yunnanensis* sp. nov. Des. Ruan & Douglas, 2019. • 1♀ (IZCAS), labels: 1) **Yunnan**, Xi-shuang-ban-na, Meng-hun (勐混), 1000–1200 m, Chinese Academy of Sciences [in Chinese]; 2) 1958.V.21, leg. Leyi Zheng [in Chinese]; 3) Paratype *Phorocardius yunnanensis* sp. nov. Des. Ruan & Douglas, 2019. • 2♂1♀ (IZCAS), labels: 1) **Yunnan**, Xi-shuang-ban-na, Meng-hun (勐混), 1200–1400 m, Chinese Academy of Sciences [in Chinese]; 2) 1958.V.17–24, leg. Xuwu Meng [in Chinese]; 3) Paratype *Phorocardius yunnanensis* sp. nov. Des. Ruan & Douglas, 2019. • 1♂ (IZCAS), labels: 1) **Yunnan**, Xi-shuang-ban-na, Meng-hun (勐混), 1200 m, Chinese Academy of Sciences [in Chinese]; 2) 1958.V.17, leg. Xuwu Meng [in Chinese]; 3) Paratype *Phorocardius yunnanensis* sp. nov. Des. Ruan & Douglas, 2019. • 1♂ (IZCAS), labels: 1) **Yunnan**, Xi-shuang-ban-na, Da-meng-long (大勐龙), 650 m, Chinese Academy of Sciences [in Chinese]; 2) 1958.VI.9, leg. Shuyong Wang [in Chinese]; 3) Paratype *Phorocardius yunnanensis* sp. nov. Des. Ruan & Douglas, 2019. • 1♀ (IZCAS), labels: 1) **Yunnan**, Jing-dong (景东), Dong-jia-fen, 1250 m, 1956.V.27, leg. Zha-gu-liang-ye-fu [in Chinese]; 2) Paratype *Phorocardius yunnanensis* sp. nov. Des. Ruan & Douglas, 2019. • 1♀ (IZCAS), labels: 1) **Yunnan**, Jing-dong (景东), 1170 m, 1956.VI.30, leg. Zha-gu-liang-ye-fu, light trap [in Chinese]; 2) Paratype *Phorocardius yunnanensis* sp. nov. Des. Ruan & Douglas, 2019. • 1♂ (IZCAS), labels: 1) **Yunnan**, Jing-dong (景东), Dong-jia-fen, 1250 m, 1956.VI.29, leg. Krizhanovsky [in Chinese]; 2) Paratype *Phorocardius yunnanensis* sp. nov. Des. Ruan & Douglas, 2019. • 2♀ (IZCAS), labels: 1) **Yunnan**, Jing-dong (景东), Dong-jia-fen, 1250 m, 1956.VI.3, leg. Krizhanovsky [in Chinese]; 2) Paratype *Phorocardius yunnanensis* sp. nov. Des. Ruan & Douglas, 2019. • 1♂ (IZCAS), labels: 1) **Yunnan**, Bao-shan (保山) to Yong-ping (永平), 1955.V.28, leg. Le Wu [in Chinese]; 2) Paratype *Phorocardius yunnanensis* sp. nov. Des. Ruan & Douglas, 2019. • 1♂1♀ (IZCAS), labels: 1) **Yunnan**, east of Bao-shan (保山), Lang-cang river 1200 m, 1955.V.28, leg. Bu-xi-ke [in Chinese]; 2) Paratype *Phorocardius yunnanensis* sp. nov. Des. Ruan & Douglas, 2019. • 2♂ (IZCAS), labels: 1) **Yunnan**, Si-mao (思茅), 1380 m, Chinese Academy of Sciences [in Chinese]; 2) 1958.VI.7, leg. Shuyong Wang [in Chinese]; 3) Paratype *Phorocardius yunnanensis* sp. nov. Des. Ruan & Douglas, 2019. • 2♂ (IZCAS), labels: 1) **Yunnan**, Si-mao (思茅), Pu-wen, 950–1200 m, 1957.V.11, leg. Guangji Hong & Zhirang Meng [in Chinese]; 2) [same information as label 1, in Russian]; 3) Paratype *Phorocardius yunnanensis* sp. nov. Des. Ruan & Douglas, 2019. • 3♂12♀ (SZPT, ex. LQCC), labels: 1) **Yunnan**, Pu-er, Si-mao (思茅), 1400 m, 9–11.V.2018, Meizihu Park, leg. Jianyue Qiu & Hao xu, Shenzhen Polytechnic [in Chinese]; 2) Paratype *Phorocardius yunnanensis* sp. nov. Des. Ruan & Douglas, 2019. • 6♂3♀ (SZPT), labels: 1) **Yunnan**, Lin-cang, Yun-xian County, Man-wang township (漫湾镇), light trap, VI–VIII, 2018, leg. Zichun Xiong, Shenzhen Polytechnic [in Chinese]; 2) Paratype *Phorocardius yunnanensis* sp. nov. Des. Ruan & Douglas, 2019. • 1♂2♀ (SZPT), labels: 1) Nabang Town, 那邦镇, Yingjiang County, **Yunnan**, 2018-IV-3, 252 m, Lu Qiu Leg.; 2) Paratype *Phorocardius yunnanensis* sp. nov. Des. Ruan & Douglas, 2019. • 4♀ (IZCAS), labels: 1) **Yunnan**, Cang-yuan (沧源), 750–790 m, Chinese Academy of Sciences [in Chinese];

2) 1980.V.19–22, leg. Jinwen Shang [in Chinese]; 3) Paratype *Phorocardius yunnanensis* sp. nov. Des. Ruan & Douglas, 2019. • 1♀ (IZCAS), labels: 1) **Yunnan**, Cang-yuan (沧源), ban-lao, 1100 m, Chinese Academy of Sciences [in Chinese]; 2) 1980.V.18, leg. Hongxing Li [in Chinese]; 3) Paratype *Phorocardius yunnanensis* sp. nov. Des. Ruan & Douglas, 2019. • 1♂ (IZCAS), labels: 1) **Yunnan**, Lu-xi (路西), 1250 m, Chinese Academy of Sciences [in Chinese]; 2) 1980.V.18, leg. Jinwen Shang [in Chinese]; 3) Paratype *Phorocardius yunnanensis* sp. nov. Des. Ruan & Douglas, 2019. • 1♀ (IZCAS), labels: 1) **Yunnan**, Rui-li (瑞丽), 1400 m, 1956.VI.6, leg. Benshou Zhou [in Chinese]; 2) [same information as label 1, in Russian]; 3) Paratype *Phorocardius yunnanensis* sp. nov. Des. Ruan & Douglas, 2019.

Remarks. Based on specimen information, this species is currently only known from mountainous southwest Yunnan, China. It inhabits mainly middle elevations (ca. 650–1400 m). Southwest Yunnan is rainy and humid, subtropical to tropical with subtropical evergreen broad-leaf forest or tropical rain forest. Specimens were collected by sweep-netting and light traps, indicating both diurnal and nocturnal activity.

11. *Phorocardius zhiweii* Ruan, Douglas & Qiu, sp. nov.

<http://zoobank.org/6DFDF68D-2147-4055-8034-243A6FEBEA72>

Figs 21, 22, 23J, 24J, 25I

Type locality. Yunnan: Long-chuan county, Hu-sa township, Gun-bang-jian-shan [i.e., Bang-gun-jian-shan 邦棍尖山].

Etymology. This species is named after its collector, Mr Zhiwei Dong, who generously provided specimens for this study.

Distribution. China (Yunnan).

Differential diagnosis. Body length greater than 7.0 mm; pronotum with integument red, elytra metallic green. Prothorax: procoxal cavities open; prosternal process not strongly narrowed posterad to ventral apex in ventral view, with ventral apex rounded. Pterothorax: scutellar shield with posterior edge pointed. Tarsal claw with ventral apex not smaller than dorsal apex. Male genitalia: paramere without preapical lateral expansion, but with apical mesal callus. Female unknown.

This species is distinct among *Phorocardius* in its entirely metallic green elytra and red pronotum. It is the second species having metallic color on elytra, as the type species of the genus (i.e., *P. florentini* (Fleutiaux, 1895)) also has slight blue metallic luster on elytra.

Phorocardius zhiweii Ruan, Douglas & Qiu, sp. nov. resembles *P. manuleatus* most in body shape and color of leg and prothorax. They can be easily separated by elytral color and aedeagus shape. In *P. zhiweii* Ruan, Douglas & Qiu, sp. nov., elytra are metallic green with slight purple luster; in ventral view, the aedeagus has apical fourth slightly narrowed, robust in both ventral and lateral views; and the paramere has preapical lateral expansion absent, apical mesal callus present; while in *P. manuleatus*, elytra are black to yellow, without metallic color; and the aedeagus in ventral view has the apical fourth greatly narrowed. The aedeagus is slender in

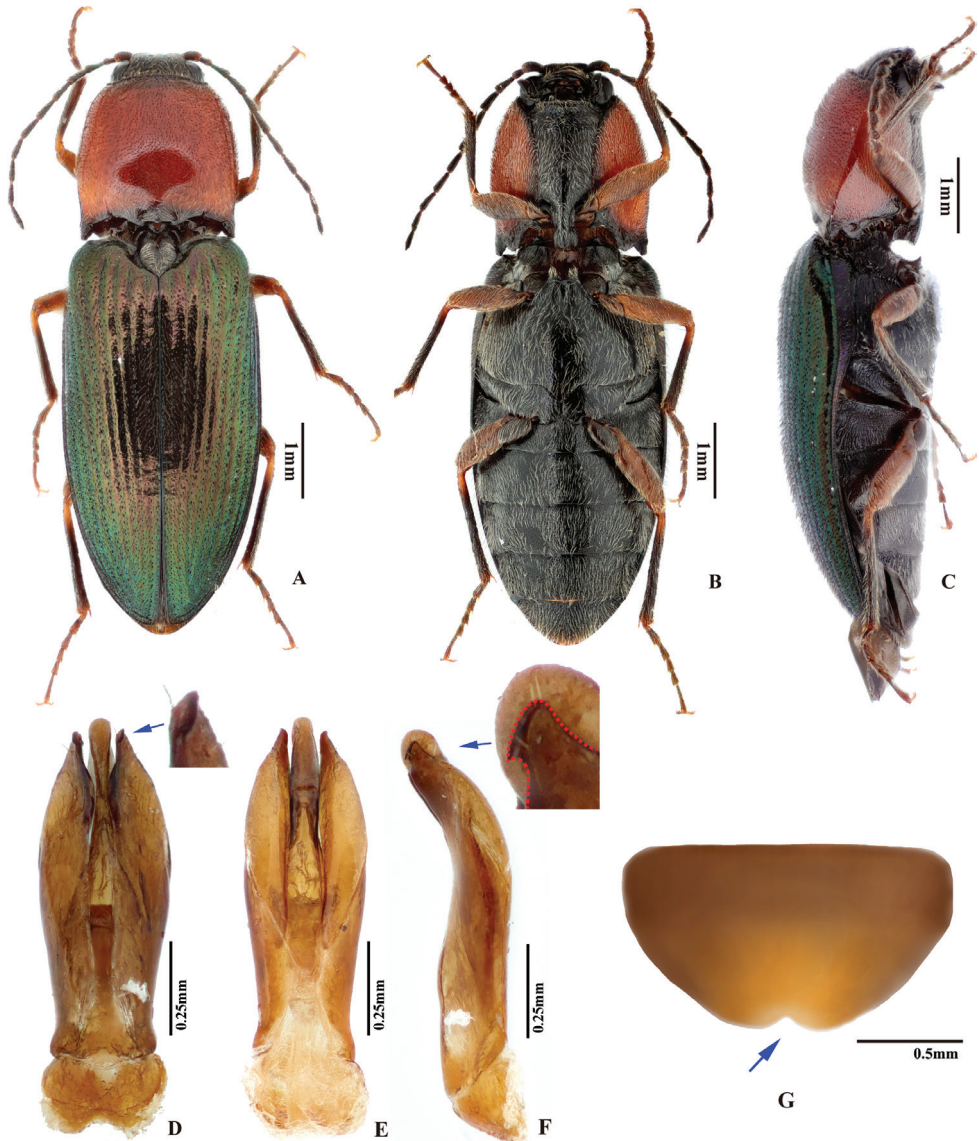


Figure 21. *Phorocardius zhiwei* Ruan, Douglas & Qiu, sp. nov., holotype, male. **A** habitus, dorsal view. **B** habitus, ventral view **C** habitus, lateral view **D** aedeagus ventral view, arrow indicating apex and apical mesal callus of paramere **E** aedeagus, dorsal view **F** aedeagus, lateral view, arrow indicating apices of paramere and median lobe **G** tergite 7, dorsal view, hand drawing, arrow indicating posterior concavity.

both ventral and lateral views with parameres lacking acute preapical lateral expansions or apical mesal calli.

Description. (based on holotype) Dorsum shiny. Head black, with mouthparts red-brown to brown. Antennae brown. Pronotum orange, with posterior edge dark brown (Fig. 22A). Scutellar shield black. Elytra entirely metallic green, with purple luster. Hypomera orange; rest of ventral surface black (Fig. 21B). Epipleura metallic

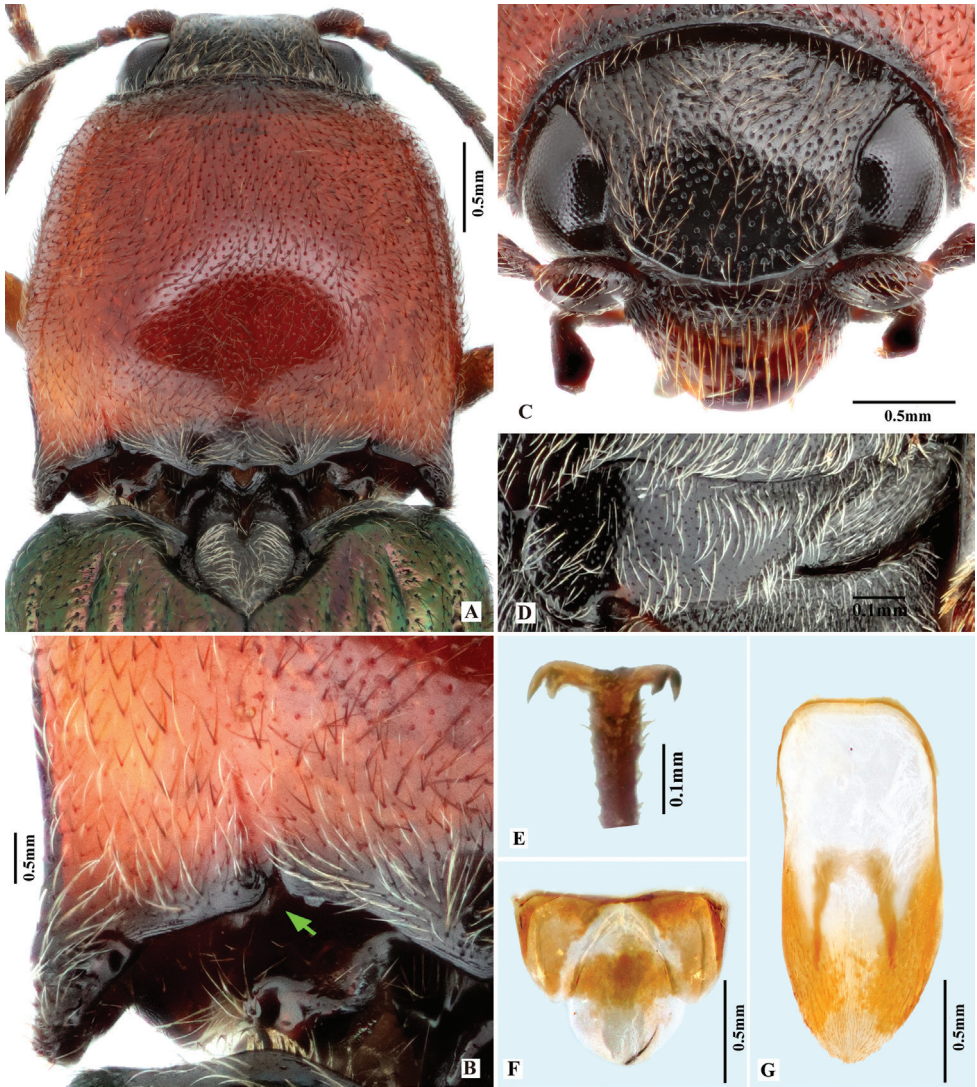


Figure 22. *Phorocardius zhiweii* Ruan, Douglas & Qiu, sp. nov. **A** pronotum and scutellar shield, dorsal view **B** left posterior edge of pronotum, showing sublateral incision (arrow) **C** head, frontal view **D** metacoxal plate, ventral view **E** tarsal claws **F** male abdominal tergites IX–X, dorsal view **G** male abdominal sternite IX, dorsal view.

purple. Legs black on coxa, pale brown on femur and basal half of tibia, dark brown from mid-length of tibia to apex. Body with short, yellow-grey pubescence, brown setae also present on disc of pronotum.

Measurements. (based on holotype) Body length 8.0 mm, width 2.8 mm. Body length to width ratio 2.9. Pronotal width to length ratio 1.1. Pronotal width to body width ratio 0.80. Elytral length to pronotal length ratio 2.5; elytron length to width ratio 3.8.

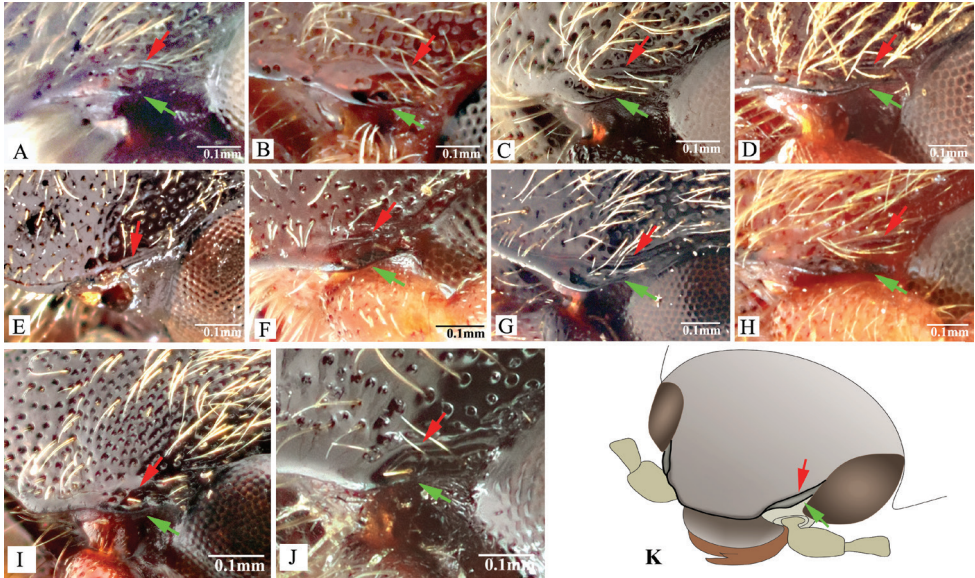


Figure 23. Shape of supraantennal carina of Chinese *Phorocardius* species. Arrows indicating supraantennal carina forked near eye. **A** *P. alterlineatus* Ruan & Douglas, sp. nov. **B** *P. flavistriolatus* Ruan & Douglas, sp. nov. **C** *P. florentini*. **D** *P. magnus*. **E** *P. manuleatus*. **F** *P. minutus* Ruan & Douglas, sp. nov. **G** *P. rufiposterus* Ruan & Douglas, sp. nov. **H** *P. unguicularis*. **I** *P. yunnanensis* Ruan & Douglas, sp. nov. **J** *P. zhiweii* Ruan, Douglas & Qiu, sp. nov. **K** head, frontal-lateral view, arrows indicating forked supraantennal carina.

Head. Frons and vertex with interspaces between punctures $1-3 \times$ average puncture diameter (Fig. 22C). Frontal carina in frontal view convex. Antenna with apex extending to basal edge of elytron. Distance between eyes to width of eye ratio 2.7. Antenna length to body length ratio 0.42. Proportions of antennomere lengths (male): 100 (scape); 71; 76; 100; 100; 105; 103; 90; 90; 88; 116.

Prothorax. Pronotum in dorsal view (Fig. 22A): sides slightly convex from anterior edge to concavity near posterior fourth, widest near posterior third; posterior angles with lateral sides almost straight, not bulged; surface with interspaces between punctures $2-2.5 \times$ average puncture diameter. In ventral view, ventral surface of prosternal process with sides carinate and slightly and gradually narrow from anterior to mid-length, parallel from mid-length to near posterior end, apex broadly rounded. In lateral view, prosternal process with ventral surface curved slightly dorsad, posterior end concave (Fig. 24J). Procoxal cavities open.

Pterothorax (Figs 24J, 25I). Mesepisternum in ventral view with antero-mesal corner right-angled (Fig. 25I, upper, green arrow). Projections on posterior edge of mesosternum: in ventral view present (Fig. 25I, red arrow); in lateral view present, strongly developed, produced anteriorly (Fig. 24J, red arrow). Scutellar shield: width to length ratio 1.0; anterolateral edges slightly sinuate; posterior apex pointed. Elytra: upper edge of epipleura with minute serrations.

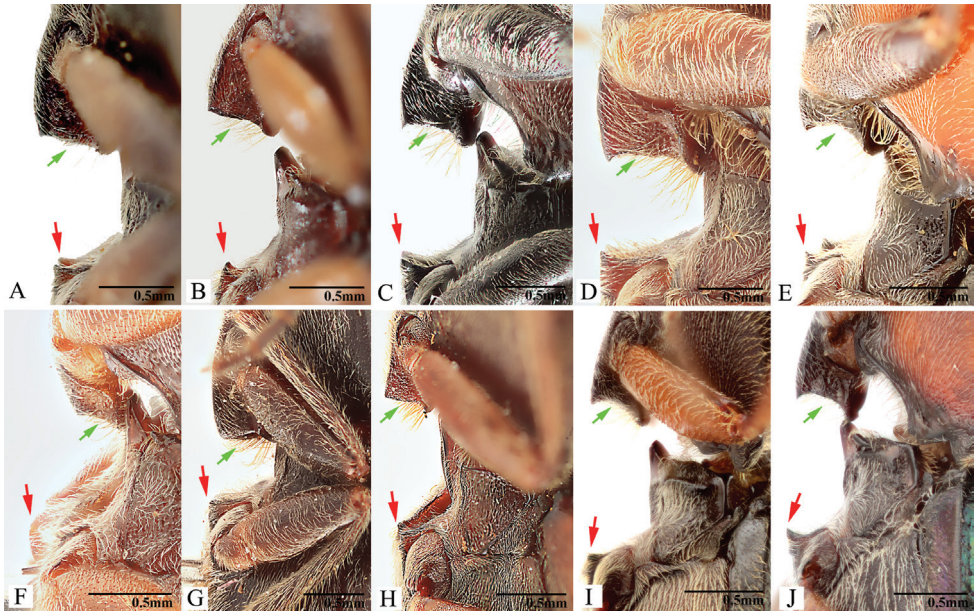


Figure 24. Lateral view of prosternal process and mesosternum of Chinese *Phorcardius* species. Upper green arrows indicating shape of posterior end of prosternal process; lower red arrows indicating projections (absent or present) on posterior edge of mesosternum (i.e., on anteroventral angle of mesosternal fossa according to Douglas 2003). **A** *P. alterlineatus* Ruan & Douglas, sp. nov. **B** *P. flavistriolatus* Ruan & Douglas, sp. nov. **C** *P. florentini*. **D** *P. magnus*. **E** *P. manuleatus*. **F** *P. minutus* Ruan & Douglas, sp. nov. **G** *P. rufiposterus* Ruan & Douglas, sp. nov. **H** *P. unguicularis*. **I** *P. yunnanensis* Ruan & Douglas, sp. nov. **J** *P. zhiweii* Ruan, Douglas & Qiu, sp. nov.

Legs. Length ratio of metatarsomeres I–V (excluding claws): 100; 71; 53; 50; 120. Claw with ventral apex almost as large as dorsal apex.

Abdomen. Lateral edges of visible abdominal ventrites I–V with minute serrations.

Male genitalia. Robust in ventral and lateral views. Median lobe in ventral view with sides nearly parallel, slightly narrowed near apex; apex broadly rounded (Fig. 21D). Median lobe in lateral view gently bent ventrad, apex dilated and broadly rounded (Fig. 21F). Paramere in ventral view: wide, widest near mid-length, sides convex to near apex; preapical ventral expansion absent, mesal side of apex with ovoid disc-shaped callus (Fig. 21D, indicated by blue arrow); paramere 2–3 × wider than median lobe (measured at mid-length of paramere and median lobe respectively). Paramere in lateral view: robust, almost straight at basal half, bent ventrad at apical half; preapical ventral expansion hook-like, with acute tip facing ventrad (Fig. 21F, indicated by blue arrow).

Female. Unknown.

Type material. Holotype. male (IZCAS, ex. LQCC), labels: 1) **Yunnan**, Longchuan county, Hu-sa township (户撒), Mang-dong road, Gun-bang-jian-shan Mt., leg. Zhiwei Dong, 2018-VI-5 [label in Chinese]; 2) **Holotype**, *Phorcardius zhiweii* sp. nov., Des. Ruan et al., 2019.

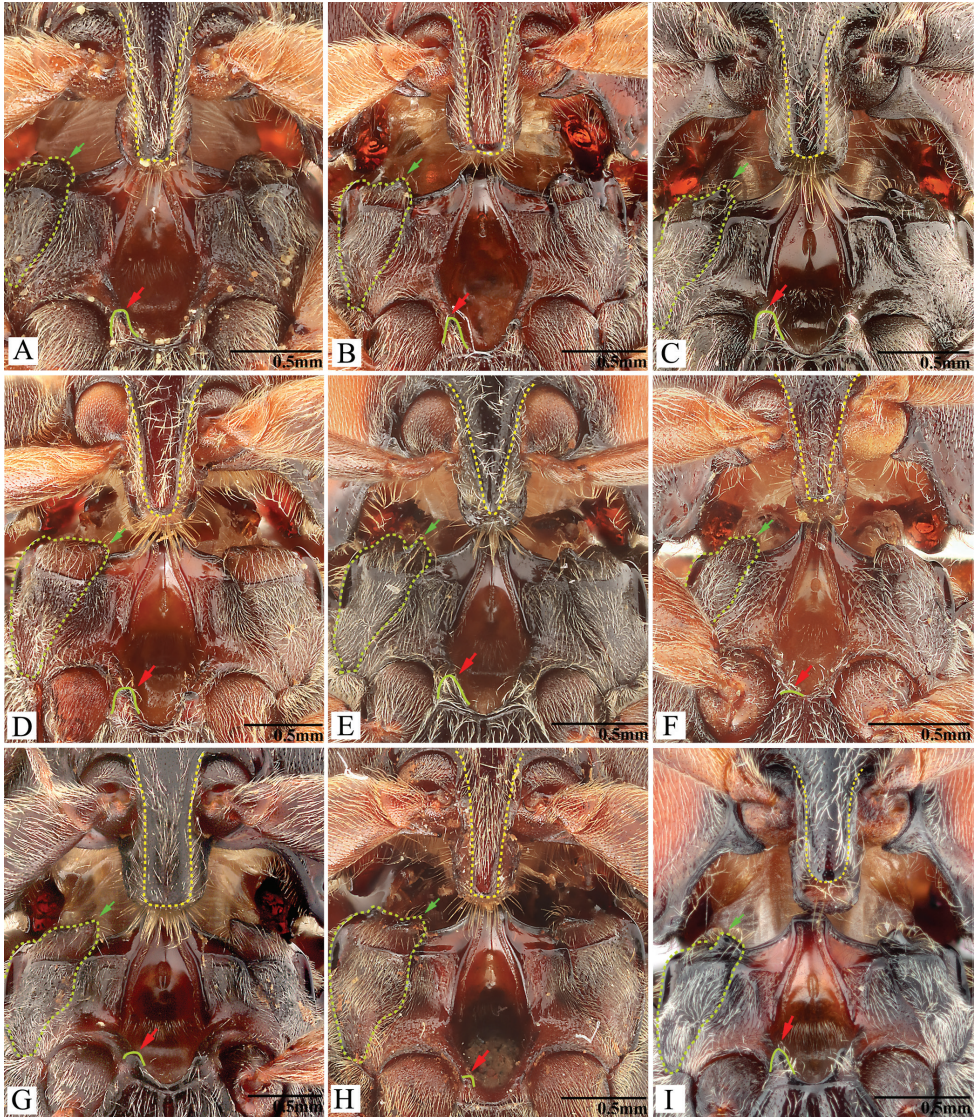


Figure 25. Ventral view of pro- and mesothorax of Chinese *Phorocardius* species. Showing shape of ventral surface of prosternal process (upper, yellow dashed line), mesepisternum (middle, green arrow and dashed line) and projections on posterior edge of mesosternum (lower, red arrow and solid line) middle, green arrows indicating anterior-mesal angle of mesepisternum. **A** *P. alterlineatus* Ruan & Douglas, sp. nov. **B** *P. flavistriolatus* Ruan & Douglas, sp. nov. **C** *P. florentini*. **D** *P. magnus*. **E** *P. manuleatus*. **F** *P. minutus* Ruan & Douglas, sp. nov. **G** *P. rufiposterus* Ruan & Douglas, sp. nov. **H** *P. unguicularis*. **I** *P. zhiwei* Ruan, Douglas & Qiu, sp. nov.

Remarks. This species inhabits middle elevations (around 1500 m) in Yunnan Prov., south China. This area is rainy, subtropical to tropical, with subtropical evergreen broad-leaf forest or tropical rain forest. This species is known only from the Oriental Region.

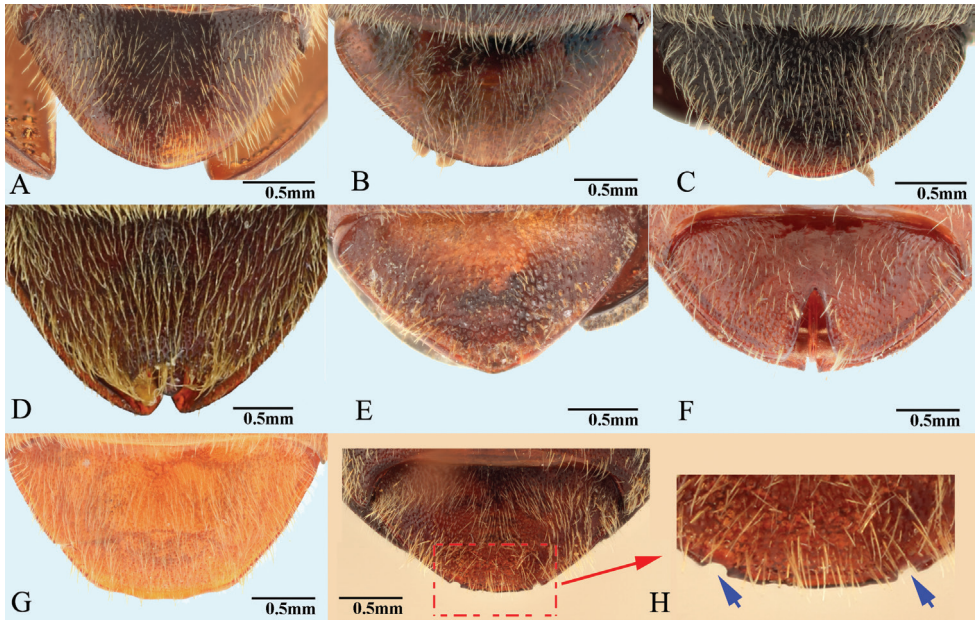


Figure 26. Female abdominal ventrite V in Chinese *Phorocardius* species (ventral view). **A** *P. alterlineatus* Ruan & Douglas, sp. nov. **B** *P. flavistriolatus* Ruan & Douglas, sp. nov. **C** *P. florentini*. **D** *P. magnus*. **E** *P. manuleatus* **F** *P. rufiposterus* Ruan & Douglas, sp. nov. **G** *P. unguicularis* **H** *P. yunnanensis* Ruan & Douglas, sp. nov, arrows showing incisions near apex.

There are two undetermined female specimens (SZPT) from Xi-shuang-ban-na (西双版纳), Yunnan that have metallic blue elytra and a black pronotum. One male specimen (SZPT) from Ying-jiang (盈江), Yunnan also has metallic blue elytra and a black pronotum. Its aedeagus is extremely close to that of *Phorocardius zhiweii* Ruan, Douglas & Qiu, sp. nov. However, it is still not entirely clear whether these are conspecific. More specimens should be studied before a reliable determination can be made.

Removal of a questionable distributional record:

Phorocardius comptus (Candèze, 1860) [removed from distribution of mainland China and Taiwan]

Fig. 28

Cardiophorus comptus Candèze, 1860: 202. Type locality: Hindoustan méridional, Mysore (interpreted as India, Karnataka, Mysuru). Lectotype designated here.

Phorocardius comptus: Miwa 1934: 209 (distribution).

Dicronychus comptus: Ôhira 1973: 38 (as comb. nov. from *Cardiophorus*, distribution).

Phorocardius comptus: Ôhira 1978: 96 (as comb. nov. from *Dicronychus*, distribution, photograph of habitus).

Phorocardius comptus: Cate et al. 2007: 206 (distribution).

Distribution. India (Candèze 1860, 1891); Nepal (Ôhira 1978); Sri Lanka (Ôhira 1973). Excluded from China here.

Remarks. *Phorocardius comptus* was recorded from Taiwan by Miwa (1927, 1931). However, Suzuki (1999) considered the record questionable. He excluded *P. comptus* from Taiwan after studying the specimens that Miwa (1927) used for the record. The same specimen was examined in our study (TARI, see Fig. 28F). We agree with Suzuki (1999) that the specimen used by Miwa (1927) is one of the “Shiraki specimens”. “Shiraki specimens” were originally housed in NHMUK, collected from tropical Oriental countries (e.g., India, Nepal, Borneo, etc.) and shipped to Taiwan by Dr Shiraki in 1916. All specimen labels were then replaced by new labels with several specific localities from Taiwan such as “Rônô”, “Kôshun”, “Kôtoshô”, “Horisha”, “Hori”, “Musha”, etc. (Kurosawa 1980; Chu and Xiao 1981; Chu 2011, 2013). Most of these Taiwan locality names refer to localities in the south and southeast Asia, the codes for these true locality names were documented in a file housed in National Taiwan University, Taipei, which was already lost shortly after world war II (Chu 2011). Additionally, under each of these specimens, there is a typical Shiraki’s label with his handwriting and a red circle mark. Therefore, the single *P. comptus* specimen in TARI is one of these “Shiraki specimens”, since it has a locality label indicating “Rônô”, and a second label with Shiraki’s handwriting and a red circle mark.

Phorocardius comptus was previously recorded by Jiang (1993) and Jiang and Wang (1999) in Hubei Prov., China. We examined the specimens used in those studies and found that these specimens are not conspecific with *P. comptus*, instead they are described as a new species in this study (i.e., *Phorocardius alterlineatus* Ruan & Douglas sp. nov. above). We consider *P. comptus* to be absent from mainland China and Taiwan.

Candèze (1860: 202) described *Cardiophorus comptus* and *C. contemptus* on the same page and stated that *C. contemptus* (see Fig. 29) may be a variety *C. comptus*. The examination of the type material of both species shows that they are similar in female genitalia and external characters (except for the elytral color). It is possible that *C. contemptus* is a junior synonym of *C. comptus*. However, as we have not studied any male specimen of *C. contemptus*, it is treated here as valid.

Three specimens (NHMUK) are designated as lectotype or paralectotypes for the following reasons: 1) they are labeled with “SYNTYPE”; 2) the labels indicate either “S. India” or “Hindoustan”, which are consistent with the original description; 3) the collection of Candèze before 1869 had been transferred to the NHMUK (Bousquet 2016); and 4) the type materials are absent in either RBINS or MNHN.

Type material. *Lectotype* of *Cardiophorus comptus* Candèze, 1860: ♂ (NHMUK), labels: 1) SYNTYPE [a circular label]; 2) 677; 3) [a small blank square label in deep-red color]; 4) *Cardioph. Comptus* Cand. Hindoustan; 5) Janson Coll. Ex. Deyrolle. 1903.130; 6) Lectotype, *Cardiophorus comptus* Candèze, 1888, Des. Ruan & Douglas, 2020.

Paralectotypes of *Cardiophorus comptus* Candèze, 1860: 1♂ (NHMUK), labels: 1) SYNTYPE [a circular label]; 2) S. India; 3) 733; 4) 11; 5) Janson coll., ex Dejean. 1903-130; 6) *C. comptus* ♂; 7) Paralectotype, *Cardiophorus comptus* Candèze, 1888, Des. Ruan & Douglas, 2020. 1♀ (NHMUK), labels: 1) S. India, ex coll.

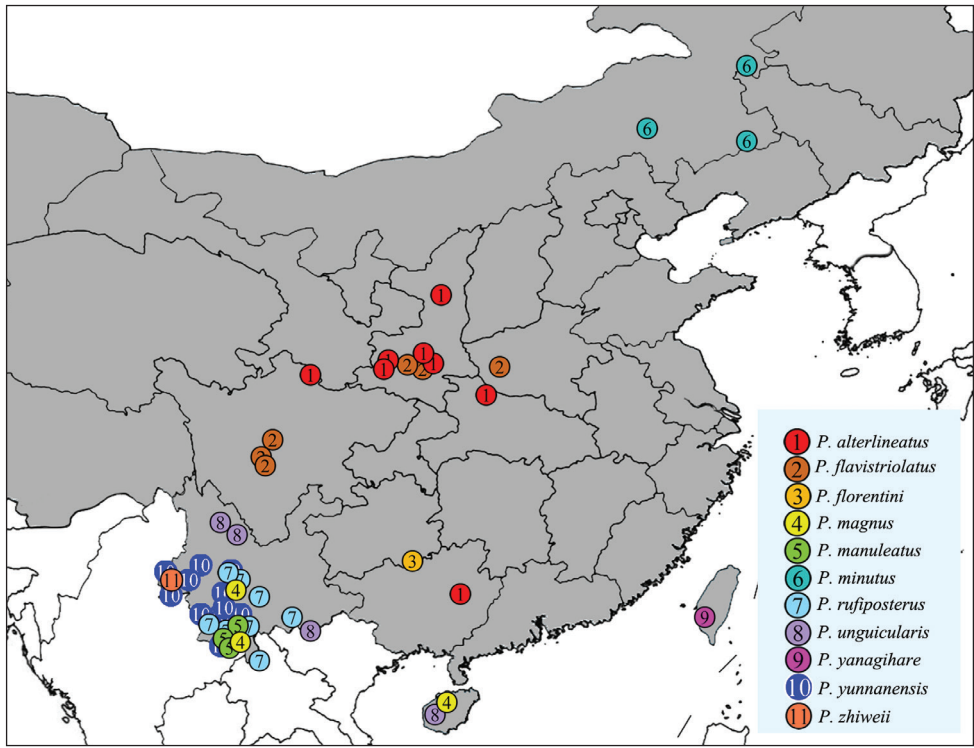


Figure 27. A distribution map of Chinese *Phorocardius* species. **1** *P. alterlineatus* Ruan & Douglas, sp. nov. **2** *P. flavistriolatus* Ruan & Douglas, sp. nov. **3** *P. florentini* **4** *P. magnus* **5** *P. manuleatus* **6** *P. minutus* Ruan & Douglas, sp. nov. **7** *P. rufiposterus* Ruan & Douglas, sp. nov. **8** *P. unguicularis* **9** *P. yanagiharae* **10** *P. yunnanensis* Ruan & Douglas, sp. nov. **11** *P. zhiweii* Ruan, Douglas & Qiu, sp. nov.

..... [characters illegible]; 2) Janson coll., ex Dejean. 1903-130; 3) 727; 4) 10; 5) *C. comptus* [characters illegible], ♀ Cdzé.; 6) ♀ genitalia See slide Coll. No. 796; 7) Paralectotype, *Cardiophorus comptus* Candèze, 1888, Des. Ruan & Douglas, 2020. [We consider this female specimen as one of the paralectotypes because the locality on the label is consistent with the original description, and the specimen has a unique red prothorax, which is described as a variation by the author (Candèze 1860). This specimen is shown in Fig. 28D].

Additional material. The specimen that was used as a distributional record by Miwa (1927) [this specimen is actually from the south or southeast Asia instead of Taiwan as discussed above]: 1 ♀ (TARI), labels: 1) Rônô; 2) *Phorocardius comptus* Cand. Det T. Shiraki; 3) Not Taiwan, Shiraki specimen, W. Suzuki, 1989.

The specimens that were misidentified as *P. comptus* and used as a distributional record by Jiang (1993) and Jiang and Wang (1999) [these specimens are identified as *P. alterlineatus* sp. nov. Ruan & Douglas in this study]: 1 ♂ (SZPT), labels: 1) Hubei, Wu-dang Mts., Chao-tian-gong (朝天宫), 1982.VII.5; 2) *Phorocardius comptus* (Candèze), det. Shihong Jiang 19; 3) 7.30*2.60 cm. • 1 ♂ (SZPT), labels: 1) Hubei, Wu-dang Mts., Zi-xiao (紫霄), 1982.VII.10; 2) *Phorocardius comptus*

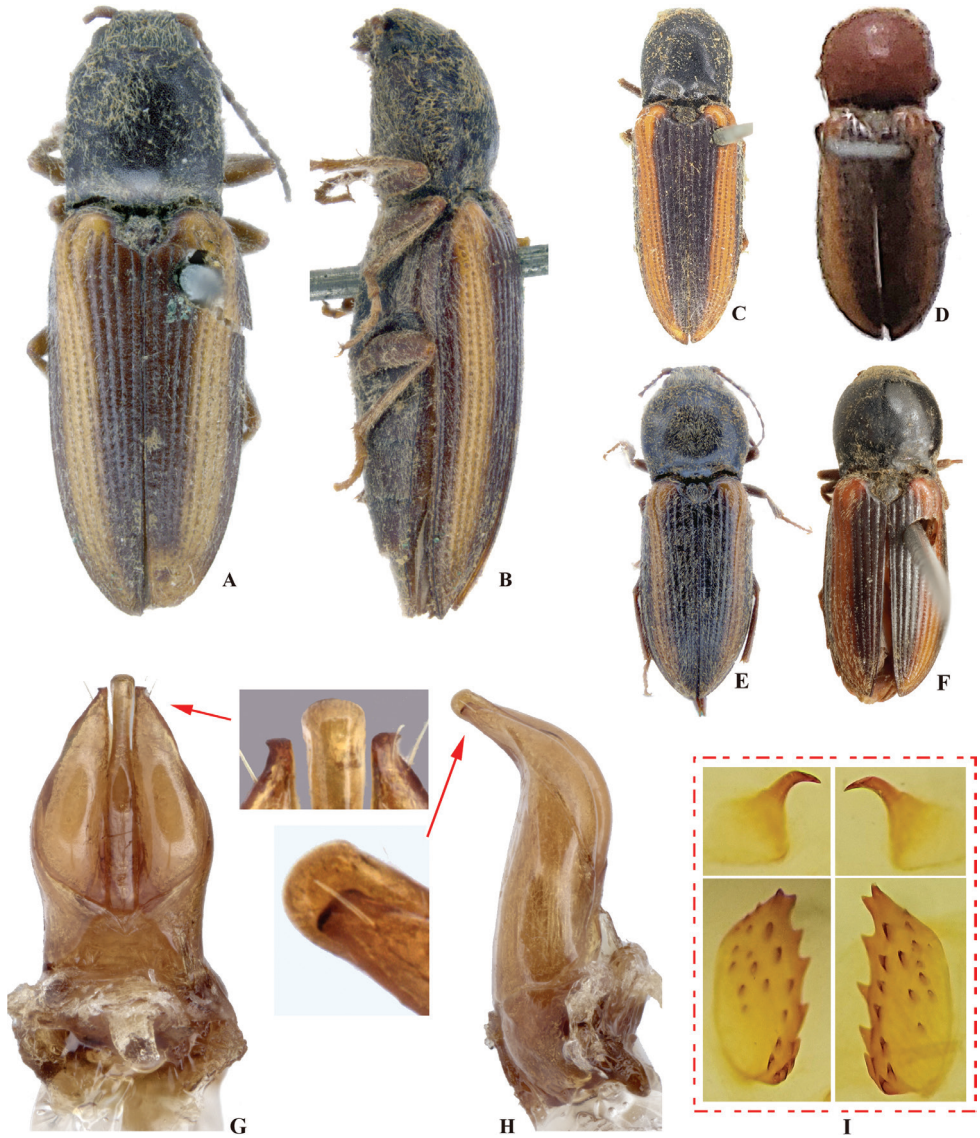


Figure 28. *Phorocardius comptus* (Candèze, 1860) (insets **A, B, E, G–I** are provided by Ms Karine Savard, Agriculture and Agri-food Canada; insets **C, D** are provided by Dr Yijie Tong, IZCAS). **A** lectotype, male, dorsal view **B** lectotype, male, lateral view **C** paralectotype, male, dorsal view **D** paralectotype, female, dorsal view **E** female, dorsal view (NHMUK, non-type specimen) **F** female, dorsal view (TARI, used for distributional record by Miwa (1927)) **G** aedeagus of lectotype, dorsal view, arrow indicating apices of parameres and median lobe **H** aedeagus of lectotype, lateral view, arrow indicating apices of parameres and median lobe **I** distal (upper side) and proximal sclerites of bursa copulatrix (paralectotype, habitus shown in **D**).

(Candèze), det. Shihong Jiang 1993. • 1♀ (SZPT), labels: 1) Hubei, Wu-dang Mts., Jin-ding (金顶), 1982.VII.9; 2) *Phorocardius comptus* (Candèze), det. Shihong Jiang 1993. • 1♀ (SZPT), labels: 1) Hubei, Wu-dang Mts., Lao-yan (老燕), 1983.VII.2;

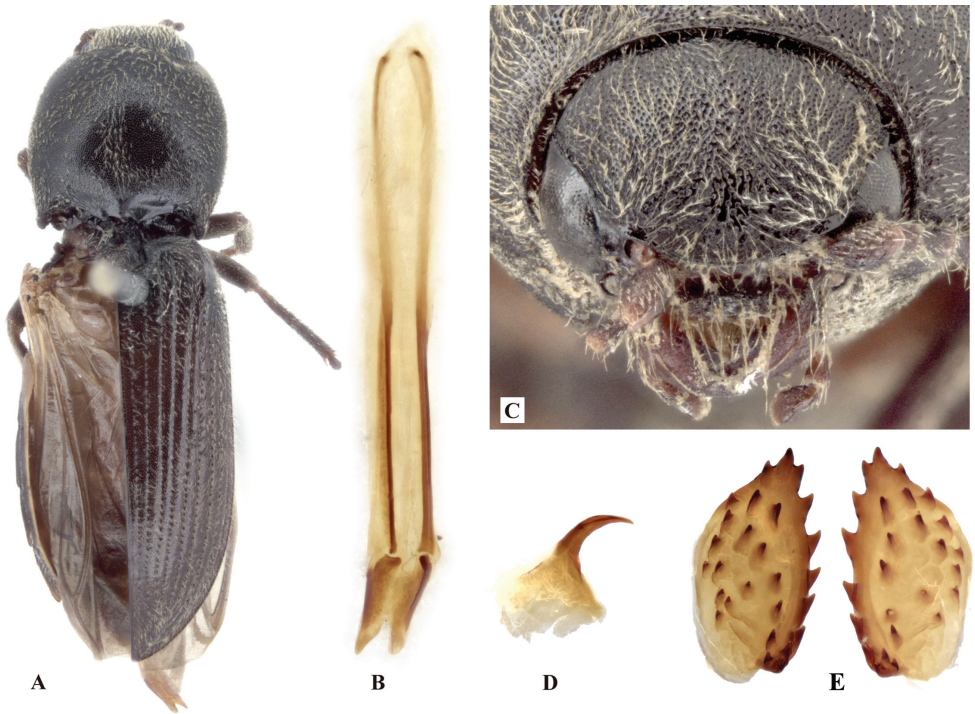


Figure 29. *Phorocardius contemptus* (Candèze, 1860) (images are provided by Ms Karine Savard, Agriculture and Agri-food Canada). **A** lectotype, female, dorsal view **B** ovipositor, dorsal view **C** head, frontal view (lectotype) **D** distal sclerite of bursa copulatrix (lectotype; only one sclerite is shown) **E** proximal sclerites of bursa copulatrix (lectotype).

2) *Phorocardius comptus* (Candèze), det. Shihong Jiang 1993. • 1♀ (SZPT), labels: 1) Hubei, Wu-dang Mts., Nan-yan (南岩), 1983.VII.2; 2) *Phorocardius comptus* (Candèze), det. Shihong Jiang 1991.

Discussion

No new *Phorocardius* species were described between 1931 and 2015, and only three *Phorocardius* species were documented from China since 1931. Our study shows that the species richness of *Phorocardius* is greater than previously known, particularly in China. Southwest China (especially the Heng-duan Mountains) is renowned as a global biodiversity hot spot (Myers et al. 2000). The high diversity of that area is most evident in that five of the six new species described in this study were discovered in this area (although other areas also require increased collecting effort).

The northernmost specimens of *Phorocardius* are of *P. minutus* Ruan & Douglas, sp. nov., collected from Ke-you-zhong-qi, Inner Mongolia, with minimum January

temperatures near -20°C . If monophyletic with other *Phorocardius*, this shows that *Phorocardius* species can inhabit not only humid tropical rain forest, but also arid and freezing grassland areas. This finding also suggests that at least some species of *Phorocardius* may not require forest soils, hollow trees, or decaying wood for larval development. The discovery of *P. minutus* expands the collective distributional records for the genus *Phorocardius* deep into the Palearctic Region for the first time.

According to specimen records, the highest elevation for Chinese *Phorocardius* species is 2750 m at the foot of Yu-long-shan Mountain (also known as Yu-long Snow Mountain), with snow present year-round above 3500 m, while the lowest elevation is around 50 m. The strongly sclerotized ovipositors of all *Phorocardius* species examined here suggests that they can oviposit in dense substrates, such as soils that are not sandy.

Phorocardius zhiweii is the second species described in the genus with metallic coloration on the elytra, with *P. florentini* also having a slight blue metallic luster on the elytra. There may be additional undescribed metallic species, as we have examined three other undetermined specimens with metallic blue elytra.

We found that using the open procoxal cavities as a generic character, as in Douglas (2017), for *Phorocardius* is incorrect because the procoxal cavities of *P. rufiposterus* are closed (Fig. 15E), only narrowly open in rare cases. The degree of the opening of procoxal cavities also slightly varied between individuals of *P. magnus* Fleutiaux, 1931, with many specimens having nearly closed (narrowly open) procoxal cavities. Douglas (2017) also incorrectly placed *Phorocardius* in the key to genera among species with the pronotal lateral carina present in the first half of couplet 4. But the proximal sclerites of the bursa copulatrix are ovoid as mentioned there. Users of that key might incorrectly identify *Phorocardius* specimens as *Ryukyucardiophorus* based on the pronotal character. However, *Phorocardius* can be distinguished from *Ryukyucardiophorus* by its apically split claws (tooth at base in *Ryukyucardiophorus*) and by having four sclerites in the bursa copulatrix (only two in *Ryukyucardiophorus*).

The shape of the male genitalia illustrated in this study is highly variable in some species, especially in *P. flavistriolatus*, *P. manuleatus* and *P. minutus*. This may be due to one or more of the following reasons:

1. Rotation of structures. The variations could be amplified in planar illustrations (photographs only show two dimensions of three-dimensional structures. For example, in *P. flavistriolatus* and *P. manuleatus*, the apical mesal part of the paramere is bent (or turned) ventrad, and a slight bending (or turning) can cause a substantial difference from ventral or dorsal views (shown in Fig. 6).

2. Variation in degree of sclerotization. Some individuals have less strongly sclerotized aedeagi than other individuals. This can result in slightly different shapes. An extreme case was observed in one specimen of *P. minutus*, whose aedeagus had one paramere normal, and the other slightly collapsed and deformed.

3. Mating activity. In a few individuals of *P. flavistriolatus* (e.g., Fig. 4J), the apical part of the parameres are much more divergent than those in other individuals. This is probably due to the aedeagi being extended at the time of death of the beetle because divergent parameres were found only in specimens preserved with the aedeagus entirely extended from the posterior end of specimens. In Cardiophorinae (and probably Negas-triinae), when the aedeagus is extended before copulation, the distal part of parameres diverge from the median lobe (the base of parameres are fused, with the apex flexible, Iablokoff-Khnzorian and Mardjanian 1981; Douglas 2017). We also observed the copulation in *Ludioschema obscuripes* for comparison. During the copulation, the distal part of the parameres diverges from the median lobe. After copulation, the aedeagus starts to retract back into the body, the parameres gradually move close to median lobe, and when the aedeagus is almost entirely retracted, the parameres return closely to median lobe.

4. Undescribed species diversity. It also remains possible that these species definitions contain undescribed cryptic species, so that further DNA comparisons should be done to test species limits.

This study also first documents that the shape of the apex of abdominal ventrite V in females is highly variable (arcuate, with arcuate median indentation, or with elongate invagination containing slender blade-like projection) between species (see Fig. 26A–H). This character system (first noted in unpublished drawings in specimen drawers in NHMUK by Christine von Hayek) provides a set of powerful diagnostic characters for some species (e.g., *P. rufiposterus*, *P. magnus*, and *P. yunnanensis*). However, in males, the same structure (usually arcuate and simple) is more evenly convex and lacks interspecific variation.

Acknowledgements

We are greatly indebted to Dr Antoine Mantilleri (MNHN), Dr Yijie Tong (IZCAS), Dr Jérôme Constant (RBINS), Dr Florence Trus (RBINS), Dr Harald Schillhammer (NHMW), Ms Karine Savard (Agriculture and Agri-food Canada), and Dr Wouter Dekoninck (RBINS) for their help with taking photographs of type specimens. We are grateful to Dr Chi-feng Lee (TARI), Dr Michael Geiser, Mr Keita Matsumoto, and Dr Maxwell Barclay (NHMUK) for their kind help with our access to type and non-type specimens. We sincerely thank Mr Zhiwei Dong (Kunming Institute of Zoology, Chinese Academy of Sciences, Yunnan), Dr Hao Xu (Mianyang Normal University, Sichuan), Dr Jianyue Qiu (Mianyang Normal University, Sichuan), Mr Qiaozhi Yang (Beijing), Mr Weipeng Qiao (Henan), Mr Hao Huang (Shandong) and Mr Zichun Xiong (Yunnan) for generously providing specimens for this study. We also express heartfelt thanks to Dr Frank Etzler and Dr Aaron Smith who have helped very much to improve the manuscript.

This research was supported by grants from the National Natural Science Foundation of China to Shihong Jiang (Grant No. 31772511) and Yongying Ruan (Grant No. 31802004).

References

- Bousquet Y (2016) Litteratura Coleopterologica (1758–1900): a guide to selected books related to the taxonomy of Coleoptera with publication dates and notes. *ZooKeys* 583: 1–776. <https://doi.org/10.3897/zookeys.583.7084>
- Candèze ECA (1860) Monographie des Élatérides 3. Mémoires de la Société royale des Science de Liège 15: 1–512.
- Candèze ECA (1878) Élatérides Nouveaux II. Annales de la Société Entomologique de Belgique 21: 1–54.
- Candèze ECA (1888) Viaggio di Leonardo Fea in Birmania e regioni vicinow XIV. Élatérides recueillis en Birmanie en au Ténasserim par M. L. Fea pendant les années 1885–1887. *Annali del Museo Civico di Storia Naturale di Genova*, (2a) 6(26): 667–689.
- Candèze ECA (1891) Catalogue Méthodique des Élatérides connus en 1890. H Vaillant-Carmanne, Liège, 245 pp. <https://doi.org/10.5962/bhl.title.47119>
- Candèze ECA (1895) Élatérides nouveaux. Cinquième fascicule. Mémoires de la Société royale des Science de Liège, ser 2 18: 1–76.
- Cate PC, Sánchez-Ruiz A, Löbl I, Smetana A (2007) Elateridae. In: Löbl I, Smetana A (Eds) *Catalogue of Palaearctic Coleoptera*, Vol. 4. Apollo Books, Stenstrup, 89–209.
- Chu Y, Xiao M (1981) Shiraki collection. *Formosan Entomologist* 1: 26–32. [In Chinese: 朱耀沂, 肖美玲 (1981) 所谓“素木标本” (Shiraki Collection) (甲虫部分) 之概略, *台湾昆虫* 1: 26–32]
- Chu Y (2011) Additional notes on the “Shiraki collection”, *Taiwan Natural Science*, 30(2): 40–47. [In Chinese: 朱耀沂 (2011) 再谈“素木标本”. *台湾博物季刊* 30(2): 40–47] <https://doi.org/10.1108/01604951111105014>
- Chu Y (2013) *History of Entomology of Taiwan (1684–1945)*. National Taiwan University Press, Taipei, 614 pp. [In Chinese: 朱耀沂 (2013) *台湾昆虫学史话 (1684–1945)*. 国立台湾大学出版中心, 台北, 614 pp.]
- Douglas HB (2003) Revision of the *Cardiophorus* (Coleoptera: Elateridae) species of eastern Canada and United States of America. *The Canadian Entomologist* 135: 493–548. <https://doi.org/10.4039/n02-003>
- Douglas HB (2011) Phylogenetic relationships of Elateridae inferred from adult morphology, with special reference to the position of Cardiophorinae. *Zootaxa* 2900: 1–45. <https://doi.org/10.11646/zootaxa.2900.1.1>
- Douglas HB (2017) World reclassification of the Cardiophorinae (Coleoptera, Elateridae), based on phylogenetic analyses of morphological characters. *ZooKeys* 655: 1–130. <https://doi.org/10.3897/zookeys.655.11894>
- Douglas HB, Kundrata R, Janosikova D, Bocak L (2018) Molecular and morphological evidence for new genera in the click-beetle subfamily Cardiophorinae (Coleoptera: Elateridae). *Entomological Science* 21(3): 292–305. <https://doi.org/10.1111/ens.12306>
- Fleutiaux E (1895) Contributions à la faune indo-chinoise. 15^e memoire. Première addition aux Cicindelidae et Elateridae. *Annales de la Société Entomologique de France* 63: 683–690.
- Fleutiaux E (1918) Coléoptères Élatérides indochinois de la collection du Muséum d'histoire naturelle de Paris, catalogue et description des espèces nouvelles. *Bulletin du Muséum national d'histoire naturelle* 24: 205–236. <https://doi.org/10.5962/bhl.part.19997>

- Fleutiaux E (1931) Les Élatérides de l'Indo-Chine Française (Catalogue raisonné). Quatrième partie. Bulletin de la Société Zoologique de France 56: 306–334.
- Fleutiaux E (1947) Révision des élatérides (Coléoptères) de l'Indo-Chine française. Notes d'entomologie chinoise 11: 233–420.
- Hallermann J, Ananjeva N, Orlov N, Tillack F (2002) Leonardo Pea's historical collection of Amphibia and Reptilia from Burma deposited at the Zoologisches Museum Hamburg. Mitteilungen aus den Hamburgischen Zoologischen Museum und Institut 99: 139–153.
- Iablokoff-Khznorian SM, Mardjanian MA (1981) On the process of copulation and structure of the aedeagus of the click beetles with the description of a new subgenus of the genus *Cardiophorus* Eschs. Doklady Akademia nauka Armyan CCP 73: 244–249.
- Jiang S (1993) A catalogue of the insect specimens preserved in the Insect Collection of Huazhong Agricultural University. Beijing Agricultural Press, Beijing, 135 pp.
- Jiang S, Wang S (1999) Economic click beetle fauna of China (Coleoptera: Elateridae). China Agriculture Press, Beijing, 195 pp.
- Kollar V (1844/1848) without title. In: Kollar V, Radtenbacher L (Eds) Aufzählung und Beschreibung der von Freiherrn Carl v. Hügel auf seiner Reise durch Kaschmir und das Himalayagebirge gesammelten Insecten [393–564]. In: Hügel CFv (Eds) Kaschmir und das Reich der Siek. Vierter Band. Zweite Abtheilung. Hallberger'sche Verlagshandlung, Stuttgart, 244–586 [1844], 587–865 [1848].
- Kurosawa Y (1980) Chelidonium Memorandums (1). Coleopterists' News 50: 7–13.
- Laporte [Castelnau FL de Laporte Comte de] (1840) Histoire naturelle des insectes, Coléoptères. Avec une introduction renfermant l'anatomie et la physiologie de animaux articulés, par M. Brullé. Tome Premier. P. Duménil, Paris, 324 pp.
- Miwa Y (1927) New and some rare species of Elateridae from the Japanese Empire. Insecta Matsumurana 2(1): 105–114.
- Miwa Y (1931) Elateridae of Formosa (V). Transaction of natural History Society of Formosa 22(113): 72–98.
- Miwa Y (1934) The fauna of Elateridae in the Japanese Empire. Department of Agriculture Government Research Institute. Report N 65, Formosa 65, 289 pp.
- Morrone JJ (2015) Biogeographical regionalisation of the world: a reappraisal. Australian Systematic Botany 28(3): 81–90. <https://doi.org/10.1071/SB14042>
- Myers N, Mittermeier RA, Mittermeier GC, da Fonseca GAB, Kent J (2000) Biodiversity hotspots for conservation priorities. Nature 403: 853–858. <https://doi.org/10.1038/35002501>
- Ôhira H (1973) Coleoptera: Elateridae from Ceylon. Entomologica Scandinavica 4: 27–38.
- Ôhira H (1978) Some elaterid-beetles from Nepal collected by the Hokkaido university scientific expeditions to Nepal Himalaya. New Entomologist 27(4): 89–96.
- Platia G (2015) Contribution to the knowledge of click beetles from Maldives (Coleoptera: Elateridae). Boletín de la Sociedad Entomológica Aragonesa 57: 182–184.
- Platia G, Ahmed Z (2016) Contribution to the fauna of click beetles (Coleoptera: Elateridae) from Pakistan. Arquivos Entomológicos 16: 3–28.
- Suzuki W (1999) Catalogue of the family Elateridae (Coleoptera) of Taiwan. Miscellaneous Reports of the Hiwa Museum for Natural History 38: 1–348.
- Wallace AR (1876) The geographical distribution of animals. Vols I & II. Harper and Brothers, New York, 574 pp.

Three new species of frogs of the genus *Pristimantis* (Anura, Strabomantidae) with a redefinition of the *P. lacrimosus* species group

Santiago R. Ron¹, Julio Carrión¹, Marcel A. Caminer¹, Yerka Sagredo¹,
María J. Navarrete¹, Jhael A. Ortega¹, Andrea Varela-Jaramillo¹,
Gabriela A. Maldonado-Castro¹, Claudia Terán¹

¹ Museo de Zoología, Escuela de Biología, Pontificia Universidad Católica del Ecuador, Av. 12 de Octubre y Roca, Aptdo. 17-01-2184, Quito, Ecuador

Corresponding author: Santiago R. Ron (santiago.r.ron@gmail.com)

Academic editor: A. Crottini | Received 23 April 2020 | Accepted 5 September 2020 | Published 16 November 2020

<http://zoobank.org/10D216B5-7C11-43A5-BBC7-68DE9D31790F>

Citation: Ron SR, Carrión J, Caminer MA, Sagredo Y, Navarrete MJ, Ortega JA, Varela-Jaramillo A, Maldonado-Castro GA, Terán C (2020) Three new species of frogs of the genus *Pristimantis* (Anura, Strabomantidae) with a redefinition of the *P. lacrimosus* species group. ZooKeys 993: 121–155. <https://doi.org/10.3897/zookeys.993.53559>

Abstract

A new phylogeny for the *Pristimantis lacrimosus* species group is presented, its species content reviewed, and three new species described from the eastern slopes of the Ecuadorian Andes. Our phylogeny includes, for the first time, samples of *P. aureolineatus*, *P. bromeliaceus*, and *P. lacrimosus*. The morphology of hyperdistal subarticular tubercles is also assessed among 21 species of *Pristimantis*. The *P. lacrimosus* species group is composed of 36 species distributed in the Chocó, Guiana, and Amazon regions of tropical South America with a single species reaching Central America. Ancestral area reconstruction indicates that, despite its high diversity in the Amazon region, the *P. lacrimosus* group originated in the Pacific basin, Chocó region of Ecuador and Colombia. *Pristimantis amaguanae* **sp. nov.** is most closely related to *P. bromeliaceus*. It differs from *P. bromeliaceus* by being smaller, having transversal dark bands in the hindlimbs (absent or faint in *P. bromeliaceus*) and the absence of discoidal fold (present in *P. bromeliaceus*). *Pristimantis nankints* **sp. nov.** and *P. romeroae* **sp. nov.** are part of a clade of predominantly light-green frogs that includes *P. acuminatus*, *P. enigmaticus*, *P. limoncochensis*, and *P. omeviridis*. *Pristimantis nankints* **sp. nov.** and *P. romeroae* **sp. nov.** can be distinguished from all of them by the presence of a dark dorsolateral stripe that borders a light green band on a green background. Hyperdistal tubercles are present in all examined species of the *P. lacrimosus* species group and its sister clade. Species with hyperdistal tubercles are characterized by having relatively long terminal phalanges and narrow T-shaped expansion at the end of the terminal phalange. We discuss the phylogenetic distribution of these characters and their potential diagnostic significance.

Keywords

Amazon, Andes, Brachycephaloidea, morphology, phalanges, phylogeny, *Pristimantis amaguanae* sp. nov., *Pristimantis nankints* sp. nov., *Pristimantis romeroae* sp. nov., subarticular tubercles, systematics, taxonomy, Terrarana

Introduction

With 540 species *Pristimantis* is the most diverse vertebrate genus and represents a majority of the formally described anuran diversity in the tropical Andes of Colombia and Ecuador (AmphibiaWeb 2019). Moreover, molecular studies are revealing a high proportion of cryptic diversity (e.g., Elmer et al. 2007; Ortega-Andrade et al. 2015; Rivera-Correa and Daza 2016). Molecular-based systematic reviews should substantially increase the number of described *Pristimantis* species in decades to come.

One phenotypically distinctive group of *Pristimantis* is the *P. lacrimosus* group. Species of this group are frequently found in bromeliad plants and have broad and flattened heads with acuminate snouts (Hedges et al. 2008). The group was first recognized by Lynch and Duellman (1980) as an assemblage of species within the *Pristimantis unistriatus* species group. It contained *P. bromeliaceus*, *P. lacrimosus*, *P. mendax*, and *P. petersi*. Subsequent reviews added more species (e.g., Guayasamin et al. 2006; Lynch 1980) until reaching 18 species by 2008 (Hedges et al. 2008) and 25 by 2014 (Padial et al. 2014). Rivera-Correa and Daza (2016) presented a molecular phylogeny showing that the group was paraphyletic because it formed two clades that were not sister to each other. One clade (named “A”) included three Colombian species, the other, “clade B”, included the remaining species of the *P. lacrimosus* group. Because the phylogenetic position of *P. lacrimosus* is unknown, they refrained from defining which of the two clades should be considered the *P. lacrimosus* species group. Nevertheless, Gonzalez-Duran et al. (2017) created a new species group for clade A, the *P. boulengeri* group. They hypothesized that clade B corresponds to the *P. lacrimosus* species group based on a figure of the neotype of *P. lacrimosus* (Lynch and Schwartz 1971) showing the absence of double distal subarticular tubercles on fingers III or IV, a diagnostic character for the *P. boulengeri* group.

During fieldwork in cloud forests of the Amazon Basin of Ecuador, field teams from Museo de Zoología at Catholic University of Ecuador found three distinctive species that belong to the *Pristimantis lacrimosus* species group. Herein we describe them and present a new phylogeny for the group including, for the first time, *P. aureolineatus*, *P. bromeliaceus*, and *P. lacrimosus*.

Materials and methods

Morphology

The format for the descriptions follows Lynch and Duellman (1997). The terminology and definition of diagnostic characters follows Duellman and Lehr (2009). Specimens were

preserved in 10% formalin and stored in 70% ethanol. Sex was determined by examining the presence of vocal slits and gonadal inspection. Measurements were taken with digital calipers (to nearest 0.01 mm) following the methodology described by Navarrete et al. (2016). Examined specimens belong to the herpetological collection at Museo de Zoología, Pontificia Universidad Católica del Ecuador, Quito (QCAZ), and are listed in Appendix 1.

Fingers and toes are numbered preaxially to postaxially from I to IV and I to V, respectively. Relative lengths of toes III and V were determined by appressing them against toe IV; lengths of fingers I and II were compared by appressing them to each other. While describing the hands and feet of the new species, we noticed the presence of an additional distal subarticular tubercle. These tubercles were recently named by Ospina-Sarria and Duellman (2019) as “hyperdistal”. We use the following terminology for the subarticular tubercles of *Pristimantis*, including hyperdistal tubercles (Fig. 1): (1) “basal” for the tubercles at the base of fingers and toes, (2) “penultimate” occurs only on toe IV and refers to the tubercle underlying the distal articulation of the first phalange, (3) “distal” for the tubercles underlying the proximal articulation of the penultimate phalange, and (4) “hyperdistal” for the tubercle underlying the articulation of the last phalange of each finger and toe. Except for the exclusion of hyperdistal tubercles, this terminology has been used in most systematic accounts of *Pristimantis* at least since Lynch and Duellman (1997) seminal publication (e.g., Duellman and Lehr 2007; Urgiles et al. 2019; Valencia et al. 2019). We recommend its use, as amended by Ospina-Sarria and Duellman (2019), for future terminological consistency.

Subarticular tubercles underly articulations between phalanges (Lynch and Duellman 1997). To understand the osteological anatomy of the hyperdistal subarticular tubercles, we obtained X-ray images of 21 species of *Pristimantis* including two of the new species and three additional members of the *P. lacrimosus* species group (*P. acuminatus*, *P. enigmaticus*, and *P. limoncochensis*). The other species represent assorted lineages within *Pristimantis* (based on the phylogeny of Jetz and Pyron 2018). Digital X-ray images were obtained with the Thermo KeveX X-ray Imaging System at the QCAZ museum. To explore the relationship between phalange size and the presence of hyperdistal tubercles, we compared the length of the ultimate and penultimate phalanges of finger III (Fig. 2). *Pristimantis* have T-shaped terminal phalanges for which we measured the terminal expansion width in finger III. We measured the left hand except when fingers were twisted as result of fixation problems. If both hands had fixation problems, we excluded the specimen. All measurements were made with software ImageJ 2 version 1.52q (Rasband 2020).

Phylogeny

We estimated the phylogenetic relationships of the new species based on DNA sequences of mitochondrial genes 12S rRNA (12S), 16S rRNA (16S), NADH dehydrogenase subunit 1 (ND1), their flanking tRNAs and the nuclear gene Recombination activating gene 1 (RAG-1). DNA was extracted from muscle or liver tissue preserved in 95% ethanol, using standard guanidine thiocyanate extraction protocols. We used a polymerase chain reaction (PCR) to amplify DNA fragments.

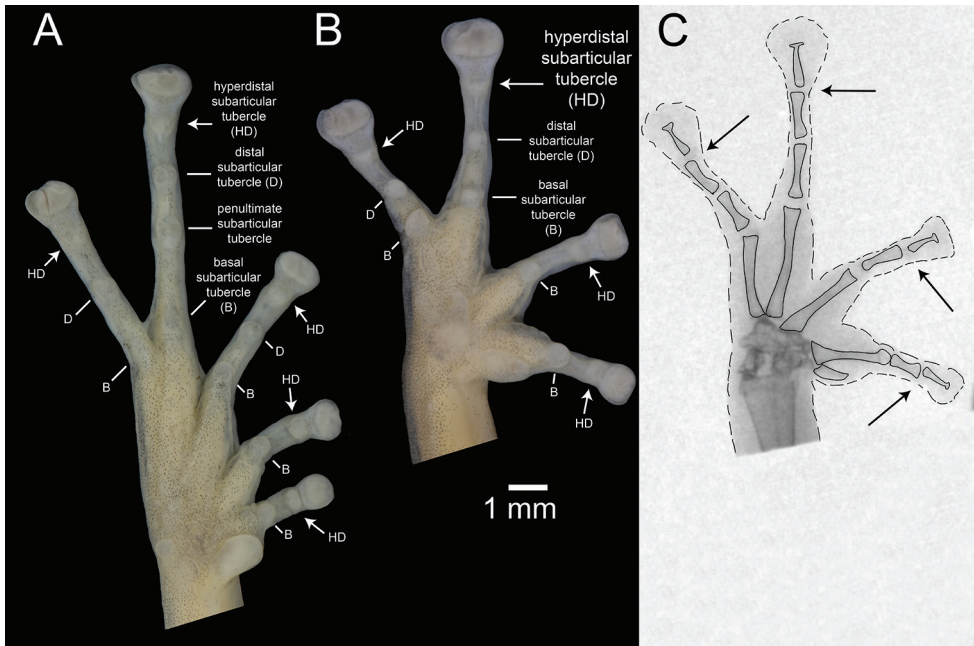


Figure 1. Palmar and plantar surfaces of *Pristimantis romeroae* sp. nov. and X-ray of the hand **A** ventral view of the left foot **B** ventral view of left hand **C** X-ray of the left hand. Holotype (QCAZ 41121). Arrows point to the hyperdistal subarticular tubercles. Abbreviations: B = basal, D = distal, HD = hyperdistal. In the x-ray image, dashed lines indicate the border of soft tissues; continuous lines indicate edges of bones.

The primers used for the 12S amplification were obtained from Goebel et al. (1999), for 16S from Heinicke et al. (2007), for ND-1 from Zhang et al. (2013), Wiens et al. (2005), Moen and Wiens (2009) and Brito et al. (2017) and for RAG-1 from Hedges et al. (2008). PCR amplification was performed under standard protocols and sequenced by the Macrogen Sequencing Team (Macrogen Inc., Seoul, Korea).

Our matrix included 74 newly generated sequences of *Pristimantis* (Table 1). We also included congeneric sequences available on GenBank. To optimize taxon sampling, we blasted the 16S sequences of the new species to the GenBank database (blastn procedure). This search showed that the most similar sequences belong to species of the *Pristimantis lacrimosus* group. Therefore, we concluded that the new species are closely related to the *P. lacrimosus* species group clade B (*sensu* Rivera-Correa et al. 2016). We included all GenBank sequences of that clade as well as closely related species (based on Guayasamin et al. 2017) and representative samples of other species groups of *Pristimantis*. The GenBank sequence of specimen QCAZ 19664 (EU130579) was assigned to *P. acuminatus* by Elmer et al. (2007) but is updated to *P. omeviridis* based on Ortega-Andrade et al. (2015). For the outgroup we included several species of the subgenus *Hypodictyon*.

The new sequences were assembled in Geneious 9.0 and then exported to Mesquite 3.61 (Maddison and Maddison 2019) where each genomic region was aligned using default parameters with Muscle 3.8 (Edgar 2004). Phylogenetic relationships were inferred for all genes concatenated using maximum likelihood (ML) as optimality cri-

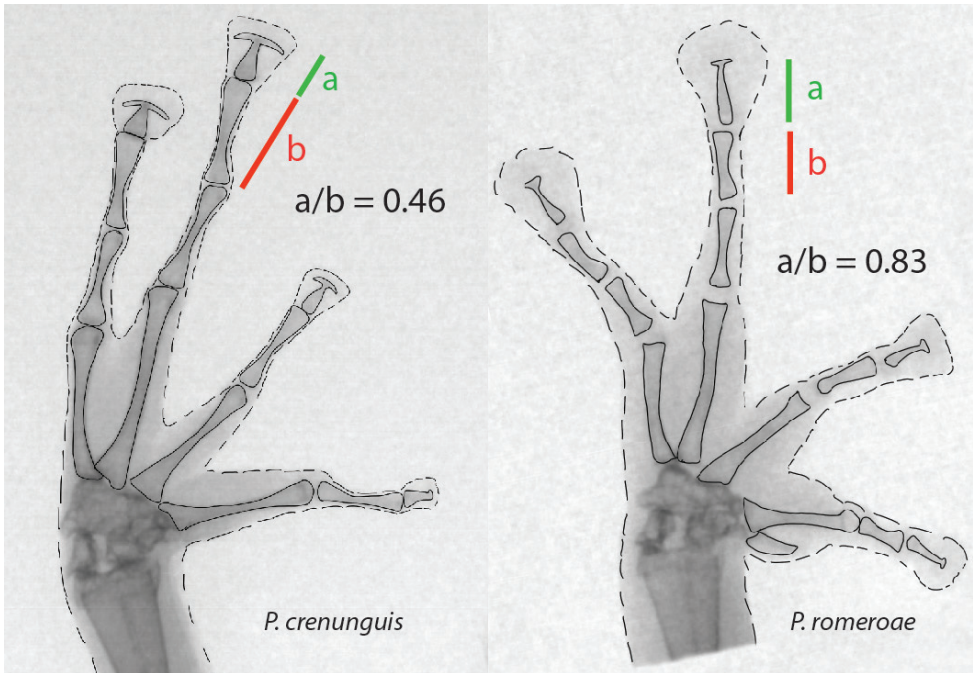


Figure 2. X-ray images of the left hand of adult *Pristimantis romeroae* sp. nov. and *P. crenunguis*. The ratios of the length of the ultimate and penultimate phalanges of finger III are shown. Dashed lines indicate the border of soft tissues; continuous lines indicate the edge of bones. *Pristimantis romeroae* sp. nov., QCAZ 41121, SVL = 31.1 mm; *P. crenunguis*, QCAZ 56506, SVL = 46.7 mm.

terion. The concatenated DNA matrix had 3974 bp and is available at <http://zenodo.org> under <https://doi.org/10.5281/zenodo.4005737>. Because different evolutionary processes have influenced each gene, we partitioned the data by gene and codon position to find the best model of evolution and partition scheme. To accomplish both tasks, we used the command MFP + MERGE (Chernomor et al. 2016; Kalyaanamoorthy et al. 2017) in software IQ-TREE multicore version 2.0 (Nguyen et al. 2015). To find the best phylogeny we run a search using IQ-TREE 2.0 under default settings. To assess branch support, we made 200 non-parametric bootstrap searches (-b 200 command) and 1000 replicates for the SH-like approximate likelihood ratio test (-alrt 1000 command; Guindon et al. 2010). We considered that branches with bootstrap values > 70 and SH-aLRT values > 80 had strong support. To calculate uncorrected *p*-distances of 16S we used MEGA 7.0 (Kumar et al. 2016).

Biogeographic origin of the *P. lacrimosus* species group

Most species of the *Pristimantis lacrimosus* group occur in the Amazon and Pacific basins. To determine the biogeographic origin of the group, we carried out ancestral state reconstruction. Regions were coded as a binary character (Pacific or Amazon) and the reconstruction employed maximum likelihood as optimality criterion. The

Table 1. GenBank accession numbers for DNA sequences used in the phylogenetic analyses.

Species	Voucher	12S	16S	RAG-1	ND1
<i>P. acerus</i>	KU 217786	EF493678.1	EF493678.1	NA	NA
	KU 217830	NA	EF493696.1	EF493432.1	NA
<i>P. alamazonicus</i>	KU 215460	EF493670.1	EF493670.1	NA	NA
<i>P. amaguanae</i> sp. nov.	QCAZ 39274	MT636506	MT636529	MT635622	MT635661
<i>P. angustilineatus</i>	UVC 15828	NA	JN371034.1	NA	NA
<i>P. appendiculatus</i>	KU177637	EF493524.1	EF493524.1	NA	NA
<i>P. aureolineatus</i>	QCAZ 42286	MT636509	MT636530	MT635626	NA
<i>P. boulengeri</i>	MHUAA 8951	NA	KU724435.1	NA	NA
<i>P. brevifrons</i>	nrps 0059	JN991498.1	JN991433.1	NA	NA
<i>P. bromeliaceus</i>	QCAZ 16699	MT636505	MT636527	MT635618	MT635659
	QCAZ 62940	MT636512	MT636523	NA	MT635669
<i>P. calcarulatus</i>	KU 177658	EF493523.1	EF493523.1	NA	NA
<i>P. cedros</i>	MZUTI 1713	NA	KT210155.1	NA	NA
<i>P. cf. mendax</i>	MTD 45080	EU186659.1	EU186659.1	NA	NA
<i>P. crucifer</i>	KU 177733	EU186736.1	EU186718.1	NA	NA
<i>P. diadematus</i>	KU 221999	EU186668.1	EU186668.1	NA	NA
	KU179090	EF493522.1	EF493522.1	NA	NA
<i>P. dorsopictus</i>	MHUAA7638	KP082864.1	KP082874.1	NA	NA
<i>P. ecuadorensis</i>	CJ 5350	KX785339	KX785343	NA	KX785347
	CJ 5351	KX785340	KX785344	NA	KX785348
<i>P. enigmaticus</i>	QCAZ 40918	MT636513	MT636520	MT635636	MT635670
<i>P. galdi</i>	QCAZ 32368	EU186670.1	EU186670.1	EU186746	NA
<i>P. glandulosus</i>	KU 218002	EF493676.1	EF493676.1	NA	NA
<i>P. imitatrix</i>	KU 215476	EF493824.1	EF493667.1	NA	NA
<i>P. inusitatus</i>	KU 218015	EF493677.1	NA	NA	NA
<i>P. jaguensis</i>	MHUAA 7249	KP082862.1	KP082870.1	NA	NA
<i>P. jorgevelosai</i>	JDL 26123	NA	DQ195461.1	NA	NA
<i>P. lacrimosus</i>	QCAZ 55238	NA	MT636518	MT635629	MT635667
	QCAZ 59474	NA	MT636517	MT635633	NA
	QCAZ 40261	NA	MT636524	MT635623	MT635671
	QCAZ 59469	NA	MT636516	MT635632	NA
<i>P. limoncochensis</i>	QCAZ 43794	NA	MT636525	MT635627	MT635665
	QCAZ 19180	MN128395	MT636532	MT635620	NA
<i>P. melanogaster</i>		EF493826.1	EF493664.1	NA	NA
<i>P. mindo</i>	MZUTI 1382	NA	KF801584.1	NA	NA
	MZUTI 1381	NA	KF801583.1	NA	NA
	QCAZ 56512	NA	MT636522	MT635630	MT635668
	MZUTI 1756	NA	KF801581.1	NA	NA
	QCAZ 42197	MT636508	MT636531	MT635625	MT635664
<i>P. moro</i>	AJC 1860	JN991520.1	JN991454.1	JQ025191.1	NA
	AJC 1753	JN991519.1	JN991453.1	JQ025192.1	NA
<i>P. nankints</i> sp. nov.	QCAZ 69137	NA	MT636514	MT635635	NA
<i>P. nyctophylax</i>	KU 177812	EF493526.1	EF493526.1	NA	NA
	QCAZ 32288	NA	MT636519	MT635621	MT635660
<i>P. omeviridis</i>	QCAZ 10564	MN128400	MK881398	MK881312	MT635658
	QCAZ 19664	NA	EU13057	MT635619	NA
<i>P. orcesi</i>	KU 218021	EF493679.1	EF493679.1	NA	NA
<i>P. ornattissimus</i>	MZUTI 4798	KU720464	KU720463	NA	KU720480
	MZUTI 4806	KX785337	KX785341	NA	KX785345
	MZUTI 4807	KX785338	KX785342	NA	KX785346
<i>P. pabuma</i>	MZUTI 493	NA	KT210158.1	NA	NA

Species	Voucher	12S	16S	RAG-1	ND1
<i>P. platydactylus</i>	MNCN 5524	FJ438811.1	EU192255.1	NA	NA
<i>P. pulvinatus</i>	KU 181015	EF186741.1	EF186723.1	NA	NA
<i>P. pycnodermis</i>	KU 218028	EF493680.1	EF493680.1	NA	NA
<i>P. romeroae</i> sp. nov.	QCAZ 41121	MT636507	MT636528	MT635624	MT635662
<i>P. rubicundus</i>	QCAZ 58932	NA	MT372670	MT372613	NA
<i>P. schultei</i>	KU 212220	EF493681.1	EF493681.1	NA	NA
<i>P. subsigillatus</i>	KU 218147	EF493525.1	EF493525.1	NA	NA
	QCAZ 49637	NA	MT636521	MT635628	MT635666
	MECN 10117	NA	KF801580.1	NA	NA
<i>P. urani</i>	MHUA 7471	NA	KU724442.1	NA	NA
<i>P. w-nigrum</i>	QCAZ 45200	MT636510	MT372703	MT372600	MT372569
	QCAZ 46256	NA	MT372704	MT372603	MT372571
	QCAZ 41818	NA	MT372691	NA	MT635663
<i>Pristimantis</i> sp.	ROM 43978	EU186678.1	EU186678.1	NA	NA
	KU 291702	EF493351.1	EF493351.1	NA	NA
	QCAZ 60398	NA	MT636515	MT635634	NA
	QCAZ 58956	MT636511	MT636526	MT635631	NA

analysis was carried out in Mesquite 3.61 (Maddison and Maddison 2019) under the asymmetrical two parameter Markov-k model. The model finds the ancestral states that maximize the probability of the geographic distribution of the contemporary species given the phylogeny (see Pagel 1999 for a detailed description of the model). Ancestral states were traced using the best tree obtained from the maximum likelihood search (see above). Species distributed outside both basins (e.g., *P.* sp. ROM 43978, *P. jorgevelosai*) were coded as unknown because the two parameter Markov-k maximum likelihood model is binary and does not allow additional states. This restriction imposed by the Markov-k model was inconsequential to the results because only two species of the *P. lacrimosus* group (*P. moro* and *P.* sp.) were affected. Species distribution data was obtained from Anfíbios del Ecuador (Ron et al. 2019), Lista de Anfíbios de Colombia (Acosta-Galvis 2019), and the IUCN Red List website (<https://www.iucnredlist.org/>). River basin assignment was based on a digital map of South American basins obtained from the Food and Agriculture Organization GeoNetwork website (<http://www.fao.org/geonetwork>).

Results

Phylogeny and biogeography

The phylogeny (Fig. 3) shows strong support (SH-aLRT = 97, bootstrap = 73) for a clade that includes the species of the *Pristimantis lacrimosus* group (clade B, sensu Rivera-Correa et al. 2016) as well as *P. amaguanae* sp. nov., *P. crucifer*, *P. galdi*, *P. ecua-dorensis*, *P. eremitus*, *P. enigmaticus*, *P. jorgevelosai*, *P. limoncochensis*, *P. nankints* sp. nov., *P. nyctophylax*, *P. omeviridis*, *P. ornatissimus*, *P. romeroae* sp. nov., and *P.* sp. Within this

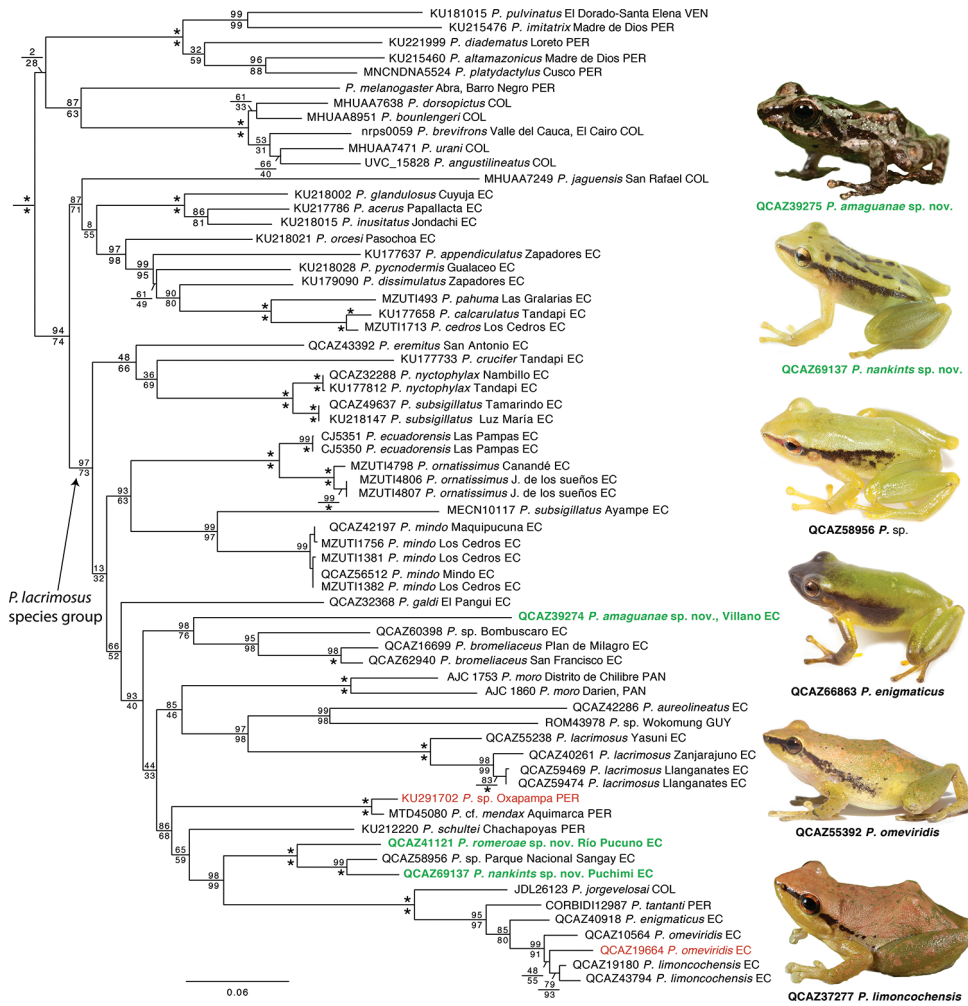


Figure 3. Phylogenetic relationships of the *Pristimantis lacrimosus* species group. Maximum likelihood tree for genes 12S, 16S, ND1 and RAG-1. SH-aLRT support (above) and non-parametric bootstrap support (below) are shown as percentages on branches. Asterisks indicate support values of 100 (bootstrap). Voucher number, species, and locality of the samples are shown next to each terminal; country is indicated by the following abbreviations: COL = Colombia, EC = Ecuador, GUY = Guyana, PAN = Panama, PER = Peru, VEN = Venezuela. The new species are shown with bold green characters. Changes in species identifications relative to the GenBank database are shown with red. Photographs show five species of the clade of green species and *P. amaguanae* sp. nov.. Outgroup is not shown.

clade, the first two clades to diverge are distributed in the Pacific basin of Ecuador and include *P. crucifer*, *P. ecuadorensis*, *P. mindo*, *P. nyctophylax*, *P. ornatissimus*, and *P. subsigillatus*. The remaining species form a large clade distributed in the Amazon basin with the exception of *P. moro* (Central America), *P. jorgevelosai* (Magdalena River basin), and *P. sp.* (Guyana).

We also found strong support (SH-aLRT = 94, bootstrap = 74) for a sister clade relationship between the *P. lacrimosus* group (as redefined below) and a clade composed of 11 species including *P. appendiculatus*, *P. calcarulatus*, *P. cedros*, *P. jaguensis*, *P. pycnodermis*, and *P. orcesi*. Within the *P. lacrimosus* species group, *Pristimantis amaguanae* sp. nov. is most closely related to *P. bromeliaceus* and an undescribed species from Bombuscaro, Podocarpus National Park, Ecuador. Branch lengths in the phylogeny and its morphological distinctiveness indicate that *P. amaguanae* sp. nov. is evolutionarily independent from *P. bromeliaceus* and the undescribed species from Bombuscaro. Uncorrected *p*-genetic distances (gene 16S) between *P. amaguanae* sp. nov. and its sister clade range between 13.0 and 13.8%. *Pristimantis nankints* sp. nov. is sister to an undescribed species from Sardinayacu, Sangay National Park, Ecuador. Their genetic distance is 2.7%. Both species are sister to *P. romeroae* sp. nov. from Napo Province. They are separated by distances of 6.9 (*P. sp.*) and 7.0% (*P. nankints* sp. nov.) These three species are sister to a clade composed by *P. jorgevelosai*, *P. enigmaticus*, *P. limoncochensis*, *P. omeviridis*, and *P. tantanti*.

The reconstruction of ancestral basin indicates that the group originated in the Pacific basin with a single colonization event to the Amazon basin (Fig. 4). There is one colonization event from the Amazon to Central America and the Pacific basin in *P. moro* and to the Río Magdalena basin (Colombia) in *P. jorgevelosai*.

Hyperdistal subarticular tubercles and phalange morphology

Most examined species of *Pristimantis* lack hyperdistal tubercles (Table 2). However, the five species of the *P. lacrimosus* group have hyperdistal tubercles as well as *P. eriphus*, *P. katoptroides*, and *P. orcesi*. As expected, the hyperdistal tubercle is located in the articulation of the two terminal phalanges (Fig. 1). Among the 21 species of *Pristimantis*, the five examined species of the *P. lacrimosus* group are characterized by having: (1) long terminal phalanges, and (2) narrow T-shaped expansions in the terminal phalanges. Species with shorter terminal phalanges and long T-shaped expansions lack distinct hyperdistal tubercles (e.g., *P. crenunguis*, *P. condor*; Fig. 2). We found large variation in width of the T-shaped expansion in the terminal phalange. In some species the expansion is almost as long as the phalange (*P. crenunguis*) while in others it represents less than 1/3 of its length (*P. acuminatus*).

Systematic accounts

Pristimantis lacrimosus species group

Content. We present a new definition of the group based in our phylogeny and recent taxonomic reviews. We define the *P. lacrimosus* species group to include all species descendant of the most recent common ancestor of *P. eremitus* and *P. lacrimosus* (Fig. 3). Our definition is based on our phylogeny and the data presented by Arteaga et al. (2013), Padial et al. (2014), Ortega-Andrade et al. (2015), Rivera-Correa and Daza (2016),

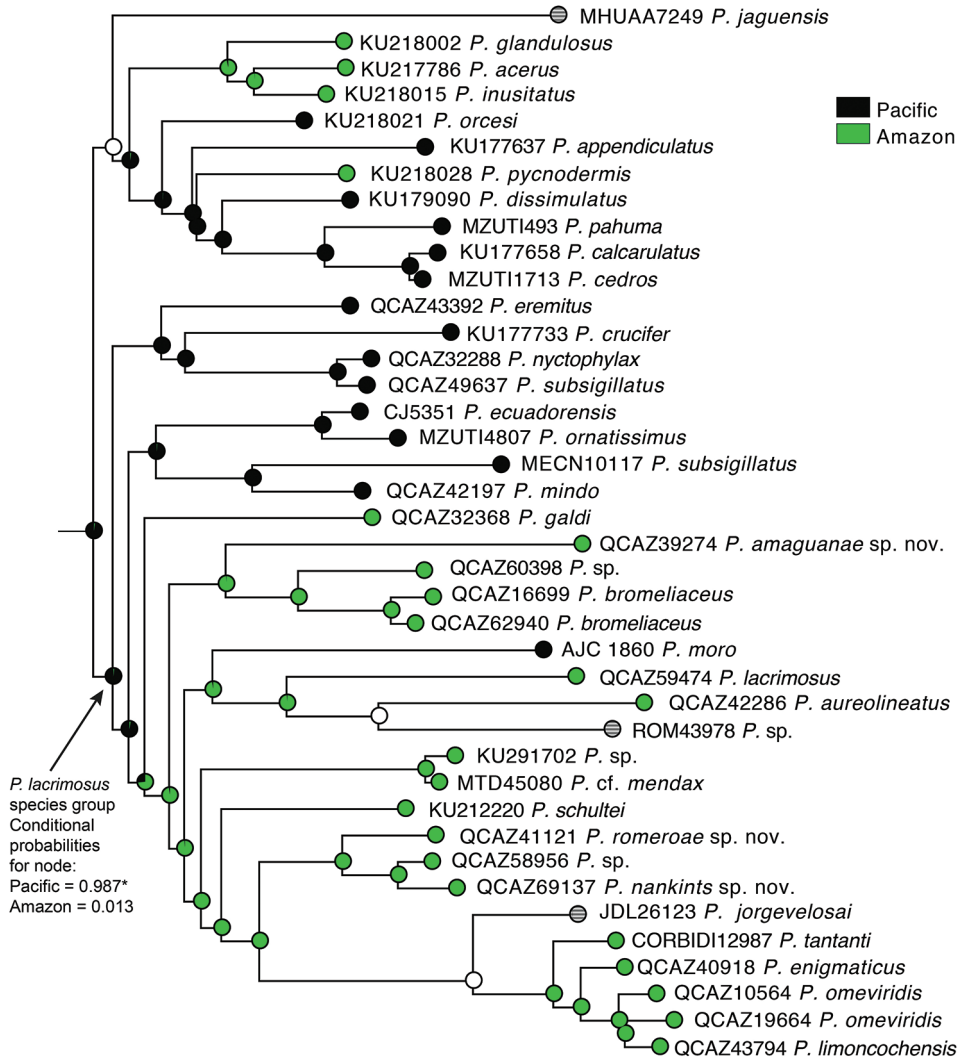


Figure 4. Ancestral reconstruction for geographic basin (Pacific vs. Amazon) in the *Pristimantis lacrimosus* species group. Reconstructions were based on maximum likelihood inference. Pie charts at nodes represent conditional probabilities for the Pacific (black) and Amazon (green) basins. The asterisk indicates significant support for the Pacific basin as ancestral area for the most recent common ancestor of the *P. lacrimosus* species group. White circles indicate equivocal state, striped circles indicate distribution outside the Pacific or Amazonian basins (coded as missing data).

Shepack et al. (2016), Gonzalez-Duran et al. (2017), and Ospina-Sarria and Duellman (2019). We exclude *P. apiculatus* from this group based on its close resemblance to *P. calcarulatus* (Lynch and Duellman 1997), a species that is not closely related to the *P. lacrimosus* species group (e.g., Pyron 2014). We exclude from the group *P. eugeniae* based on the phylogeny by Carrión (2020) which shows that it belongs to the sister clade of the *P. lacrimosus* species group. Ospina-Sarria and Duellman (2019) indicated that

Table 2. Phalange morphometry and hyperdistal tubercle condition in several species of *Pristimantis*. Species of the *Pristimantis lacrimosus* species group are shown in bold. Species are ordered according to the relative length of the terminal phalanges (from low to high, terminal/penultimate). The five lowest T-width/terminal values are shown with italics. Note that species of the *P. lacrimosus* species group are characterized by having longer terminal phalanges, narrower T-expansions at the end of the terminal phalange, and hyperdistal tubercles. Hyperdistal tubercles were coded as “present” when they were similar in size to other hyperdistal tubercles in the same finger or toe.

QCAZ	Species	Terminal/ penultimate	T-width/ terminal	Hyperdistal tubercle
56506	<i>P. crenunguis</i>	0.463	0.980	absent
40057	<i>P. buckleyi</i>	0.467	0.597	absent
2308	<i>P. unistrigatus</i>	0.473	0.574	absent
63435	<i>P. bicantus</i>	0.485	0.578	absent
43313	<i>P. quinquagesimus</i>	0.535	0.921	absent
66850	<i>P. condor</i>	0.550	0.608	absent
39122	<i>P. lantbanites</i>	0.558	0.652	absent
26209	<i>P. appendiculatus</i>	0.574	0.538	absent
49633	<i>P. achatinus</i>	0.601	0.461	absent
61831	<i>P. pycnodermis</i>	0.626	0.455	absent
47731	<i>P. chomskyi</i>	0.670	0.583	absent
66559	<i>P. eriphus</i>	0.732	0.539	present
66881	<i>P. katoptroides</i>	0.743	0.495	present
39763	<i>P. orcesi</i>	0.752	0.754	present
67662	<i>P. crucifer</i>	0.757	0.307	absent
65062	<i>P. phoxocephalus</i>	0.772	0.494	absent
41121	<i>P. romeroae</i> sp. nov.	0.828	0.317	present
30954	<i>P. limoncochensis</i>	0.831	0.294	present
71457	<i>P. nankints</i> sp. nov.	0.839	0.314	present
73812	<i>P. enigmaticus</i>	1.044	0.500	present
56418	<i>P. acuminatus</i>	1.060	0.293	present

P. sneiderni is most similar to *P. schultei* and *P. deyi*, two members of the *P. lacrimosus* species group. However, they also stated a resemblance to *P. boulengeri*, a species belonging to the *P. boulengeri* species group. Given this inconsistency we refrain from assigning *P. sneiderni* to the *P. lacrimosus* group until genetic evidence is available. We suspect *P. sneiderni* is not a member of the *P. lacrimosus* species group because it inhabits paramo, a habitat type on which the *P. lacrimosus* species group is absent. Most species of the *P. lacrimosus* species group inhabit foothill Andean forest or lowland tropical rain forest.

The group contains 36 described species: *P. acuminatus* (Shreve 1935), *P. amaguanae* sp. nov. (herein), *P. aureolineatus* (Guayasamin et al. 2006), *P. bromeliaceus* (Lynch 1979), *P. calima* Ospina-Sarria and Duellman 2019, *P. crucifer* (Boulenger 1899), *P. deyi* Lehr et al. 2013, *P. ecuadorensis* Guayasamin et al. 2017, *P. enigmaticus* (Ortega-Andrade et al. 2015), *P. eremitus* (Lynch 1980), *P. galdi* (Jiménez de la Espada 1870), *P. jorgevelosai* (Lynch 1994), *P. lacrimosus* (Jiménez de la Espada 1875), *P. latericius* Batallas and Brito 2014, *P. limoncochensis* Ortega-Andrade et al. 2015, *P. mendax* (Duellman 1978), *P. mindo* Arteaga et al. 2013, *P. moro* (Savage 1965), *P. nankints* sp. nov. (herein), *P. nyctophylax* (Lynch 1976), *P. olivaceus* (Köhler et al. 1998), *P. omeviridis* Ortega-Andrade et al. 2015, *P. ornatissimus* (Despax 1911), *P. padiali* Moravec et al. 2010, *P. pardalinus*, (Lehr et al. 2006), *P. petersi* (Lynch and Duellman 1980), *P. pluvialis* Shepack et al.

2016, *P. royi* (Morales 2007), *P. pseudoacuminatus* (Shreve 1935), *P. romeroae* sp. nov. (herein), *P. schultei* (Duellman 1990), *P. subsigillatus* (Boulenger 1902), *P. tantanti* (Lehr et al. 2007), *P. tayrona* (Lynch and Ruíz-Carranza 1985), *P. waoranii* (McCracken et al. 2007), and *P. zimmermanae* (Heyer and Hardy 1991).

***Pristimantis amaguanae* sp. nov.**

<http://zoobank.org/EE43D069-D9E5-456F-A026-3B783EFB2146>

Figures 5–7

Material. Holotype. QCAZ 39274 (field no. VH 1105; Figs 5–7), adult female from Ecuador, Provincia Pastaza. Surroundings of Villano, AGIP oil camp, K10, Unit 3. (1.4727°S, 77.5359°W), 430 m above sea level, collected by Edwin Carrillo, Galo Díaz, Yadira Mena and Fernando Ayala on 12 October 2008. **Paratype (1).** QCAZ 39275, adult male collected in amplexus with the holotype.

Suggested common name. English: Amaguaña's Rain Frog. Spanish: Cutín de Amaguaña.

Diagnosis. A species of *Pristimantis* characterized by the following combination of characters: (1) skin on dorsum shagreen with conical tubercles, skin on venter areolate with light green warts on the chest; discoidal fold absent; dorsolateral folds absent (Fig. 5); (2) tympanic membrane and tympanic annulus present, its dorsoposterior border converges with supratympanic fold; (3) snout acuminate in dorsal, protruding in lateral profile, with rostral papilla; (4) upper eyelid with several small conical tubercles; cranial crests absent; (5) dentigerous processes of vomers absent; (6) male having vocal slits, nuptial pads absent; (7) finger I shorter than finger II; discs of digits expanded, rounded (Fig. 6); (8) fingers with lateral fringes; hyperdistal subarticular tubercles present; (9) ulnar tubercles present, low and rounded; (10) heel bearing conical tubercles varying from prominent to inconspicuous; inner tarsal fold absent; (11) inner metatarsal tubercle ovoid, elevated, five times the size of round outer metatarsal tubercle; supernumerary plantar tubercles present; (12) toes with narrow lateral fringes; basal toe webbing absent; toe V much longer than toe III (disc on toe III reaches the proximal border of the penultimate subarticular tubercle on toe IV, disc on toe V reaches the distal subarticular tubercle on toe IV); hyperdistal subarticular tubercles present; toe discs as large as those on fingers (Fig. 6); (13) in life, dorsal surfaces of body and limbs olive green or olive brown with black markings; canthal stripe and supratympanic fold black; lips cream with black bars; flanks cream with one broad oblique black bar; chest light green with greenish cream warts; belly yellowish white; iris bronze to reddish copper with black reticulations (Fig. 5); (14) SVL in adult female 20.4 mm ($n = 1$), in adult male 16.3 mm ($n = 1$).

Comparison with other species. In this section, coloration refers to live individuals unless otherwise noticed. The coloration of *Pristimantis amaguanae* resembles that of *P. bromeliaceus* and *P. petersi* (Fig. 5). *Pristimantis amaguanae* can be easily recognized by the presence of transversal dark bands in the hindlimbs (absent or faint in *P. bromeliaceus* and *P. petersi*) and the absence of discoidal fold (present in *P. bromeliaceus* and *P. petersi*).



Figure 5. Live adult individuals **A** holotype of *Pristimantis amaguanae* sp. nov., adult female, QCAZ 39274 (SVL = 20.4 mm) **B** paratype of *Pristimantis amaguanae* sp. nov., adult male, QCAZ 39275 (SVL = 16.3 mm). Photographs by Jorge Valencia.

Pristimantis amaguanae further differs from *P. bromeliaceus* by its smaller adult size (female SVL = 20.4 mm, males SVL = 16.3 mm vs. *P. bromeliaceus* female SVL = 23.0–28.5 mm, male SVL = 16.7–22.8 mm; Lynch and Duellman 1980). Another small, green *Pristimantis* from the Amazon basin is *P. paululus*. The new species differs by having more tuberculate dorsal skin, discoidal folds absent (folds prominent in *P. paululus*, Lynch 1974), and scattered enlarged light green warts in the venter (small white points in *P. paululus*; Lynch 1974). *Pristimantis pseudoacuminatus* differs by having a truncate snout in profile (acuminate in *P. amaguanae*, Fig. 7) and by having a lighter and more uniform coloration in preservative.

Description of the holotype. Adult female (QCAZ 39274). Measurements (in mm): SVL 20.4; tibia length 9.5; foot length 8.7; head length 8.7; head width 7.7; eye diameter 2.8; tympanum diameter 1.1; interorbital distance 2.5; upper eyelid width 1.9; internarial distance 2.0; eye-nostril distance 2.3; tympanum-eye distance 0.8. Body slender; head slightly longer than wide, wider than body; snout acuminate in dorsal view, protruding in lateral profile, with rostral papilla; canthus rostralis distinct, curved in dorsal view; loreal region concave; interorbital space flat, no cranial crests; eye large, protuberant; upper eyelid bearing numerous small tubercles; tympanic membrane and annulus distinct, rounded in shape, with supratympanic fold partially covering upper and posterodorsal edges; choanae large, rounded, not concealed by

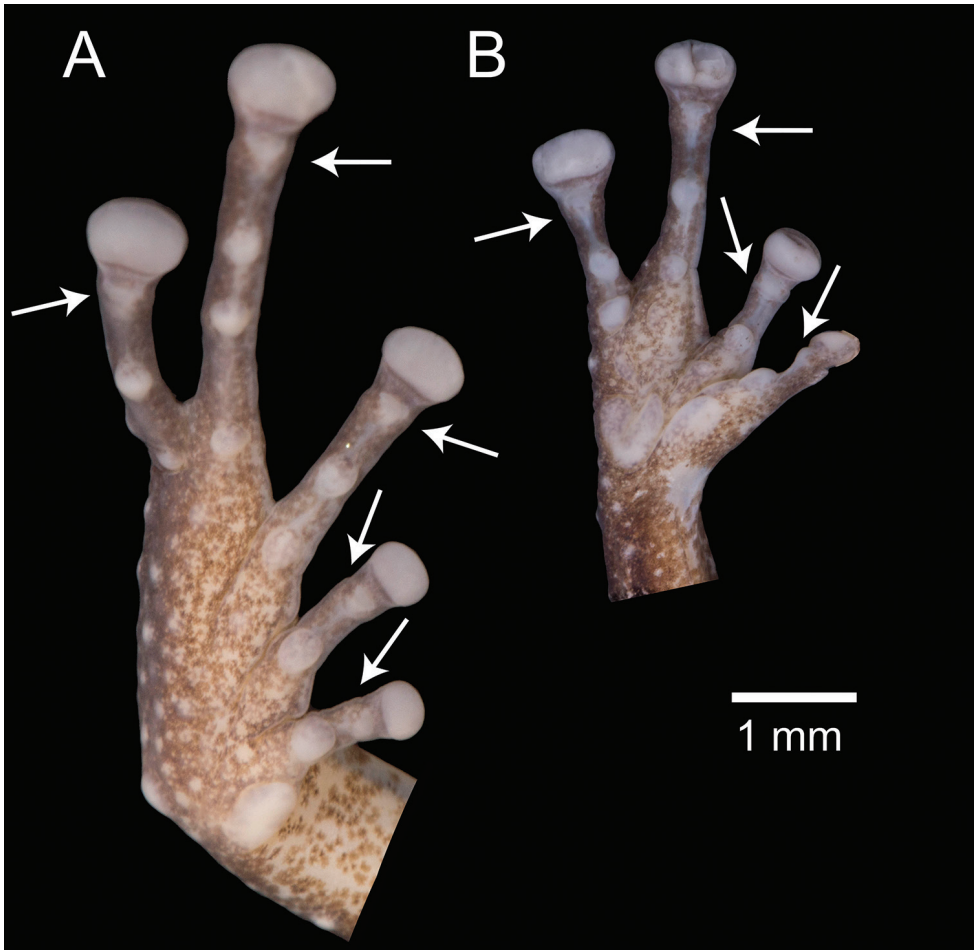


Figure 6. Ventral views of the left hand and foot of *Pristimantis amaguanae* sp. nov. Holotype (QCAZ 39274). Hyperdistal subarticular tubercles are pointed with arrows. Photographs by Julio C. Carrión.

palatal shelf of maxillary arc; dentigerous processes of vomers absent; tongue elliptical, posterior border notched, one-third not adherent to floor of mouth.

Skin on dorsum shagreen with scattered tubercles; dorsolateral folds absent; skin on lower flanks and belly areolate with scattered tubercles; skin on throat and chest smooth; discoidal fold absent; skin in upper cloacal region shagreen, wrinkled ventrally, with several tubercles below the cloacal sheath. Forearms slender; conical ulnar tubercles present along outer edge of forearm; all digits bearing pads and discs, broadly expanded and rounded but those of fingers II–IV clearly larger than that on thumb; fingers bearing narrow lateral fringes; relative lengths of fingers $I < II < IV < III$; subarticular tubercles single, well defined, round in ventral and lateral view; hyperdistal subarticular tubercles present in all fingers; several supernumerary tubercles

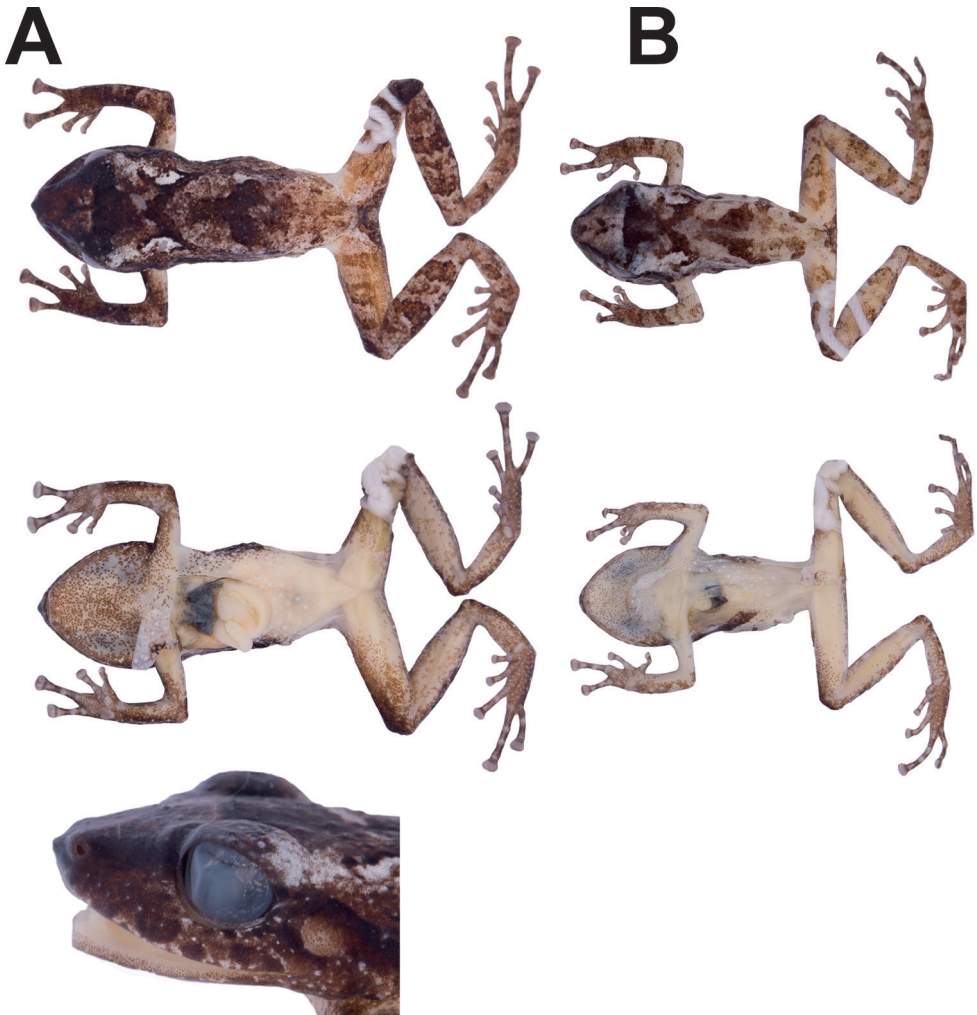


Figure 7. Variation in preserved specimens of *Pristimantis amaguanae* sp. nov. **A** adult female, QCAZ 39274 (SVL = 20.4 mm) **B** adult male, QCAZ 39275 (SVL = 16.3 mm). Photographs by Maricela Rivera.

at base of fingers present, distinct; palmar tubercle bifid, approximately 1.5 size of ovoid thenar tubercle (Fig. 6).

Hindlimbs slender; upper surfaces of hindlimbs smooth; posterior surfaces of thighs smooth, ventral surfaces of thighs slightly areolate; heel bearing low conical tubercles; inner surface of tarsus bearing small, low tubercles; toes with lateral fringes; webbing between toes absent; discs on toes expanded, elliptical, as large as those on fingers; all toes having pads surrounded by circumferential grooves; relative lengths of toes: $I < II < III < V < IV$; subarticular tubercles rounded, simple; hyperdistal subarticular tubercles present; plantar surface with supernumerary tubercles; inner metatarsal tubercle prominent, ovoid approximately five times of rounded outer metatarsal tubercle (Fig. 6).

Color of holotype in preservative. (Fig. 7) Background color pale brown with a dark brown interorbital bar and chevron marks in the scapular and sacrum region; a white mark extending from the posterior border of the upper eyelid to the scapular region; canthal and supratympanic stripe black, extending as a post-axial stripe on lower flanks; a dark brown Y-shaped mark at the tip of snout; dark brown transversal bars on dorsal surfaces of the limbs (three on the forearm, four to five on the thigh, five on the shank, and four on the foot); anal triangle dark brown; flanks and hidden surfaces of thighs pale brown; venter cream with white tubercles; scattered brown flecks on the neck, chest, and lips; ventral surfaces of hindlimbs and forelimbs creamy white with a brown suffusion.

Color of holotype in life. (Fig. 5) Dorsal surfaces of body and limbs olive green with black markings; canthal stripe and supratympanic fold black; flanks cream with one broad oblique bar; chest light green with small white spots; belly yellowish white; ventral surfaces of forelimbs and shanks faint green wash; ventral surfaces of thighs pale brown; iris bronze with black reticulations.

Variation. In this section, variation refers to a preserved male QCAZ 39275 (Fig. 7) collected with the holotype in amplexus. The adult male (SVL = 16.3 mm) is smaller than the single known female (SVL = 20.4 mm). Measurements (in mm): tibia length 8.4; foot length 7.1; head length 6.4; head width 5.7; eye diameter 2.1; tympanum diameter 0.8; interorbital distance 2.1; upper eyelid width 1.7; internarial distance 1.7; eye-nostril distance 2.2; tympanum-eye distance 0.5. Male having vocal slits; nuptial pads absent.

Color in life (based on digital photographs; Fig. 5). Background coloration is olive brown with faint green dorsolaterally. Marks on dorsum and flanks are similar to the holotype, except for the interorbital bar that is interconnected with the chevron mark in the scapular region. Iris is reddish copper.

Distribution, natural history, and conservation status. This species is only known from the type locality in Provincia de Pastaza, Ecuador at 430 m above sea level (Fig. 8). Natural region is Amazonian Tropical Rainforest (as defined by Ron et al. 2019). The forest is characterized by a high canopy (up to 30 m) with emergent trees that can reach 40 m. Annual precipitation is above 3000 mm and seasonality is low. The amplexant pair was on a leaf 0.4 m above the ground in primary forest near a stream at night.

We recommend assigning *Pristimantis amaguanae* to the Endangered Red List category according to the B2ab(iii) criteria (based on IUCN 2017 guidelines) because it is known from a single locality, its Area of Occupancy is less than 500 km² and its only known locality is at a distance of 1.5 km from deforested areas (based on Google Earth satellite images dating from 2017). A road was built in the area ca. five years ago. Road building is the main predictor of forest destruction in the Ecuadorian Amazon (Sierra 2013).

Etymology. The specific name *amaguanae* is a noun in the genitive case and is a patronym for Tránsito Amaguaña, a leading female figure of the indigenous movement in Ecuador. In 1930 she helped to form the first indigenous organization in Ecuador and during all her life she fought for equality and justice for Ecuadorian poor people.

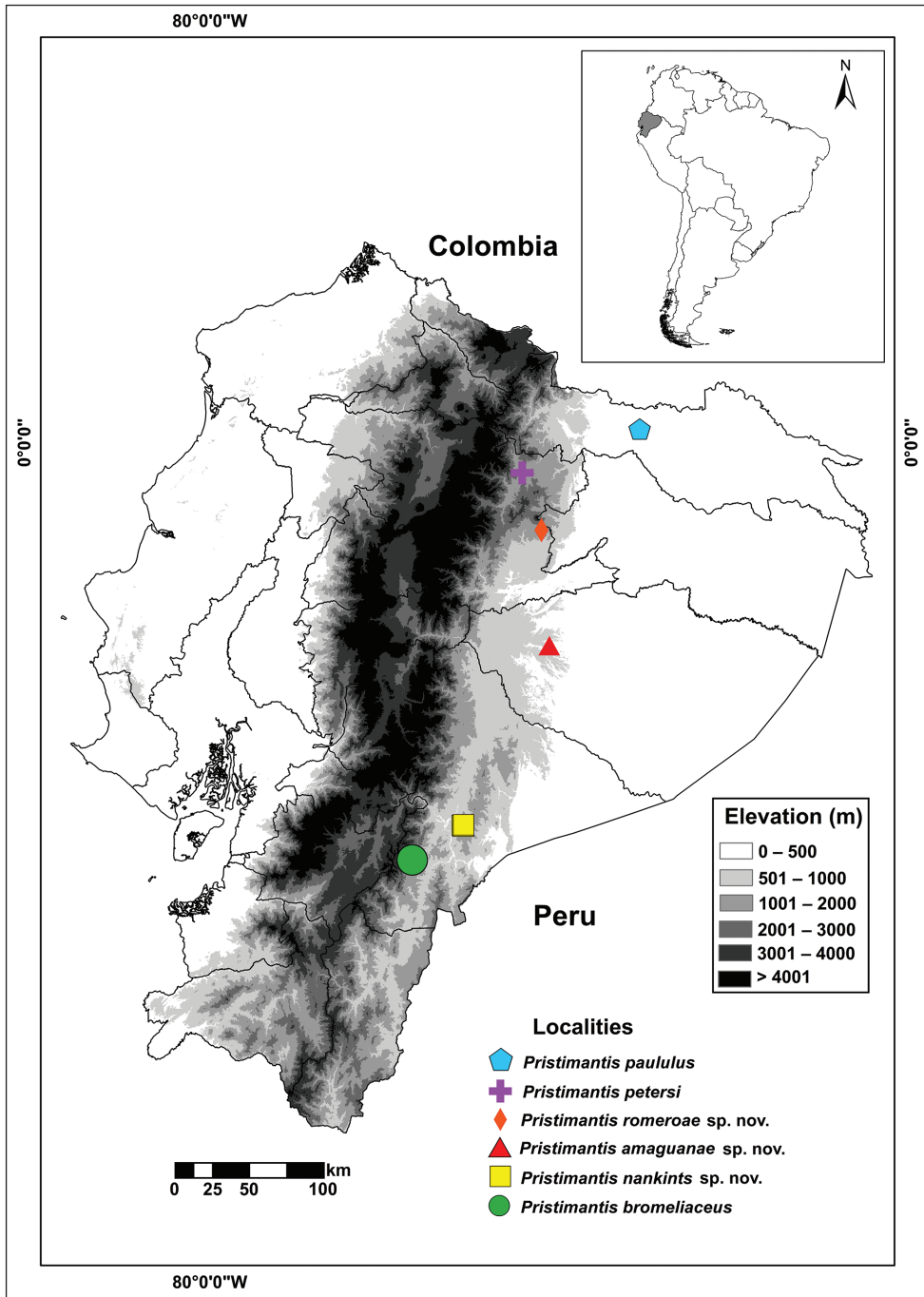


Figure 8. Known distribution of the three new species and type localities of *P. paululus*, *P. petersi*, and *P. bromeliaceus*. Localities are based on specimens deposited at Museo de Zoología of Pontificia Universidad Católica del Ecuador and from Lynch (1974), Lynch (1979), and Lynch and Duellman (1990).

***Pristimantis nankints* sp. nov.**

<http://zoobank.org/F3D2457F-6AB8-49F7-9608-1A24A4054782>

Figures 9–12

Material. Holotype. QCAZ 71457 (field no. SC-PUCE 61965; Figs 9–11), adult female from Ecuador, Provincia Morona Santiago, Cantón Santiago de Méndez. Low part of the Cutucú mountain range in the vicinity of the house of Mr. Carlos Hurtado (2.78325°S; 78.15878°W), 1413 m above sea level. Collected by Diego Almeida, Diego Paucar, Darwin Núñez, Eloy Nusirquia and Ricardo Gavilanes on 01 January 2018.

Paratypes (2). All specimens were collected in Ecuador, Provincia Morona Santiago. QCAZ 71458 (field no. SC-PUCE 61965), adult female collected with the holotype. QCAZ 69137 (field no. SC-PUCE 60012); adult male from Ecuador, Cantón Santiago, Puchimi (2.7780°S, 78.1682°W), 1364 m above sea level, collected by Diego Almeida, Darwin Núñez, Eloy Nusirquia and Jefferson Mora on 14 September 2017.

Suggested common name. English: Nankints Rain Frog. Spanish: Cutín de Nankints.

Diagnosis. A species of *Pristimantis* characterized by the following combination of characters: (1) skin on dorsum shagreen, skin on venter areolate with scattered warts, smooth on throat; discoidal fold absent; dorsolateral folds absent; (2) tympanic membrane and tympanic annulus present, upper edge of tympanic annulus covered by supratympanic fold; (3) snout short, protruding in lateral profile, acuminate in dorsal view, with rostral papilla; (4) upper eyelid without conical tubercles; cranial crests absent; (5) dentigerous processes of vomers present, prominent, oblique; (6) male having vocal slits, nuptial pads absent; (7) finger I shorter than finger II; discs of digits moderately expanded, rounded; (8) fingers bearing narrow lateral fringes; hyperdistal subarticular tubercles present; (9) ulnar and tarsal tubercles present, those on the tarsus are flattened and low, nearly inconspicuous; (10) heel without conical tubercles; inner tarsal fold present; (11) inner metatarsal tubercle prominent, elliptical, approximately 3× as large as rounded, conical outer metatarsal tubercle; outer metatarsal tubercle small, rounded; supernumerary plantar tubercles inconspicuous (Fig. 10); (12) toes bearing narrow lateral fringes; toe webbing absent except for basal webbing between toes III and IV; toe V much longer than toe III (disc on toe III extends to the distal edge of the medial subarticular tubercle on toe IV, disc on toe V extends beyond the proximal edge of the distal subarticular tubercle on toe IV); hyperdistal subarticular tubercles present; toe discs smaller than those on fingers (Fig. 10); (13) in life, dorsum lime green to olive green with black to brown marks on dorsum; flanks green with black to brown longitudinal stripes on upper edge; chest and belly greenish cream, throat yellowish green; ventral surface of thighs lime green to pinkish green. Iris bronze with a broad dark brown horizontal band and black reticulations; (14) SVL in adult females 29.4 mm ± 2.2 (27.8–30.9, n = 2), SVL in one adult male 19.6 mm.

Comparisons with other species (Fig. 12). In this section, coloration refers to live individuals unless otherwise noticed. *Pristimantis nankints* and *P. romeroae* have similar coloration in preservative. *Pristimantis nankints* differs by having small warts in the ven-



Figure 9. Live individuals of *Pristimantis nankints* **A** paratype, subadult male QCAZ 69137 (SVL = 19.6 mm) **B** holotype, adult female QCAZ 71457 (SVL = 30.9 mm). Photographs by Darwin Nuñez (**A**), Gustavo Pazmiño (**B**).

ter (numerous large warts in *P. romeroae*) and by the size and shape of discs on fingers: expanded and truncate in *P. romeroae* vs. moderately expanded and rounded in *P. nankints*. Its green dorsal coloration resembles that of *P. acuminatus*, *P. enigmaticus*, *P. limoncochensis*, *P. omeviridis*, *P. pseudoacuminatus*, and *P. tantanti*. It differs from all of them by having a dark stripe bordering the upper edge of the flanks (dark stripe absent or present, it is an oblique-lateral stripe starting behind the eye and ending near the ventral edge of the flank at midbody). It further differs from *P. acuminatus*, *P. limoncochensis*, and *P. tantanti* by having a prominent tympanum (tympanum absent in the three species; Duellman and Lehr 2009). *Pristimantis enigmaticus* and *P. omeviridis* differ by having a smaller tympanum (12–13% of head length [Ortega-Andrade et al. 2015] vs. 20–25% in *P. nankints*). *Pristimantis pseudoacuminatus* differs by having sparse tubercles and warts on the dorsum (tubercles and warts absent in *P. nankints*; Shreve 1935).

Description of the holotype. Adult female (QCAZ 71457; Figs 9–11). Measurements (in mm): SVL 30.9; tibia length 13.2; foot length 14.9; head length 11.4; head width 10.6; eye diameter 3.0; tympanum diameter 2.3; interorbital distance 3.8; upper eyelid width 2.8; internarial distance 2.3; eye-nostril distance 3.7; tympanum-eye distance#1.7. Body slender; head slightly wider than long, wider than body; snout short, protruding in lateral profile, acuminate in dorsal view, with rostral papilla;

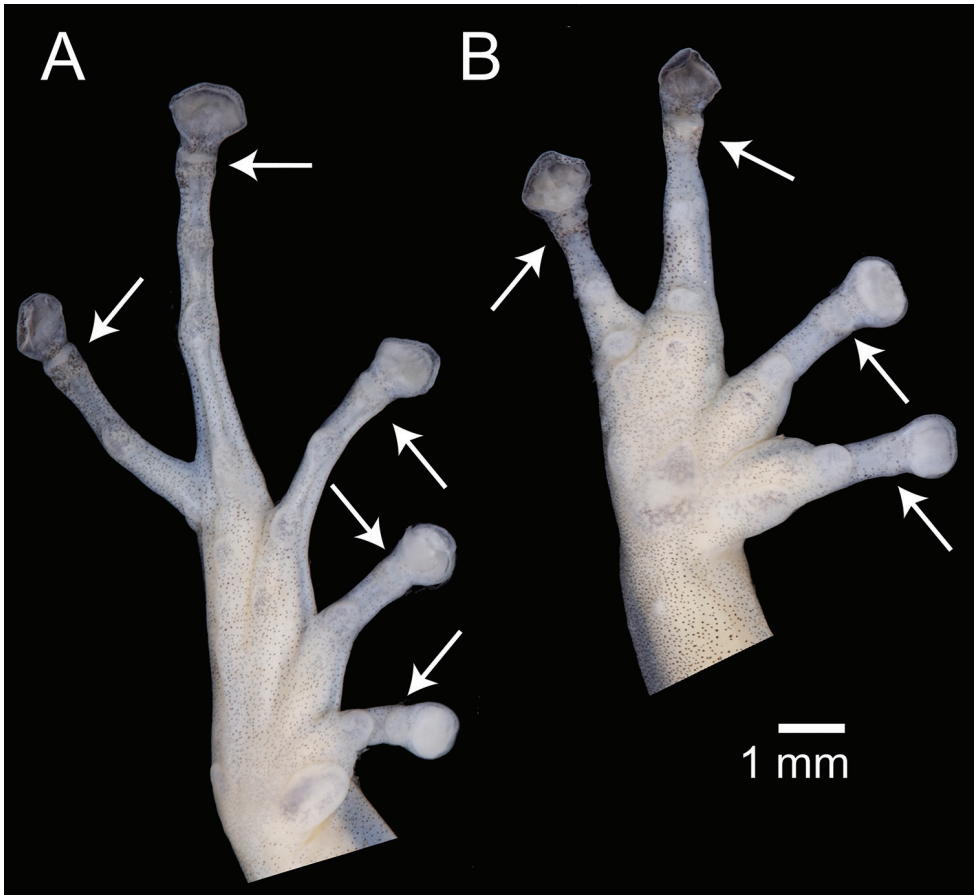


Figure 10. Ventral views of the left hand and foot of *Pristimantis nankints* sp. nov. Holotype (QCAZ 71457). Hyperdistal subarticular tubercles are pointed with arrows. Photographs by Julio C. Carrión.

canthus rostralis distinct, slightly curved in dorsal view; loreal region slightly concave; interorbital space flat, no cranial crests; upper eyelid ca. 75% of interorbital distance; lacking tubercles, no interocular fold. Tympanic membrane and annulus present, rounded in shape, with supratympanic fold covering upper edge; horizontal diameter of tympanum ca. 75% of eye diameter, separated from eye by a distance of a complete tympanum length; choanae large, rounded, not concealed by palatal shelf of maxillary arc; dentigerous processes of vomers present, prominent, oblique, bearing 5 teeth, tongue cordiform.

Skin on dorsum shagreen; dorsolateral folds absent; skin on belly and posterior half of chest areolate with scattered warts; skin on anterior half of chest and throat smooth; discoidal fold absent; skin in upper cloacal region shagreen. Forearms slender with a row of four conical ulnar tubercles in outer edge of forearm; fingers large and slender, all with round discs; fingers bearing narrow lateral fringes; relative lengths of fingers I < II < IV < III; subarticular tubercles single, well defined, round in ventral view; hy-

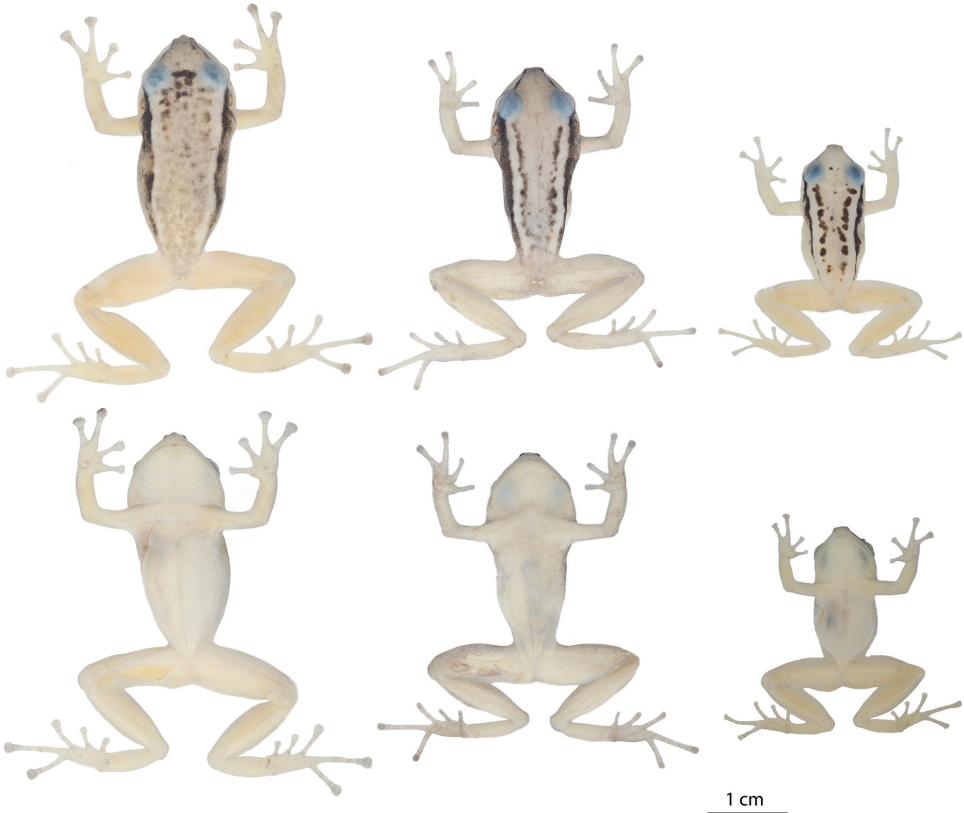


Figure 11. Variation in preserved specimens of *Pristimantis nankints* sp. nov. From left to right, first and second rows: QCAZ 71457 (holotype, adult female, SVL = 30.9 mm), QCAZ 71458 (adult female, SVL = 27.8 mm), QCAZ 69137 (adult male, SVL = 19.6 mm). Photographs by Julio C. Carrión.

perdistal subarticular tubercles present in all fingers; supernumerary palmar tubercles present, distinct; palmar tubercle bifid, 2× size of ovoid thenar tubercle (Fig. 10).

Hindlimbs slender; tibia length ca. 50% of SVL; upper surfaces of hindlimbs smooth; foot length ca. 46 % of SVL, posterior surfaces of thighs smooth, ventral surfaces of thighs slightly areolate; knee and heel lacking tubercles; inner surface of tarsus lacking tubercles; toes bearing narrow lateral fringes; webbing between III and IV toes present at the base; discs on toes broadly expanded, rounded, relatively smaller than fingers; all toes having pads surrounded by circumferential grooves; relative lengths of toes: I < II < III < V < IV; subarticular tubercles rounded; hyperdistal subarticular tubercles present in all toes; plantar surface with inconspicuous supernumerary tubercles; inner metatarsal tubercle prominent, elliptical, approximately three times as large as rounded, conical outer metatarsal tubercle (Fig. 10).

Color of holotype in preservative. (Fig. 11) Background color pale gray with dark brown interorbital bar; light canthal and supratympanic black stripe continued by a long dorsolateral stripe bordering the upper flank; dorsal brown marks scattered on

Table 3. Morphometric variables of *Pristimantis nankints* sp. nov. and *Pristimantis romeroae* sp. nov. Mean \pm SD is given with range in parentheses. All measurements are in millimeters.

Variable	<i>P. nankints</i> sp. nov.		<i>P. romeroae</i> sp. nov.	
	male n = 1	female n = 2	male n = 1	female n = 3
Snout-vent length	19.6	29.4 \pm 2.2 (27.8–30.9)	23.8	32.0 \pm 1.6 (31.1–33.8)
Tibia length	10.4	13.3 \pm 0.2 (13.2–13.5)	9.9	14.6 \pm 0.6 (14.2–15.2)
Foot length	10.8	14.5 \pm 0.6 (14.1–14.9)	11.1	15.8 \pm 0.3 (15.6–16.1)
Head length	7.0	10.7 \pm 1.0 (10.0–11.4)	8.2	11.4 \pm 0.6 (10.8–12.0)
Head width	6.3	10.3 \pm 0.4 (10.0–10.6)	7.7	11.3 \pm 0.4 (11.0–11.7)
Eye diameter	2.6	2.8 \pm 0.2 (2.7–3.0)	2.8	3.2 \pm 0.3 (2.9–3.4)
Tympanum diameter	1.8	2.3 \pm 0.1 (2.3–2.4)	2.3	2.8 \pm 0.5 (2.4–3.3)

all dorsum except for two longitudinal bands adjacent to the dark dorsolateral stripe; color of venter, chest, and ventral surfaces of the limbs pale cream.

Color of holotype in life. (Fig. 9) Dorsal surfaces dark green with black spots and limbs yellowish green; canthal stripe and supratympanic fold black, continued by black dorsolateral stripe bordering the upper flank, the black stripe gradually fades in the upper flank and limits dorsally with a parallel light green band; chest and belly greenish cream, throat yellowish cream; ventral surfaces of forelimbs yellowish green and shanks faint green; ventral surfaces of thighs pinkish green; iris bronze with a broad dark brown horizontal band and black reticulations.

Variation. (Fig. 11) In this section, coloration refers to preserved individuals. In the type series, the adult male has an SVL = 19.6 mm and the adult female 27.8 mm; (Table 3). The male has vocal slits and lacks nuptial pads. Dorsal coloration in preservative is light gray (e.g., QCAZ 71458) to yellowish cream (e.g., QCAZ 69137) with black dorsolateral bars and a black canthal stripe. Both paratypes have a lighter dorsolateral band bordered by the dark dorsolateral stripe and delimited medially by a faint black stripe (QCAZ 71458) or a row of black marks (QCAZ 69137). Both paratypes lack an interorbital bar but QCAZ 69137 has two dark marks instead. In QCAZ 69137 the flanks are yellowish cream; in QCAZ 71458 the flanks are gradually darker towards the black dorsolateral stripe. The tips of the fingers have the same color as the rest of the finger in QCAZ 69137 while in QCAZ 71458 they are darker.

Color in life (based on digital photographs of an adult male QCAZ 69137) (Fig. 9): dorsal surfaces are lime green; black-reddish canthal stripe is continued by black supratympanic fold and black dorsolateral stripe bordering the upper flank, the black stripe limits dorsally with a parallel light lime green band limited medially by two rows of black round marks; flanks, ventral and dorsal surfaces of limbs are green; belly and chest are greenish cream, throat greenish yellow; fingers, and toes greenish yellow; iris bronze.

Distribution, natural history, and conservation status. *Pristimantis nankints* has been recorded at one locality in the eastern Andean slopes of Ecuador, Provincia Morona Santiago, Cordillera del Cutucú, 1364–1413 m above sea level (Fig. 8). Natural Region is Andean Eastern Montane Forest (according to Ron et al. 2019 classification) which is characterized by evergreen trees covered by mosses and abundant epiphytic plants.

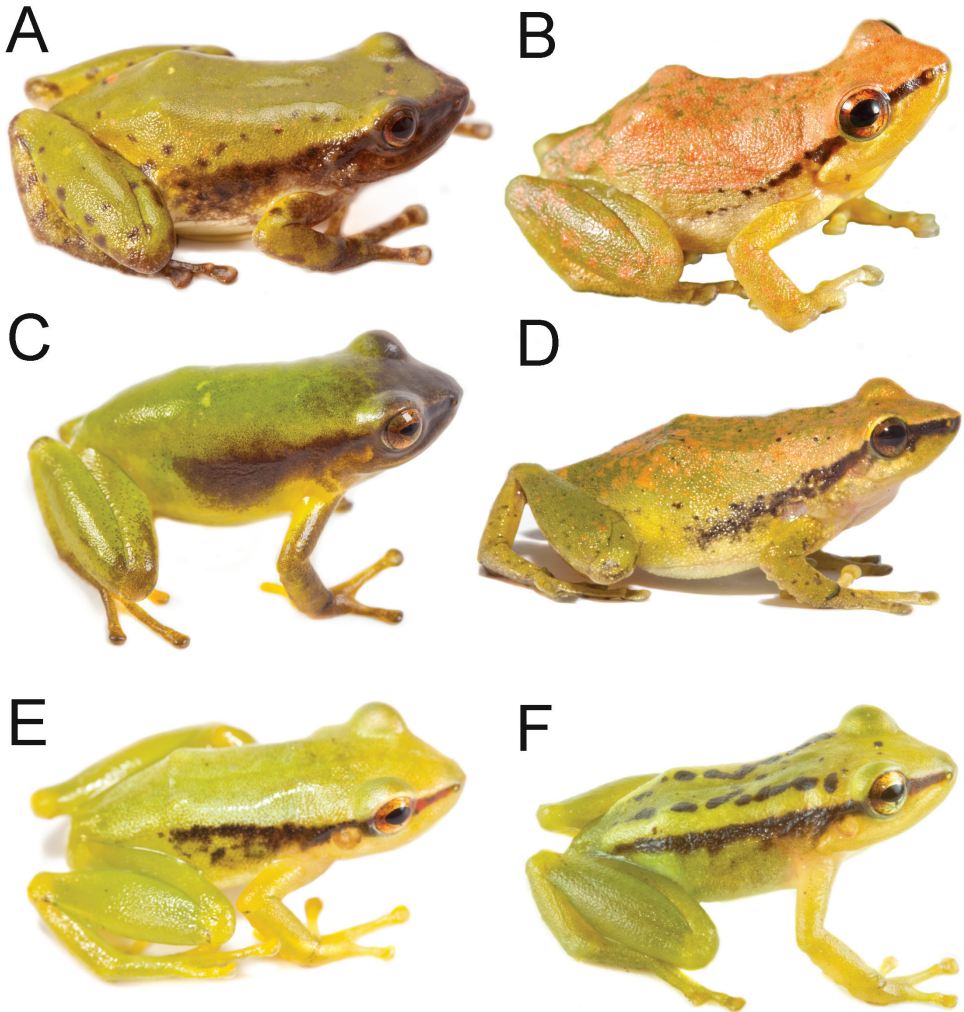


Figure 12. Live adult individuals of the clade of green *Pristimantis* within the *P. lacrimosus* complex and their closest relatives **A** *Pristimantis acuminatus*, QCAZ 53845 **B** *P. limoncochensis*, QCAZ 37277 **C** *P. enigmaticus*, QCAZ 66863 **D** *P. omeviridis*, QCAZ 55392 **E** *P. sp.*, QCAZ 58956 **F** *P. nankints* sp. nov. QCAZ 69137 (SVL = 19.6 mm). Photographs by Santiago R. Ron (**A–B**), Gustavo Pazmiño (**C**), Diego Quirola (**D**), Juan Carlos Sánchez (**E**) and Darwin Nuñez (**F**).

Specimens were found at night along crystalline creek surrounded by secondary forest. The holotype was perching on a leaf 2 m above the ground, next to the stream; after capture, while in the plastic bag, the female deposited 22 eggs. The adult male was collected on secondary forest, on a terrestrial bromeliad. The female paratype was perching on a leaf 30 cm above the ground.

Pristimantis nankints distribution area is a mosaic of forest and deforested areas (based on Ministerio de Ambiente del Ecuador 2013). Its occurrence in secondary

forest, near artificial open areas, indicates at least some level of resilience to anthropogenic habitat change. Nevertheless, there is not enough information to assess its risk of extinction. Therefore, we recommend its assignment to the Data Deficient Red List Category (DD) (based on IUCN 2017 guidelines).

Etymology. The species name is a noun in apposition that refers to Nankints, a small hamlet in Cordillera del Cóndor, Ecuador, that used to be inhabited by Shuar native Americans. Its dwellers were violently evicted and Nankints was destroyed in 2016 to establish a mining camp. Large scale mining projects generate widespread deforestation and pollution in the Andes. The species name is a tribute to Ecuadorian people who have resisted mining activities in defense of the environment. *Nankints* is a shuar word that means spear.

***Pristimantis romeroae* sp. nov.**

<http://zoobank.org/41809854-F7F5-4D0D-B023-97425E666D0C>

Figures 1, 13, 14

Material. Holotype. (Figs 1, 13, 14) QCAZ 41121 (field no. SC-PUCE 27602), adult female from Ecuador, Provincia de Napo, Cantón Archidona, Parroquia Cotundo, Pacto Sumaco-Volcán Sumaco road, El Mirador cottage, 3 km from the cottage to the volcano on Río Pucuno, SSE slope of the Sumaco volcano, 10 km airline distance from the summit (0.633915°S, 77.59228°W), 1602 m above sea level, collected by Elicio Tapia and Raúl E. Ruiz on 21 March 2009.

Paratypes (3). Provincia de Napo: QCAZ 41103, 41128 adult females, QCAZ 41122 adult male. Collected at the type locality with the holotype by Elicio Tapia and Raúl E. Ruiz on 21 March 2009.

Suggested common name. English: Romero's Rain Frog. Spanish: Cutín de Romero.

Diagnosis. A species of *Pristimantis* characterized by the following combination of characters: (1) skin on dorsum shagreen, skin on venter areolate with scattered warts; discoidal fold absent; dorsolateral folds absent; (2) tympanic membrane and tympanic annulus present, upper edge of tympanic annulus covered by supratympanic fold; (3) snout short, truncate in dorsal view, slightly protruding in lateral profile, with small rostral papilla; (4) upper eyelid with several small tubercles; cranial crests absent; (5) denticulate processes of vomers present, prominent, moderately oblique; (6) male having vocal slits, nuptial pads present on finger I; (7) finger I slightly shorter than finger II; discs of digits expanded, truncate; (8) fingers with lateral fringes; hyperdistal subarticular tubercles present; (9) ulnar tubercles absent, tarsal tubercles present, subconical, conspicuous; (10) heel with one, nearly inconspicuous, small subconical tubercle or without tubercles; inner tarsal fold absent; (11) inner metatarsal tubercle prominent, elliptical, approximately three times as large as rounded, conical outer metatarsal tubercle; supernumerary plantar tubercles present (Fig. 1); (12) toes with lateral fringes; toe webbing absent; toe V much longer than toe III (disc on toe III extends to the distal edge of the medial subarticular tubercle on toe IV, disc on toe V extends beyond the proximal edge



Figure 13. Variation in preserved specimens of *Pristimantis romeroae* sp. nov. From left to right, first and second rows: QCAZ 41121 (holotype, SVL = 31.1 mm, adult female), QCAZ 41103 (SVL = 33.8 mm, adult female), QCAZ 41128 (SVL = 31.15 mm, adult female), QCAZ 41222 (SVL = 23.8 mm, adult male). All specimens are shown at the same scale. Photographs by Julio C. Carrión.

of the distal subarticular tubercle on toe IV); hyperdistal subarticular tubercles present in all toes; toe discs smaller than those on fingers (Fig. 1); (13) life, coloration unknown; (14) SVL in adult females 31.1–33.8 mm ($n = 3$), adult male = 23.8 mm ($n = 1$).

Comparisons with other species. In this section, coloration refers to preserved individuals (Fig. 13). *Pristimantis romeroae* resembles *P. nankints* in coloration. *Pristimantis romeroae* differs by having numerous large warts on the venter (small warts in *P. nankints*) and by the size and shape of discs on fingers: expanded and truncate in *P. romeroae* vs. moderately expanded and rounded in *P. nankints*. Its predominately pale creamy orange dorsal coloration resembles that of preserved *P. acuminatus*, *P. enigmaticus*, *P. limoncochensis*, *P. omeviridis*, *P. pseudoacuminatus*, and *P. tantanti*. It differs from all of them by having a dark stripe bordering the upper edge of the flanks (dark stripe absent or if present, it is an oblique-lateral stripe starting behind the eye and ending near the ventral edge of the flank at midbody). It also differs from *P. acuminatus*, *P. limoncochensis*, and *P. tantanti* by having a conspicuous tympanum (absent in the three species). *Pristimantis romeroae* can be further distinguished from *P. enigmaticus* and *P. omeviridis* by having a larger tympanum (21–27% of head length in *P. romeroae* vs. 12–13% in both species; Ortega-Andrade et al. 2015). *Pristimantis pseudoacuminatus* differs by having sparse tubercles and warts on the dorsum (absent in *P. romeroae*; Shreve 1935).

Description of the holotype. Adult female (QCAZ 41121). Measurements (in mm): SVL 31.1; tibia length 14.3; foot length 15.7; head length 11.2; head width

11.0; eye diameter 3.2; tympanum diameter 2.4; interorbital distance 4.0; upper eyelid width 3.0; internarial distance 3.4; eye-nostril distance 3.2; tympanum-eye distance 0.9. Semi-slender body; head much wider than long, wider than body; snout short, truncate in dorsal view, slightly protruding in lateral profile, with rostral papilla; canthus rostralis distinct, slightly curved in dorsal view; loreal region concave; interorbital space flat, lacking cranial crests; eye large; upper eyelid ca. 73% of interorbital distance; lacking tubercles, no interocular fold. Tympanic membrane and annulus present, rounded in shape, its upper and posterodorsal edges covered by supratympanic fold; horizontal diameter of tympanum ca. 54% of eye diameter, separated from eye by a distance ca. 45% tympanum length; choanae large, elliptical, non-concealed by palatal shelf of maxillary arc; dentigerous processes of vomers present, prominent, moderately oblique, narrowly separated, bearing seven teeth, tongue large, rounded, posterior border notched, 15% not adherent to floor of mouth.

Skin on dorsum and flanks shagreen; dorsolateral folds absent; skin on belly and posterior half of chest areolate with scattered warts; skin on throat and anterior half of chest smooth; discoidal fold absent; skin in upper cloacal region smooth. Forearms slender with three ill-defined, low ulnar tubercles in distal, medial and proximal outer edge of forearm; fingers large and slender, all fingers with pads surrounded by circumferential grooves, truncate discs; bearing narrow lateral fringes; relative lengths of fingers $I < II < IV < III$; subarticular tubercles single, round in ventral and lateral view; hyperdistal subarticular tubercles present; bearing few, inconspicuous, low supernumerary tubercles, palmar tubercle bifid, twice the size of elliptical thenar tubercle (Fig. 1).

Hindlimbs slender; tibia length ca. 50% of SVL; upper surfaces of hindlimbs smooth; foot length ca. 45 % of SVL, posterior surfaces of thighs shagreen, ventral surfaces of thighs smooth; knee and heel lacking tubercles; inner surface of tarsus lacking tubercles; toes bearing narrow lateral fringes; webbing between toes absent; discs on toes broadly expanded, truncate, the same size than fingers; all toes having pads surrounded by circumferential grooves; relative lengths of toes: $I < II < III < V < IV$; subarticular tubercles rounded, simple; hyperdistal subarticular tubercles present; plantar surface with numerous indistinct supernumerary tubercles; inner metatarsal tubercle prominent, elliptical, approximately 3 times the size of rounded, conical outer metatarsal tubercle (Fig. 1).

Color of holotype in preservative. (Fig. 13) Background color pale creamy orange with faint interorbital line; long, thick, dark brown dorsolateral bars; dorsum with paler blotches clustered in two parallel stripes at the scapular region approximately half the length of the dorsolateral bars; face with dark brown canthal and supratympanic stripes, supratympanic stripe suffused with the dark brown dorsolateral bar; flanks the same back ground color with minute dark spots (visible under magnification) densely distributed; dorsal surfaces of limbs yellowish cream brighter than dorsum with scattered minute dark brown spots visible under magnification; ventral surface of body yellowish cream; plantar and palmar surfaces dirty cream.

Color of holotype in life. Unknown but presumably green, similar to its most closely relatives (e.g., *P. nankints*, *P. enigmaticus*) which have a similar clear coloration in preservative (Figs 9 and 12).



Figure 14. X-rays of *Pristimantis nankints* sp. nov. and *Pristimantis romeroae* sp. nov. Left, *Pristimantis nankints* sp. nov. holotype, QCAZ 71457; right, *Pristimantis romeroae* sp. nov. holotype, QCAZ 41121.

Variation. (Fig. 13) In this section, coloration refers to preserved individuals unless otherwise noted. In the type series, the adult male has an SVL = 23.8 mm, lower than the adult female SVL (range 31.1–33.8 mm; Table 3). Males have vocal slits and nuptial pads on finger I. Dorsal coloration is creamy tan (e.g., QCAZ 41121) with a black canthal stripe followed by black dorsolateral stripes. Marks on dorsum vary from scattered dark brown spots (e.g., QCAZ 41103) to two longitudinal brown strips starting behind the head and converging medially in the sacral region (QCAZ 41122) with or without a fine interorbital bar. Flanks are cream; venter and ventral surfaces of limbs vary from creamy white (e.g., QCAZ 41122) to yellowish cream (e.g., QCAZ 41103). The belly has scattered white warts (e.g., QCAZ 41103, 41121).

Color in life: unknown but presumably green (see description of the holotype).

Distribution, natural history, and conservation status. *Pristimantis romeroae* is known from one locality at the eastern Andean slopes of Ecuador, Provincia de Napo, on the SSE slope of the Sumaco volcano, 1602 m above sea level (Fig. 8). Natural Region is Andean Eastern Montane Forest (according to Ron et al. 2019 classification) which is characterized by evergreen trees covered by mosses and abundant epiphytic plants. Except for QCAZ 41128, all specimens were found on a spiny bromeliad 6 cm from the ground by the day. QCAZ 41128 was found also by day on a bromeliad of a recently fallen tree.

In 2008, one year before the specimens were collected, the type locality was at a distance of < 1 km from agricultural deforested areas (based on Ministerio de Ambiente del Ecuador 2013) suggesting at least some level of tolerance to habitat degradation. Available information is insufficient to determine the risk of extinction of this species

known from a single locality. Lack of records may partly be a consequence of its association with bromeliads which generally grow at heights unreachable during herpetological searches. We suggest to assigning *P. romeroae* to the Data Deficient Red List Category (DD) (based on IUCN 2017 guidelines).

Etymology. The species name is a noun in the genitive case and is a patronym for Giovanna Romero, an Ecuadorian botanist and SRR's wife. For almost two decades, she has supported SRR's research in countless ways and this is a long-overdue tribute.

Discussion

Subarticular tubercles and phalange morphology in *Pristimantis*

Subarticular tubercles are round dermal protuberances, below the articulations of phalanges, on the underside of the hands and feet of anurans. According to the most recent comprehensive reviews of morphological characters of *Pristimantis* (Lynch and Duellman 1997; Duellman and Lehr 2007), strabomantid frogs have: (1) one subarticular tubercle on fingers I, II and toes I, II, (2) two subarticular tubercles on fingers III, IV and toes III, IV, and (3) three subarticular tubercles on toe IV. While describing the morphology of the new species, we noticed the presence of an additional subarticular tubercle underlying the articulation of the last phalange on each finger and toe (arrows in Fig. 1). Those tubercles are similar in size to other subarticular tubercles. While preparing this publication, we became aware of a recent publication by Ospina-Sarria and Duellman (2019) on which they report the same tubercles and named them “hyperdistal tubercles”. Prior to Ospina-Sarria and Duellman (2019), the only mention we could find of hyperdistal tubercles in Strabomantid frogs was made by Lynch (1999) who stated “in many species there is a tubercle poorly defined that corresponds to the articulation of the terminal phalange (which supports the disk) and the penultimate phalange. This is a subarticular tubercle but because it is not as developed as the others, conventionally we do not take it into account”. Our observations indicate that hyperdistal tubercles can be as large or larger than other subarticular tubercles (e.g., Fig. 1). Variation between presence and absence of hyperdistal tubercles appear to be continuous. In some species, like *P. phoxocephalus*, there is an inconspicuous tubercle at the base of the disk. In others, like *P. katoptroides*, the tubercle is larger than that of *P. phoxocephalus* but smaller than the hyperdistal tubercles observed in the *P. lacrimosus* species group. Future studies on the evolution and functional significance of hyperdistal tubercles would require methodologies to code it as a continuous character.

The available information on the phylogenetic distribution of hyperdistal tubercles and the morphology of the terminal phalanges suggest that they have phylogenetic signal and diagnostic value. Hyperdistal tubercles are present in all examined species of the *P. lacrimosus* species group (ten species: Table 2, Ospina-Sarria and Duellman 2019). They are also present in *P. orcesi* and *P. eugeniae*, two members of the sister clade

of the *P. lacrimosus* species group (Table 2, Ospina-Sarria and Duellman 2019). In contrast, they were absent in the distantly related *P. crenunguis*, *P. achatinus*, *P. condor*, and *P. lanthanites* (Table 2). The available evidence suggests that the hyperdistal tubercles may be shared by the *P. lacrimosus* species group and its sister clade. Hyperdistal tubercles were also found in three species belonging to the closely related *P. boulengeri* and *P. leptolophus* species groups: *P. angustilineatus*, *P. boulengeri*, and *P. leptolophus* (Ospina-Sarria and Duellman 2019). They are also present in *P. eriphus*, *P. katoptroides*, and *P. orpacobates*, species that are not closely related to the *P. lacrimosus* species group (Table 2). The distribution of hyperdistal tubercles among *Pristimantis* suggests several independent origins. An exhaustive analysis of the distribution of hyperdistal tubercles on a phylogenetic context is necessary to understand its evolution.

Interestingly, our results suggest that the presence of hyperdistal tubercles is linked to two osteological characters of the terminal phalanges (Table 2). First, species with hyperdistal tubercles tend to have long terminal phalanges (relative to the penultimate phalange; Fig. 2, Table 2). Second, they tend to have narrow T-shaped expansions at the end of the terminal phalange. Our results on 21 species of *Pristimantis* (Table 2) suggest future venues of research to discover morphological synapomorphies for *Pristimantis* clades, a task that has been elusive until now.

The correlation between the presence of hyperdistal tubercles and the morphology of the terminal phalanges has not been tested. We suspect that in species with short ultimate phalanges, like *P. crenunguis* (Fig. 2), the disk pad overlaps the phalange articulation and, therefore, the hyperdistal tubercle. This overlap may explain the absence of hyperdistal tubercles in species with short terminal phalanges (Fig. 2). In species with long terminal phalanges, like *P. romeroae*, the disk pad does not overlap with the articulation and the subarticular tubercle is separate from the disk pad and, therefore, is distinct.

The *Pristimantis lacrimosus* species group originated in the Chocoan forests

Our reconstruction of ancestral basin indicates that the *P. lacrimosus* species group originated in the Chocoan forests of the Pacific basin of Ecuador and Colombia. This result was unexpected because, by far, most species of the group occur in the Amazon basin (26 described species out of 36). Our reconstruction suggests that the Amazon basin was colonized on a single event. The paucity of colonization events across the Andes demonstrates the pivotal role of the Andean barrier in the diversification of *Pristimantis*. There is a single colonization event from the Amazon Basin to the Chocoan forests with *P. moro*. Because *P. moro* is also distributed in Central America, we suspect that its presence in the Chocoan forest is a result of a colonization from central America instead of colonization across the Andes. The Amazon basin was also the origin of *P. jorgevelosai*, a species distributed in the Magdalena river basin and embedded in an otherwise Amazonian clade (Fig. 4).

Our biogeographic reconstruction suggests that the *P. lacrimosus* species group had higher diversification rates in the Amazon basin relative to the Chocó region. There are two clades inhabiting the Chocoan region. One of them is older than the Amazonian

clade and yet it only has four species. The second clade is sister to the Amazonian clade. Although both clades have the same age, the Chocoan clade has only four species compared to 19 species in the Amazonian clade. These differences in diversification rates are inconsistent with the time-for-speciation hypothesis, which predicts the highest richness in first colonized regions (Stephens and Wiens 2003). Additional studies are needed to determine if the higher diversification rate in the Amazon region, relative to the Chocó, observed in the *P. lacrimosus* group is a generality among *Pristimantis* inhabiting both regions.

Acknowledgments

Ana Belén Carrillo helped with laboratory work. For specimen collection, locality data, and field assistance, we are indebted to Diego Almeida, Fernando Ayala, Edwin Carrillo, Galo Díaz, Ricardo Gavilanes, Yadira Mera, Jefferson Mora, Darwin Núñez, Kunam Nusirquia, Diego Paucar, Raúl E. Ruiz, and Elicio Tapia. Research and collecting permits were issued by the Ministerio de Ambiente del Ecuador (003-17 IC-FAU-DNB/MA, 008-09 IC-FAU-DNB/MA and MAE-DNB-CM-2015-0025). Field and laboratory work in Ecuador were funded by Secretaría Nacional de Educación Superior, Ciencia, Tecnología e Innovación del Ecuador SENESCYT (Arca de Noé initiative; SRR and Omar Torres principal investigators) and a grant from Pontificia Universidad Católica del Ecuador, Dirección General Académica. We thank Santiago Guamán, Diego Paucar, and Fernando Ayala for assisting access to the QCAZ collection. Additionally, we thank Gustavo Pazmiño, Maricela Rivera, Diego Quirola, Juan Carlos Sánchez, Darwin Núñez and Jorge Valencia for providing specimen photographs. Fernando Ayala made x-ray images of the specimens.

References

- Acosta-Galvis A (2019) Lista de los Anfibios de Colombia: Referencia en línea v.09.2019. Villa de Leyva, Colombia. <http://www.batrachia.com>
- AmphibiaWeb (2019) AmphibiaWeb: information on amphibian biology and conservation. University of California Berkeley. <http://amphibiaweb.org/>
- Arteaga A, Yáñez-Munoz M, Guayasamin JM (2013) A new frog of the *Pristimantis lacrimosus* group (Anura: Craugastoridae) from the montane forests of northwestern Ecuador. Adendum to: “The amphibians and reptiles of Mindo: life in the cloudforest”. Serie de Publicaciones Científicas, Universidad Tecnológica Indoamérica 1: 198–210.
- Batallas D, Brito J (2014) Nueva especie de rana del género *Pristimantis* del grupo *lacrimosus* (Amphibia: Craugastoridae) del Parque Nacional Sangay, Ecuador. Papeis Avulsos de Zoologia (Sao Paulo) 54: 51–62. <https://doi.org/10.1590/0031-1049.2014.54.05>
- Boulenger GA (1899) Descriptions of new reptiles and batrachians collected by Mr. P. O. Simons in the Andes of Ecuador. Annals and Magazine of Natural History 7, 4: 454–457. <https://doi.org/10.1080/00222939908678229>

- Boulenger GA (1902) Descriptions of new batrachians and reptiles from north-western Ecuador. *Annals and Magazine of Natural History, Series 7*, 9: 51–57. <https://doi.org/10.1080/00222930208678538>
- Brito J, Almendáriz A, Batallas D, Ron SR (2017) Nueva especie de rana bromelícola del género *Pristimantis* (Amphibia: Craugastoridae), meseta de la cordillera del Cóndor, Ecuador. *Papeis Avulsos de Zoologia (Sao Paulo)* 57: 177–195. <https://doi.org/10.11606/0031-1049.2017.57.15>
- Carrión JC (2020) Systematics of *Pristimantis lacrimosus* group (Anura, Strabomantidae) with the description of a new species from the eastern slopes of the Ecuadorian Andes. Quito, Ecuador: Pontificia Universidad Católica del Ecuador. Unpublished Licenciatura thesis.
- Chernomor O, von Haeseler A, Minh BQ (2016) Terrace Aware Data Structure for Phylogenomic Inference from Supermatrices. *Systematic Biology* 65: 997–1008. <https://doi.org/10.1093/sysbio/syw037>
- Despax MR (1911) Mission géodésique de l'Équateur. Collections recueillies par M. le Dr. Rivet. Batraciens anoures. *Bulletin du Museum national d'Histoire naturelle, Paris* 17: 90–94.
- Duellman WE (1978) Three new species of *Eleutherodactylus* from Amazonian Perú (Amphibia: Anura: Leptodactylidae). *Herpetologica* 34: 264–270.
- Duellman WE (1990) A new species of *Eleutherodactylus* from the Andes of Northern Peru (Anura: Leptodactylidae). *Journal of Herpetology* 24: 348–350. <https://doi.org/10.2307/1565048>
- Duellman WE, Lehr E (2009) Terrestrial breeding frogs (Strabomantidae) in Perú. Natur- und Tier-Verlag, Naturwissenschaft, Münster.
- Edgar RC (2004) MUSCLE: multiple sequence alignment with high accuracy and high throughput. *Nucleic Acids Research* 32: 1792–1797. <https://doi.org/10.1093/nar/gkh340>
- Elmer KR, Davila JA, Lougheed SC (2007) Cryptic diversity and deep divergence in an upper Amazonian leaf litter frog, *Eleutherodactylus ockendeni*. *BMC Evolutionary Biology* 7: 247. <https://doi.org/10.1186/1471-2148-7-247>
- Goebel AM, Donnelly MA, Atz M (1999) PCR primers and amplification methods for 12S ribosomal DNA, the control region, cytochrome oxidase I, and cytochrome b in bufonids and other frogs, and an overview of PCR primers which have amplified DNA in amphibians successfully. *Molecular Phylogenetics and Evolution* 11: 163–199. <https://doi.org/10.1006/mpev.1998.0538>
- Gonzalez-Duran GA, Targino M, Rada M, Grant T (2017) Phylogenetic relationships and morphology of the *Pristimantis leptolophus* species group (Amphibia: Anura: Brachycephaloidea), with the recognition of a new species group in *Pristimantis* Jimenez de la Espada, 1870. *Zootaxa* 4243: 42–74. <https://doi.org/10.11646/zootaxa.4243.1.2>
- Guayasamin JM, Hutter CR, Tapia EE, Culebras J, Penafiel N, Pyron RA, Morochz C, Funk WC, Arteaga A (2017) Diversification of the rainfrog *Pristimantis ornattissimus* in the lowlands and Andean foothills of Ecuador. *PLOS ONE* 12: e0172615. <https://doi.org/10.1371/journal.pone.0172615>
- Guayasamin JM, Ron SR, Cisneros-Heredia DF, Lamar W, McCracken SF (2006) A new species of frog of the *Eleutherodactylus lacrimosus* assemblage (Leptodactylidae) from the Western Amazon Basin, with comments on the utility of canopy surveys in lowland rainforest. *Herpetologica* 62: 191–202. <https://doi.org/10.1655/05-40.1>

- Guindon S, Dufayard JF, Lefort V, Anisimova M, Hordijk W, Gascuel O (2010) New algorithms and methods to estimate maximum-likelihood phylogenies: assessing the performance of PhyML 3.0. *Systematic Biology* 59: 307–321. <https://doi.org/10.1093/sysbio/syq010>
- Hedges SB, Duellman WE, Heinicke MP (2008) New World direct-developing frogs (Anura: Terrana): molecular phylogeny, classification, biogeography, and conservation. *Zootaxa* 1737: 1–181. <https://doi.org/10.11646/zootaxa.1737.1.1>
- Heinicke MP, Duellman WE, Hedges SB (2007) Major Caribbean and Central American frog faunas originated by ancient oceanic dispersal. *Proceedings of the National Academy of Sciences of the United States of America* 104: 10092–10097. <https://doi.org/10.1073/pnas.0611051104>
- Heyer WR, Hardy LM (1991) A new species of frog of the *Eleutherodactylus lacrimosus* assembly from Amazonia, South America (Amphibia: Anura: Leptodactylidae). *Proceedings of the Biological Society of Washington* 104: 436–447.
- ImageJ 2. <https://imagej.nih.gov/ij/> [accessed 11 January 2020]
- IUCN Standards and Petitions Subcommittee (2017) Guidelines for Using the IUCN Red List Categories and Criteria. Version 13. IUCN Standards and Petitions Subcommittee, 108 pp. <http://www.iucnredlist.org/documents/RedListGuidelines.pdf>
- Jetz W, Pyron RA (2018) The interplay of past diversification and evolutionary isolation with present imperilment across the amphibian tree of life. *Nature Ecology & Evolution* 2: 850–858. <https://doi.org/10.1038/s41559-018-0515-5>
- Jiménez de la Espada M (1870) Fauna neotropicalis species quaedam nondum cognitae. *Jornal de Ciências, Matemáticas, Physicas e Naturaes* 3: 57–65.
- Jiménez de la Espada M (1875) Vertebrados del Viaje al Pacifico: Batracios. Imprenta de Miguel Ginesta, Madrid, xvi + 208 pp.
- Kalyaanamoorthy S, Minh BQ, Wong TKF, von Haeseler A, Jermiin LS (2017) ModelFinder: fast model selection for accurate phylogenetic estimates. *Nature Methods* 14: 587–589. <https://doi.org/10.1038/nmeth.4285>
- Köhler J, Morales VR, Lotters S, Reichle S, Aparicio J (1998) A new green species of frog, genus *Eleutherodactylus*, from Bolivia and Peru (Amphibia, Anura, Leptodactylidae). *Studies on Neotropical Fauna and Environment* 33: 93–99. <https://doi.org/10.1076/snfe.33.2.93.2158>
- Kumar S, Stecher G, Tamura K (2016) MEGA7: Molecular Evolutionary Genetics Analysis version 7.0 for bigger datasets. *Molecular Biology and Evolution* 33: 1870–1874. <https://doi.org/10.1093/molbev/msw054>
- Lehr E, Gregory C, Catenazzi A (2013) A new species of *Pristimantis* (Amphibia: Anura: Strabomantidae) from the Rio Abiseo National Park, Peru. *Zootaxa* 3731: 201–211. <https://doi.org/10.11646/zootaxa.3731.2.1>
- Lehr E, Lundberg M, Aguilar C, von May R (2006) New species of *Eleutherodactylus* (Anura: Leptodactylidae) from the eastern Andes of central Peru with comments on central Peruvian *Eleutherodactylus*. *Herpetological Monographs* 20: 105–128. [https://doi.org/10.1655/0733-1347\(2007\)20\[105:NSOEAR\]2.0.CO;2](https://doi.org/10.1655/0733-1347(2007)20[105:NSOEAR]2.0.CO;2)
- Lehr E, Torres-Gastello CP, Suárez-Segovia J (2007) A new species of arboreal *Eleutherodactylus* (Anura: Leptodactylidae) from the Amazonian lowlands of central Peru. *Herpetologica* 63: 94–99. [https://doi.org/10.1655/0018-0831\(2007\)63\[94:ANSOAE\]2.0.CO;2](https://doi.org/10.1655/0018-0831(2007)63[94:ANSOAE]2.0.CO;2)

- Lynch JD (1976) New species of frogs (Leptodactylidae: *Eleutherodactylus*) from the Pacific versant of Ecuador. Occasional Papers of the Museum of Natural History, University of Kansas 55: 1–33. <https://doi.org/10.5962/bhl.part.29037>
- Lynch JD (1980) *Eleutherodactylus eremitus*, a new trans-Andean species of the *lacrimosus* assembly from Ecuador (Amphibia: Leptodactylidae). Breviora 462: 1–7. <https://doi.org/10.2307/1444513>
- Lynch JD (1994) A new species of frog (genus *Eleutherodactylus*: Leptodactylidae) from a cloud forest in Departamento de Santander, Colombia. Revista de la Academia Colombiana de Ciencias Exactas, Físicas y Naturales 19: 205–208.
- Lynch JD, Duellman WE (1980) The *Eleutherodactylus* of the Amazonian slopes of the Ecuadorian Andes (Anura: Leptodactylidae). Miscellaneous Publications Museum Natural History University of Kansas 69: 1–86. <https://doi.org/10.5962/bhl.title.16222>
- Lynch JD, Duellman WE (1997) Frogs of the genus *Eleutherodactylus* in Western Ecuador. Special Publication The University of Kansas Natural History Museum 23: 1–236.
- Lynch JD, Ruíz-Carranza PM (1985) A synopsis of the frogs of the genus *Eleutherodactylus* from the Sierra Nevada de Santa Marta, Colombia. Occasional Papers of the Museum of Zoology, University of Michigan 711: 1–60.
- Lynch JD, Schwartz A (1971) Taxonomic disposition of some 19th century Leptodactylid frog names. Journal of Herpetology 5: 103–114. <https://doi.org/10.2307/1562732>
- McCracken S, Forstner M, Dixon JR (2007) A new species of the *Eleutherodactylus lacrimosus* assemblage (Anura, Brachycephalidae) from the lowland rainforest canopy of Yasuni National Park, Amazonian Ecuador. Phyllomedusa 6: 23–34. <https://doi.org/10.11606/issn.2316-9079.v6i1p23-35>
- Ministerio de Ambiente del Ecuador (2013) Sistema de Clasificación de los Ecosistemas del Ecuador Continental. Subsecretaría de Patrimonio Natural, Quito, Ecuador.
- Maddison WP, Maddison DR (2019) Mesquite: a modular system for evolutionary analysis. Version 3.61. <http://www.mesquiteproject.org>
- Moen DS, Wiens JJ (2009) Phylogenetic evidence for competitively driven divergence: body-size evolution in Caribbean treefrogs (Hylidae: *Osteopilus*). Evolution 63: 195–214. <https://doi.org/10.1111/j.1558-5646.2008.00538.x>
- Morales VR (2007) Una especie nueva de *Eleutherodactylus* (Amphibia: Anura: Brachycephalidae) de la Amazonía central del Perú. Biotempo Lima 7: 5–11. <https://doi.org/10.31381/biotempo.v7i0.868>
- Moravec J, Lehr E, Pena PEP, Lopez JJ, Urrutia GG, Tuanama IA (2010) A new green, arboreal species of *Pristimantis* (Anura: Strabomantidae) from Amazonian Peru. Vertebrate Zoology 60: 225–232.
- Navarrete MJ, Venegas PJ, Ron SR (2016) Two new species of frogs of the genus *Pristimantis* from Llanganates National Park in Ecuador with comments on the regional diversity of Ecuadorian *Pristimantis* (Anura, Craugastoridae). ZooKeys 593: 139–162. <https://doi.org/10.3897/zookeys.593.8063>
- Nguyen LT, Schmidt HA, von Haeseler A, Minh BQ (2015) IQ-TREE: a fast and effective stochastic algorithm for estimating maximum-likelihood phylogenies. Molecular Biology and Evolution 32: 268–275. <https://doi.org/10.1093/molbev/msu300>

- Ortega-Andrade HM, Rojas-Soto OR, Valencia JH, Espinosa de Los Monteros A, Morrone JJ, Ron SR, Cannatella DC (2015) Insights from integrative systematics reveal cryptic diversity in *Pristimantis* frogs (Anura: Craugastoridae) from the upper Amazon Basin. *PLoS One* 10: e0143392. <https://doi.org/10.1371/journal.pone.0143392>
- Ospina-Sarria JJ, Duellman WE (2019) Two new species of *Pristimantis* (Amphibia: Anura: Strabomantidae) from southwestern Colombia. *Herpetologica* 75: 85–95. <https://doi.org/10.1655/D-18-00019>
- Padial JM, Grant T, Frost DM (2014) Molecular systematics of terraranas (Anura: Brachycephaloidea) with an assessment of the effects of alignment and optimality criteria. *Zootaxa* 3825: 1–132. <https://doi.org/10.11646/zootaxa.3825.1.1>
- Pagel M (1999) The maximum likelihood approach to reconstructing ancestral character states of discrete characters on phylogenies. *Systematic Biology* 48: 612–622. <https://doi.org/10.1080/106351599260184>
- Pyron RA (2014) Biogeographic analysis reveals ancient continental vicariance and recent oceanic dispersal in amphibians. *Systematic Biology* 63: 779–797. <https://doi.org/10.1093/sysbio/syu042>
- Rivera-Correa M, Daza JM (2016) Molecular phylogenetics of the *Pristimantis lacrimosus* species group (Anura: Craugastoridae) with the description of a new species from Colombia. *cordillera occidental* 11: 31–45.
- Ron SR, Merino-Viteri A, Ortiz DA (2019) Anfibios del Ecuador. Version 2019.0. <https://bioweb.bio/faunaweb/amphibiaweb/> [accessed March 8, 2019]
- Savage JM (1965) A new bromeliad frog of the genus *Eleutherodactylus* from Costa Rica. *Bulletin of the Southern California Academy of Sciences* 64: 106–110.
- Shepack A, von May R, Tito A, Catenazzi A (2016) A new species of *Pristimantis* (Amphibia, Anura, Craugastoridae) from the foothills of the Andes in Manu National Park, southeastern Peru. *ZooKeys* 594: 143–164. <https://doi.org/10.3897/zookeys.594.8295>
- Shreve B (1935) On a new Teiid and Amphibia from Panama, Ecuador, and Paraguay. *Occasional Papers of the Boston Society of Natural History* 8: 209–218.
- Sierra R (2013) Patronos y factores de deforestación en el Ecuador continental, 1990–2010. Y un acercamiento a los próximos 10 años. *Conservation International Ecuador y Forest Trends*, Quito, Ecuador.
- Stephens PR, Wiens JJ (2003) Explaining species richness from continents to communities: the time-for-speciation effect in emydid turtles. *American Naturalist* 161: 112–128. <https://doi.org/10.1086/345091>
- Urgiles VL, Székely P, Székely D, Christodoulides N, Sanchez-Nivicela JC, Savage AE (2019) Genetic delimitation of *Pristimantis orestes* (Lynch, 1979) and *P. saturninoi* Brito et al., 2017 and description of two new terrestrial frogs from the *Pristimantis orestes* species group (Anura, Strabomantidae). *Zookeys* 864: 111–146. <https://doi.org/10.3897/zookeys.864.35102>
- Valencia JH, Valladares-Suntasig F, Tipantiza-Tuguminago L, Duenas MR (2019) A new species of terrestrial-breeding frog of the genus *Pristimantis* (Anura: Terrarana: Craugastoridae) from the eastern Andean slopes of the southern Ecuador. *Zootaxa* 4658: 509–525. <https://doi.org/10.11646/zootaxa.4658.3.4>

- Wiens JJ, Fetzner JW, Parkinson CL, Reeder TW (2005) Hylid frog phylogeny and sampling strategies for speciose clades. *Systematic Biology* 54: 778–807. <https://doi.org/10.1080/10635150500234625>
- Zhang P, Liang D, Mao RL, Hillis DM, Wake DB, Cannatella DC (2013) Efficient sequencing of Anuran mtDNAs and a mitogenomic exploration of the phylogeny and evolution of frogs. *Molecular Biology and Evolution* 30: 1899–1915. <https://doi.org/10.1093/molbev/mst091>

Appendix I

Examined specimens

Pristimantis petersi. ECUADOR: PROVINCIA NAPO: Cantón: Archidona. Cocodrilos, Cocodrilo Station (0.6545°S, 77.7848°W) 1732 m, (QCAZ 31416, 31417); road from Baeza to Archidona (77.7929°W, 0.6711°S) 1575 m, (QCAZ 63452, 63453, 63454, 63455, 63456). PROVINCIA PASTAZA: Cantón Mera, Ankaku Private Station (78.0779°W, 1.2792°S) 2300 m (QCAZ 45846, 45847, 45848, 45849, 45850, 45892, 45898).

Pristimantis bromeliaceus. ECUADOR: PROVINCIA MORONA SANTIAGO: Cantón: Gualaquiza. Chinguida (3.2263°S, 78.7105°W) 1930 m (QCAZ 56454); Zuñac (2.1934°S, 78.3597°W) 2371 m, (QCAZ 61836). PROVINCIA ZAMORA CHINCHIPE: Cantón: Nangaritza. Campo Maicu (4.1195°S, 78.5766°W) 1667 m (QCAZ 55469); La Canela (4.5728°S, 78.8915°W) 1736 (QCAZ 63272).

Pristimantis paululus. ECUADOR: PROVINCIA NAPO. Jatun Sacha Biological Reserve (1.05°S, 77.6000°W) 388 m (QCAZ 09099); (1.0660°S, 77.6170°W) 405 m, (QCAZ 53002, 53016). PROVINCIA ORELLANA. San José de Payamino (0.4794°S, 77.2945°W) 318 m, (QCAZ 56656). Cantón: Joya de los Sachas. La Parquer (0.34243°S, 76.8665°W) 284 m, (QCAZ 63130).

